THE UNIVERSITY *of* EDINBURGH

The Habitability of Ammoniacal Waters on Icy Moons and Earth

Cassie M. Hopton

University of Edinburgh
UK Centre for Astrobiology
September 2025

A thesis presented for the degree of Doctor of Philosophy

ABSTRACT

The search for life has expanded to include the icy moons of Jupiter (Europa, Ganymede, and Callisto) and Saturn's moons Titan and Enceladus. These moons feature surfaces encrusted in ice ranging from several to hundreds of kilometres thick, beneath which substantial subsurface oceans of liquid water are thought to exist. Liquid water is a prerequisite for life, and thus the habitability prospects of these oceans is speculated. Preservation of this liquid water is thought possible by freezing point depressants, such as ammonia. Indeed, the Cassini-Huygens mission revealed not only active cryovolcanism on Enceladus but also the presence of ammonia. On Earth, ammonia facilitates biotic chemistry at low concentrations and is a common pollutant from agricultural and industrial processes. As a proton acceptor, elevated concentrations of ammonia are known to disrupt biological chemistries. The presence of ammonia in extraterrestrial oceans, as well as terrestrial ecosystems, could therefore constrain the habitability prospects of these environments. In this thesis, I explore whether the presence of ammonia could impact the potential for habitability in icy moon oceans, with additional implications for the habitability of Earth environments. I use growth dynamics and cellular viability assays to establish the growth response and cultivation limits of the extremophile *Halomonas meridiana* Slthf1 in concentrations of aqueous ammonia relevant to the oceans of Enceladus, Titan, and Europa. Through these approaches, I also examine the growth impacts of indirect ammonia exposure occurring by volatilized ammonia gas. The morphological and physiological changes exerted by ammonia on *H. meridiana* are additionally examined by transmission electron microscopy and metabolomics. Through this research I show that aqueous ammonia exposure, either as dissolved ammonia gas (NH_3) or as a salt ($(NH_4)_2SO_4$), can extend lag phase duration and doubling time, slow growth rate, diminish cell density and reduce cell viability, even in cultures indirectly exposed to NH_3 by volatilization. I elucidate that exposure to ammonia can disfigure cell morphology and elevate the occurrence of cell lysis events. I present evidence that ammonia toxicity is distinct from external pH toxicity and could be encouraged by internal and potentially destructive NH_3-driven reactions. Toxicity of ammonia may also be driven by modulation to essential nitrogen, carbon, and energy metabolism. Possible survival strategies, such as cell wall remodelling, were indicated by metabolomics. The results demonstrate that at specified molar thresholds, ammonia can impose constraints on growth, viability, and the metabolism of *H. meridiana*. This data cannot suggest whether icy moons oceans are or have been inhabited but can provide a foundation for which to assess the potential for habitability. The molar concentrations at which the outlined effects occur exceed the putative ammonia concentrations in the oceans of Enceladus and Europa. Based on this evidence, it is plausible dissolved or volatilized ammonia in these environments may not pose as a limiting factor for habitability. For Titan, the ammonia content of the interior ocean ranges to as high as 15%. High accumulations of ammonia from agricultural and industrial sources are also possible on Earth. In the case of these higher concentration thresholds, the results of this research indicate ammonia could constrain the habitability potential of both Titan's ocean and certain Earth environments. These findings advance the current understanding of bacterial life in ammonia and demonstrate the importance of ammonia concentration when assessing conditions that could support life in extraterrestrial and terrestrial environments.

LAY SUMMARY

We know that, on Earth, all life requires liquid water. Liquid water is an excellent solvent; that is, it has a strong ability to dissolve a range of substances (e.g., salts, sugars, gases). In liquid water, these substances can chemically interact with each other as well as with water itself. Chemical reactions of increasing complexity in liquid water are the basis of how life formed on Earth. The presence of liquid water on extraterrestrial planets is therefore of great interest when conducting missions in the search for life. Moons in our solar system are surprising reservoirs of liquid water. While Earth has a single moon, Jupiter has almost 100 moons, and Saturn has over 250 moons, and some of these moons contain liquid water. Jupiter and Saturn are much further from the Sun, and thus these planets, along with their moons, have surface temperatures below -100 °C. As a result, the moons of these planets have icy surfaces, and are dubbed 'icy moons'.

In 1997, NASA's Cassini-Huygens mission was launched, equipped to study Saturn and its system. While flying by Saturn's moon Enceladus in 2005, proof of what was long thought was finally found: liquid water ejected from the Southern pole. Along with this, gravity measurements and surface features of both Enceladus and the largest of Saturn's moons, Titan, hinted strongly at global liquid water oceans beneath the surface ices. Such reservoirs of liquid water are also expected, and strongly indicated, in Jupiter's moons Europa, Ganymede and Callisto. Thus, these icy moons are prominent targets in the search for life.

Given the freezing point of water is 0 °C, the presence of liquid water with surface temperatures below -100 °C appears paradoxical. However, liquid water could be sustained if the freezing temperature of water is lowered. This can occur with the addition of salt or ammonia. Indeed, ammonia was detected within the liquid water ejected from Enceladus. Ammonia is also believed to be a constituent of the subsurface oceans of Titan, Europa, Ganymede and Callisto. In small amounts, ammonia is a nitrogen source for living organisms. However, in larger amounts, ammonia is toxic. Ammonia increases the pH (i.e., portion of OH^- ions) of solutions and, as a gas, can readily permeate into biological matter. Both of these actions disrupt internal chemical reactions, the ones needed to sustain life. The presence of ammonia within the oceans of icy moons may therefore reduce the suitability of these environments to host life as we know it. The impact of ammonia on life is also relevant to Earth; in terrestrial environments, ammonia is a common pollutant due to use in agricultural fertilizer and industrial processes.

The impact of ammonia on life, particularly bacterial, is not well defined. This thesis therefore seeks to explore how ammonia may impact the natural habitability of icy moons and also how, on Earth, habitability could be impacted by ammonia pollution. I explore this hypothesis with the most simple of lifeforms, a bacteria, *Halomonas meridiana*. Due to its deep-sea origins, *H. meridiana* has shown an ability to survive in extreme cold, saline, and high pH waters that are under pressure. *H. meridiana* therefore serves as an excellent model for assessing the habitability of icy moon oceans, as these environments share similar properties. In this thesis, *H. meridiana* is directly grown in varying concentrations of ammonia-water and at varying distances from an ammonia-water source. Through this, I define the concentration and spatial

limits at which growth and survival are affected by ammonia. I also explore how ammonia exposure affects the internal chemistry and cell structure of *H. meridiana*. These research avenues illuminate the habitability potential of ammonia-water mixtures, and environments in proximity to ammonia-water mixtures.

Through this research, I show that the growth and survival of *H. meridiana* is affected at defined concentrations of ammonia, whether *H. meridiana* is grown directly in ammonia-water or at a distance from an ammonia-water source. Cell structure was altered from exposure to ammonia as well as internal chemistry. The changes to cell structure indicated significant internal damage. Changes to internal chemistry also indicated the formation of large and potentially disruptive compounds, and disturbance to chemistries that are essential to life, such as the basic processing of nitrogen, carbon, and energy. However, internal chemistry also indicated potential survival strategies that included restructuring of the outer shell of the cell, possibly to counteract ammonia permeation. By comparing growth of *H. meridiana* in ammonia to growth in high pH solutions without ammonia, toxicity of ammonia was found to be distinct from an external rise in pH, further confirming internal disturbance by ammonia as the cause of toxicity.

The defined concentrations of ammonia identified as affecting growth and survival are above those estimated in the oceans of icy moons Enceladus and Europa. This indicates the presence of ammonia may not limit the potential for habitability in these oceans or water networks in the overlying ice shell. However, the defined concentrations are generally below those estimated for Titan, and could be above those found in polluted environments on Earth. Thus, the concentrations of ammonia found in these environments may preclude the growth and survival of life similar to *H. meridiana*, and may alter the internal and external features as described. Taken together, these results confirm ammonia-water mixtures can alter habitability potential in a concentration-dependent manner, and must be considered on a case-by-case basis when assessing the habitability of extraterrestrial and Earth environments.

DECLARATION

I declare that this thesis has been composed by myself and that the work has not been submitted for any other degree or professional qualification. I confirm that the work submitted is my own, except where work which has formed part of jointly-authored publications has been included. My contribution and those of the other authors to this work have been explicitly indicated below. I confirm that appropriate credit has been given within this thesis where reference has been made to the work of others.

Publications in Chapter 4 and 6 appeared respectively in *Scientific Reports* and *Frontiers in Microbiology* by Cassie M. Hopton, Peter Nienow and Charles S. Cockell. I, Cassie M. Hopton, was involved in the conceptualization of the studies, methodology, validation, formal analysis, investigation, data curation, data visualization, and writing of the original drafts. Peter Nienow conducted review and edits of the original drafts as well as project supervision. Charles S. Cockell provided research conceptualization, methodology, supervision, project administration, funding acquisition and review

M. Hopton, September 2025

ACKNOWLEDGEMENTS

The work in this thesis would have not been possible without the generous support and guidance provided to me. Firstly, I am grateful to the Natural Environment Research Council (NERC) E4 Doctoral Training Partnership (DTP) for granting me the opportunity to pursue a PhD at the University of Edinburgh. The NERC E4 DTP funded not only this research, but also contributed towards the costs essential for my participation in the JPL Visiting Student Research Program at NASA's Jet Propulsion Laboratory.

Most earnestly, I would like to express gratitude to my supervisor Charles S. Cockell. I initially encountered Charles's work as a first-year undergraduate studying BSc Biochemistry at the University of Bristol. While watching the documentary television series *Cosmos*, I was inspired to find out how my developing knowledge in biochemistry could intersect with space studies. A quick search immediately led me to the UK Centre for Astrobiology, my first introduction to the field of astrobiology. Here, I was enthralled by Charles's research and was surprised to learn that he, too, had studied BSc Biochemistry at the University of Bristol. It was by chance and luck that Charles not only had a PhD opening coinciding with the end of my master's degree, but for a project which was directly linked with my skill set and interests. During my PhD, Charles guided and inspired me with his knowledge, enthusiasm, and creative ideas but afforded me the trust and independence to pursue my research in my own direction. Being part of the UK Centre for Astrobiology has been an invaluable experience. I feel honoured to have been mentored by Charles who is a leader in the field of astrobiology and an expert in extreme microbiology.

My extended supervision team of Peter Nienow, Simon Titmuss and Aidan Brown also deserve my thanks. Each individual provided crucial guidance that shaped my research and deepened my scientific thinking, for which I am profoundly appreciative. I would also like to thank Tessa Moses of EdinOmics and Steve Mitchell of the School of Biological Sciences whom provided essential assistance with the complexities of metabolomics and transmission electron microscopy, respectively. I am deeply grateful to the experience and skills they imparted that were essential for the completion of this project.

The support of the wider team at the UK Centre for Astrobiology has also been vital to this work. From assistance in the lab to troubleshooting unexpected results to simply brightening Monday lab meetings with sweet treats, my past and present colleagues have contributed in countless ways to every stage of this project. Their knowledge, experience, and kindness has helped me become a better scientist and collaborator.

It is not without mention that my family deserve a special thanks. I owe immense gratitude to my Mum and Dad whose unwavering support throughout my almost decade-long educational journey has allowed me to pursue my interests and face challenges with confidence. My parents, grandparents and family as a whole have never hesitated in encouraging my aspirations and were a constant source of comfort. A special mention to Naomi who always provided a source of laughter when it was needed, and Tess who ensured I took regular writing breaks.

Finally I would like to thank my partner, Cameron. He uprooted his life in London to accompany me in Edinburgh. In the face of experiments gone wrong or an overwhelming workload, Cameron provided a source of strength through his calm and reassuring presence. Without him, the challenges I faced would have been even greater, and I would not have had Desmond, who provided companionship during the solitary days of data analysis and thesis writing.

Contents

List of Figures

List of Tables

1

Introduction

Since the turn of the century, the search for habitable environments beyond Earth has expanded to include the icy moons of Jupiter and Saturn. Lying beyond the habitable zone, the extreme distances of these moons from solar radiation has driven the formation of substantial ice surfaces. Observations by Voyager 1 and 2 in the 1980's provided tentative indications of active cryovolcanism on Jupiter's moon Europa and Saturn's moon Enceladus (Smith et al., 1979, 1982). In 1998, data from the Galileo spacecraft provided strong evidence for a subsurface liquid, saline ocean beneath the ice crust of Europa, providing compelling evidence for liquid water and, therefore, potentially habitable conditions beyond the traditional habitable zone (Khurana et al., 1998, Rathbun et al., 1998, Carr et al., 1998, Pappalardo et al., 1998). However, it was not until the Cassini-Huygens mission arrived at Saturn in 2004 that our understanding of icy moons was redefined. Once thought geologically inert, Cassini revealed plumes of liquid water expelled from the Southern pole of Enceladus and provided substantial evidence for a global subsurface ocean beneath the ice crust of both Enceladus and Titan (Porco et al., 2006, Lorenz et al., 2008, Waite et al., 2009, Bills and Nimmo, 2011). Since these landmark discoveries, icy moons have been labelled "ocean worlds" and are prime candidates in the search for life.

Without solar heat, the preservation of a liquid layer in these moons has been hypothesised from tidal heating or the presence of freezing point depressants such as salt or ammonia. Ammonia-water mixtures can lower the freezing point of water to as low as -100 °C (Johnson and Nicol, 1987, Croft et al., 1988, Leliwa-Kopystyński et al., 2002, Chua et al., 2023). Indeed, Cassini detected ammonia in the plumes of Enceladus. Methane and ^{40}Ar in the atmosphere of Titan are also consistent with models of an ammonia-water ocean (Waite et al., 2009). On Earth, ammonia has been implicated in facilitating prebiotic chemistry (Wigley and Brimblecombe, 1981, Martin et al., 2008, Sojo et al., 2016, Nishizawa et al., 2021), and in modern systems plays an integral role in the global nitrogen cycle and the synthesis of nucleic

acids and amino acids (Fowler et al., 2013). Ammonia is also a constituent of agricultural fertilizers (Tyagi et al., 2022), and a common pollutant in the environment due to discharge from agricultural lands as well as industrial processes (Matthews et al., 2000, Guthrie et al., 2016, Powlson and Dawson, 2022).

High concentrations of ammonia have been shown toxic across the domains of life (Eno et al., 1955, Thurston et al., 1981, Leejeerajumnean et al., 2000, Hachiya et al., 2021). Ammonia can exist in two molecular forms: a weak base, unionized ammonia (NH_3), and a weak acid, ionized ammonium ion (NH_4^+), with the position of equilibrium between the two species dictated primarily by pH. While NH_4^+ can disrupt ionic balance, the permeation of this species is regulated by membrane transporters (Moser, 1987, Wacker et al., 2014). NH_3 is a proton (H^+) acceptor, and has properties (e.g., small size, uncharged) which facilitate passive permeation through biological membranes. As a result, NH_3 readily reacts with H^+ to raise both extracellular and intracellular pH, disrupt the proton motive force and form NH_4^+ intracellularly (Rose et al., 2005, Bosoi and Rose, 2009, Angelova et al., 2022). High concentrations of intracellular NH_4^+ can disrupt membrane potential, ionic balance and metabolism (Wang et al., 2018, Shi et al., 2020, Xiao et al., 2019). NH_3 therefore has the potential to significantly disrupt the physicochemical environment and biochemistry within living organisms and may limit the habitability potential of icy moon oceans, as well as polluted Earth environments, if present at sufficient concentrations.

The current physicochemical models of Enceladus and Titan estimate high pH oceans ($>$ pH 10) whereby ammonia would be expected in the NH_3 form (Brassé et al., 2017, Leitner and Lunine, 2019, Glein and Truong, 2025). NH_4^+ would be expected to predominate in the more acidic ocean of Europa ($<$ pH 8.4) (Johnson et al., 2019). In considerations of potential life on icy moons, simple cellular organisms, such as prokaryotes, are frequently regarded as plausible candidates. Ammonia toxicity has been established for a select few prokaryotes. But, there has been limited research indicating thresholds for survival and physiological changes in ammonia, particularly in solutions of high NH_3. There has been no research utilising extremophilic prokaryotes that have physiologies analogous to the physical and chemical conditions on icy moons. These research avenues could provide indications as to whether the presence of ammonia in the oceans of icy moons could constrain the potential for habitability.

1.1 Thesis scope and objectives

The notion of ammonia as a chemical parameter that could influence habitability on icy moons has been seldom explored by proof-of-concept experiments in literature, but has been hypothesised. A selection of experiments show survival thresholds in ammonia, but do so in solutions where the relative abundance of NH_4^+ to NH_3 is high, or with organisms that do not have relevance to astrobiology. The core objective of this thesis was to develop an understanding of ammonia as a habitability factor on icy moons Enceladus, Titan and Europa. For this, an extremophile bacteria and solutions with both a high relative abundance of NH_3 and a high relative abundance of NH_4^+ were utilised to address three primary questions:

(**a**) What are the limits of life and physiological changes for an extremophile in aqueous ammonia with high proportions of NH_3?

(**b**) How does the atmospheric dispersal of NH_3 gas impact growth and viability in nearby habitats?

(**c**) What are the limits of life and physiological changes for an extremophile in aqueous ammonium sulphate ($(NH_4)_2SO_4$) with high proportions of NH_4^+?

1.2 Thesis outline

The thesis is divided into seven chapters including this introductory chapter. Chapter 2 presents a thorough synthesis of the relevant background information to the thesis, including current knowledge regarding the properties of ammonia, ammonia content on icy moons, the function of ammonia in prebiotic and biotic systems, the known inhibitory concentrations and physiological effects of ammonia in bacteria, and finally the habitability implications of ammonia. The protocols and justification for experimental methods common to multiple chapters are outlined in Chapter 3. Specific methodologies and protocols are outlined in each individual research chapter.

The research results of this thesis are presented in Chapter 4, Chapter 5, and Chapter 6. All research chapters utilise the extremophile *Halomonas meridiana* Slthf1. Chapter 4 addresses question **(a)** by identifying the survival thresholds in ammonia, changes to growth dynamics, growth kinetics, ultrastructural morphology and metabolism in *H. meridiana* upon exposure to aqueous ammonia solutions of high pH. Chapter 5 details the spatial impact of NH_3 gas on surrounding cultures of *H. meridiana*, directly comparing growth and viability to direct aqueous ammonia exposure, and the temporal recovery of *H. meridiana* growth following NH_3 dispersal. This addresses **(b)**. Finally, **(c)** is pursued by exploring the concentration thresholds for growth, alterations to growth kinetics, and the morphological and metabolomic response of *H. meridiana* in aqueous $(NH_4)_2SO_4$ solutions.

The conclusion to this thesis is presented in Chapter 7. This includes a synopsis of the main findings and implications for the habitability of icy moons and Earth. Limitations of the thesis as well as important future research avenues are highlighted.

2

Background

Contents

2.1 Icy ocean worlds

The concept of life beyond Earth has been the subject of both philosophical and scientific interest for two millennia. As early as the 6th century BCE, Greek philosopher Anaximander speculated of multiple worlds which may harbour extraterrestrial life, and a water origin of human life on Earth (Rovelli, 2023). This early curiosity evolved with scientific discovery; in the 17th century, four moons of Jupiter (Io, Europa, Ganymede and Callisto) were discovered

by Galileo and subsequently dubbed the "Galilean moons" (Soderblom, 1980). This discovery expanded the known celestial bodies in the Solar System. The role of water in the emergence of life became evident in the 20th century; in the 1950s, Stanley Miller and Harold Urey demonstrated that amino acids could form from a mixture of ammonia, methane, hydrogen, and water (Miller, 1955). This experiment provided evidence for the theory of abiogenesis, a "primordial soup" origin of life hypothesis whereby a mixture of inorganic compounds in water gave rise to living organisms.

To much controversy, water-bearing minerals were detected almost two decades later in lunar samples returned by Apollo 11 (Goles, 1971, Levinson and Taylor, 1971). This was the first physical evidence of water beyond Earth. Further indication of liquid water beyond Earth was established by the Galileo spacecraft. The Galileo mission provided evidence for a subsurface ocean of liquid water below the thick ice crust of one of Galileo's moons, Europa (Anderson et al., 1998, Greeley et al., 1998), a prospect previously indicated by Voyager 1 and Voyager 2 in 1977 (Smith et al., 1979). At the turn of the 21st century, the National Aeronautics and Space Administration (NASA) introduced a new scientific approach as part of the Mars Exploration Program: "follow the water" (Hubbard et al., 2002). While designed initially to discover records of biological processes on Mars, in 2005 the Cassini-Huygens mission revealed plumes of water vapour and ice erupting from Saturn's moon Enceladus (Waite et al., 2006). Strong evidence for subsurface oceans of liquid water encased below surface ice have since been established not only on Europa and Enceladus (Tobie et al., 2008, Roberts and Nimmo, 2008), but Saturn's largest moon Titan (Tobie et al., 2005, Bills and Nimmo, 2011, Baland et al., 2011), and the other Galilean moons of Jupiter: Ganymede (Showman et al., 2004, Saur et al., 2015) and Callisto (Zimmer et al., 2000, Cochrane et al., 2025).

Since these discoveries, "follow the water" has expanded to include the icy moons of Jupiter and Saturn, which have emerged as compelling targets in the search for life beyond Earth.

2.1.1 Ammoniacal waters

Ammonia is a primordial molecule. It is found in celestial bodies across the universe, including stars (Schmidt et al., 2011, Wong et al., 2018), planets (Henderson-Sellers and Schwartz, 1980, Moeckel et al., 2023, Cleland and Rimmer, 2022, Irwin et al., 2025), moons (Waite et al., 2009, Nelson et al., 2009, Holler et al., 2017), comets (Wyckoff et al., 1989, Feldman et al., 1993, Poch et al., 2020), asteroids (Pizzarello et al., 2011, Glavin et al., 2025), galaxies (Ao et al., 2011, Mills and Morris, 2013), and interstellar mediums (Cheung et al., 1968, Doherty et al., 2022).

In ocean worlds, ammonia has been detected (Waite et al., 2006, 2009, 2017) or otherwise hypothesised to form a constituent of the interior oceans (Khurana et al., 1998, Mousis et al., 2002, Tobie et al., 2012, Sohl et al., 2014, Vance et al., 2018, Leitner and Lunine, 2019, Spohn and Schubert, 2003, Ramkissoon et al., 2025). In the near vacuum pressures of space, ammonia is primarily solid ice as temperatures are below the sublimation point (-73 °C), the temperature at which ammonia transitions directly from solid ice to gas (Glasser, 2009). Ammonia ice can be trapped during accretion of cold bodies such as icy moons. Internal heating from radioactive decay or tidal forces can later release ammonia as a gas as interiors

warm and subsurface oceans form (Spohn and Schubert, 2003, Tobie et al., 2012, Vance et al., 2018). As a gas, ammonia readily dissolves in water (Hales and Drewes, 1979, Dasgupta and Dong, 1986, Simonelli et al., 1998). The resulting ammoniacal waters, a mixture of ammonia-water, can have a freezing point as low as -100 °C. Dissolution of ammonia in water interferes with water-water hydrogen bonding, thus acting to lower the freezing point. This antifreeze behaviour has led to the speculation that ammonia-water may maintain subsurface liquid oceans in icy moons, despite cold surface temperatures (Johnson and Nicol, 1987, Croft et al., 1988, Leliwa-Kopystyński et al., 2002, Chua et al., 2023).

As a H^+ acceptor, the dissolution of ammonia into water protonates unionized ammonia (NH_3), a weak base, to give rise to ammonium ion (NH_4^+) and hydroxide ions (OH^-):

$$NH_3 + H_2O \rightleftharpoons NH_4^+ + OH^-$$

The position of equilibrium between NH_3 and NH_4^+ is dictated primarily by pH as per the Henderson-Hasselbalch equation, where acidic pH promotes the formation of NH_4^+ and high pH promotes the formation of NH_3. However, the speciation of ammonia is also influenced by salinity, temperature, and pressure. In aqueous geochemical systems, the effect of salinity on ammonia speciation is often described in terms of ionic strength. In the context of this thesis, ionic strength is estimated using stoichiometric ionic strength, calculated directly from the analytical concentrations of dissolved salts. Higher salinity, colder temperatures, and higher pressures increase the negative log of the acid dissociation constant, the pK_a, of the $NH_3 \rightleftharpoons NH_4$ system, and thus the protonation of NH_3 (forming NH_4^+). Lower salinity, warmer temperatures, and lower pressure exert the opposite effect (Neuhausen and Patrick, 1921, Emerson et al., 1975, Hales and Drewes, 1979, Dasgupta and Dong, 1986). Thus, the speciation of ammonia in icy moon interiors is dictated by these physicochemical parameters (Figure 2.1).

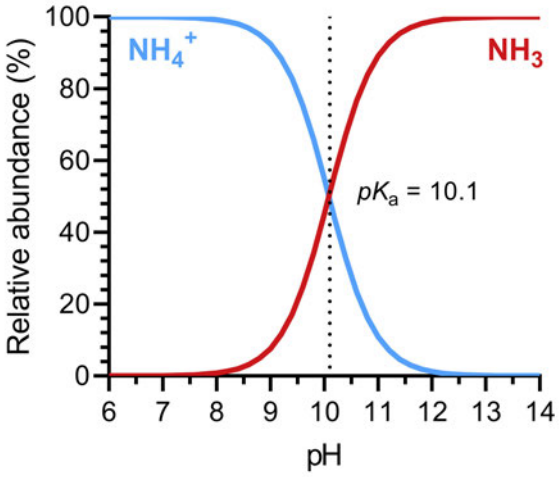

Figure 2.1: Abundance of NH_3/NH_4^+ as a function of pH. The pK_a of the $NH_3 \rightleftharpoons NH_4^+$ system was calculated based upon an ionic strength of 0.3 M, a temperature of 0 °C and 1 bar pressure (refer to section 3.5). Pressure may vary, but these ionic strengths and temperatures are parameters expected within the ocean of Enceladus (Glein and Truong, 2025). A pK_a of 10.1 was calculated, indicated by a dotted line from the x-axis.

When considering ammonia salts, speciation may likewise vary by pH, temperature, and salinity. For example, while aqueous ammonium sulphate ($(NH_4)_2SO_4$) does not remain intact as $(NH_4)_2SO_4$ molecules, but dissociates to form hydrated ions (NH_4^+ and SO_4^{2-}), the

precise aqueous speciation may nevertheless vary with physicochemical conditions. Lower pH can promote partial protonation of SO_4^{2-} to hydrogen sulfate ion (HSO_4^-) (Vielma and Hefter, 2022), while increasing salinity or ionic strength can alter ion activities and favour ion pairing, where weak and transient electrostatic interactions would occur between NH_4^+ and SO_4^{2-} (Raeispour Shirazi et al., 2025). These effects can slightly alter the relative abundances and activities of aqueous species, although NH_4^+ and SO_4^{2-} may remain the dominant ions across most conditions. Temperature may also influence $(NH_4)_2SO_4$ solutions through several mechanisms. For example, the solubility of $(NH_4)_2SO_4$ is known to increase at elevated temperatures (Mullin et al., 1970). With rising temperature, the pK_a of HSO_4^- and NH_4^+ would also decrease (Young et al., 1978, Emerson et al., 1975), favouring SO_4^{2-} at higher temperatures and the formation of NH_3 if the pH of the aqueous system was suitable. Thus, while NH_4^+ and SO_4^{2-} are considered the dominant aqueous species in this thesis, the effective chemical environment may vary with pH, temperature, salinity, and pressure.

In addition to speciation, temperature and pressure can also alter the phase behaviour of ammonia. On icy moons, gravitational forces combined with the substantial thickness of the ice shell—in the order of several to hundreds of kilometres—generate pressures tens to thousands of bar on the subsurface oceans (Billings and Kattenhorn, 2005, Nimmo and Bills, 2010, Baland et al., 2014, Čadek et al., 2016, Lucchetti et al., 2017, Vance et al., 2018, Levin et al., 2026). In mixtures of ammonia-water, the boiling point would remain above 0 °C, and may only be depressed by a few degrees from the standard boiling point of water (100 °C) when mixed with low concentrations, i.e., 1% ammonia. Pressure only increases the boiling point (Clifford and Hunter, 1933). The freezing point is also altered by pressure. At 1000 bar pressure, the freezing point of ammonia-water with a concentration of 1% ammonia by weight is approximately -9 °C, slightly colder than the freezing point at 1 bar (-3 °C) (Figure 2.2). At 3000 bar, the freezing point temperature decreases substantially to approximately -33 °C, and so on (Leliwa-Kopystyński et al., 2002).

Current models estimate the oceanic temperature of icy moons to range from -50 °C to near zero (Kargel et al., 2000, Marion et al., 2003, Melosh et al., 2004, Matson et al., 2012, Sohl et al., 2014, Glein et al., 2015). Given these conditions, ammonia would most likely exist in the liquid phase within icy moon oceans, with warmer regions exhibiting ammonia gas and some colder regions possibly exhibiting ammonia ice depending on the temperature and pressure of the region. If permitted by sub-zero temperatures (e.g., less than -98 °C) ammonia-water may also form solid, crystalline ammonia hydrate structures (Figure 2.2) (Hogenboom et al., 1997, Muñoz-Iglesias and Prieto-Ballesteros, 2021).

In the following sections, the ammonia composition and speciation in icy moons is discussed. Unionized ammonia and ammonium ion are denoted as NH_3 and NH_4^+, respectively. Henceforth, the term 'ammonia' refers collectively to the total concentration of both NH_3 and NH_4^+ in an aqueous environment.

2.1.2 Enceladus: plumes of ammonia

In the 1980's, Voyager 2 investigated the 6th largest moon of Saturn, Enceladus (Figure 2.3A). This investigation revealed a geologically young surface, and co-occurrence of the densest

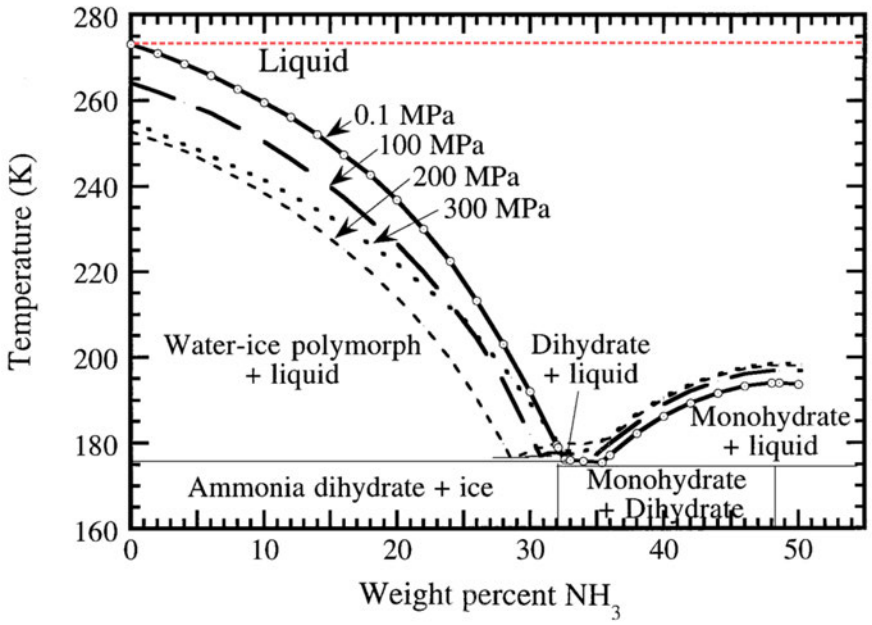

Figure 2.2: Phase diagram of ammonia-water mixtures. Phase behaviour against the concentration-temperature plane depicted. Influence of pressures at 0.1 MPa (1 bar), 100 MPa (1000 bar), 200 MPa (2000 bar), and 300 MPa (3000 bar) on phase behaviour is shown. The ammonia-water solidus at 176.16 K is illustrated with a solid line. A red dashed line has been superimposed on the figure to highlight phase behaviour at a temperature of 273.15 K (0 °C). Figure adapted from Hogenboom et al. (1997) with permission from Elsevier.

region of Saturn's E ring with Enceladus' orbit, possible evidence of eruptive activity (Smith et al., 1982). Over two decades later, ground-breaking revelations were made from Cassini. Multiple flybys of Enceladus revealed jets of icy particles erupting from 130 km long fractures in the Southern pole, the "tiger stripes", and confirmed deposition of particles into Saturn's E ring (Spitale and Porco, 2007, Porco et al., 2006). Analysis of the plumes by two mass spectrometers onboard Cassini, the Ion and Neutral Mass Spectrometer (INMS) and Cosmic Dust Analyzer (CDA), elucidated the presence of water vapour, ice particles, simple organics (e.g., benzene), complex macromolecular organics, and gases such as deuterium, hydrogen, carbon dioxide, carbon monoxide, methane, and NH_3 (Waite et al., 2006, 2009, 2017, Postberg et al., 2018).

The discoveries made by Cassini reshaped Enceladus into a prime candidate for astrobiology and further exploration. In particular, the discovery of vapour and NH_3 on Enceladus posed an enthralling question as to whether there could be liquid water beneath the ice crust. As aforementioned, ammoniacal solutions can remain liquid as low as -100 °C, depending on the concentration of NH_3 (Johnson and Nicol, 1987, Croft et al., 1988, Leliwa-Kopystyński et al., 2002, Chua et al., 2023). The detection of NH_3 by Cassini therefore provided strong indirect evidence for the existence of subsurface liquid water on Enceladus (Waite et al., 2009). Further evidence for a liquid subsurface reservoir was gleaned by the presence of ^{40}Ar in the plume. Originally in reference to Titan, Engel et al. (1994) suggested that a water ocean

preserved in the liquid state by NH_3 could dissolve sodium and potassium from silicate rock into fluid, leading to eventual decay of potassium-40 into ^{40}Ar that could later surface into the atmosphere by cryovolcanism. The detection of ^{40}Ar therefore provided further indications of an ocean with active chemical exchange with its rocky core. This was only supplemented by the detection of sodium-rich salts, such as sodium chloride (NaCl) and sodium bicarbonate ($NaHCO_3$), in Saturn's E ring and freshly ejected plume particles. Such salts can only arise from a liquid water origin (Postberg et al., 2009, 2011).

Cassini's INMS data supported an observed mixing ratio of NH_3 in the plumes of Enceladus between 0.4 to 1.3%, with variability reflecting compositional variability in the plumes (Waite et al., 2006, 2009, 2017). The ratio aligns well with NH_3-to-water ratios observed in comets between 0.01 to 1.5% (Wyckoff et al., 1989, Palmer et al., 1996, Meier et al., 1994), supporting the theory of primordial incorporation of solid NH_3 into Enceladus during accretion. Mass spectra from the CDA analysed by Khawaja et al. (2019) subsequently indicated spectral features consistent with NH_4^+ in the ejected ice grains, further supporting the notion of a subsurface ocean with dissolved ammonia. Incorporating the NH_3 data reported by Waite et al. (2017), Fifer et al. (2022) derived a bulk molecular abundance of ammonia in the Enceladus ocean between 0.011 to 0.169%, approximating to an oceanic concentration of ammonia between ≈0.01 to 0.1 M. This corresponds to 0.001 to 0.006% NH_3 and 0.01 to 0.163% NH_4^+ in an ocean between pH 7.95 to 9.05 (Fifer et al., 2022). Fifer et al. (2022) reason that the NH_3 plume composition does not directly reflect oceanic NH_3 concentration; volatile gases such as NH_3 likely undergo exsolution from the liquid phase during plume formation, depleting ammonia concentrations in the plume compared to the ocean.

However, the estimations of ammonia in the ocean of Enceladus are evolving with new data. Following the study by Fifer et al. (2022), Postberg et al. (2023) revealed the discovery of phosphate-rich grains in plume ejecta, with species of Na_2HPO_4 and Na_3PO_4 reproducing the peak pattern of the CDA spectra most accurately. Phosphorous in ionic forms of HPO_4^{2-} and PO_4^{3-} occur at pH values between 7 and 12 and greater than 12, respectively. Thus, the presence of these phosphate species constrain the ocean from pH 10.1 to 11.6 according to recent geochemical modelling (Glein and Truong, 2025). Reconstruction of the ocean chemistry by Glein and Truong (2025) place concentrations of NH_3 at 0.0181 molal (≈0.0181 M) (Glein and Truong, 2025). These concentrations are low; thermodynamic modelling of ammonia-water mixtures indicate such concentrations would not be sufficient to sustain liquid water if the ocean temperature was found to be below sub-zero (Croft et al., 1988, Kargel, 1992, Hogenboom et al., 1997).

The ocean of Enceladus is placed at 0 °C (Glein et al., 2015, Matson et al., 2012). At near 0 °C, the pK_a for the reaction $NH_3 \rightleftharpoons NH_4^+$ is approximately 10.1 (Bates and Pinching, 1949). Thus, as per the Henderson-Hasselbalch equation and current pH estimations, the ocean would indeed bear ammonia predominately as NH_3 (Figure 2.3B). However, at the concentrations estimated, it is unlikely NH_3 contributes significantly to the maintenance of liquid water. NH_3 may facilitate the liquid state in colder regions of the ocean where the temperature may fall slightly below 0 °C, but NH_3 is not the primary source of antifreeze behaviour. Indeed, internal heat generated by tidal heating is thought to be the primary driver of liquid state preservation (Nimmo et al., 2007, Roberts and Nimmo, 2008, Chen et al., 2014).

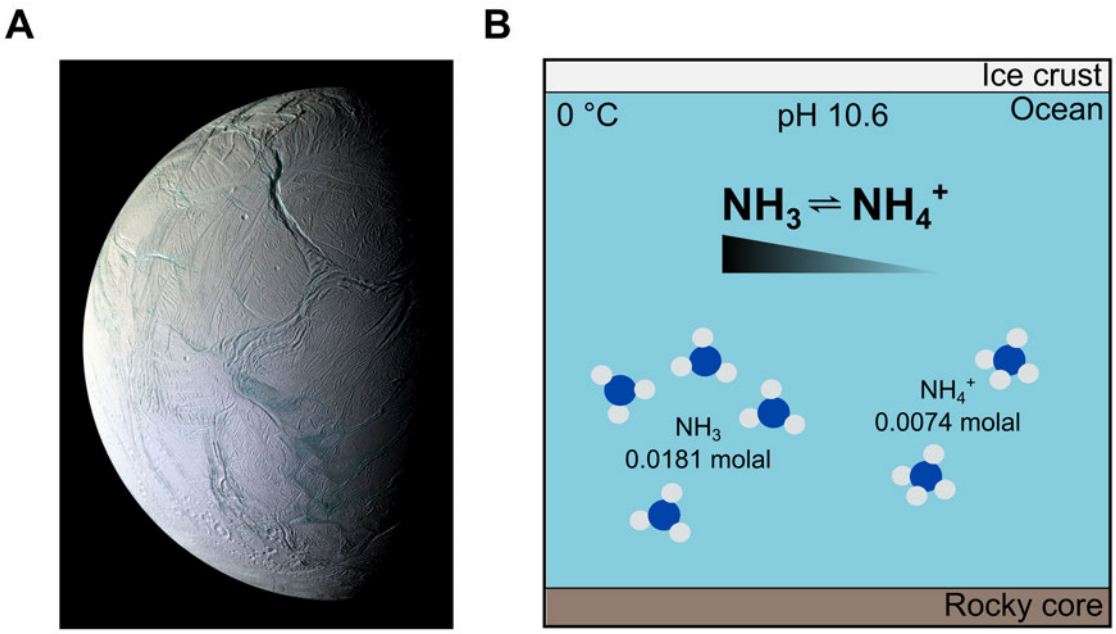

Figure 2.3: Aqueous ammonia within Enceladus. (A) Surface of Enceladus captured by the Cassini Imaging Science Subsystem. Portions of the tiger stripe fractures from which plumes of water emanate are visible along the lower right, surrounded by a circumpolar belt of mountains. Image credits: NASA/JPL/Space Science Institute. (B) Subsurface ocean ammonia concentration determined by Glein and Truong (2025), and speciation speculated as part of this chapter based upon estimated physicochemical characteristics of the ocean.

2.1.3 An ammonia reservoir on Titan

Until Cassini, the surface of Saturn's largest moon, Titan (Figure 2.4A), was shrouded in uncertainties as dense atmosphere concealed the surface. Earth observations indicated a dense atmosphere consisting of methane (Kuiper, 1944). The atmosphere, denser than that of Earth's, was unlike that observed on any other known moon. This motivated inspection by the Voyager 1 spacecraft in 1980 (Coustenis, 2014).

The discoveries made by Voyager 1 revealed a thick nitrogen-methane atmosphere with hydrocarbons and a surface entirely concealed by haze (Smith et al., 1982). But in 2005, close flyby's of the surface by Cassini unveiled what was long hidden; a hydrologic-like cycle with methane and ethane, resulting in liquid hydrocarbon clouds, rivers, lakes and seas, and methane rainfalls (Stofan et al., 2007, Turtle et al., 2009, Poggiali et al., 2024), as well as a dynamic surface decorated with drainage networks, fluvial channels (Hörst, 2017), mountains (Radebaugh et al., 2007) and possible cryovolcanoes (Lopes et al., 2007, Hörst, 2017). The mission also provided evidence of a subsurface ocean below the ice crust (Lorenz et al., 2008, Bills and Nimmo, 2011).

A subsurface ocean on Titan had been proposed long before Cassini. The persistence of methane in the atmosphere of Titan, despite continual elimination by photochemical processes,

suggested the presence of an internal replenishment mechanism. Lunine and Stevenson (1987) proposed that Titan harboured a subsurface water ocean maintained in the liquid state by the antifreeze properties of NH_3. In this model, methane retained during Titan's accretion was thought to be stored in clathrate hydrates (i.e., crystalline solids where water molecules form cages that trap gas molecules) and periodically released to the surface by cryovolcanic eruptions (Lunine and Stevenson, 1987). The pH of Titan's ocean remains undetermined, but is modelled at greater than pH 7.3 (Marion et al., 2012, Brassé et al., 2017, Leitner and Lunine, 2019). In an ocean of 5% NH_3, a pH of 11.83 is expected (Brassé et al., 2017). Lower temperatures increase pK_a (Zahn, 2017b,a, Samuelsen et al., 2019). Titan's ocean could be -18 °C (Sohl et al., 2014). Thus, the ocean would likely bear considerable quantities of ammonia as NH_3.

Engel et al. (1994) considered an ocean of up to 15% NH_3 based upon thermochemical models of the Saturnian nebula. Indeed, cosmochemical models indicate that Titan accreted with solar volatiles, and may have incorporated significant levels of NH_3 into its interior (Mousis et al., 2009). The discovery of NH_3 on Enceladus by Cassini circumstantially supported the presence of NH_3 on Titan (Waite et al., 2009). As on Enceladus, further indirect evidence of liquid water in contact with the silicate core in Titan's history was provided by the detection of ^{40}Ar in the atmosphere (Niemann et al., 2005). An aqueous NH_3 subsurface ocean on Titan could be a plausible source of atmospheric nitrogen (Owen, 2000). Indeed, cryovolcanic flows observed by the Cassini Titan Radar Mapper exhibited rheological properties consistent with aqueous NH_3, and possibly methanol, slurries (Lopes et al., 2007, Mitri et al., 2008). However, recent models place the abundance of NH_3 at 1.5 to 5%; a lower NH_3 concentration fits the observed bulk density of Titan (Vance et al., 2018, Tobie et al., 2012), thermal profiles and mechanical behaviour of the ice shell (Sohl et al., 2014) and the tidal deformation data provided by Cassini (Leitner and Lunine, 2019). In addition to NH_3, radiogenic heating may support the liquid state in Titan's ocean (Grasset et al., 2000, Sohl et al., 2014).

In an ocean of 1.5 to 15% NH_3, and an ocean density of 1,091 g/L (Goossens et al., 2024), a molar concentration of NH_3 can be calculated between 0.96 to 9.6 M as per Eq. 2.1, where ρ is the oceanic density at 1,091 g/L (Goossens et al., 2024), $\%NH_3$ is 1.5 to 15% NH_3, and the molar mass of ammonia is 17.031 g/mol.

$$M = \frac{\rho \times \%NH_3}{Molar\ mass} \tag{2.1}$$

The presence of aqueous NH_3 is largely accepted when modelling Titan's interior (Grasset and Sotin, 1996, Grasset et al., 2000, Tobie et al., 2005), and found probable by Cassini's gravitational data (Goossens et al., 2024). An aqueous NH_3 ocean is depicted in Figure 2.2B. However, it is geochemically plausible that NH_3 dissolved in aqueous solution would react with internal silicates to yield ammonium salts (Kargel, 1992, Marion et al., 2012). An ocean of aqueous $(NH_4)_2SO_4$ is thermodynamically more stable than a NH_3 and water ocean. An aqueous $(NH_4)_2SO_4$ ocean also has a density that may create a Rayleigh–Taylor instability within the ice crust that leads to the rise of buoyant diapirs, a possible mechanism of cryovolcanism (Fortes et al., 2007, Grindrod et al., 2008). The presence of $(NH_4)_2SO_4$ would indicate an oceanic pH less than 10.1 (pK_a at 0 °C) which does not align with current estimations. However, salinity and pressure can increase pK_a (Clegg and Whitfield, 1995, Samuelsen et al.,

2019), and thus the pH required for the $NH_4^+ \rightarrow NH_3$ transition may become higher. This would support the persistence of NH_4^+ despite the high pH of the ocean (Figure 2.4B). Indeed, a pressure of 8,000 bar is estimated at the seafloor (Journaux et al., 2020).

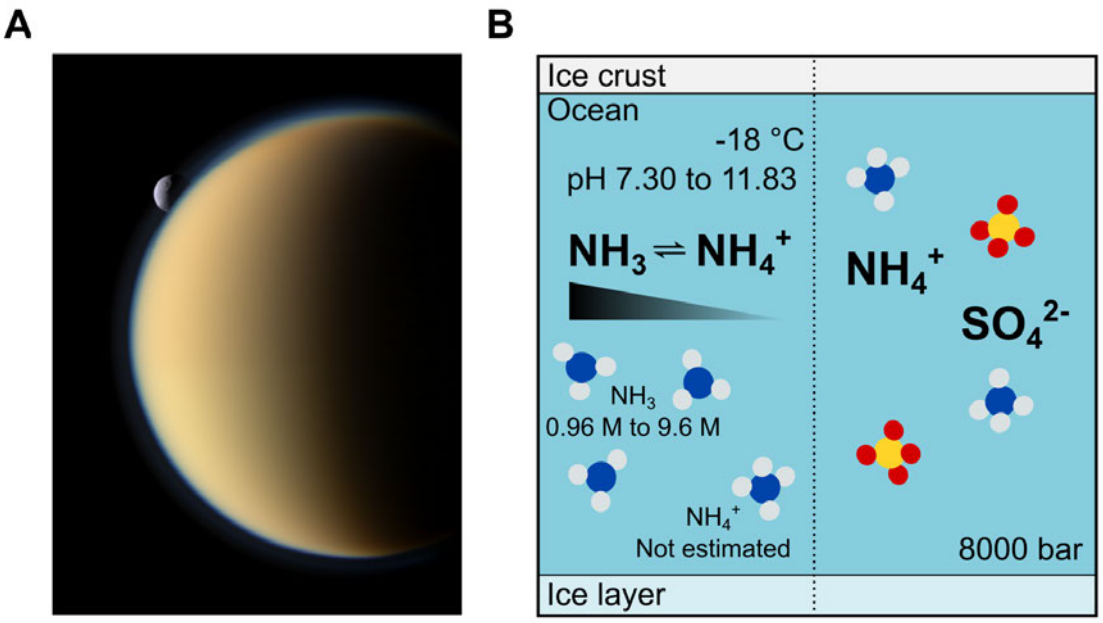

Figure 2.4: Titan as an abode of ammonia. (A) Titan captured by the Cassini Imaging Science Subsystem. The thick atmosphere of Titan is visible by a haze across the surface and lack of surface details. Saturn's other moon, Tethys, is observed behind Titan. Image credits: NASA/JPL-Caltech/Space Science Institute. (B) The possible ammonia chemistries of Titan. The subsurface ocean could be comprised of 1.5 to 15% ammonia, calculated at a molarity of 0.96 to 9.6 M (left-hand pane). Alternatively, the ocean may bear considerable ammonia in the form of ammonium sulphate ($(NH_4)_2SO_4$) (right-hand pane).

Freezing point depression can also be achieved without NH_3. The liquid state of Titan's ocean could be preserved by a high concentration of salts (Mitri et al., 2014). The possibility of a magnesium sulphate ($MgSO_4$) ocean has been considered and models of a $MgSO_4$ ocean align well with Titan's density (Vance and Brown, 2013, Mitri et al., 2014, Vance et al., 2018). Indeed, accretion with $MgSO_4$ is plausible as C1 and C2 carbonaceous chondrites contain up to 10% $MgSO_4$ (Fredriksson and Kerridge, 1988). However, the atmosphere and surface of Titan exhibit reducing conditions. In addition to methane, a suite of reduced organic molecules are present in the atmosphere (e.g., ethane, acetylene, tholins) and there is a lack of oxidants, such as oxygen (Maguire et al., 1981, Kunde et al., 1981, Sagan et al., 1992, Niemann et al., 2005, Nixon, 2024). Sulphur salts form from oxidation reactions, and thus the redox state of Titan favours NH_3. Surface analysis by NASA's mission Dragonfly may provide clarifications into the subsurface ocean composition (Lorenz et al., 2018, Barnes et al., 2021).

2.1.4 Europa's subsurface ocean

Jupiter's moon Europa was first observed by Galileo in 1610 (Soderblom, 1980). Later, high-resolution images of Europa's surface by Voyager 1 and 2 revealed a smooth terrain minimally impacted by craters and intersected by a network of fractures and ridges (Figure 2.5A) (Smith et al., 1979). These morphological features led to the hypothesis that active cryovolcanoes may periodically resurface the moon by emplacement of subsurface material. Subsequent magnetic field measurements of Europa by the Galileo spacecraft were consistent with a saline liquid layer (Khurana et al., 1998), and further surface features revealed the presence of mobile icebergs and ice diapirs (Rathbun et al., 1998, Carr et al., 1998, Pappalardo et al., 1998). While the evidence for a subsurface ocean is strong, conclusive evidence of active plumes or cryovolcanic activity is lacking. Evidence of such activity may be illuminated by NASA's Europa Clipper (Howell and Pappalardo, 2020, Vance et al., 2023), and the European Space Agency's (ESA) Jupiter Icy Moons Explorer (JUICE) (Fletcher et al., 2023, Poulet et al., 2024), that will reach the Galilean moon in 2030 and 2032, respectively.

For now, the ocean below Europa remains *terra incognita*. The ocean is encased below an ice crust estimated between 4 and 170 km (Anderson et al., 1998, Hand and Chyba, 2007, Howell, 2021). Thus, without subsurface information provided by active surface venting, the composition of the subsurface ocean is indicated only by surface chemistries and theoretical modelling. Thermal models by Lewis (1971) indicated that the Galilean satellites likely contain an ammonia-rich liquid water layer. Kargel (1991) argued that water or salt brines, rather than ammoniacal mixtures, likely drive cryovolcanism on Europa. This is because, unlike the colder Saturn nebula, the thermal properties of the Jovian nebula would have sustained ammonia as NH_3 gas. Gas is not well incorporated into smaller bodies during accretion, thus preventing significant incorporation of ammonia into the Jovian moons including Europa (Kargel, 1991). Indeed, nitrogen-bearing species have yet to be conclusively detected on Europa, and evidence of tidal heating indicates an antifreeze component such as NH_3 would not be required to maintain liquid water (Carr et al., 1998, Chen et al., 2014, Běhounková et al., 2021). However, an ammoniacal ocean is still plausible by thermal transport and thermochemical models (Spohn and Schubert, 2003, Ramkissoon et al., 2025). Indeed, NH_3 may have been a key chemical in the primordial ocean-atmosphere system (Moulanier et al., 2025).

If present, dissolution of NH_3 from the primordial atmosphere into the ocean of Europa may have encouraged the formation and incorporation of NH_4^+ (Moulanier et al., 2025). Notably, $(NH_4)_2SO_4$ forms one of the candidate species that may have been detected on the surface of Europa by the Galileo spacecraft (Mermy et al., 2023). Surface salts such as $(NH_4)_2SO_4$ could have been emplaced by venting from the ocean below or ice shell convection. As depicted in Figure 2.5B, the presence of an ammonium salt as opposed to NH_3 would align with the estimated oceanic pH of less than 8.4 (Johnson et al., 2019, Pasek and Greenberg, 2012, Tan et al., 2021), and temperatures up to 0 °C (Marion et al., 2003, Melosh et al., 2004), where NH_4^+ would predominate. Whether ammonia is indeed a constituent of Europa's internal chemistry may be illuminated by Europa Clipper through the analysis of atmospheric gases and plumes and ejecta, if any (Becker et al., 2024, Howell and Pappalardo, 2020, Vance et al., 2023).

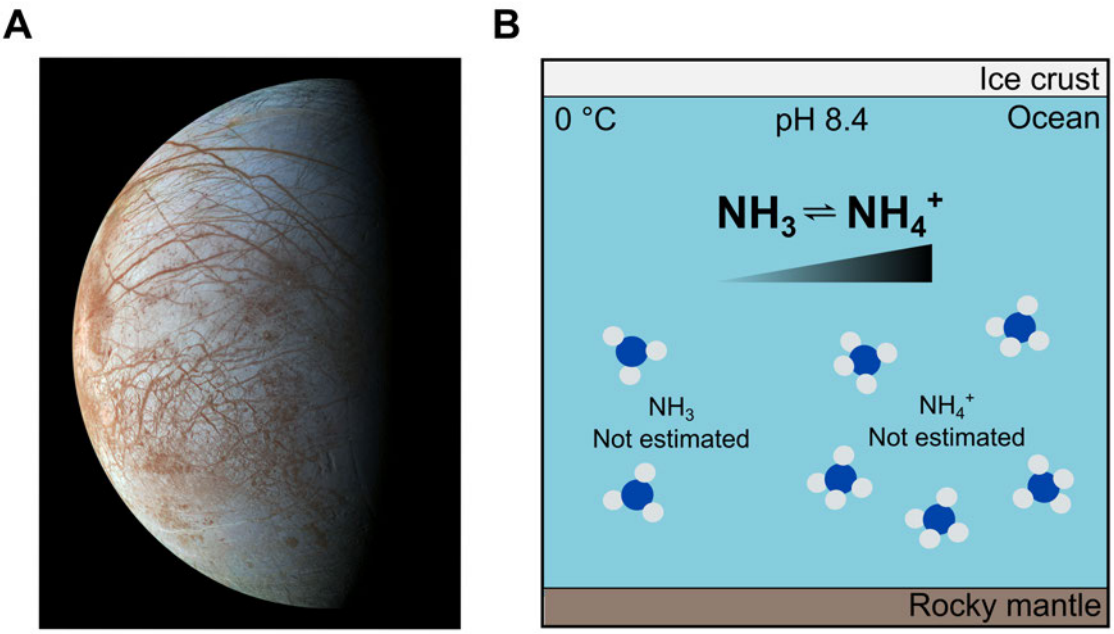

Figure 2.5: The ammonia content of Europa's subsurface ocean. (A) Europa's mosaic surface captured by the Galileo spacecraft. Long, linear ridges and cracks decorate the surface, along with distinct surface colouration arising from geological components. Image credits: NASA/JPL-Caltech/SETI Institute. (B) Ammonia speciation in the subsurface ocean of Europa. Ammonia concentration in the ocean has not been estimated. However, most models constrain the waters as acidic (Johnson et al., 2019, Pasek and Greenberg, 2012, Tan et al., 2021). Thus, if ammonia is present, NH_4^+ would predominate in the ocean.

2.1.5 Ammonia beyond the big three

Enceladus, Titan, and Europa represent icy moons for which extensive data has been gathered. However, the other Galilean moons, Ganymede and Callisto, are also subjects of scientific interest. In the case of Ganymede, this icy moon is the primary target of ESA's JUICE (Fletcher et al., 2023, Poulet et al., 2024). Along with Titan, Ganymede and Callisto are the largest known icy satellites, and both moons are expected to feature subsurface oceans (Zimmer et al., 2000, Kivelson et al., 2002, Saur et al., 2015, Cochrane et al., 2025). However, there is no strong evidence for tidal heating on either of these Jovian moons. An antifreeze component within the waters such as NH_3 is therefore hypothesised (Khurana et al., 1998, Mousis et al., 2002, Spohn and Schubert, 2003, Vance et al., 2018). Indeed, Ganymede and Callisto formed in the outer, cooler regions of the Jovian disk where the incorporation of frozen ammonia could be plausible (Mousis and Gautier, 2004, Mousis and Alibert, 2006).

It is not without mention that ammonia-bearing liquid reservoirs are not confined to the icy moons of Jupiter and Saturn but are hypothesised across a wide range of outer Solar System bodies. For example, an ocean is expected on Neptune's moon, Triton. Thermal-structural models of Triton indicate the strong possibility of a long-lived subsurface ocean, probably enriched in ammonia. However, the presence of ammonia in this ocean has not yet been

directly confirmed (Gaeman et al., 2012). Similarly, Charon, Pluto's largest moon, and the moons of Uranus (Ariel, Umbriel, Titania, and Oberon) may also host internal liquid water oceans with ammonia (Brown and Calvin, 2000, Cheng et al., 2014, Rhoden et al., 2015, Cochrane et al., 2021, Castillo-Rogez et al., 2023). Pluto itself could also host a subsurface liquid ammonia-water ocean (Robuchon and Nimmo, 2011, Nimmo et al., 2016). Indeed, ammonia has been detected on the surface (Dalle Ore et al., 2019). More broadly, several Kuiper Belt Objects are predicted to contain subsurface liquid water oceans, in which ammonia may be a constituent (Hussmann et al., 2006, Brown, 2012). However, few of these bodies have confirmed surface detections of ammonia, and the composition and extent of their internal liquids remain uncertain.

In contrast to these examples, the dwarf planet Ceres represents one of the few bodies in the Solar System for which there is strong evidence for ammonium-rich brines. Ceres is the largest object in the main asteroid belt between Mars and Jupiter. Observations from NASA's Dawn mission revealed that Ceres' surface is globally enriched in ammoniated phyllosilicates, identified through near-infrared spectral features associated with NH_4^+-bearing minerals (De Sanctis et al., 2024). The widespread presence of these phases suggests that ammonia was incorporated into the crust during aqueous alteration processes early in Ceres' history. In addition, several localised bright surface deposits, particularly within Occator crater, have been interpreted as residues formed from subsurface brines that reached the surface and subsequently lost water through sublimation (Zolotov, 2017, Nathues et al., 2022). These deposits contain sodium carbonates and ammonium salts, consistent with precipitation from ammonia-bearing brines. Gravity data and geological analyses from the Dawn mission further indicate that Ceres may host long-lived subsurface brine reservoirs within its crust, which can be mobilised by impacts or cryovolcanic processes to feed these surface deposits (Raymond et al., 2020, Singh et al., 2021). Together, these observations suggest that Ceres represents a chemically distinct aqueous environment within the Solar System, where interactions between water, salts, and ammonia have played a major role in shaping the planet's geochemical evolution.

While many planetary bodies in the Solar System may host liquid water and ammonia, compositional data on these planetary bodies are lacking. These limited physicochemical constraints do not allow for the estimation of ammonia abundance, speciation, and phase behaviour, and thus these bodies were not included as a the primary research focus as part this thesis.

2.2 Life in ammonia: Earth

To understand how ammonia may influence the habitability of extraterrestrial systems, it is critical to assess how ammonia shapes the habitability of terrestrial environments. At 25 °C, the $NH_3 \rightleftharpoons NH_4^+$ equilibrium has a pK_a of 9.25, and thus a pH above or below this value (salinity, temperature, and pressure will also adjust marginally this value) dictates whether NH_3 ($>$ pH 9.25) or NH_4^+ ($<$ pH 9.25) predominate (Bates and Pinching, 1949, Bower and Bidwell, 1978). Many environmental systems are temperate and operate at near neutral pH and standard atmospheric pressure. Thus, in most water, soil and living systems on Earth, NH_3 occurs in gas form. However, the natural levels of NH_3 are trace amounts ($<$ 6 ppm) (Roney

et al., 2004). As such, there are limited natural environments that mirror a cold and saline aquatic environment with NH_3 present, such is speculated in icy moons. There are, however, a few cases where life has been documented to thrive in high NH_3-bearing environments. In bat caves, decomposition of bat urea drives high concentrations of gaseous NH_3 (McFarlane et al., 1995). Yet microbes, along with bats, colonise this habitat (Studier, 1966, Newman et al., 2018, Leon et al., 2018). Similarly, in the alkaline waters of Mono Lake, United States, concentrations of NH_3 incrementally increase with depth to a final concentration near 500 µM at 35 m. Despite high NH_3 concentrations, bacteria have been isolated at these depths (Ward et al., 2000, Humayoun et al., 2003). Both examples indicate that life can persist in concentrated NH_3 environments on Earth. However, NH_3 is also characterised as a toxic substance. To assess the potential for extraterrestrial habitability, the following sections discuss the role and impact of NH_3 as well as NH_4^+ in terrestrial ecosystems.

2.2.1 Ammonia in prebiotic and biotic chemistry

The origin of life on Earth is speculated to have arisen from increasingly complex interactions that led to the formation of functional cellular bodies (Monnard and Walde, 2015, Goldman, 2023). It is known nitrogen was a key molecule involved in this process as it is required to produce amino acids in modern systems (Miflin and Lea, 1982, Bender, 2012). In primordial systems, alkaline hydrothermal vents may have acted as vectors for prebiotic chemistry as these sites provide heat, chemical gradients, and mineral catalysts (Martin and Russell, 2006, Russell et al., 2010, Lane and Martin, 2012, Sojo et al., 2016). It is hypothesised that ammonia produced in early hydrothermal vents could have been the nitrogen resource for prebiotic chemistry (Martin et al., 2008, Sojo et al., 2016, Nishizawa et al., 2021). Indeed, ammonia has been demonstrated to form amino acids under early Earth conditions (Miller, 1955, Lowe et al., 1963, Furukawa et al., 2009), as well as those present on Titan (Neish et al., 2009, 2010). Very low partial pressures of ammonia, on the order of 10^{-8} atm, would have been sufficient to sustain prebiotic chemistry in a seawater origin of life scenario (Wigley and Brimblecombe, 1981). It is of interest to note that hydrothermal-derived ammonia could have been prevalent as part of the primordial atmosphere within the Hadean era, and that ammonia production was less in the Archean when the earliest known life formed (Brandes et al., 1998, Nishizawa et al., 2021, Shang et al., 2023b,a). It is perhaps that the heightened levels of ammonia in the Hadean era may have been one of the factors that precluded the formation of life.

In modern systems, ammonia sustains habitability by forming a vital part of the nitrogen fixation cycle. NH_4^+ is the form of ammonia that predominates in this process due to the moderate pH of many ecosystems (Fowler et al., 2013), however NH_3 may also be present and utilised. Ammonia is formed naturally by diazotrophic bacteria, cyanobacteria and archaea that perform nitrogen fixation. In this process, atmospheric nitrogen (N_2) is reduced to ammonia (Burris and Roberts, 1993, Ribbe, 2011, Shin et al., 2016). Ammonia may also be available as a result of ammonification by decomposition of organic excretion or tissue (including DNA, proteins, amino acids) by various fungi and prokaryotes (Ladd and Jackson, 1982, Strock, 2008, Singh, 2016). The subsequent pool of NH_4^+ and NH_3 in the environment is sequestered by nitrifying bacteria such as ammonia-oxidising bacteria (AOB) to produce nitrate via nitrite (Wallace and Nicholas, 1969, Schmidt and Belser, 1983, Koops and Pommerening-Röser, 2001, Caranto and Lancaster, 2017). Ammonia may be also directly assimilated into microbes and

plants and incorporated into the synthesis of amino acids and nucleotides, whereby glutamate, a nitrogen donor, is the first and most central amino acid formed from ammonia (Smith et al., 1980, Rogers and Aneja, 1980, Tesch et al., 1999, Vo et al., 2013, Hachiya and Sakakibara, 2017). The nitrogen cycle is completed by denitrifying bacteria such as *Paracoccus* and *Pseudomonas* that process nitrate back into biologically inert N_2 (Alexander, 1965, Rajta et al., 2020, Ji et al., 2015). The presence of NH_4^+ and NH_3 in the environment thus plays a crucial role in supporting diverse microbial communities and plant growth. These compounds ensure the continuous availability of biologically usable nitrogen, which is essential for life on Earth.

2.2.2 Toxicity of ammonia

While ammonia forms a vital part of the global nitrogen cycle, high concentrations of ammonia are widely documented as toxic to life as we know it. On Earth, the speciation of ammonia dictates the degree of toxicity exerted. The small size and uncharged nature of gaseous NH_3 permits passive, unregulated permeation across lipid membranes (Ritchie and Gibson, 1987a,b, Ritchie and Islam, 2001, Brazier, 2016). Due to the lone pair of electrons on the nitrogen atom, NH_3 may act as a H^+ acceptor. Under biological pH (pH 7.4 to 7.8), permeated NH_3 combines with cytoplasmic H^+ to form NH_4^+. The capture of H^+ increases cytosolic pH (Bosoi and Rose, 2009).

In eukaryotic cells, such intracellular NH_3-driven alkalization has been associated with disrupted calcium signalling (Horie et al., 1995, Rose et al., 2005), disrupted organelle acidification, and with enzyme dysfunction (Moriwaki et al., 2024). Additionally, capture of H^+ can dissipate the proton motive force required for ATP generation (Bai et al., 2001, Angelova et al., 2022), causing oxidative stress by production of reactive oxygen species (Angelova et al., 2022, Han et al., 2020). In archaea, NH_3 transport has been correlated with dissipation of the transmembrane pH gradient in methanogen *Methanospirillum hungatei* (Sprott et al., 1984). These cellular toxicity mechanisms are depicted in Figure 2.6. For prokaryotes, specific effects of NH_3-driven reactions remain poorly characterised. Increased NH_4^+ and NH_3 has been correlated with reduced ATP production and electron transport system activity in *Enterobacter cloacae* HNR (Weng et al., 2022). Internal alkalization can elicit a stress response in prokaryotes (Schuldiner et al., 1986), but specific cellular and molecular targets and outcomes of internal NH_3 are not defined well within prokaryotes overall.

In addition to an internal rise in pH, the external rise in pH caused by NH_3 has also often been implicated as the cause of toxicity in living organisms (Figure 2.6) (Taglicht et al., 1987, Vines and Wedding, 1960). Indistinguishable toxicity between ammonia and solutions of identical pH have been characterised for *Bacillus subtilis*, *Sporosarcina*, *Paenibacillus*, *Staphylococcus*, *Brevibacillus*, *Streptomyces*, *Pseudomonas* and *Arthrobacter* (Deal et al., 1975, Kelly et al., 2012). In *Escherichia coli*, results vary. In the same study by Deal et al. (1975), ammonia was shown to be distinctly more toxic than NaCl solutions at pH 9.5, but indistinct toxicity was observed at pH 10. Likewise, for *Bacillus subtilis*, toxicity between ammonia and NaCl was distinct at pH 9 but indistinct at pH 10 (Deal et al., 1975). Vines and Wedding (1960) indicated that, in plants, high pH is not a direct toxicity mechanism of ammonia per se, but rather a vehicle through which larger amounts of gaseous NH_3 can enter cells and disrupt biological processes (Vines and Wedding, 1960). Thus far, studies have utilised neutrophilic organisms

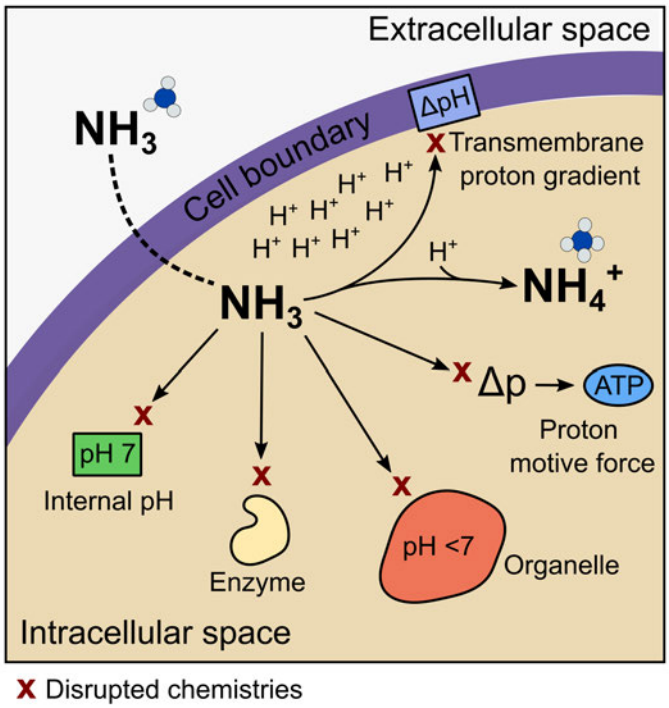

Figure 2.6: Mechanisms of cellular ammonia toxicity. Research across the domains of life has revealed several pathways of cellular NH_3 toxicity caused by disrupted internal chemistries (red X). These toxic effects are exerted firstly by the disruption of the intracellular proton pool, as the conversion of $NH_3 \rightarrow NH_4^+$occurs following unregulated, passive diffusion of NH_3. Downstream chemistries such as intracellular pH, the transmembrane proton gradient and proton motive force can become disrupted as a result. Enzyme and organelle function may also become disrupted by changes in pH.

to examine external NH_3 toxicity. These organisms are sensitive to both extracellular and intracellular alkalization. This has hindered clarity as to whether an external rise in pH induced by NH_3 is a factor that causes, or merely facilitates, bacterial toxicity.

In contrast to NH_3, the positive charge of NH_4^+ prevents passive diffusion through the hydrophobic core of lipid membranes. Instead, NH_4^+ is transported through ammonium transport (Amt) membrane proteins (Kim et al., 2012, Wacker et al., 2014), which may also facilitate passive NH_3 diffusion (Soupene et al., 1998, 2002). Due to similarities in charge, ionic radius and hydration properties, NH_4^+ can compete with potassium ions (K^+) for transport through ion channels (Neijssel et al., 1990, Moser, 1987, Bosoi and Rose, 2009). This facilitated diffusion and active transport of NH_4^+ regulates cellular uptake, thereby reducing toxicity of NH_4^+ relative to NH_3. However, high accumulations of NH_4^+, such as that caused by cation channel influx (Ramirez et al., 1999, Burckhardt and Frömter, 1992), or unregulated permeation of NH_3, can upset cell homeostasis. NH_4^+ can acidify the intracellular medium (Burckhardt and Frömter, 1992, Ramirez et al., 1999) and influence membrane potential (Golby et al., 1990, Wang et al., 2018). Elevated NH_4^+ can also disrupt K^+ balance (Sprott and Patel, 1986, Szczerba et al., 2008, Kong et al., 2014, Shi et al., 2020) which is essential for pH balance, membrane potential, intracellular communication, electrical signalling, and osmo-

protection (for extended reviews, see Beagle and Lockless (2021) and Benarroch and Asally (2020) for bacteria, Johnson et al. (2022) for plants and McLean and Wang (2021) for humans).

The whole cell outcomes of NH_4^+ toxicity are much more defined in literature across a breadth of species compared to NH_3. Such effects include disruption of amino acid, lipid and nucleotide metabolism in shrimp (Xiao et al., 2019), production of reactive oxygen species, interruption of Ca^{2+} homeostasis, and induction of cell apoptosis in mammalian cells (Wang et al., 2018), acidification in plants (Hachiya et al., 2021), and decline of motility and energy metabolism in bacteria (Weng et al., 2022). Accumulating concentrations of NH_4^+, as opposed to increasing NH_3 or pH, have also been found to be a contributing factor suppressing the abundance of *Anaerobranca*, *Tepidimicrobium* and *Proteiniborus* in anaerobic digesters (Dai et al., 2016).

Ammonia toxicity occurring by the independent action of NH_4^+ is thus possible, although less common due to the regulated transport of this ion. Further research is needed to clarify the intracellular effects of NH_3 on prokaryotes. However, evidence thus far indicates the overall picture of NH_3 toxicity is one where both species of ammonia act in concert against biological components. NH_3 bypasses membrane regulation and passively diffuses into cells. NH_4^+ is formed following the permeation of NH_3 into cells. Damaging cellular effects occur by the actions of both NH_3 and NH_4^+.

2.2.3 Ammonia in the anthropocene

The bioavailability and uptake of NH_4^+ through specialised transporters makes NH_4^+ one of the preferred nitrogen sources of many prokaryotes and photolithotrophs on Earth (Kleiner, 1981, Raven et al., 1992, Britto et al., 2001, Reitzer, 2003). Thus, it is by design that ammonia, $(NH_4)_2SO_4$ and calcium ammonium nitrate represent the major nitrogenous fertilizers used in agriculture (Tyagi et al., 2022). In the United Kingdom, agriculture accounts for 82% of all atmospheric NH_3 pollution (Guthrie et al., 2016). Atmospheric and aquatic pollution of ammonia can also occur by industrial processes (Behera et al., 2013, Matthews et al., 2000). The accumulations of excess NH_4^+ and NH_3 can be toxic to life, as described in section 2.2.2. While fertilizer supports crop growth, application of NH_4^+ to soils leads to acidification (Gijsman, 1990, Gorissen et al., 1993, Tyagi et al., 2022) and increased ionic strength (Gorissen et al., 1993). The downstream effects of this are evident; application of ammonium fertilizer has shown to reduce bacterial populations in the roots of Douglas-firs (Gorissen et al., 1993) and reduce bacterial richness and diversity in soils (Witter et al., 1993, Toljander et al., 2008, Du et al., 2019, Hu et al., 2023).

Application of ammonium fertilizer also can lead to the release of NH_3 when deposited into high pH soils—volatilization (Eno et al., 1955, Powlson and Dawson, 2022, Luo et al., 2022). Volatilization is a process in which a substance transitions from the liquid to the gas phase, escaping into the surrounding air or vacuum. During this phenomenon, the gaseous substance physically leaves liquid and enters the atmosphere or space. Global NH_3 emissions from agriculture are estimated at up to 78 tetragrams per annum (Luo et al., 2022). NH_3 losses from $(NH_4)_2SO_4$ fertilizer application range between 20-40%, but could be as high as 66%, in soils with a pH > 7 (Powlson and Dawson, 2022). Between the years of 2002 to 2016,

NH_3 emission and concentrations globally were only found to increase (Warner et al., 2017). Atmospheric pollution of NH_3 is significant as NH_3 can mobilise from the initial, local site of release to distant environments (Lô et al., 2025, Leytem et al., 2024, Sutton et al., 1998, Bouet et al., 2005). Ammonia has been detected up to 3 kilometres from a source pollution site and could be detected at a level of 5.1 μg/m^3 in natural reserves (≈7 ppb) (Lô et al., 2025). This is far above the trace averages expected. The subsequent effect of volatilized NH_3 on an ecosystem is likely to be concentration-dependent: low concentrations of ammonia could stimulate growth of plants and bacteria (Bollmann et al., 2002, Hernández-Guzmán et al., 2022, Hao et al., 2023), but, ammonia at sufficient concentrations could disrupt biological processes across the domains of life. Indeed, application of anhydrous ammonia in soil has shown to decrease the number of nematodes, fungi and bacteria where pH, and thus NH_3 volatilization, was increased (Eno et al., 1955). Whether long-range delivery of volatilized NH_3, as often occurs on Earth, could also exert such a detrimental biological impact has not been explicitly shown in literature.

2.3 The habitability of ammoniacal oceans

It is evident ammonia can have a paradoxical influence on life on Earth. Many of these findings are derived from relatively benign environments (i.e., moderate pH, temperature, salinity, and pressure). Ocean worlds are, relative to conditions on Earth, extreme environments. As described previously, oceans of high pH are estimated on Enceladus and Titan (Marion et al., 2012, Leitner and Lunine, 2019). Temperatures range from 0 to 90 °C on Enceladus (Glein et al., 2015, Matson et al., 2012), near 0 to -20 °C in the waters of Europa (Kargel et al., 2000, Marion et al., 2003, Melosh et al., 2004), and to -18 °C on Titan (Sohl et al., 2014). The pressure exerted on these oceans can also be immense; at the ocean floor, pressures are estimated at 8,000 bar on Titan (Journaux et al., 2020). At the ice-ocean interface, pressure estimates on Europa are between 840 and 2,050 bar (Kargel et al., 2000). On Enceladus, pressures could be as low as 0.5 bar but as high as 600 bar (Neveu et al., 2020, Xu et al., 2025, Vance et al., 2018, Schoenfeld et al., 2023). Plume vent regions likely exhibit pressures significantly lower than 1 bar (Glein and Truong, 2025).

Salinity is also a factor in these oceans. Tentative estimates place the oceanic salinity of Enceladus, primarily composed of NaCl, $NaHCO_3$, Na_2CO_3, below 4% (Hsu et al., 2015). This ocean likely falls between 2 and 20 g/kg (Zolotov, 2007). At 2 g/kg, these estimates are lower than the salinity of seawater on Earth (approximately 35 g/kg or 3.5% (Ludwig, 2022)). Comparatively, the subsurface oceans of Titan is expected to be much more saline. Tidal distortion analysis suggests a dense internal ocean with high amounts of sulphur, sodium and potassium salt (Mitri et al., 2014), with a salinity as high as 200 g/kg (Idini and Nimmo, 2024). Salinities between 3 g/kg and upwards of 100 g/kg are expected on Europa (Sahai et al., 2024), whereby a sulphate-rich and magnesium-rich ocean is supposed (Kargel et al., 2000, Fanale et al., 2001, Zolotov and Shock, 2001, Melwani Daswani et al., 2021).

As per Cockell et al. (2016), habitability can be defined by "an environment capable of supporting the activity of at least one known organism". Organisms that could develop under these extremes of pH, temperature, salinity, and pressure would have to utilise specialised adaptations to survive. On Earth, such organisms are known as extremophiles. Acidophiles,

alkaliphiles, psychrophiles, thermophiles, halophiles, and piezophiles exclusively colonise habitats of extreme acidity (less than pH 3), high pH (greater than pH 9), low temperature (between -20 and 10 °C), high temperature (60 to 122 °C), salinity (greater than 1.7%) and pressure (exceeding 100 bar), respectively (Martin and McMinn, 2018, Rothschild and Mancinelli, 2001). By definition, extremophiles are restricted to environments that reflect their specialized adaptations. However, some organisms merely tolerate such extremes without requiring them for growth. When evaluating the potential for life beyond Earth, extremophiles serve as ideal analogues for investigating the survival limits and physiological traits that may be compatible with the extreme physicochemical conditions of icy moon subsurface oceans. Indeed, extremophiles on Earth already demonstrate that life can thrive in waters of sub-zero temperature (Franzmann et al., 1992), pH 11 (Suzuki et al., 2014) and upwards of 200 g/kg salinity (Meinzer et al., 2023), for example.

Some prokaryotes even display ammonia-dependent metabolisms. These "ammoniaphiles" include ammonia-oxidizing archaea (AOA) and AOB. These are chemolithotrophs that utilise ammonia as an energy resource, oxidizing NH_3 to nitrite in the first-rate limiting step of nitrification (Zorz et al., 2018, Koops et al., 2006). However, *-phile* often implies thriving in highly concentrated or extreme conditions. AOA and AOB are tolerant to high NH_4^+ (0.01 to 0.43 M) but not NH_3 (activity reduced 15.9% in less than 0.001 M NH_3) (Tourna et al., 2011, Vejmelkova et al., 2012, Qian et al., 2017). It follows that these organisms are often neutrophilic or, at most, alkalitolerant (Koops et al., 2006, Lu et al., 2021). When assuming the conditions in icy moons would require the formation of ammonia-dependent physiologies, haloalkaliphilic AOA or AOB could make suitable analogues. However, most known haloalkaliphilic AOA and AOB, such as *Nitrosomonas halophila*, are limited to growth at pH 9 (Sorokin et al., 2001), and are not widely available from culture collections. This limits their use for examining the habitability of ammoniacal waters on icy moons.

When considering the habitability of icy moons, the low ammonia concentrations estimated in the oceans beckons the question as to whether would life need ammonia adaptations to thrive. Methanogens, without ammonia adaptations, can continue metabolic functions in low NH_3 (0.002 to 0.006 M) (Yi et al., 2023). Methanogens are often considered ideal analogues for life within icy moon oceans. Methanogens have been isolated from an array of extreme environments on Earth, use simple energy sources (e.g., hydrogen and carbon dioxide), produce methane (methane has been detected on both Enceladus and Titan), and are anaerobic (McKay et al., 2008, Taubner et al., 2015). Due to limited oxygen delivery to the oceans, anaerobic respiration was thought to be a requirement in the oceans of icy moons.

Models now suggest oxygen generated on the surface of icy moons by radiation could be transported to the oceans below (Teolis et al., 2017, Ray et al., 2021, Hesse et al., 2022, Szalay et al., 2024). This expands the metabolic possibilities in the oceans to aerobes, such as bacteria. Like methanogens, extremophilic bacteria have been widely documented in literature (see Pikuta et al. (2007) or Bowers et al. (2009)). However, bacteria possess a wider range of metabolisms that could be suitable to the chemistries within icy moons (e.g., sulphur oxidation, nitrate reduction, ammonia oxidation) (Yin et al., 2014, Kilic et al., 2017, Koops et al., 2006). Notably, bacteria without ammonia adaptations were isolated at depths of 35 m in the NH_3-laden Mono Lake (Humayoun et al., 2003). Bacteria have also been isolated from apt icy

moon analogue environments, such as the hypersaline and -13 °C waters of ice-sealed Lake Vida (Murray et al., 2012). The use of extremophile bacteria in limits-of-life research could therefore offer a nuanced perspective on the habitability potential of icy moons. The following sections examine whether the ammoniacal subsurface oceans of icy moons could sustain life by drawing on known bacterial survival thresholds in ammonia. This includes an analysis of physiological changes that may preclude the existence of or alter the biology of bacteria, such as specific toxic effects and adaptative mechanisms.

2.3.1 Icy moons *in vitro*: ocean habitability

As life could be entrained in the ejected ice grains from the plumes of Enceladus, much microbiology research in astrobiology has focussed on viability and detectability of microbes following simulated entombment in ice (Kelly et al., 2012, Bywaters et al., 2020, Parker et al., 2023, Klenner et al., 2024). Few experiments have provided *in vitro* assessments of how simulated icy moon conditions with ammonia could afflict bacterial life. Those that have, have done so from a planetary protection perspective, assessing the risk of surface contamination on icy moons with common terrestrial bacteria carried by spacecraft, not extremophiles. However, this data can still provide valuable constraints on habitability in ammonia. Molton and Ponnamperuma (1972) demonstrated survival thresholds of four bacteria, *E. coli*, *Serratia marcescens*, *Aerobacter aerogenes* and *B. subtilis*, to a simulated Jovian atmosphere of H_2 (56%), He (43%), CH_4 (0.5%) and NH_3 (0.5%). Pressure-temperature regimes included those that could be applicable to icy moon interiors (≈50 bar and -13 °C, and ≈68 bar and 0 °C). Survival varied with these conditions. Near-total mortality occurred under the colder treatment (deaths as %—*E. coli*, 97%; *S. marcescens*, 93%; *A. aerogenes*, 63%; *B. subtilis*, 100%), while fewer proportional deaths occurred at 0 °C (deaths as %—*E. coli*, 19%; *S. marcescens*, 50%). Although not designed to assess oceanic habitability, these findings indicate that microbial persistence in ammonia mixtures may be constrained at sub-freezing temperatures or supported at near 0 °C.

The multi-extreme conditions employed by Molton and Ponnamperuma (1972) make it difficult to attribute a single parameter, or combination of parameters, to bacterial death. Namely, the influence of ammonia on bacterial survival limits cannot be established. Subsequent studies, however, have isolated the impact of ammonia by examining bacterial viability in simple, aqueous ammonia solutions under extreme temperatures. Deal et al. (1975) defined that 0.1 M ammonia was toxic to *E. coli* and *B. subtilis* in solutions at 25 °C and pH 9.5 to 10.5 ($NH_3 > 50\%$). Molar limits of toxicity were not assessed, but cell viability at 25 °C was reduced at a higher rate as pH increased. This correlates to an increased relative proportion of NH_3. Reduction to cell viability still occurred at 0 °C, albeit at a slower rate. From this, we can make two assumptions: (i) abundance of NH_3 is proportional to toxicity, and (ii) lower temperatures reduce toxicity. The latter phenomenon could be explained by a reduction to kinetic energy associated with lower temperatures that ultimately limits substantial membrane permeation of NH_3. The parameters utilised in this study (pH 10.5, temperatures at 0 °C, and 0.1 M ammonia) align well with the physicochemical properties expected on Enceladus (see 2.1.2). These findings imply that terrestrial organisms like *E. coli* and *B. subtilis* would face significant physiological stress, if not outright mortality, under such conditions.

2.3.2 Bacterial thresholds in ammonia

Simulated icy moon environments *in vitro* have indicated that the presence of ammonia can contribute to the toxicity of an aqueous solution. But these experiments do not define the concentration thresholds for life in aqueous ammonia. As presented in Table 2.1, estimated concentrations of ammonia between icy moons vary. Not only this, but speciation also varies.

The speciation of ammonia, as well as concentration, plays a critical role in bacterial inhibition. In accordance with the toxicological data, aqueous environments with NH_3, such as those hypothesized for Enceladus and/or Titan, may present a more significant physiological challenge to microbial survival and adaptation if present at sufficient concentrations. However, the definition of "sufficient concentrations" is loose; the concentration thresholds for growth of bacteria in ammonia have not yet been properly established.

Table 2.1: Ammonia concentration and speciation estimated for icy moon subsurface oceans

	Predominant species[1]	**Est. [NH_3] (M)**	**Est. [NH_4^+] (M)**
Enceladus	NH_3	0.0181[2]	0.00744[2]
Titan	NH_3 or NH_4^+	0.96 to 9.6 M[1]	Not estimated
Europa	NH_4^+ or nil	Not estimated	Not estimated

[1] Speculated in this chapter as per physicochemical expectations of oceans (Eq. 2.1)
[2] Estimated by Glein and Truong (2025)

There is not a significant body of work that intersects microbiology, icy moon physicochemical conditions and ammonia. In lieu of this, survival thresholds in ammonia can be gleaned from research in other fields. For example, much existing work regarding survival thresholds of bacteria in ammonia has been conducted from the perspective of wastewater treatment in anaerobic digesters. However, anaerobic digesters are often maintained below pH 9.25, whereby the relative abundance of NH_3 is less than 50%. These conditions are not comparable with those estimated in the oceans of Enceladus and Titan. However, an indication of limits of bacterial life in ammonia can still be drawn from this research. The minimal inhibitory concentration (MIC) for a wide variety of bacteria in ammonia is presented in Table 2.2. Where MIC was not stated outright, an estimate was derived from the pH of the experiment using the pK_a of ammonia and the Henderson-Hasselbalch equation. In this case, the MIC was defined as the lowest concentration of ammonia that limited visible growth and function. While the physicochemical conditions underpinning the MIC of ammonia given in Table 2.2 may not be comparable to icy moons, some of the bacteria utilised exhibit alkaliphilic and halotolerant metabolisms (*B. linchenformis*) or alkalitolerance and halotolerance (*B. subtilis*, *B. cereus*, *E. faecium*, *E. durans*, *M. luteus*) that are relevant to the high pH and saline properties expected in icy moon oceans.

Table 2.2: Minimal inhibitory concentration (MIC) of NH_3 and NH_4^+ across bacterial species

Species	**Strain**	**MIC ([NH_3], M)**	**MIC ([NH_4^+], M)**
Enterobacter cloacae[a]	HNR	≈0.00049	≈0.0138
Escherichia coli[b]	MG1655	0.0042	0.750[§]
Corynebacterium glutamicum[b]	ATCC 13032	0.0112	1.989[§]
Bacillus subtilis[b]	-	0.0133	0.750[§]
Escherichia coli[c]	K-12	>0.02, <0.04[†]	-
Bacillus subtilis[c]	168	>0.02, <0.04[†]	-
Enterococcus durans[c]	ST2	>0.02, <0.04[†]	-
Pseudomonas sp.[c]	-	>0.02, <0.04[†]	-
Enterobacter faecalis[d]	NCTC 00775	0.025	0.465
Listeria innocua[d]	NCTC 11288	0.025	0.465
Escherichia coli[d]	NCTC 10538	0.025	0.465
Bacillus subtilis[d]	T1, T2, T19, T22, T33, T39, DK-W1, N3, N4 and N5	0.05	0.931
Bacillus cereus[d]	T31 and T38	0.05	0.931
Bacillus megaterium[d]	T3, T4, T21, T34, T37 and T40	0.05	0.931
Pseudomonas aeruginosa[d]	NCTC 10299	0.05	0.931
Bacillus subtilis[e]	168	≈0.064	≈1.456
Bacillus subtilis[d]	T5 and DA2	0.15	0.279
Bacillus cereus[d]	NCIMB 9373	0.15	0.279
Sulphate-reducing bacteria[f]	-	0.2[‡]	0.166[‡]
Bacterial isolate[c]	4-1	≈0.3[†]	-
Bacterial isolate[c]	4-2	≈0.3[†]	-
Bacillus subtilis[d]	T20, N1, N2, DA1 and NCIMB 3610	0.3	0.559
Bacillus cereus[d]	T41	0.3	0.559
Bacillus licheniformis[d]	ATCC 39302	0.3	0.559
Enterococcus faecium[d]	DK-C1	0.3	0.559
Micrococcus luteus[d]	NCDO 0982	0.3	0.559
Staphylococcus aureus[d]	NCDO 0949	0.3	0.559
Salmonella typhimurium[d]	NCIMB 10248	0.3	0.559
Bacillus subtilis[d]	T36	0.5	0.931
Proteus morgani[d]	NCIMB 00067	0.5	0.931
Bacillus pumilus[d]	NCIMB 9369	>0.5	0.931
Bacillus pasteurii[d]	NCIMB 8841	>0.5	0.931

[a] From Weng et al. (2022)
[b] From Müller et al. (2006)
[c] From Tada et al. (2021)
[d] From Leejeerajumnean et al. (2000)
[e] From Hamill et al. (2020)
[f] From Dai et al. (2017)
[§] Growth impairment attributed to osmotic or ionic effects of NH_4^+

† Cultured in NH_3 gas
‡ MIC derived from ammonia concentrations in reactor 3

The proceeding comparison is not meant to imply the presence of life, but rather explore whether known biological limits intersect with extraterrestrial conditions. Any similarity in chemical ranges should not be interpreted as evidence for life but rather as a point of interest for further study. The ammonia concentrations estimated on Enceladus fall below the MIC of NH_3 established for a majority of the bacteria in Table 2.2. The exceptions are *E. cloacae* HNR, *E. coli* MG1655, *B. subtilis* and *Corynebacterium glutamicum* ATCC 13032, which exhibit sensitivity to concentrations of NH_3 below 0.0181 M. It is notable the maximal inhibitory threshold for *B. subtilis* is 0.5 M. Spore-formation of *B. subtilis* has been implicated for the survival of this species when frozen in 35% NH_3 (Kelly et al., 2012). *Bacillus pumilus* and *Bacillus pasteurii* have demonstrated a tolerance up to and possibly exceeding 0.5 M NH_3, the current upper limit of bacterial survival in ammonia recorded in literature. The high level of tolerance can be attributed to ammonia utilisation; in *Bacillus pasteurii*, NH_3 supports substrate oxidation (Wiley and Stokes, 1962), permeability of substrates (Wiley and Stokes, 1963) and ATP generation (Jahns, 1996). This could indicate concentrations of 0.96 M NH_3 could be survived by some species, however, survival in 0.96 M NH_3 has not been explicitly demonstrated. Based on the data presented in Table 2.2, the known NH_3 tolerance in bacteria does not overlap with the NH_3 concentrations estimated for Titan. On Europa, the concentration of ammonia in the subsurface ocean of is not estimated. However, Table 2.2 demonstrates that the toxicity of NH_4^+ for bacteria is low and, as such, the limits of bacteria in NH_4^+ is high. Bacteria demonstrate growth in up to 2 M NH_4^+. If it is true that Europa incorporated only low amounts of ammonia into its interior during accretion, the levels of NH_4^+ in the subsurface ocean of Europa could fall within a range that has been observed to support bacterial survival of Earth.

2.3.3 Physiology in ammonia

Having considered the concentration thresholds for bacterial survival in ammonia, it is pertinent to consider the physiological influence of ammonia on extracellular bacterial structure and intracellular processes. Physiology determines successful propagation within an environmental niche. The structure-function relationship between a biological entity and its environment is an essential prerequisite for a habitable environment becoming inhabited. As such, physiological responses to external ammonia can indicate adaptations that may be suitable for surviving in high ammonia, as well as indicate the molecular and cellular stress responses that may preclude the persistence of viable biology. Physiological characteristics elevated in response to extreme environments, such as compatible solutes, proteins, lipids, fatty acids, and other metabolites can additionally be used as biological markers for life. For this reason, instrumentation capable of detecting such biological components feature onboard NASA's Europa Clipper (Klenner et al., 2024), and could implemented on future missions to Enceladus, the Enceladus Orbilander (MacKenzie et al., 2021), and are to be incorporated on the Titan-bound Dragonfly (Barnes et al., 2021).

To date, the physiological response to ammonia is not well characterised in bacteria. Much work has been dedicated to the transcriptomics and metabolomics of methanogens under ammonia stress (Dai et al., 2016, Kato et al., 2014, Zhang et al., 2014, Gao et al., 2015). In

bacteria, the physiological response to ammonia limitation, as opposed to ammonia replete conditions, is predominantly represented in literature (Behrends et al., 2012, Alarico et al., 2014). Studies that have examined physiological changes associated with ammonia exposure have done so at relatively low concentrations (0.001 to 0.035 M), within a pH range where NH_4^+ predominates by a significant margin (pH 7.8) (Sedlacek et al., 2019, Goude et al., 2004, Zorz et al., 2018, Sayavedra-Soto et al., 2015). These concentrations and conditions are unlikely to be comparable to the oceanic environments on Enceladus or Titan, and transcriptomic, proteomic and metabolomic insight into the bacteria physiological response to high proportions of NH_3 is absent. However, they could possibly bear resemblance to the internal chemistries of Europa and are nonetheless worthy of discussion. The following material is summarised in Figure 2.7.

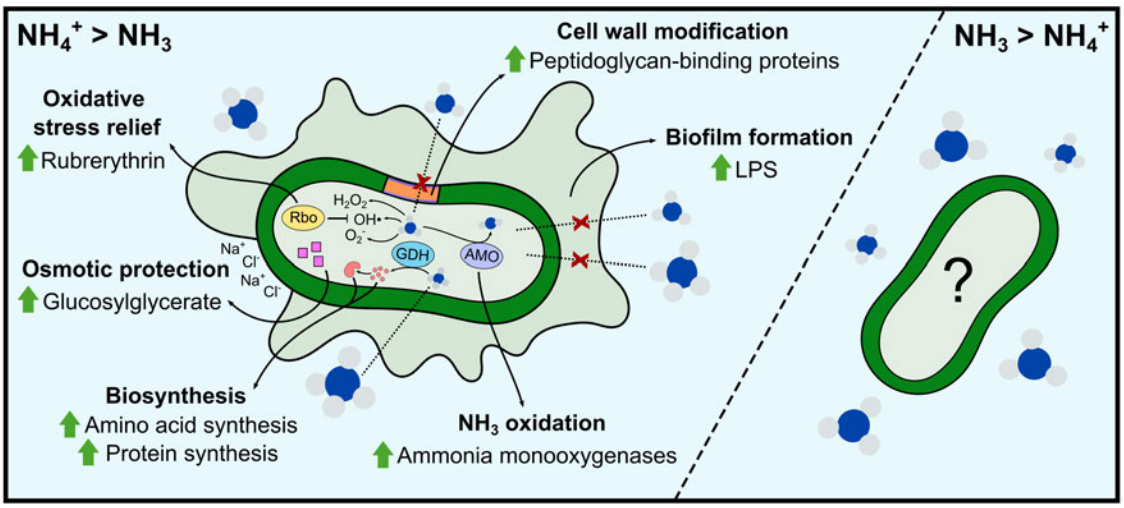

Figure 2.7: Bacterial physiological changes to ammonia exposure. Several changes to internal molecular features have been characterised in bacteria exposed to ammonia solutions where the relative abundance of NH_4^+ is higher than NH_3. This includes altered nitrogen metabolism resulting in NH_3 oxidation and biosynthesis of amino acids and proteins, cell wall modification, oxidative stress relief, biofilm formation, and altered mechanisms in osmotic protection. To date, there is a lack of literature indicating the physiological response of a cell to ammonia where the relative abundance of NH_3 is higher than NH_4^+. AMO, ammonia monooxygenase; GDH, glutamate dehydrogenase; LPS, lipopolysaccharide; Rbo, rubrerythrin.

Firstly, it has been shown that a major response to elevated ammonia is alteration to nitrogen metabolism. AOB within the genus of *Nitrosomonas* cultivated in ammonia exhibit elevation to nitrogen reducers: nitrite reductase and cytochrome c-552, as well as ammonia oxidizers, ammonia monooxygenases (Zorz et al., 2018). Sedlacek et al. (2019) demonstrated that a cluster of *Nitrosomonas* spp. were capable of faster growth rates in ammonia compared to *Nitrosomonas* spp. of a separate cluster. The fast-growing *Nitrosomonas* spp. exhibited the putative nitric oxide-scavenging module *ncgABC* within the genome. This module is speculated to encode a suite of proteins that work in conjunction with the nitrogen reductase NirK (Sedlacek et al., 2019). NirK has been implicated as an electron shuffle that supports ammonia oxidation (Cantera and Stein, 2007). These physiologies are thus indicative of two

biochemical responses to ammonia: energy-generating NH_3 oxidation, and the activation of a secondary process such as nitrifier denitrification or flexible nitrogen metabolism. In the latter case, this may be a response to excess electron generation from ammonia oxidation and the need to maintain redox balance. However, these physiological adaptations to ammonia are specific to AOB as most other bacterial groups do not perform ammonia oxidation.

In bacteria without ammonia adaptations, ammonia is primarily assimilated for amino acid biosynthesis through the glutamine synthetase-glutamate synthase (GS-GOGAT) pathway or the glutamate dehydrogenase (GDH) pathway. GS has a higher affinity for NH_4^+ and thus is preferentially utilised at low NH_4^+ concentrations (Nagatani et al., 1971, Kanamori et al., 1987b, Yan et al., 1996). Use of either the GS-GOGAT or GDH pathway yields glutamate, the primary nitrogen reservoir. It is therefore logical an increase in ammonia would lead to increased nitrogen assimilation and biosynthesis of amino acids. Indeed, in excess ammonia, elevation to amino acid transcripts have been reported in *E. cloacae*. In accordance with higher levels of NH_4^+, *E. cloacae* exhibited downregulation of the GS-GOGAT pathway (Weng et al., 2022). Amplification to factors involved in protein translation, translocation and folding have also been reported in *N. winogradskyi* (Sayavedra-Soto et al., 2015) and *Nitrosomonas* spp. (Zorz et al., 2018) upon ammonia exposure.

In addition to nitrogen metabolism, glutamate has a secondary function as a compatible solute. Compatible solutes accumulate under osmotic stress to balance osmotic pressure and maintain cellular hydration. Notably, the presence of ammonia has been found to alter the pool of osmolytes synthesised. Cultivation of *Erwinia chrysanthemi* under high salt and 0.01 M ammonia saw the accumulation of the osmolyte glucosylglycerate, as opposed to the commonly synthesised glutamate, in response to osmotic stress (Goude et al., 2004). Both glucosylglycerate and glutamate are charged at biological pH and thus increase the ionic strength of cytoplasm. However, the accumulation of glucosylglycerate as a dominant osmolyte under stressing salt conditions has not been reported in other bacteria. It is possible this is a symptom of a downregulated GS-GOGAT pathway as has been observed in *E. cloacae* (Weng et al., 2022). While glutamate can be produced through the GDH pathway, it is not as efficient and may led to a comparative reduction in glutamate compared to glucosylglycerate when utilised (Wakisaka et al., 1989, Yan et al., 1996). This discovery is particularly apt for waters that could impose both osmotic and ammonia stress, such as the highly saline ammoniacal ocean of Titan.

Further physiological alterations in response to ammonia are those of protective adaptations. While NH_4^+ translocation across the cell membrane is generally regulated and controlled, excess permeation can still disrupt intracellular processes. Even at neutral pH, small but appreciable amounts of NH_3 would exist in equilibrium with NH_4^+ and contribute to internal biochemical perturbation. In ammonia, *Nitrosomonas* spp. have exhibited elevated proteins in cell wall modification (e.g., peptidoglycan-binding proteins) and oxidative stress relief (e.g., rubrerythrin) (Zorz et al., 2018). These proteins likely support restricted NH_3 diffusion across the membrane and manage NH_3-driven production of harmful reactive oxygen species, respectively. Upregulation to transcripts in oxidative stress relief have likewise been reported in bacteria without ammonia adaptations, such as *E. cloacae* (Weng et al., 2022).

Further physiological defensive mechanisms against ammonia have been identified in the form of biofilms. Biofilms are an organized collation of bacteria adhered to one another and an external surface through a matrix formed of extracellular polymeric substances (EPS). The EPS can consist of polysaccharides, lipopolysaccharides (LPS), proteins, and DNA that provide a physical barrier to external stresses. In bacteria without ammonia adaptations, the synthesis of the EPS constituent LPS has been reported in *E. cloacae* (Weng et al., 2022) and *N. winogradskyi* (Sayavedra-Soto et al., 2015). Amplification to protein and polysaccharide synthesis has also been reported in *E. cloacae*, coinciding with upregulation to the protein secretion system known as the type 2 secretion system (T2SS) which supports extracellular export of proteins for EPS formation (Weng et al., 2022). Both bacteria exhibited a reduction to motility and motility related genes in response to ammonia which is characteristic of bacteria encased in EPS. However, it should be highlighted that these adaptations reflect a general stress response that are not exclusively triggered by ammonia (Storz and Hengge, 2010, Jolivet-Gougeon and Bonnaure-Mallet, 2014).

The lack of specific adaptations to ammonia do not reflect an inability to adapt but rather limited opportunity to adapt; ammonia concentrations occur at low levels in natural environments on Earth. Where ammonia levels are naturally higher, organisms might be expected to incorporate ammonia into multiple biological metabolisms, such is the case for AOB. Although, it is not without question that additional factors such as those akin to oxidative stress relief and biofilm formation could support life in concentrated aqueous ammonia. Indeed, within Earth oceans, biofilms are widespread and are essential for microbial survival, ecology and contribution to global biogeochemical cycles (Zhang et al., 2019, Qian et al., 2022, Antunes et al., 2019).

2.3.4 Lessons from a polluted planet: ice habitats

Oceans are not the only environments within icy moons that could hold water, and thus, potential habitats. The ice shells of icy moons could support brine channels, veins, pockets and fractures (Kargel et al., 2000, Buffo et al., 2021, Wolfenbarger et al., 2022, Buffo et al., 2023). On Earth, such brine networks have shown to sustain life. Organisms can be entrained into liquid inclusions of ice shells during ice formation. The subsequent labyrinth of brine networks connected to the ocean below can provide liquid water, nutrients and dissolved gas that preserve viable life (Loose et al., 2011, Dieckmann, 2002). Viruses, prokaryotes and eukaryotes have been isolated from terrestrial sea ice (Maranger et al., 1994, Brown and Bowman, 2001, Lizotte, 2003, Mueller et al., 2005). *Chroococcidiopsis* CCMEE 029 and CCMEE 171 have been shown capable of surviving in sodium sulphate (Na_2SO_4), $MgSO_4$ and NaCl ice frozen to -40 °C (Cosciotti et al., 2019). It has therefore been suggested that cryobrine networks in ice shells of icy moons could offer viable habitats. Particularly those near the ice-ocean interface where temperatures are more suitable for biological propagation (Kargel et al., 2000, Wettlaufer, 2009). While a majority ($\sim$ 80%) of these brine habitats on Europa may not supply enough nutrients to become inhabited, it is estimated $\sim$ 20% could sustain life without active growth under nutrient-limited conditions. A smaller portion of nutrient-rich brine channels, isolated near the ice-ocean interface, could also support active growth (Wolfenbarger et al., 2022). Such habitable ice environments proximal to the ice-ocean interface on Europa and Enceladus have also been suggested by Buffo et al. (2021).

When considering the permeation of ammonia into ice shell niches, several scenarios are possible (Figure 2.8). Brine compositions within ice shells could reflect the composition of the ocean from which the brine is derived. Brine channels, veins, pockets, and fractures within the ice could therefore contain ammonia. Exclusion from the ice lattice during ocean water freezing may even concentrate ammonia into the brines (Hammond et al., 2018). Upward shift of brines into the ice shell may encourage exsolution of NH_3 (i.e., separation of NH_3 from the liquid phase and release as a gas). This occurs as per Henry's Law that states as pressure decreases, as does solubility of gas. Fractures that are open to the surface may enable NH_3 volatilization, depending on local pH, pressure, and temperature. Volatilized NH_3 could then migrate along the fracture system and potentially enter other intersecting brine networks within the ice shell. NH_3 may also adsorb onto the ice sheet. NH_3 has been shown to adsorb onto ice between -50 and -25 °C (Richter et al., 2025). NH_3 gas could also be delivered through secondary sources, such as plume activity at sites like the tiger stripes on Enceladus. At the ocean-plume interface, brine rises from the ocean into the vent system, where exsolution of NH_3 occurs. Within the plume shaft, NH_3 gas could begin condensing onto the ice walls or become incorporated into the ice shell via plume fallback. A hypothetical scenario might proceed as follows: NH_3 adsorbs onto ice; the adsorbed NH_3 migrates slowly through the ice shell by surface or bulk diffusion; NH_3 may enter liquid inclusions within the shell, where it dissolves into liquid brine.

The dispersal and accumulation NH_3 in brine channels, veins, pockets, or fractures of icy moons is analogous to NH_3 volatilization on Earth. Volatilized NH_3 disperses from an ammonia source into surrounding environments. Although more proof-of-concept data is required, dispersed NH_3 occurring as a consequence of volatilization has shown to influence the habitability of soil for bacteria and eukaryotic organisms (Eno et al., 1955), and could alter the habitability of distant terrestrial environments. Taking lessons from a polluted planet, NH_3 from icy moon oceans could likewise alter the potential for habitability not just locally within the ocean, but also at a distance in ice shell brine networks where dispersal of NH_3 is plausible. Understanding this interaction could also help us demonstrate and characterise the repercussions of terrestrial ammonia pollution on the habitability environments both local to sites of ammonia emission and distant.

2.4 Astrobiology of ocean worlds: uncertainties, challenges and perspectives

Potential habitability constraints imposed by ammonia within icy moon oceans have been noted (McKay et al., 2008), but experiments validating this hypothesis are limited. Of experiments that have explored the limits of life in ammonia, these have either utilised a pH below 9.25, where the relative abundance of NH_3 to NH_4^+ is small, or bacteria that do not have physiological adaptations that could be relevant to the physicochemical conditions on icy moons. While low concentrations of ammonia and near neutral pH may be suitably applicable for the ocean of Europa, these experiments do not inform habitability assessments of the high pH oceans of Enceladus and Titan. Indeed, a closer examination of limits-of-life research reveals additional underlying gaps in knowledge that continue to challenge our understanding of ammonia as a habitability factor. For example, whether external pH contributes to NH_3

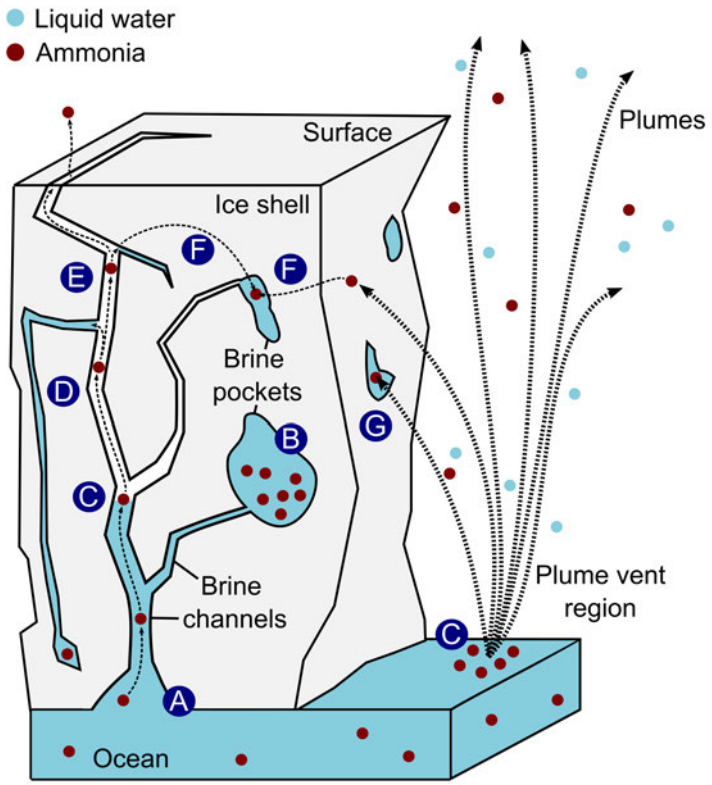

Figure 2.8: Penetration of ammonia into icy moon ice shell habitats. Brine may percolate into channels from the ocean below, delivering chemical constituents, including ammonia and liquid water, to these habitats (A). In some instances, depicted in (B), ammonia may concentrate within brine channels or pockets as a result of exclusion from the ice lattice. Exsolution (C) may occur at regions where liquid water is open to the vacuum or air, such as plume vent regions, permitting volatilization (D) if fractures are open to the surface, and dissolution of ammonia into intersecting brine channels higher in the ice shelf or release from the surface (E). Ammonia adsorbed (F) onto the ice shell may migrate to brine channels and pockets. Alternatively, ammonia could be deposited directly onto and within the ice shell if brine networks are exposed to plumes at the plume vent region (G).

toxicity, the physiological effects of NH_3 on bacteria, and the implications of NH_3 dispersal on microbial viability and ecology. Such information would allow us to consider whether toxicological challenges presented by ammonia could be overcome by suitable biological adaptations, or be merely detrimental to the development of life as we know it. We could also consider how distance-based dispersal of ammonia could affect the potential for habitability.

In addition to several outstanding uncertainties, there are several challenges presented when considering the suitability of oceans worlds to permit life beyond Earth. Firstly, we cannot directly compare icy moon oceans to any known environment on Earth. There are terrestrial environments that contain high concentrations of ammonia effluent. However, these environments do not present the other physicochemical extremes (e.g., pH, temperature, pressure) that would make them suitable as an analogue for icy moon ocean environments. We also

do not yet have precise physicochemical information regarding the oceans. Icy moon oceans are sealed below ice shells in the order of several to hundreds of kilometres thick, generating hydrostatic pressures of tens to a few hundred MPa at the seafloor, and up to a few GPa at the seafloor of larger moons (Billings and Kattenhorn, 2005, Nimmo and Bills, 2010, Baland et al., 2014, Čadek et al., 2016, Lucchetti et al., 2017, Vance et al., 2018, Levin et al., 2026). While missions could incorporate ice drilling instrumentation, technological advancements in drilling are limited as ice sheets on Earth reach a maximum thickness of 4.9 kilometres (Fretwell et al., 2013). Thus, the ocean chemistries, including ammonia, are not fully clarified.

The challenges presented mean the presence and abundances of salts, volatile organics, and the temperature, pH, and pressure of the oceans can only be estimated from surface observations. In turn, conditions within *in vitro* experiments can only be based upon these estimations or speculative assumptions. This is a particular challenge when considering ammonia as a habitability factor: what is the concentration of ammonia within the oceans? What is the speciation of ammonia in the oceans? Could the concentration of ammonia, along with pressure and temperature conditions in the oceans, sequester NH_3 into non-toxic solid hydrates? Could ammonia-based life develop, thus negating the lethality of ammonia? These questions cannot be defined with precision, yet define ammonia toxicity.

What we do know is that as well as an antibiotic, ammonia is a prebiotic molecule. Alkaline hydrothermal vents coinciding with ammonia could have supported the emergence of life on Earth. We also know that several prebiotic prerequisites for the emergence of life on Earth are also present on Enceladus, Titan and Europa. For example, there is evidence of tidal heating (Carr et al., 1998, Nimmo et al., 2007, Roberts and Nimmo, 2008, Chen et al., 2014, Běhounková et al., 2021) or radiogenic heating (Grasset et al., 2000, Sohl et al., 2014) on all three ocean worlds. Hydrothermal activity at the ocean floor of Enceladus and Europa (Zolotov, 2007, Matson et al., 2007, Hand et al., 2007, Vance et al., 2007, Hsu et al., 2015) is plausible, akin to origin-of-life hydrothermal vents on Earth. Redox chemistry on Titan could supply essential chemical energy (McKay and Smith, 2005, McKay, 2016). The essential elements for life on Earth, the CHNOPS suite (carbon, hydrogen, nitrogen, oxygen, phosphorus, sulphur), have been detected or are otherwise feasible on Enceladus (Waite et al., 2009, 2017, Postberg et al., 2023, Xu et al., 2025). Many of the CHNOPS have also been detected on Titan (Sagan et al., 1992, Hiscox, 2000, Owen, 2000, Nixon, 2024) and Europa (Hiscox, 2000, Szalay et al., 2024). Organics have been directly detected in the plume of Enceladus (Waite et al., 2009, Postberg et al., 2018), in the atmosphere of Titan (Lellouch et al., 1989, Niemann et al., 2005), and have been tentatively detected on the surface of Europa (McCord et al., 1998). The combination of liquid water, heat, chemical energy, and organic molecules would suggest these environments could feasibly host habitable environments. The geological chemistries presented on icy moons, in addition to ammonia, thus make ocean worlds strong astrobiology targets in the search for life.

When considering the potential for biological life on other celestial bodies, it must be considered that conditions within icy moons may be habitable but not inhabited (Cockell, 2014, 2020). We must also consider that many other conditions in addition to ammonia (i.e., temperature, pressure, and salinity) also play critical roles in microbial viability. However, before we can philosophise of ammonia-water habitability, or explore the impact of multi-extremes on

life including ammonia, we must first understand fundamental aspects of life in ammonia that remain in question. These will not determine whether ammoniacal environments are truly habitable, but they will assess the potential for habitability on both icy moon and Earth environments as a function of this single parameter.

3

Methodology

Contents

3.1 Bacterial strain selection

For all experiments, the aerobic, gram negative bacterium *Halomonas meridiana* Slthf1 (DSM 15724) was selected (Figure 3.1). *Halobacteria* are often polyextremophilic and thus ideal models for astrobiology (Wu et al., 2022). This strain was originally isolated at a depth of 2000 m from a low temperature hydrothermal fluid in the East Pacific Rise. As a consequence of this deep, low temperature ocean environment, *H. meridiana* exhibits several adaptations to extremes of salinity, pH, temperature, and pressure. Firstly, *H. meridiana* is a halophile with optimum growth at 2 to 7% (w/v) NaCl, and can exhibit growth in up to 22% (w/v) NaCl. *H. meridiana* is also alkalitolerant, growing optimally at pH 8 but with growth tolerance up to pH 12. *H. meridiana* can also continue to grow in temperatures as low as -1 °C and shows piezotolerance; growth under 550 bar has been recorded (Kaye and Baross, 2004, Kaye et al., 2004). These adaptations categorise *H. meridiana* as an extremophile.

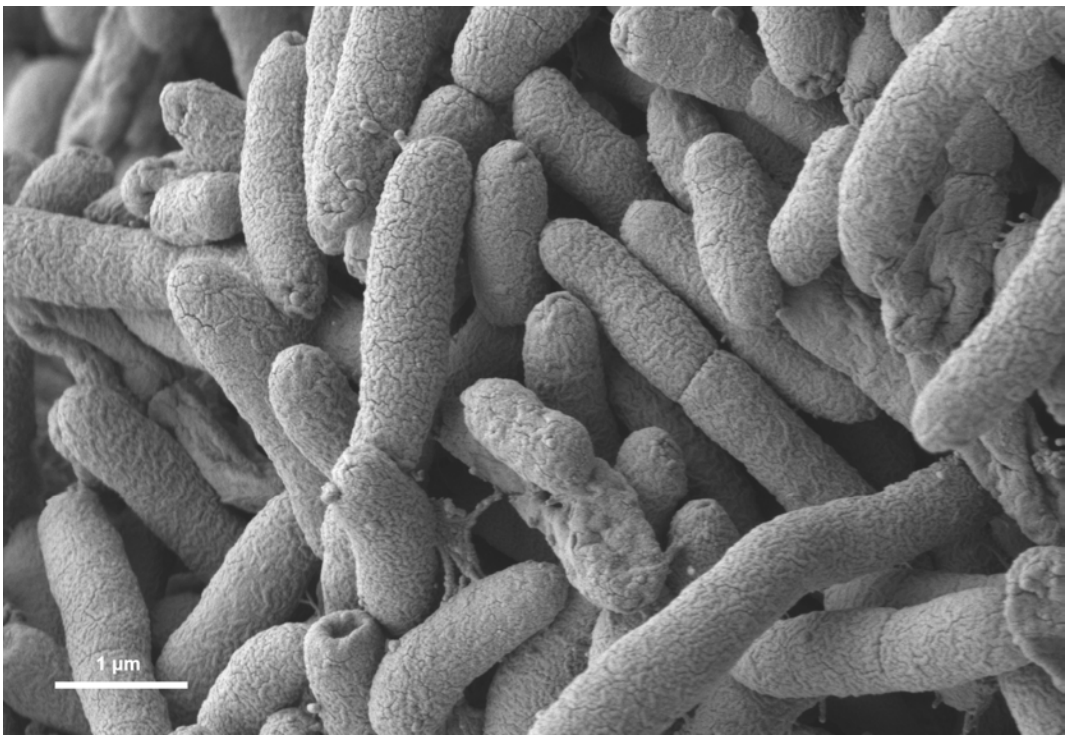

Figure 3.1: Cryo-SEM of *Halomonas meridiana* Slthf1. Scale bar = 1 µm. Imaged using a FIB-SEM (FEI) with SESI signal detection. Accelerating voltage: 2.00 kV, probe current: 100 pA, working distance: 5.0 mm, ESB grid: 300 V, magnification: 14,000 ×.

For the purpose of this thesis, the selection of *H. meridiana* was underpinned by three criteria:

1. An isolation location with geological and physicochemical similarities to those that could occur in icy moons oceans. Icy moons subsurface oceans such as those of Enceladus and Europa are hypothesised to contain hydrothermal vent systems (Glein et al., 2007, Matson et al., 2007, Hand et al., 2007, Vance et al., 2007, Hsu et al., 2015), and could have available oxygen for aerobic metabolism (Teolis et al., 2017, Ray et al., 2021, Hesse et al., 2022, Szalay et al., 2024). The waters of Enceladus, Titan, and Europa are also thought to be saline, and with exception of Titan, could exhibit salinities comparable to Earth's ocean (Zolotov, 2007, Sahai et al., 2024). The waters of these deep extraterrestrial oceans are also cold, likely below 0 °C (Kargel et al., 2000, Marion et al., 2003, Melosh et al., 2004, Matson et al., 2012, Sohl et al., 2014, Glein et al., 2015), and under hydrostatic pressure (Kargel et al., 2000, Vance et al., 2018, Journaux et al., 2020, Neveu et al., 2020, Schoenfeld et al., 2023, Xu et al., 2025). The environment of isolation is therefore highly relevant to icy moons.
2. This bacterium has associated physiological metabolisms that support its survival in fluids with properties similar to icy moons. The extremophilic adaptations presented by *H. meridiana* are relevant to survival in low temperature, high pH brines under pressure, characteristics comparable to the ocean waters of icy moons.
3. *H. meridiana* exhibits no known adaptation to ammonia. The purpose of this thesis was not to study ammonia adaptation as is found in AOB, but rather to study the limits of

life in ammonia. Icy moons such as Enceladus and Europa are estimated to contain only small concentrations of ammonia, and the concentration of ammonia on Titan could be as low as 1.5%. Thus, it was not necessary to study an ammonia adapted bacterium but rather assess whether ammonia could be a chemical parameter which limits habitability for organisms without ammonia adaptations.

An additional rationale for the selection of *H. meridiana* was availability of the genome sequence (Takahashi et al., 2020) [DDBJ, accession no. AP022821]. As described below, metabolomic analysis formed a part of this work. While a complete genome sequence is not a requirement for metabolomics, it provides benefits in scientific accuracy and validity. For example, the genome sequence can provide a point of reference to confirm whether a certain metabolite or pathway identified in the metabolomic analysis is substantiated by genes present in the whole genome. These factors made *H. meridiana* the ideal candidate to explore the objectives of this thesis.

3.2 Bacterial culture

Standard microbial techniques were used throughout this thesis. All materials used in culturing were either sterile single-use plastic or sterilised by autoclaving at 121 °C for 20 minutes. Aerobic culture of *H. meridiana* was performed in glass conical Erlenmeyer flasks at 28 °C in an orbital bench-top shaking incubator set to rotate at 150 RPM. Aerobic cultures were initiated and manipulated with sterile pipette tips using aseptic technique in a laminar flow hood. *H. meridiana* was grown in yeast media consisting of 1g/100 mL Bacto™ yeast extract (Becton, Dickinson and Company), 0.2 M NaCl (Thermo Fisher Scientific, CAS Number: 7647-14-5) and distilled water (dH2O). Yeast extract was chosen to simulate an aqueous environment where there is an availability of nutrients via single-cell organic debris, as opposed to peptone or tryptone which contain materials derived from more complex animals. A concentration of 0.2 M NaCl was selected as this is the concentration of NaCl estimated within the ocean of Enceladus (Postberg et al., 2009). Although several salts and organics comprise the waters of icy moon oceans, the addition of too many variables would restrict the ability to attribute microbiological effects to ammonia.

3.3 Preparation of ammoniacal solutions

All aqueous ammonia solutions were prepared from 35% ammonium hydroxide (Fisher Scientific, CAS Number: 1336-21-6) in yeast media to desired concentrations. Solutions of ammonium sulphate ($(NH_4)_2SO_4$) were prepared from a 2 M stock solution of $(NH_4)_2SO_4$ in yeast media. These solutions were assumed to dissociate fully into NH_4^+ and SO_4^{2-} ions in aqueous solution. Although minor speciation such as HSO_4^- formation or ion pairing may occur depending on pH, temperature, and ionic strength, NH_4^+ and SO_4^{2-} were expected to dominate under the experimental conditions used in this study. To preserve the relative proportion of NH_3 and NH_4^+ and ensure microbiological effects observed were derived purely from ammonia, the pH of these solutions was not adjusted. However, pH-matched solutions of yeast media were created by addition of either sodium hydroxide (NaOH) or hydrochloric acid (HCl). The pH of solutions was determined with a Jenway 3510 bench-top pH meter. pH was

matched to within ± 0.01 pH units. All solutions were filter-sterilised through a 0.22-micron pore before use. Ammonia concentrations were selected in a range that includes the lowest concentration threshold of ammonia estimated for the ocean of Enceladus (≈0.01 M) (Fifer et al., 2022, Glein and Truong, 2025), as well as the highest concentration threshold (≈0.1 M) (Fifer et al., 2022). Values that could be representative of the ammonia concentrations within the ocean of Titan (greater than 0.5 M) were also utilised (Brassé et al., 2017).

3.4 Measurement of ammonia

In Chapters 4 and 5, changes in ammonia concentration over time were assessed by direct measurement. For this, ammonia concentration were deduced by a direct nesslerization reaction using the CHEMetrics High Range VACUette Ammonia Test Kit (K-1510C). Direct nesslerization determines ammonia concentration by a reaction of ammonia with potassium mercuric iodide. This produces a yellow-coloured complex, the Nessler reaction product, which can be measured at 420 nm (Jeong et al., 2013). The K-1510C kit features a detection range of 0-10,000 ppm ammonia and a detection limit of 100 ppm, along with standards of ammonia. The standards were utilised to create a calibration curve of known concentrations of ammonia in ppm against absorbance at 420 nm (Figure 3.2).

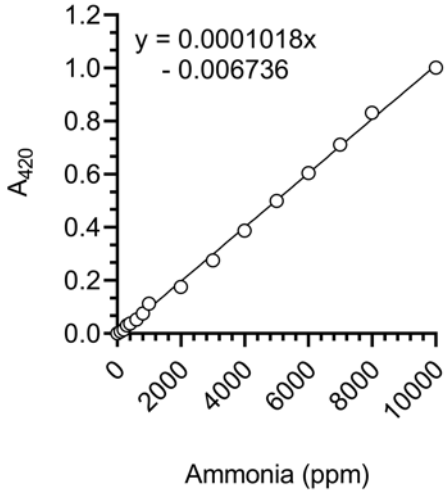

Figure 3.2: Absorbance of ammonia at 420 nm as a function of standard ammonia concentrations (ppm). Data points were obtained by direct nesserlization reaction of known concentrations of ammonia and subsequent absorbance readings at 420 nm. The calibration curve was created by linear regression. Samples of unknown ammonia concentration were determined by calculation of x (Eq. 3.1).

Ammonia concentration of a sample was determined by rearrangement of the linear regression equation (Eq. 3.1).

$$x = \frac{A_{420} + 0.006736}{0.0001018} \tag{3.1}$$

Molarity of ammonia was derived from ppm as shown in Eq. 3.2, where 1 ppm≈1 mg/L, and molar mass refers to the molar mass of ammonia expressed in g/mol.

$$M = \frac{ppm \div 1000}{Molar\ mass} \tag{3.2}$$

3.5 Relative abundance of NH_3 and NH_4^+

In Chapter 4, the relative abundance of NH_3, and thus NH_4^+, in a sample was deduced indirectly by calculation. In solution, NH_3 and NH_4^+ exist in equilibrium:

$$NH_3 + H_2O \rightleftharpoons NH_4^+ + OH^-$$

The proportion of NH_3 in an ammonia sample is primarily influenced by pH. Alterations in pH alter the protonation environment, thereby changing the relative proportions of protonated and deprotonated ammonia in accordance with the Henderson–Hasselbalch relationship between pH and the negative log of the acid dissociation constant (pK_a). As such, the concentration of NH_3 in a sample can be derived by the total ammonia concentration ($[NH_3] + [NH_4^+]$), as in Eq. 3.3.

$$[NH_3] = [NH_3 + NH_4^+]/1 + 10^{(pK_a - pH)} \tag{3.3}$$

However, salinity, temperature, and pressure also impact the abundance of NH_3. Salinity (ionic strength), pressure, and temperature can alter the pK_a of NH_4^+ in solution. Theoretical calculations by Whitfield (1974) on the hydrolysis of NH_4^+ in sea water, and the subsequent use of these calculations by Hampson (1977) to derive the relationship between total ammonia and NH_3 in ocean waters, were used in this thesis to calculate the proportion of NH_3 in a sample based upon changes in salinity, temperature, and pressure. The steps in this calculation are outlined below.

Step 1: pK_a as a function of salinity
Whitfield (1974) and Hampson (1977) provided the relationship between ionic strength (*I*) and pK_a as a function of salinity (pK_a^s) (Eq. 3.4), and provided pK_a^s values of NH_3/NH_4^+ at various ionic strengths. These data points were plotted in a linear regression analysis (Figure 3.3). Using the linear regression equation, pK_a^s could be calculated by Eq. 3.5.

In this thesis, ionic strength refers to the stoichiometric ionic strength, calculated from the analytical concentrations of dissolved ions in solution. Stoichiometric ionic strength assumes ideal behaviour, calculating the total potential concentration of ions assuming full dissociation of salts. An alternative definition is effective ionic strength, which incorporates non-ideal solution behaviour. This considers activity coefficients or ion pairing effects that may occur in concentrated electrolyte solutions. However, because the solutions used in this thesis were prepared from defined salt compositions and were of moderate ionic strength, the stoichiometric ionic strength provides a practical and widely adopted approximation for calculating equilibrium constants such as pK_a. The use of stoichiometric ionic strength is therefore appropriate for estimating the NH_3/NH_4^+ speciation. For this work, a salinity of 11.688 ppt was utilised. An *I* of 0.236 M and a pK_a^s of 9.274 was calculated.

$$I = \frac{19.9273 \times S}{1000 - 1.005109 \times S} \tag{3.4}$$

$$pK_a^s = 0.1179(I) + 9.246 \tag{3.5}$$

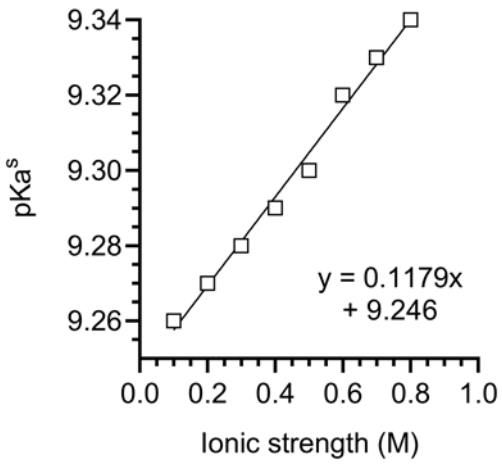

Figure 3.3: Ionic strength vs. pK_a^s values. Data points were obtained from Hampson (1977), and plotted to provide a regression for calculating pK_a^s. The linear regression line is shown. The linear regression equation, $y = 0.1179x + 9.246$, was used to calculate pK_a^s, where $pK_a^s = y$ and $I = x$. This is shown in Eq. 3.5.

Step 2: pK_a as a function of temperature
Calculations by Fouad (1955) demonstrated the linear relationship between temperature (T) and the hydrolysis of NH_4^+ in salt solutions (pK_a^T). The linear equation is shown in Eq. 3.6.

$$pK_a^T = 18.915 - 0.0324(T) \tag{3.6}$$

Whitfield (1974) deduced that, assuming data lines by Fouad (1955) were parallel to the line defined by Eq. 3.6, it is possible to predict temperature effects in salt solutions from experimental or calculated values at the relevant ionic strength at 25 °C (298 K) (Eq. 3.7). In this thesis, a temperature of 28 °C (301.15 K) was used.

$$pK_a^T = pK_a(\text{at 298 K}) + 0.0324(298 - T) \tag{3.7}$$

Step 3: pK_a as a function of pressure
Finally, Whitfield (1974) deduced a linear regression equation describing the relationship between pressure (P) and pK_a (pK_a^P) (Eq. 3.8). A pressure of 1 atm was used in this thesis.

$$pK_a^P = pK_a(\text{at 1 atm}) + 0.0415(P/T) \tag{3.8}$$

Step 4: Integration
pK_a can be calculated by the sum total of $pK_a^s + pK_a^T + pK_a^P$ (Eq. 3.9).

$$pK_a = pK_a^s + 0.0324(298 - T) + 0.0415(P/T) \tag{3.9}$$

Integrating Eq. 3.9 into Eq. 3.3, NH_3 concentration can be calculated by Eq. 3.10, and the percentage abundance of NH_3 and NH_4^+ calculated respectively by Eq. 3.11 and Eq. 3.12.

$$[NH_3] = [NH_3 + NH_4^+]/1 + 10^{(pK_a^s + 0.0324(298-T) + 0.0415(P/T) - pH)} \tag{3.10}$$

$$\%NH_3 = \frac{[NH_3]}{[NH_3 + NH4^+]} \times 100 \tag{3.11}$$

$$\%NH_4 = 100 - \%NH_3 \tag{3.12}$$

3.6 Spectrophotometry

Throughout this thesis, optical density (OD) measurements using visible light spectrophotometry were utilised to characterise *H. meridiana* growth and dynamics. OD measurements are based on the absorption of visible light. Specifically, the detection of light transmitted through a material at a specified wavelength. A sample of suspended bacterial cells will scatter light, thus reducing the amount of light detected in a spectrophotometer. A higher number of bacterial bodies therefore correlate with a reduction of light detected. This is characterised by a higher absorbance value, although light is technically scattered. The absorbance value given is thereby proportional to bacterial density, and can be continually measured over a specified time period to provide information on propagation and growth phases. An OD of 600 nm (OD_{600}) was chosen as this wavelength is not known to cause damage or hinder the growth of bacteria.

The measurement of transmitted light is sensitive and can be affected by culture media components. Each OD reading was therefore blanked with the specific solution used for culture. All growth experiments were conducted in a 96-well plate with readings taken by a BMG SPECTROstar Nano Microplate Reader at 28 °C. To examine growth limits, 190 µL of a selected experimental solution was inoculated with 10 µL overnight *H. meridiana* culture to OD_{600} = 0.05 in a 96-well plate. Inoculation to OD_{600} = 0.05 was chosen as this provides a low, but still measurable, starting point for experiments. An initial cell density of OD_{600} = 0.05 would be expected to exhibit a lag and log phase before reaching a stationary phase and death phase, thus recording the full spectrum of growth dynamics. Positive controls were 190 µL yeast media inoculated with 10 µL overnight *H. meridiana* culture to OD_{600} = 0.05. Negative controls were 200 µL yeast media with no inoculant. Experiments were conducted to yield three standard microbiological growth parameters: lag phase duration, doubling time or growth rate, and final OD. The calculation of these parameters are described in more detail in each research chapter. These growth kinetics were utilised as a tool to define the limits of life in ammonia by assessing bacterial health and proliferation.

3.7 Colony-forming units

In addition to OD, the viability of *H. meridiana* was also characterised throughout this work. Cell viability was assesed by plating diluted bacterial samples onto agar plates made with yeast media. A colony-forming unit (CFU) is formed when viable cells settle on the nutrient agar plate and divide to form a visible colony. The number of visible colonies is therefore directly proportional to the number of viable cells in the original sample, after accounting for any serial dilution during the plating process. While bacterial density in the form of OD is a useful methodology that provides insight into bacterial growth, it does not define whether the bacterial cells are alive. Bacterial bodies do not need to be viable to scatter light. This technique therefore allowed me to characterise cell death as a consequence of ammonia exposure.

Additionally, standard microplate lids for 96-well plates utilised in spectrophotometry do not provide an air-tight seal. In Chapter 4, I consider the growth of *H. meridiana* in a closer-air growth system in which NH_3 cannot escape. For this, I utilised an air-tight falcon tube with

sufficient head space for oxygen as the culture vessel. Transparent, air-tight seals that are gas impermeable are available for microplates, however these would equally limit the exchange of oxygen, essential for bacterial growth, as well as ammonia. In instances where bacteria were grown under these closed-air environments, and thus could not be assessed in a 96-well plate, bacterial growth was assessed by CFU at the end of a treatment condition. In all instances, agar plates were stored at 28 °C prior to enumeration of colonies.

3.8 Untargeted metabolomic analysis

In Chapter 4 and Chapter 6, an untargeted metabolomics approach was employed. Metabolomics offers an end-point biochemical snapshot not accessible through transcriptomic or proteomic analyses. The untargeted approach was utilised to gain a broad overview of the *H. meridiana* metabolome following exposure to different conditions: 0.25 M ammonia in yeast media, 0.5 M $(NH_4)_2SO_4$ in yeast media, yeast media adjusted to pH 10.18 with NaOH, and unamended yeast media (control).

The metabolomics process is divided into three steps: (1) sample preparation, (2) metabolite separation and detection, and (3) annotation and data analysis. The complete metabolomics approach is detailed in Chapter 4 and Chapter 6, however the essential steps are summarised here. In the first step, samples of *H. meridiana* were grown to and harvested at a defined OD_{600} of 0.5. To preserve the metabolomic response, further cellular metabolism was halted by quenching. Samples were aliquoted into microcentrifuge tubes and quenched by rapid cooling through submersion in a dry ice and 70% (v/v) ethanol bath. Surplus media was removed through centrifugation. Extraction of metabolites was achieved by submerging *H. meridiana* in ice-cold chloroform/methanol/water (1:3:1 ratio). The application of chloroform and methanol disrupts the cell membrane through lipid interactions and precipitates proteins. Methanol and water act to solubilise semi-polar and polar metabolites, while chloroform acts to solubilise non-polar metabolites. Metabolites were separated from cell debris by centrifugation at 13,000 $\times$ g. A quality control (QC) sample mirroring the total metabolite diversity of the study was created by pooling an aliquot of all samples.

The second step of metabolomics and a portion of the third step were carried out by the EdinOmics research facility at the University of Edinburgh [RRID: SCR_021838]. In the second phase, metabolites were separated by their chemical properties using ultra high performance liquid chromatography (UHPLC) to reduce complexity and signal overlap. Metabolites were subsequently analysed by ion mobility (IM) quadrupole time-of-flight (TOF) mass spectrometry (MS) using electrospray ionization (ESI). ESI ionizes intact metabolites by adding or removing protons, allowing their detection as charged species. Ions passed firstly through the IM cell. The IM component of MS consists of an internal environment filled with gas under an electric field. The travel time of ions through the IM spectrometer defines the drift time. As drift time is dependent on the size, shape and charge of an ion, the effective size and shape of ions is also characterised. This is known as the collision cross section, and is measured based on how ions interact and collide with gas molecules while travelling through the IM cell.

The ions then travel through the quadrupole mass analyser and the TOF flight tube containing a detector. The quadrupole component filters ions through an electric field that only permits

the travel of ions with certain mass-to-charge ratios (m/z), thus determining the mass and charge of ions. The TOF component measures the time taken for an ion to reach a detector from an ion source. TOF depends on both the ion's mass (i.e., heavier ions travel slower) and charge (i.e., ions with higher charge accelerate faster through the electric field), and thus indirectly infers the m/z value. The m/z is utilised to derive the accurate mass (i.e., the exact mass of an ion) and precise mass (i.e., the consistency of mass measurements across repeated analyses). In this process, the QC sample was injected at the beginning of the experiment and after every five test samples. Since the QC composition is constant, any changes in signal over time can be attributed to instrumental drift or technical variation, not biological difference. Repeated processing of the QC allows technical variation to be monitored and corrected if needed.

Chemical data retrieved from MS was subsequently processed to annotate metabolites. As multiple ions were measured simultaneously in a multiplexed approach, data was demultiplexed using the PNNL PreProcessor software. Accuracy and consistency in the mass and drift time data was ensured by recalibration against known reference compounds using the AgtTofReprocessUi and IM-MS Browser 10.0 in the Agilent MassHunter software suite. Molecular features including retention time in UHPLC, drift time and accurate mass in MS were extracted and grouped using the Agilent MassHunter Mass Profiler 10.0 to begin building a profile of individual ions. Metabolites were identified using the McLean CCS Compendium PCDL library 80, an online tool that matches molecular features of accurate mass and collision cross section to known compounds in the library.

With the annotated list of metabolites, I then carried out a comparative analysis of metabolites across the different treatment conditions. The annotated list of metabolites were uploaded to the MetaboAnalyst 6.0 web-based platform. Data was log-transformed and Pareto-scaled. Log transformation reduces data skewness and improves normality. Pareto-scaling normalizes data by reducing, but not eliminating, the dominance of variables with large variance. Unlike auto-scaling which equalizes variance, or mean-centring which retains the original variance scale, this preserves metabolites with naturally large variation. This often occurs naturally in living systems. Pareto-scaling also prevents variables with smaller variance from being overshadowed. The metabolite data was then subjected to multivariate (principal component analysis, heatmap) and univariate (ANOVA, volcano plots, box and whisker plots) statistical analysis. The raw metabolomics dataset associated with Chapter 4 and Chapter 6 is publicly available on GitHub [`https://github.com/cmhopton/Metabolomics.git`].

3.9 Transmission electron microscopy

Transmission electron microscopy (TEM) was utilised in Chapter 4 and Chapter 6 to explore the ultrastructural changes in *H. meridiana* associated with aqueous ammonia and $(NH_4)_2SO_4$ exposure. As cells can be sectioned in TEM and the internal structures analysed, this phenotypic data was used to inform ammonia toxicity and adaptation mechanisms, and support the metabolomics data. In Chapter 4, overnight cultures of *H. meridiana* were pelleted by centrifugation at 5,000 $\times$ *g* and resuspended for 2 h in one of the following solutions: 1 M aqueous ammonia in yeast media, yeast media adjusted to pH 10.78 with NaOH, or unamended yeast media (control). In Chapter 6, *H. meridiana* grown in 0.5 M $(NH_4)_2SO_4$ in yeast media and unamended yeast media were harvested prior to metabolomics processing. *H. meridiana*

was separated from the aqueous $(NH_4)_2SO_4$ growth media by centrifugation at 5,000 $\times$ g followed by removal of supernatant.

The procedure in both Chapter 4 and Chapter 6 proceeded as follows. Cell pellets were washed with and resuspended in phosphate buffered saline (PBS). PBS is a non-toxic isotonic solution that maintains a stable osmotic environment, thus preventing cell rupture, while also cleansing cells of unwanted material such as remaining culture media. *H. meridiana* were centrifuged at 5,000 $\times$ g and PBS supernatant removed, followed by resuspension of the pellet in 3% glutaraldehyde in 0.1 M sodium cacodylate buffer, pH 7.3. Glutaraldehyde preserves cell structure by cross-linking proteins. Sodium cacodylate was utilised to stabilize pH and maintain osmotic balance. *H. meridiana* was stored in glutaraldehyde fixative until further processing for TEM.

The following procedures were carried out by Steve Mitchell within the TEM facility, School of Biological Sciences, University of Edinburgh. Specimens of *H. meridiana* were washed in 0.1 M sodium cacodylate for 10 minutes to remove excess fixative. This was repeated in triplicate. The membrane of *H. meridiana* was stabilised and stained using 1% osmium tetroxide in 0.1 M sodium cacodylate for 45 minutes. Osmium tetroxide preserves cell structure by cross-linking lipids. Osmium tetroxide also reacts with fatty acid double bonds; this process reduces osmium tetroxide and deposits metallic osmium into the cell, increasing the electron density of cell structures.

Long-term preservation of cell structure was achieved by embedding samples in resin, which also creates a solid matrix for ultra-thin sectioning. As resin is hydrophobic and immiscible with water, the water contents within *H. meridiana* cells were firstly removed by replacement with ethanol in a gentle, gradual process. This involved application of 50%, 70%, 90% and then 100% ethanol three times for 15 minutes each. This was followed by two 10-minute changes in propylene oxide. Propylene oxide is miscible in both ethanol and resin and therefore acts as a transition solvent between these stages. Following embedment in resin, thick sections of preserved *H. meridiana* were cut using a Leica Ultracut ultramicrotome. The sections were stained with toluidine blue, and areas of interest identified under a light microscope. From the identified areas, ultra-thin 60 nm sections were cut and stained with uranyl acetate and lead citrate. Uranyl acetate stains nucleic acids and proteins, while lead citrate stains membranes, nucleoli, cytoplasmic proteins, granules and ribosomes, increasing the electron density of these structures.

The fixed, stained and sectioned *H. meridiana* specimens were subsequently imaged by myself using the JEOL JEM-1400 Plus TEM. Images were collected on a GATAN OneView camera at 4K resolution. Ultra-thin sections are required for TEM as this technique operates by penetrating electrons through samples; electrons do not penetrate well through thick samples. TEM relies on an electron gun, electromagnetic lenses, sample, electron interaction and a detector.

Firstly, the cathode electron gun emits a beam of high energy electrons which are accelerated in vacuum into a focused beam using an anode. The positive charge of the anode attracts and accelerates the negatively charged electrons emitted from the cathode. The beam of electron is

focused by a series of electromagnetic condenser lenses which control beam illumination. The beam is narrowed to a fine point by a condenser aperture before interacting with the sample specimen. The sample is placed within the beam path.

As the electron beam passes through the sample, electrons are scattered by the electron-dense materials and transmitted through the less electron dense regions. The scattered and transmitted electrons are collected and focused by a further series of electromagnetic lenses (i.e., the objective lens, intermediate lens and projector lens) to a detector. These lenses form the initial magnified image of the sample (objective lens), further magnify and position the image (intermediate lens), and project the final, magnified image onto the detector (projector lens). A greyscale image is formed from electron-dense structures (dark) and electron-light structures (bright) that are captured on a fluorescent screen (for manual, real-time observation) and a CMOS digital detector—the GATAN OneView camera. Although TEM sample processing was primarily conducted by Steve Mitchell, I, Cassie Hopton, was responsible for identifying ultrastructural areas of interest, capturing images, and processing images using the image processing program ImageJ.

4

Ammonia sets limit to life and alters physiology independently of pH in *Halomonas meridiana*

This publication originally appeared in *Scientific Reports*, 4th June 2025.
DOI: 10.1038/s41598-025-03858-z

4.1 Introduction

Icy moons Enceladus and Titan are predicted to contain aqueous ammonia oceans (Lunine and Stevenson, 1987, Glein and Truong, 2025). A higher relative abundance of NH_3 to NH_4^+ is estimated as driven by the high pH of the oceans (Marion et al., 2012, Brassé et al., 2017, Leitner and Lunine, 2019, Glein and Truong, 2025). NH_3 readily permeates cell membranes in an unregulated manner that induces significant intracellular damage (Ritchie and Gibson, 1987a,b, Brazier, 2016). NH_3 is also a weak base that can increase both the external and internal pH of the cell environment (Vines and Wedding, 1960, Taglicht et al., 1987, Horie et al., 1995, Rose et al., 2005). The presence of NH_3 in these oceans may therefore limit the potential for habitability. While the presence of life within the subsurface oceans of icy moons is only speculative, the potential for habitability can be assessed by establishing the limits of terrestrial life in ammoniacal waters. Thus, in this chapter, the potential for habitability in icy moon and Earth environments was assessed by characterising the limits of life in ammoniacal solutions with a high relative abundance of NH_3. The growth, survival limits and physiological response of an extremophile, *Halomonas meridiana*, were characterised in ammonia under two culture systems: a 'closed-air' culture, where all ammonia was retained, and an 'open-air' culture, permitting escape of NH_3 and gradual reduction of ammonia concentration. These systems were utilised as ammonia is presumed to be retained at a constant concentration in the oceans of icy moons (closed-air). However, open-air dispersal could be relevant if cryovolcanic expulsion diminishes ammonia concentrations over time. The open-air system is also relevant to terrestrial environments where NH_3 can readily disperse into the atmosphere. The pH of all ammonia solutions was unmodified; this was to ensure only pure ammonia-water solutions were used. This also maintained a broad spectrum of pH ranges in line with the variable pH ranges characterised for icy moons and high pH soils on Earth. As to provide a comprehensive understanding of the limits of habitability exerted by ammonia, this paper also deconvolutes whether the toxicity of ammonia is based upon an intrinsic rise in external aqueous pH, as indicated in many neutrophilic bacteria (Deal et al., 1975, Kelly et al., 2012).

scientific reports

Check for updates

OPEN

Ammonia sets limit to life and alters physiology independently of pH in *Halomonas meridiana*

Cassie M. Hopton[1]✉, Peter Nienow[2] & Charles S. Cockell[1]

The subsurface oceans of icy moons, expected to retain appreciable concentrations of ammonia, are of significant interest to astrobiology. On Earth, ammonia is released in large quantities, primarily through anthropogenic activities. Ammonia is toxic to many forms of life at high concentrations, and thus it is necessary to understand the habitability impact of ammonia on these environments. The survival limits and physiological response of aerobic bacteria in ammonia, and whether ammonia toxicity is distinct from toxicity by high pH, is poorly understood. Here, we investigate the survival thresholds, growth kinetics, and metabolomic response of *Halomonas meridiana* in ammonia-water solutions and pH-matched sodium hydroxide solutions. Using closed- and open-air systems to mimic environments with NH_3 retention or dispersion, we found complete and partial cell death above 0.05 M ammonia, respectively. In open-air systems, a sub-set of cells survived up to 0.25 M ammonia; metabolomics revealed unique physiological responses to ammonia, including elevation of cyclic compounds and Coenzyme A metabolites, suggesting mechanisms of ammonia toxicity and adaptation. Ammonia and high pH toxicity were found to be distinct. These findings show that ammonia can impose a distinct geobiological limit, potentially constraining the habitability of ammonia-rich terrestrial and extraterrestrial environments.

Ammonia (hereafter considered as total ammonia, ammonia (NH_3) + ammonium (NH_4^+)) is a primordial molecule, formed in the early universe and found abundantly in various environments including Earth's early atmosphere and on other celestial bodies within the solar system[1–3]. Terrestrially, ammonia plays a critical role in the synthesis of amino acids and nucleic acids[4,5], and has an integral role in the global nitrogen cycle[6,7]. Yet, despite biochemical significance, the toxicity of NH_3 has been well-documented across the domains of life[8–11]. NH_3 is gaseous under temperate conditions. The small size and unchanged nature of NH_3 facilitates passive permeation through membranes[12–15], causing significant intracellular disruption[16–18]. The equilibrium between NH_3 and NH_4^+ is influenced by factors such as pH (with NH_3 predominating at pH > 9.25), salinity and temperature[19–21].

Mono Lake, California, underscores the role of NH_3 in shaping microbial ecosystems; depth-dependent shifts in biodiversity are driven by the spatial distribution of abiotic factors including ammonia, which is predominately in the NH_3 form[22,23]. This becomes relevant when considering the habitability of NH_3-rich environments. Ammonia has been detected at a volume mixing ratio of 0.4–1.3% on the icy moon Enceladus, orbiting Saturn[24,25]. The evidence of a saline, liquid water subsurface ocean[26,27], and other physicochemical conditions suitable for life[28–30], has encouraged strong astrobiological interest in this satellite. With a pH predicted at or above 9[29–31], the ocean of Enceladus would bear appreciable amounts of toxic NH_3. Due to the limited research on NH_3 tolerance in bacteria, coupled with the presence of carbon dioxide and hydrogen in the ocean, habitability assessments of Enceladus are currently limited to methanogenic organisms[32–34].

The habitability impacts of ammonia are also relevant terrestrially. Globally, several dozen tetragrams of ammonia are released annually from agriculture[35,36]. Ammonia deposition into soil, water and vegetation occurs as a consequence[37–39]. In alkaline soils (pH > 7), application of ammonium fertilizers leads to NH_3 volatilization. Indeed, applied nitrogen losses of up to 66% have been recorded in alkaline soils as a result of ammonium fertilizer application[40–42]. Although toxicological effects are presumed, the downstream impact of NH_3 volatilization on microbial diversity and community structures in alkaline environments, where the relative abundance of NH_3 exceeds NH_4^+, is not well understood.

To accurately assess the habitability impacts of ammonia, fundamental questions remain. Few studies have systematically investigated the survival limits or physiology of microorganisms under NH_3 stress, where both

[1]UK Centre for Astrobiology, School of Physics and Astronomy, University of Edinburgh, James Clerk Maxwell Building, Peter Guthrie Tait Road, Edinburgh EH9 3FD, UK. [2]School of Geosciences, University of Edinburgh, Drummond St, Edinburgh EH8 9XP, UK. ✉email: c.m.hopton@sms.ed.ac.uk

the concentration and relative abundance of NH_3 is high. Bacteria such as *Bacillus pasteurii* can grow in up to 0.5 M NH_3[43], although it is noted this species can utilise ammonia for ATP generation[44], substrate permeability[45] and oxidation of substrates[46]. Ammonia-oxidising bacteria (AOB) can metabolise both NH_3 and NH_4^+ and can survive in up to 0.5 M ammonia at pH 6[47,48], but the concentration of NH_3 in these solutions is minimal ($NH_3 \approx 0.05\%$, ≤ 0.00025 M). Without specific adaptations, toxicity at 0.1 M ammonia (pH 9.5, $NH_3 > 50\%$) has been observed in *B. subtilis* and *Escherichia coli*. However, similar toxicity was noted in sodium chloride solutions of matching pH[49]. The use of neutrophilic organisms has thus far limited our understanding of whether ammonia toxicity is intrinsically pH-based. There is compelling need for research examining the survival limits and physiological response of an alkaline adapted bacteria in ammonia solutions exceeding pH 9.25 ($NH_3 > 50\%$) and comparing with a pH matched counterpart.

Here, we use a combination of growth kinetics and cell viability assays to identify habitability limits of *Halomonas meridiana* Slfth1 in ammonia solutions with high NH_3 content. This organism lacks specific adaptations to ammonia[50], but possesses alkalitolerant traits relevant for this investigation[51]. We utilise growth systems permitting ("open-air system") or preventing ("closed-air system") gaseous escape to mimic environments where NH_3 is environmentally dispersed and retained, respectively. By using an alkaline adapted organism, we resolve that ammonia toxicity is independent from pH toxicity and, using microscopy and metabolomics analysis, define the specific toxicity effects of ammonia on bacterial physiology independent of pH. Together, these findings advance the understanding of ammonia toxicity and should foster improved habitability assessments of NH_3-rich environments.

Results

Physicochemical properties of ammonia and pH-matched solutions

Ammonia solutions were prepared from liquid ammonia to molar concentrations of 0.01, 0.025, 0.05, 0.1, 0.25, 0.5 and 1 M, equating to pH values between 8 and 11 (Fig. 1a). Positive control (PC) was unamended yeast media. The percentage abundance of NH_3 to NH_4^+ at these concentrations and pH values is given in Fig. 1b. From concentrations of 0.05 M ammonia and higher, NH_3 accounts for over 50% of the total NH_3/NH_4^+ in solution. Solutions of increasing ammonia concentration showed decreased oxygen concentrations; however, this decrease was non-significant from pH-matched counterparts (Fig. 1c). Alterations to water activity with increasing ammonia and pH were also statistically non-significant (Fig. 1d).

Ammonia sets a distinct molarity threshold for viability and growth

Bacteria were grown in ammonia solutions utilising two system types: a 'closed-air' system – to determine growth limits in a perpetually ammonia exposed environment, and an 'open-air' system – to determine growth limits in an environment permitting NH_3 dispersal following volatilization. Figure 2a shows the final colony forming units of *H. meridiana* after incubation in the closed-air system for 72 h. The closed-air system utilised an air-tight falcon tube for culture that was presumed to maintain constant ammonia concentrations by retention of both aqueous and volatilized ammonia. Colonies were evident following incubation in 0.01 M, 0.025 M and 0.05 M ammonia, but colony number decreased as NH_3 increased relative to NH_4^+ (Fig. 1b). A lower number of viable colonies compared to positive control was observed in 0.01 M ammonia ($p < 0.01$). No significant difference in colony number was observed when *H. meridiana* was incubated in 0.025 M compared to positive control ($p = 0.056$) or 0.01 M ammonia ($p = 0.323$). This concentration of ammonia has a pH within the optimum range for *H. meridiana* (pH 9) (Fig. 1a). Lower viable cell numbers were observed when incubated in 0.05 M compared to positive control ($p < 0.0001$) and 0.025 M ammonia ($p < 0.01$). No viable colonies were present following incubation in 0.1 M ammonia or ammonia solutions of higher concentration (Fig. 2a).

Figure 2b shows the growth dynamics of *H. meridiana* Slthf1 over 48 h in increasing concentrations of ammonia in an open-air system. Lag phase duration, doubling time (T_d) and final OD_{600} are presented in Fig. 2c-e, respectively, extrapolated from Fig. 2b of the open-air system. At concentrations exceeding 0.01 M ammonia, lag phase was greater with higher ammonia concentrations; incubation in 0.1 M and 0.25 M ammonia prolongs lag phase time by 6-fold and 25-fold compared to the positive control, respectively (Fig. 2c). The lag phase time in 0.1 M ammonia was higher than that in 0.05 M ammonia ($p < 0.05$). Likewise, the lag phase time in 0.25 M ammonia was higher than that in 0.1 M ammonia ($p < 0.0001$) (Fig. 2c). T_d was also higher with increasing ammonia concentration, with higher T_d compared to the positive control observed in 0.05 M ($p < 0.05$), 0.1 M ($p \leq 0.0001$) and 0.25 M ($p < 0.0001$) solutions (Fig. 2d). The T_d was not significantly altered between positive control and 0.01 M ($p = 0.965$) or 0.1 M and 0.25 M solutions ($p = 0.9972$). Final OD_{600} after 48 h growth showed no statistical difference from positive control in 0.01 M ($p = 0.932$), 0.025 M ($p = 0.330$), 0.1 M ($p = 0.248$) and 0.25 M solutions ($p = 0.135$), but higher OD_{600} values were observed in 0.05 M compared to the positive control ($p < 0.01$) (Fig. 2e). Cell density was lower in 0.5 and 1 M solutions compared to the positive control (0.5 M, $p < 0.01$; 1 M, $p < 0.001$) (Fig. 2e), where no distinguishable growth occurred within 48 h (Fig. 2b).

In Fig. 2b, ammonia appeared to extend lag phase in 0.1 M and 0.25 M ammonia cultures. Onset of the log phase following extended lag phase could indicate an inhibitory, bacteriostatic influence of ammonia that had diminished over time possibly due to NH_3 volatilization and dispersal from the culture solution. However, as the optical density at the lag phase (< 0.05) was below the detectable limit, it is possible cell death events occurring during this period were not adequately represented in the data. Thus, a bactericidal effect whereby cell numbers were reduced and gradually repopulated to numbers that were detectable by optical density could not be ruled out. To deconvolute bacteriostatic and bactericidal effects of ammonia, cell viability within lag phase and early log phase relevant time points were performed in 0.1 M and 0.25 M ammonia culture solutions. Relevant time points align to 0, 4 and 8 h for 0.1 M ammonia solutions, and 0, 4, 8, and 16 h for 0.25 M ammonia solutions. Additionally, ammonia concentrations were measured over these time points to identify whether NH_3 volatilization and dispersal correlated with growth initiation. The results for 0.1 M and 0.25 M cultures are

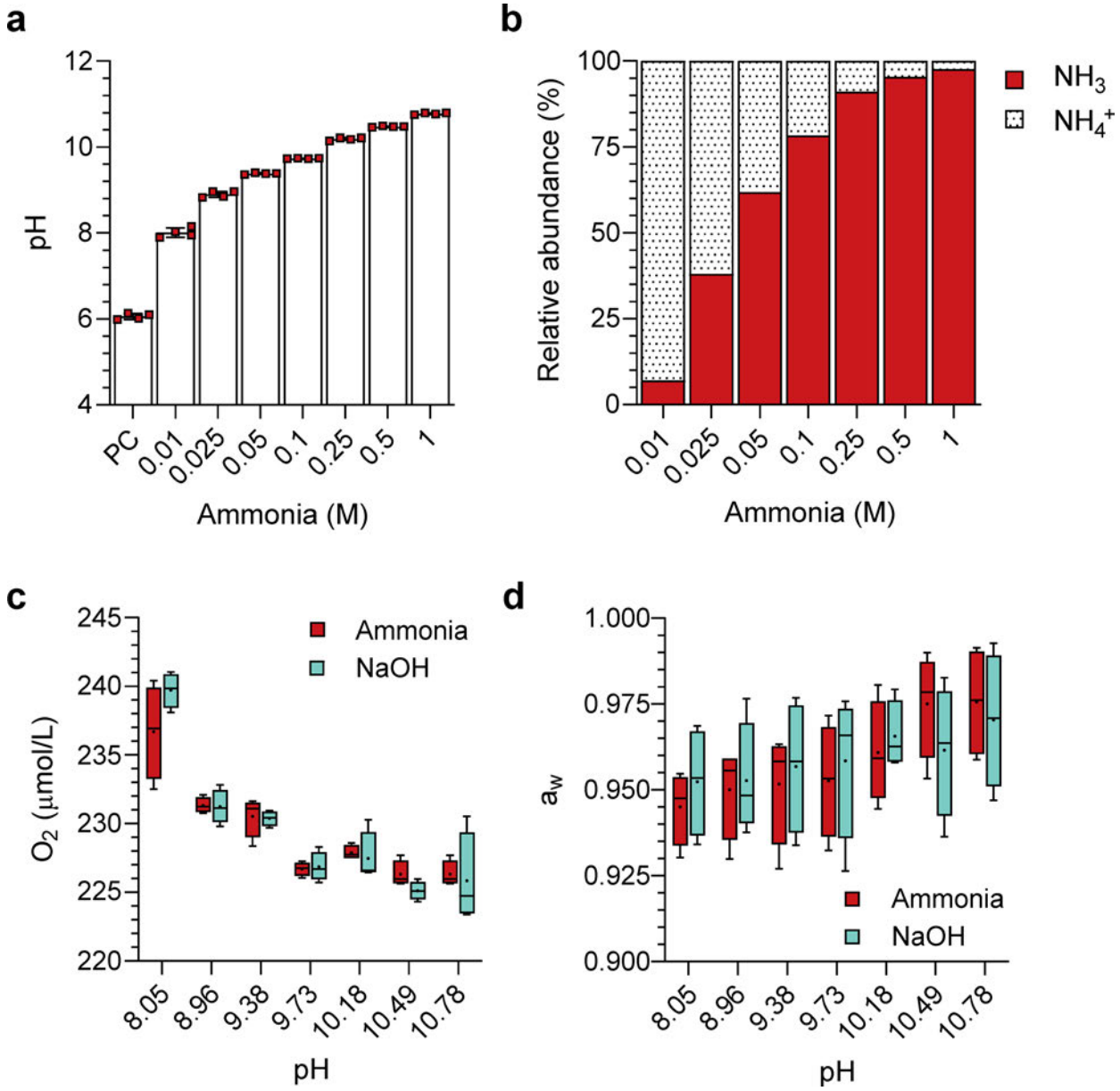

Fig. 1. Properties of ammonia and pH-matched solutions utilised in this study. (**a**) Molar levels of ammonia and corresponding pH values utilised in this study. The positive control (PC) corresponds to growth in unamended yeast media (0 M ammonia) without pH modifications. Column heights and error bars represent mean ± s.d. ($n = 4$). (**b**) Calculated percentage abundance of NH_3/NH_4^+ in molar levels of ammonia utilised in this study. (**c**) Oxygen concentration and (**d**) water activity of ammonia and pH-matched solutions utilised in this study. The upper limit, middle line and lower limit of the boxplots indicate the 25th, 50th (median) and 75th percentiles, respectively. Whiskers represent 1.5× the interquartile ranges. Mean is indicated by a plus sign (+) ($n = 4$). Alterations to oxygen concentration and water activity were found to be non-significant between all ammonia and pH-matched counterparts. Significance is given by unpaired two-tailed t-tests or Mann-Whitney test at each pH. The statistical tests and outcomes are available in Supplementary Table 1.

presented in Fig. 2f and 2g, respectively. After 4 h exposure, viable cells in 0.1 M ammonia showed a 1000-fold decrease from 0 h ($t = 28.28$, df = 4, $p < 0.0001$) (Fig. 2f). In 0.25 M ammonia, viable cells at 4 h were reduced 10-fold from 0 h ($t = 6.499$, df = 4, $p < 0.01$) (Fig. 2g). Bactericidal reduction to cell populations within 0.1 M ammonia solutions cease between 4 h and 8 h, where a small but non-significant increase in cell viability was observed ($t = 2.421$, df = 4, $p = 0.0727$) (Fig. 2f). Likewise, bactericidal effects were absent between 4 h and 8 h in 0.25 M ammonia solutions where cell numbers stabilised ($t = 0.8934$, df = 4, $p = 0.442$) and increased from 8 h to 16 h ($t = 11.76$, df = 4, $p < 0.001$) (Fig. 2g). The increase in cell viability within 0.1 and 0.25 M ammonia solutions at 8 h and 16 h, respectively, aligned with diminished ammonia levels to ≤ 0.05 M at 4 h and 13 h, respectively (Fig. 2f, g). Thus, lag phase extension in the open-air system reflects two events: (1) an immediate bactericidal

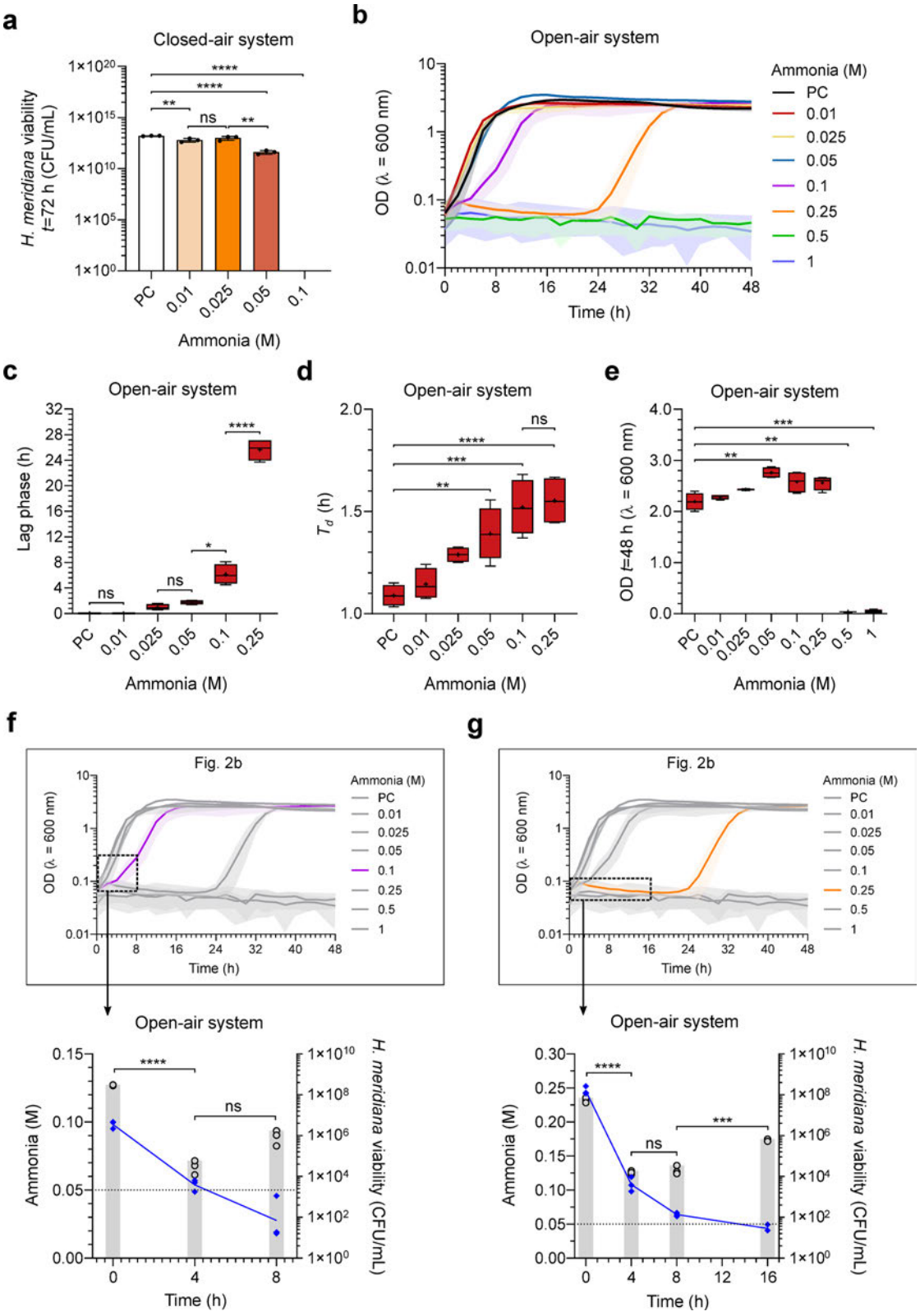

effect and (2) growth initiation after ammonia levels drop to sub-bactericidal levels (≤ 0.05 M) in surviving populations.

Ammonia toxicity is independent from pH toxicity

Ammonia is a weak base that raises solution pH with increasing concentration. To delimitate ammonia toxicity from pH toxicity, growth experiments were repeated in NaOH solutions pH-matched to ammonia solutions. Figure 3a presents the final CFU/mL of *H. meridiana* in pH-matched solutions following 72 h closed-air system incubation. No significant differences were observed between cells grown in positive control and pH-matched

◀**Fig. 2**. Survival limits of *H. meridiana* in ammonia. (**a**) CFU/mL of *H. meridiana* grown in ammonia solutions at 0 (PC), 0.01, 0.025, 0.05 and 0.1 M in a closed system for 72 h. The positive control (PC) corresponds to growth in unamended yeast media (0 M ammonia) without pH modifications. Column heights and error bars represent mean ± s.d. ($n = 3$). Statistical significance is by one-way ANOVA with Tukey's multiple comparison test (F (4, 10) = 27.70, $p < 0.0001$). (**b**) Growth curve of *H. meridiana* over 48 h in increasing ammonia concentrations. Growth curves represent mean OD_{600} values over time ± s.d. (0-0.5 M, $n = 4$; 1 M, $n = 3$). Error is indicated by area fill within error bands. Growth parameters of lag phase (**c**), doubling time (T_d) (**d**) and final OD_{600} at 48 h (**e**) extrapolated from (**b**) are presented. Box plots represent the median as well as the 25% and 75% interquartile ranges. The whiskers represent 1.5× the interquartile ranges. Plus sign (+) indicate the mean and the middle line indicate the median. Welch's ANOVA with Games-Howell's multiple comparison test was used in (**c**) W (3.000, 5.965) = 218.6, $p < 0.0001$) and (**e**) W (7.000, 9.736) = 7919, $p < 0.0001$). Statistics in (**d**) correspond to one-way ANOVA with Tukey's multiple comparison test (F (5, 18) = 14.79, $p < 0.0001$). (**f**, **g**) Time series of ammonia molarity and cell viability (CFU/mL) during the lag phase and early growth of cultures grown in 0.1 (**f**) and 0.25 M ammonia (**g**). The relevance to data points in Fig. 2b is indicated. Ammonia molarity is plotted as a line graph with blue diamond markers on the left axis. Molarity at 0.05 M is indicated by a dotted line. Cell viability is plotted as a column bar graph on the right axis. Line and column heights represent mean ± s.d. ($n = 3$). For cell viability, statistical difference between means is given by unpaired t-test. ns, no significance; *, $p < 0.05$; **, $p < 0.01$; ***, $p < 0.001$; ****, $p < 0.0001$.

solutions up to pH 10.78 (equivalent to 1 M ammonia), with exception of cells grown in pH 10.18 where cell number was higher ($p < 0.05$). The outcome of the statistical analyses are available to view in Supplementary Table 2. Figure 3b presents the growth curve of *H. meridiana* grown under pH-matched NaOH solutions in an open-air system, with extrapolated parameters of lag phase (Fig. 3c), T_d (Fig. 3d) and final OD_{600} (Fig. 3e) presented in Log_2 fold changes (Log_2FC) from growth in ammonia solutions of the same pH. For cells grown in pH 8.05 and 0.01 M ammonia, there was a non-significant difference between lag phase duration ($U = 8$, $p > 0.999$), T_d ($t = 1.55$, df = 6, $p = 0.171$), and final OD_{600} ($t = 0.798$, df = 6, $p = 0.456$). But, significantly altered lag phases, T_d and final OD_{600} were observed for higher pH and ammonia values. Lower lag phases were observed in cells grown in pH 8.96, pH 9.38, pH 9.73 and pH 10.18 compared to those grown at 0.025 M ($t = 4.399$, df = 3, $p < 0.05$), 0.05 M ($t = 11.26$, df = 3, $p < 0.01$), 0.1 M ($t = 7.663$, df = 3.02, $p < 0.01$) and 0.25 M ammonia ($t = 29.05$, df = 3.05, $p < 0.0001$) (Fig. 3c). T_d was significantly lower for cells grown in pH 8.96 ($t = 2.453$, df = 6, $p < 0.05$), pH 9.38 ($t = 4.235$, df = 6, $p < 0.01$), pH 9.73 ($U = 0$, $p < 0.05$), and pH 10.18 ($t = 2.532$, df = 6, $p < 0.05$) compared to ammonia counterparts (Fig. 3d). Final OD_{600} at 48 h was lower in NaOH pH 8.96 ($t = 4.577$, df = 3, $p < 0.05$), pH 9.38 ($t = 7.914$, df = 6, $p < 0.001$), pH 9.73 ($t = 2.786$, df = 6, $p < 0.05$) and pH 10.18 ($t = 5.173$, df = 6, $p < 0.01$) than to growth in ammonia counterparts. Higher OD_{600} was observed in pH 10.49 ($t = 16.09$, df = 3.01, $p < 0.001$) and pH 10.78 solutions ($t = 15.59$, df = 3.12, $p < 0.001$) compared to ammonia counterparts (Fig. 3e), indicating lag phase extension and absent growth in 0.5 and 1 M ammonia could not be attributed to pH increases.

To broaden the pH comparison beyond NaOH, lag phase analysis was used to explore whether the prolonged lag phase in 0.25 M ammonia (Fig. 2c) could be replicated in KOH, Na_2SiO_3, K_2CO_3, and Na_2CO_3 at pH 10.18 (Fig. 3f). No differences in lag phase duration were observed between *H. meridiana* grown in Na_2SiO_3 ($p = 0.779$) or Na_2CO_3 ($p = 0.996$) compared to NaOH. Longer lag phases were seen in KOH ($p < 0.05$) and K_2CO_3 ($p < 0.0001$) compared to NaOH, possibly reflecting reduced adaptation to potassium in *H. meridiana*. All high pH cultures showed a significantly shorter lag phase than 0.25 M ammonia cultures ($p < 0.001$), confirming the pH-independent toxicity of ammonia.

Ammonia toxicity exerts distinct changes to bacterial morphology

Specific bactericidal effects of ammonia on cells can be observed in Fig. 4. Under control growth conditions (unaltered yeast media) (Fig. 4a-b), *H. meridiana* exhibited ribosome-rich cytoplasm, visible nucleoids and clear division of outer membrane, periplasm and inner membrane. Cells exhibited irregular, undulating outer membrane, an enlarged periplasmic space and PHA-like granules. Upon 2 h treatment of 1 M ammonia (Fig. 4c-d), cells showed intracellular aggregation and loss of ribosomes with some showing cytoplasmic loss and lysis. The periplasmic space volume decreased, and detachment of the inner membrane from the outer membrane was observed. Cells showed expansion of electrolucent cavities, possibly surrounding nucleoids. Condensed material within the electrolucent cavities exhibited splayed morphologies, possibly indicating disruption to DNA supercoiling. Cells exposed to a NaOH solutions pH-matched to 1 M ammonia (10.78 pH) also showed some cell lysis events (Fig. 4e-f). However, there were few morphological differences from cells grown in control media. Differences include uniform outer membrane, and fewer PHA-like granules.

Metabolic pathways altered in response to ammonia and high pH exposure

The survival of cells in up to 0.25 M ammonia in an open-air system suggests adaptations enabling tolerance to ammonia. Untargeted metabolomics was performed on *H. meridiana* in unamended yeast media (hereafter denoted 'control') and yeast media with 0.25 M ammonia at pH 10.18 (hereafter denoted '0.25 M ammonia') to determine variations in metabolism that may account for the differences observed. To delimitate high pH adaptations from ammonia adaptations, metabolomics was also performed following exposure to yeast media adjusted to pH 10.18 with NaOH (hereafter denoted 'NaOH pH 10.18'). Growth kinetics and sampling points in these conditions are indicated in Fig. 5a. Principal component analysis (PCA) (Fig. 5b) separated 0.25 M ammonia and NaOH pH 10.18 conditions from the control, with overlap between 0.25 M ammonia and NaOH pH 10.18 conditions indicating metabolic similarity. Univariate volcano analysis identified 23 features

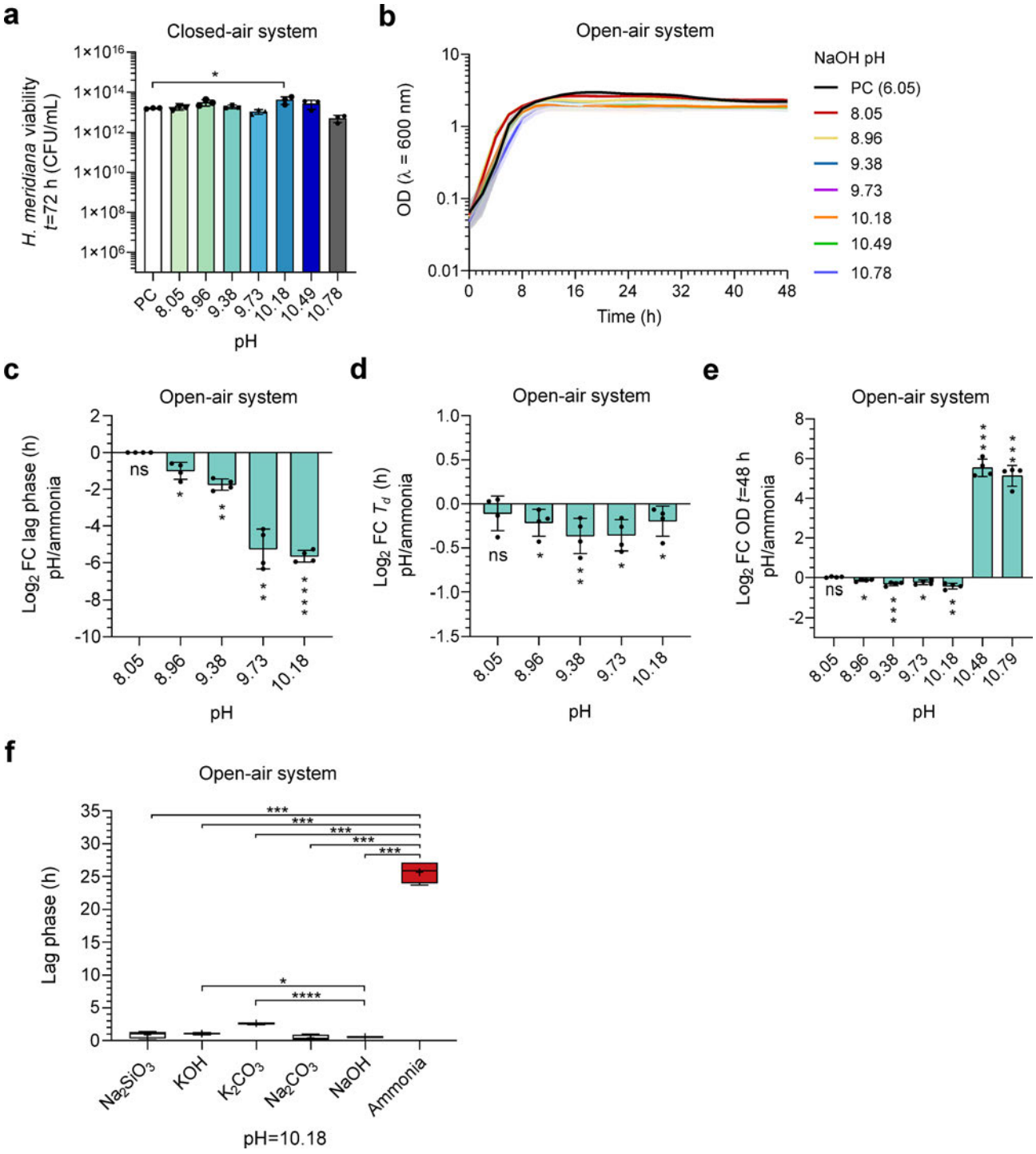

significantly altered in 0.25 M ammonia/control (Fig. 5c), 10 features significantly altered in 0.25 M ammonia/NaOH pH 10.18 (Fig. 5d), and 28 features significantly altered in NaOH pH 10.18/control (Fig. 5e). The volcano analysis dataset for each comparison group is shown in Supplementary Tables 4–6.

The most significantly altered metabolites between these conditions were identified by ANOVA (Supplementary Table 7), depicted as a heatmap (Fig. 5f). Overall, high similarity was found between 0.25 M ammonia and NaOH pH 10.18 exposed samples; both conditions generally exhibited higher levels of unsaturated phospholipid and lower levels of linoleic acid and derivatives. Intermediates that feed glycerophospholipid biosynthesis, CMP-sialic acid ($\mathbf{F} = 2021.9$, $p < 0.0001$) and glycerol-3-phosphate ($\mathbf{F} = 2022.2$, $p < 0.0001$), were more abundant compared to the control. Amino acid pathway intermediates indole-3-ethanol ($\mathbf{F} = 2327.8$, $p < 0.0001$), N, N-dimethylglycine ($\mathbf{F} = 30.626$, $p < 0.001$) and N-acetylglutamate ($\mathbf{F} = 25.653$, $p < 0.01$) were also altered compared to control. There were reduced levels of N-acetylserotonin ($\mathbf{F} = 18876$, $p < 0.0001$) and N-acetyl-L-aspartic acid ($\mathbf{F} = 24.091$, $p < 0.01$) that could suggest reactions with acetyl donors were less favourable at high pH in both conditions.

◀**Fig. 3**. Growth of *H. meridiana* in NaOH pH-matched solutions. (**a**) CFU/mL of *H. meridiana* grown in a closed system for 72 h with solutions of increasing pH that pH-match ammonia solutions of 0 (PC, pH 6.06), 0.01 (pH 8.05), 0.025 (pH 8.96), 0.05 (pH 9.38), 0.1 (pH 9.73), 0.25 (pH 10.18). 0.5 (pH 10.49) and 1 M (pH 10.78). The positive control (PC) corresponds to growth in unamended yeast media (0 M ammonia) without pH modifications. Column heights and error bars represent mean ± s.d. ($n = 3$). Statistical significance is by one-way ANOVA with Tukey's multiple comparison test (**F** (7, 16) = 5.292, $p < 0.01$). (**b**) Growth curve of *H. meridiana* over 48 h grown in NaOH solutions of increasing pH. Growth curves represent mean OD_{600} values over time ± s.d. ($n = 4$). Error is indicated by area fill within error bands. Growth parameters of lag phase (**c**), doubling time (T_d) (**d**) and final OD_{600} at 48 h (**e**) extrapolated from (**b**) are presented as Log_2 fold change (FC) values comparing pH/ammonia. Statistics correspond to unpaired two-tailed t-tests and non-parametric tests comparing the data for lag phase, T_d and final OD_{600} at each pH condition to the corresponding ammonia molarity. Statistical tests are detailed in Supplementary Table 3. Column heights and error bars represent mean ± s.d. ($n = 4$). (**f**) Box plots comparing the lag phase of *H. meridiana* grown in different pH-matched solutions at pH 10.18. Box plots represent the median as well as the 25% and 75% interquartile ranges. The whiskers represent 1.5× the interquartile ranges. The plus signs (+) indicate the mean and the central line indicate the median ($n = 4$). Welch's ANOVA with Games-Howell's multiple comparison test was used (**W** (5.000, 8.089) = 170.4). ns, no significance; *, $p < 0.05$; **, $p < 0.01$; ***, $p < 0.001$; ****, $p < 0.0001$.

Ammonia exposure elicits a unique metabolomic response

Despite general similarities between cells exposed to 0.25 M ammonia and NaOH pH 10.18, ANOVA indicated five metabolites significantly altered only in 0.25 M ammonia cultured *H. meridiana*. Box plots of these metabolites are presented in Fig. 6a-e. Samples exposed to 0.25 M ammonia showed significantly higher levels of unidentified metabolites, metabolite i at m/z = 215.084 (Fig. 6a) and metabolite ii at m/z = 157.0973 (Fig. 6b), compared to NaOH pH 10.18 exposed samples (metabolite i, $p < 0.0001$; metabolite ii, $p < 0.0001$) and control samples (metabolite i, **F** = 2112.3, $p < 0.0001$; metabolite ii, **F** = 4865.6, $p < 0.0001$). Library annotations matched metabolite i to nitrogen-containing heterocyclic compound atrazine (89.6% Q score) and metabolite ii to hydrocarbon 2,7-dimethylnaphthalene (96.5% Q score). Structures of atrazine and 2,7-dimethylnaphthalene are depicted in Fig. 6a and b, respectively. Univariate analysis also revealed exposure to 0.25 M ammonia increased the relative abundance of pantothenate (**F** = 28.839, $p < 0.001$) (Fig. 6c), and amino acids D-allo-isoleucine (**F** = 28.686, $p < 0.001$) (Fig. 6d), and alanine (**F** = 25.391, $p < 0.01$) (Fig. 6e), compared to those in NaOH pH 10.18 and control conditions.

Discussion

The influence of ammonia on habitability, particularly to microbes, is underrepresented in scientific literature. Yet, the pollution of ammonia into the environment could shape the underlying microbial community structures and biodiversity of alkaline environments. The presence of ammonia within the subsurface ocean of Enceladus, predicted at an alkaline pH, may also shape the habitability expectations of this satellite. Although the presence of life beyond Earth is speculative, terrestrial organisms can be utilised to explore the boundaries of known life under similar conditions to assess potential for habitability. In this study, we utilise alkalitolerant and halophilic *H. meridiana* as an analogue organism to investigate the molar concentration thresholds for survival, and physiological changes, that might be present in aerobic bacteria within extreme NH_3 environments.

The exposure of *H. meridiana* to increasing ammonia concentrations revealed that growth at 0.05 M ammonia, where the relative abundance of NH_3 is 62%, sets a consistent habitability limit for *H. meridiana* regardless of whether in a closed-air or open-air system. The tolerance of microbes to ammonia varies and cannot be predicted by genus or species alone; strain-specific responses to stress have been well documented[52–57]. The molarity limit established in this study aligns with data for other bacteria, including *B. subtilis* strains T1, T2, T19, T22, T33, T39[43] and *Enterobacter cloaecae* HNR[16], but is lower than the absolute limit for ammonia survival in literature which extends to above 0.716 M $(NH_4)_2SO_4$ at pH 9, correlating to above 0.5 M NH_3, survived by strains of *B. pumilus and B. pasteurii*[43]. Specific ammonia adaptations may support the survival of *B. pasteurii* in such concentrations[44–46]. The relative abundance of NH_3 to NH_4^+ in these studies is below 40%. We define an NH_3-rich solution as one where NH_3 exceeds natural environmental concentrations for ammonia (> 6 ppm, assessed by the Agency for Toxic Substances and Disease Registry)[58], and where the relative abundance of NH_3 exceeds NH_4^+. Our results characterise a habitability limit of 0.05 M in an ammonia solution that can be considered NH_3-rich by this definition (550 ppm, NH_3/NH_4^+ = 62%), which has not been previously reported for an aerobic bacterium.

Independent ammonia and pH toxicity has been characterised in *E. coli*[49], yet indistinguishable toxicity has been recorded with *B. subtilis*, *Sporosarcina*, *Paenibacillus*, *Staphylococcus*, *Brevibacillus*, *Streptomyces*, *Pseudomonas and Arthrobacter*[9,49]. Using an alkalitolerant organism, we establish ammonia toxicity is distinct from pH toxicity in *H. meridiana* and does not exert toxicity via oxygen displacement or water activity changes. However, the degree of similarly between the metabolomic profiles of cells exposed to 0.25 M ammonia and a pH-matched NaOH solution indicates *H. meridiana* primarily responds to ammonia using high pH adaptations. Unique physiological responses to ammonia in *H. meridiana* included the accumulation of two cyclic compounds, metabolite i and ii, the former of which bore amine functional groups. The presence of these compounds may be indicative of intracellular NH_3-driven reactions[59,60]. The disruption of such structures to cellular components could be a mechanism of pH-independent toxicity. Indeed, *H. meridiana* treated with ammonia exhibited aggregation to intracellular components that would suggest significant disruption to cell contents. Reductions

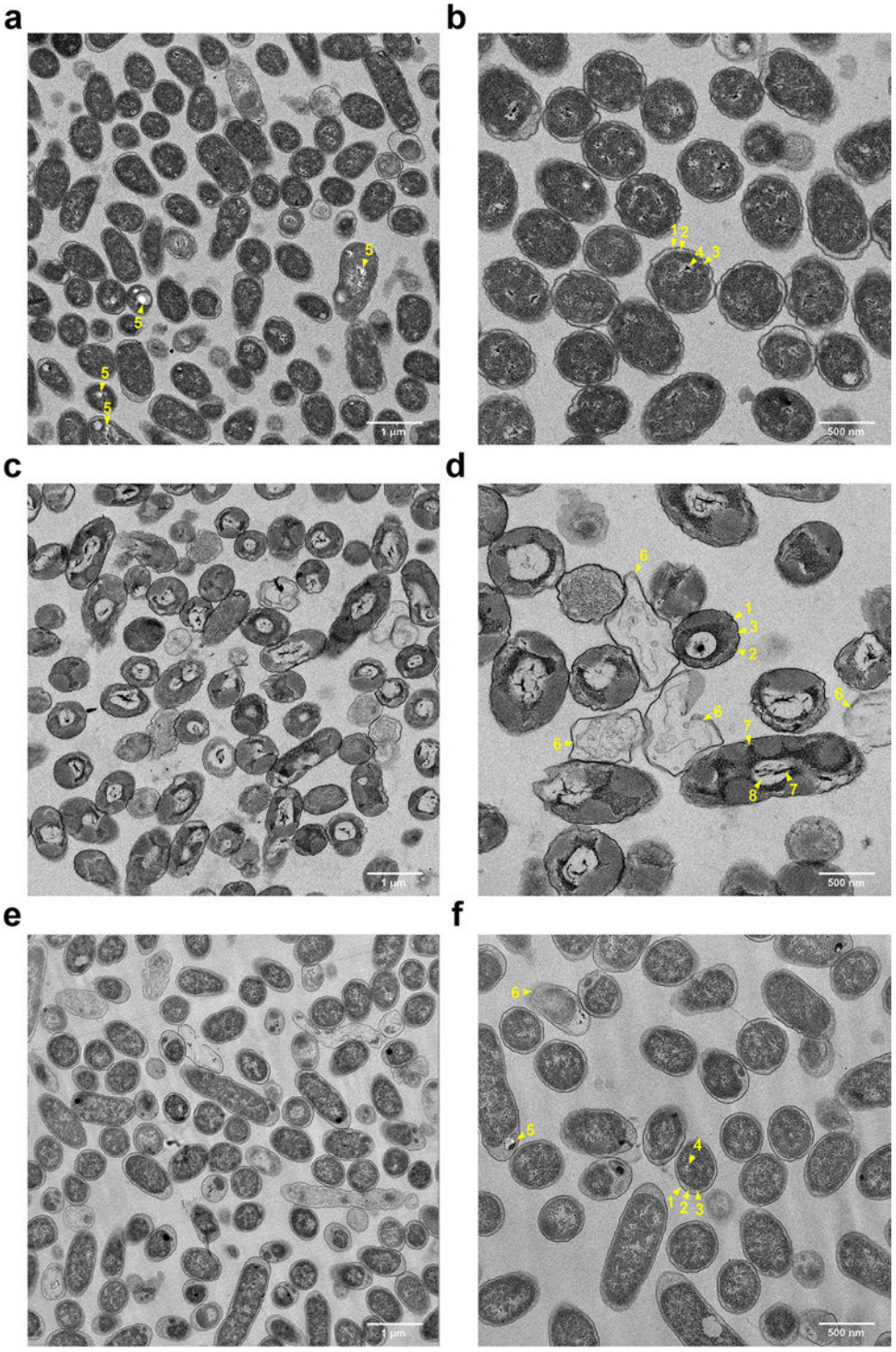

Fig. 4. TEM of *H. meridiana*. *H. meridiana* after 2 h treatment in control solutions (**a**, **b**), 1 M ammonia (**c**, **d**), and pH-matched yeast media (pH 10.78, **e**, **f**). Yellow arrows: 1, outer membrane; 2, periplasmic space; 3, inner membrane; 4, nucleoid; 5, PHA-like granule; 6, lysed cell; 7, aggregated material; 8, electrolucent cavities.

to free ammonia concentration coupled with formation of metabolites i and ii could correlate the formation of metabolites i and ii with intracellular NH_3-driven reactions.

Elevated levels of alanine, D-allo-isoleucine, and pantothenate were also exclusively observed in ammonia exposed *H. meridiana.* The presence of an isoleucine derivative and pantothenate suggested modulation to the Coenzyme A pathway that affects the cell membrane[61,62], and amino acid metabolism[62–64]. Indeed, D-amino acids have been implicated in cell wall remodelling in *Vibrio cholerae* and *B. subtilis*[65]. Alanine dehydrogenase catalyses the production of alanine by a reaction between pyruvate and ammonium[66–68]. Thus, alanine could

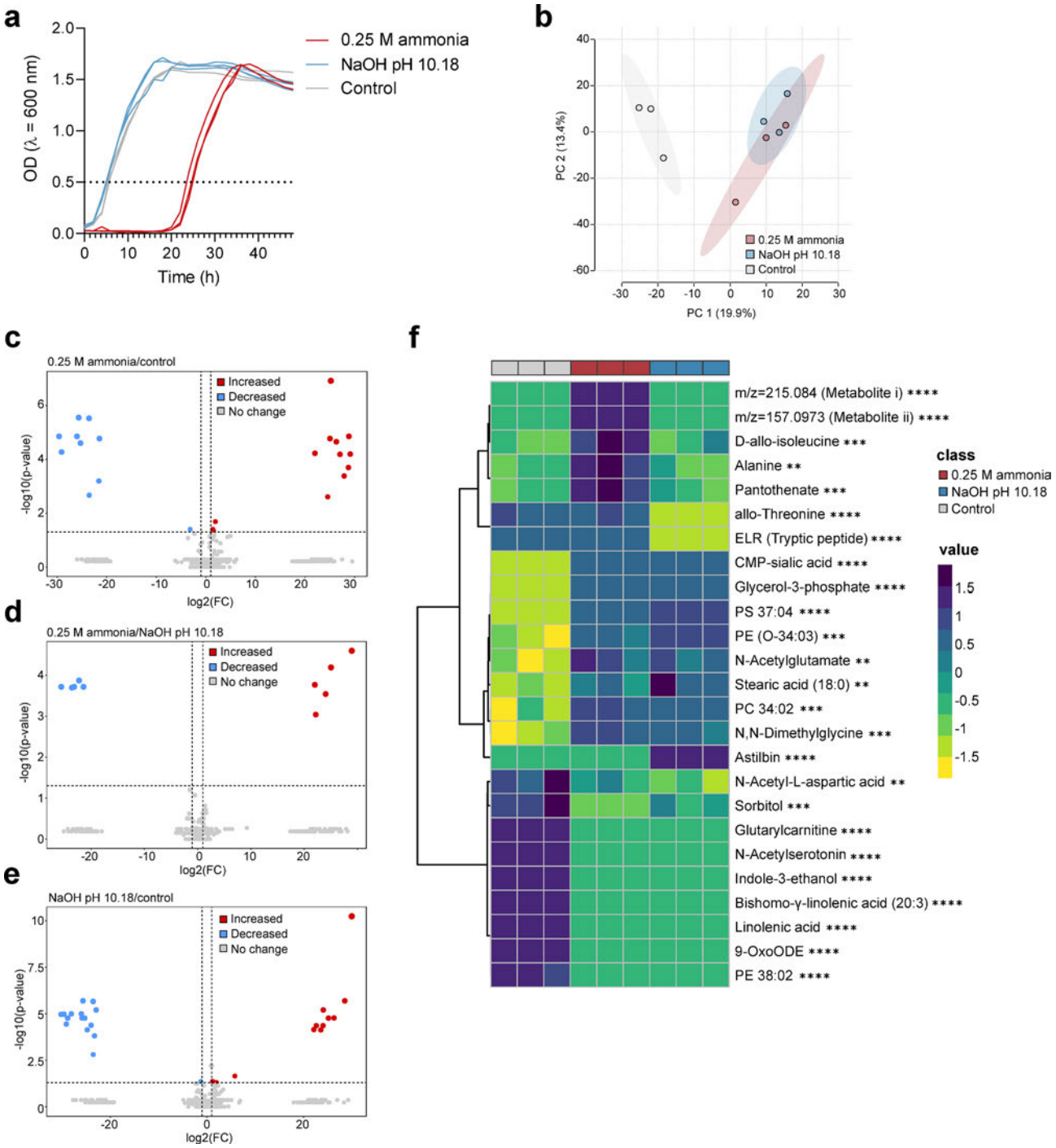

Fig. 5. Metabolic features significantly altered upon ammonia and high pH exposure in *H. meridiana*. (**a**) Growth curve of samples cultured for metabolomics processing with each replicate shown. Dotted line at $OD_{600} = 0.5$ indicates harvest point. (**b**) Scores plot of a principal component analysis (PCA). (**c**–**e**) Volcano plots depicting metabolites with a fold change greater than 2 and a *p*-value lower than 0.05 (adjusted using FDR correction) for 0.25 M ammonia/control (**c**), 0.25 M ammonia/NaOH pH 10.18 (**d**) and NaOH pH 10.18/control (**e**). Relative levels of each metabolite are presented as red dots (high) or blue dots (low). (**f**) Heatmap of the top 25 metabolites most significantly altered between ammonia, pH and control treated samples. Significance was calculated by one-way ANOVA (alpha = 0.05, two-sided) with Tukey's post-hoc test using Metaboanalyst 6.0. Significance level is indicated next to metabolites. The normalised relative abundance is presented in a gradient from dark blue (high) to yellow (low). All data compiled from three biological replicates ($n = 3$). The control corresponds to growth in unamended yeast media (0 M ammonia) without pH modifications. PCA, volcano plots and heatmap were generated using MetaboAnalyst 6.0 and amended for visual clarity in Inkscape. **, $p < 0.01$; ***, $p < 0.001$; ****, $p < 0.0001$.

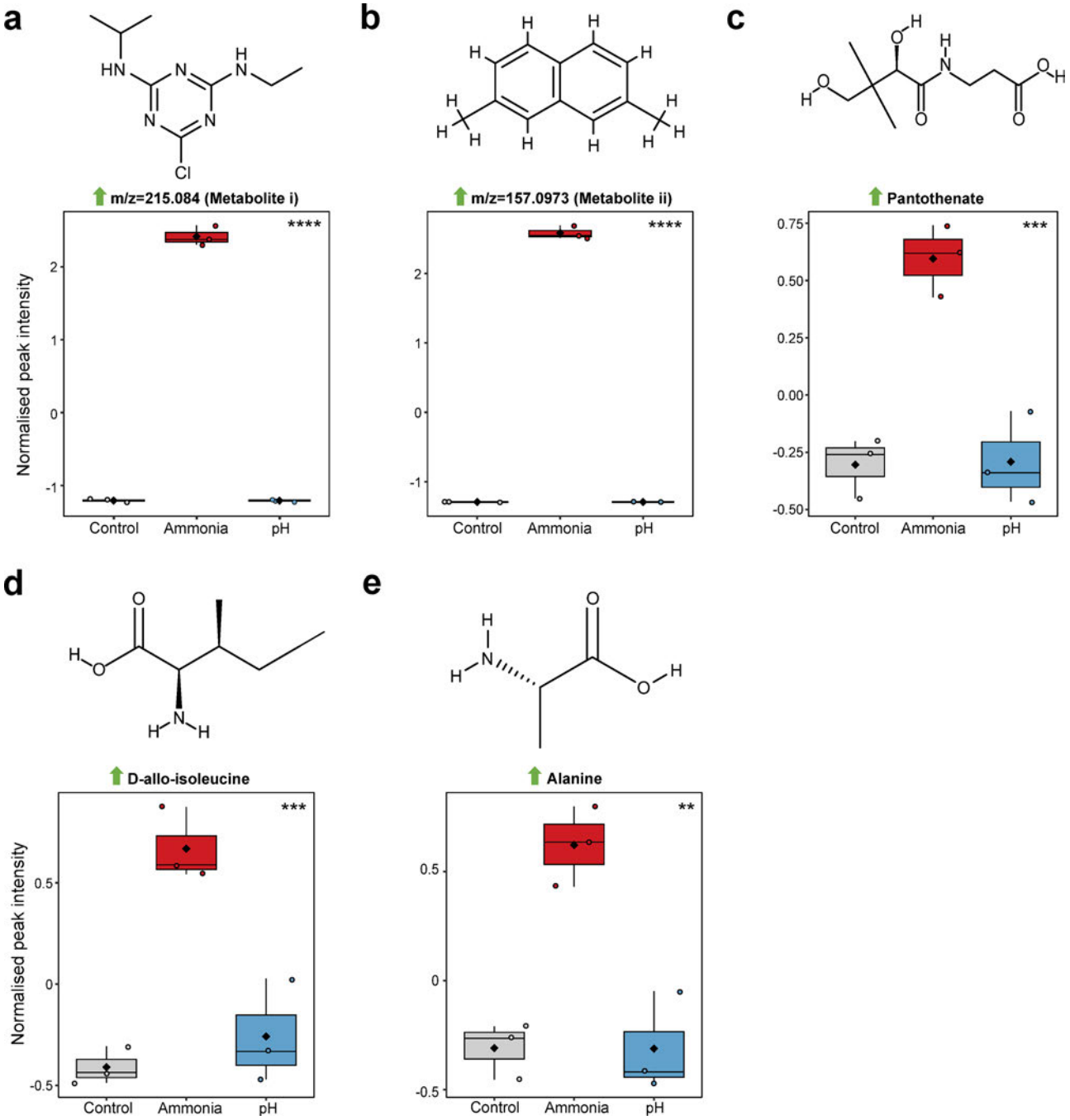

Fig. 6. Metabolic response to ammonia exposure in *H. meridiana*. (**a**–**e**) Box plots of five significantly altered metabolites found in 0.25 M ammonia exposed *H. meridiana* (ammonia) compared to NaOH pH 10.18 (pH) and control samples (control). Results are taken from ANOVA with Tukey's post-hoc test (Supplementary Table 7). The upper limit, middle line and lower limit of the boxplots indicate the 25th, 50th (median) and 75th percentiles, respectively. Whiskers represent 1.5× the interquartile ranges. Mean is indicated by a black diamond. Coloured circles represent the values from all samples ($n = 3$ for each group). Box and whiskers were generated using MetaboAnalyst 6.0 and edited for visual clarity in Inkscape. Chemical structures were created using ChemDraw. **, $p < 0.01$; ***, $p < 0.001$; ****, $p < 0.0001$.

be a by-product of elevated ammonia levels. Notably, D-amino acid aminotransferase catalyses the production of pyruvate and D-glutamate from D-alanine and 2-oxoglutarate, for which D-allo-isoleucine can act as an amino donor in *Thermotoga maritima*[69]. The presence of D-allo-isoleucine may therefore lead to enrichment of pyruvate and, in turn, enrichment of D-alanine or L-alanine via the alanine dehydrogenase pathway, or both. D-alanine may act to impede ammonia permeation; D-alanine can increase rigidity, and decrease permeability,

of the peptidoglycan layer[70–72]. L-alanine may act to prevent excessive ammonia metabolism; in some bacteria, L-alanine is an allosteric inhibitor of the nitrogen assimilation enzyme glutamine synthetase[73–75].

Interpreted from the point of view of planetary habitability, the closed-air system is the most applicable representation of icy moon subsurface oceans, as ammonia concentrations are presumed to remain constant. The ammonia toxicity limit at 0.05 M established in the closed-air system is higher than the lowest predicted concentration of ammonia at 0.01 M for the Enceladus ocean, but lower than the highest predicted concentration at 0.1 M[25,30,31]. When considering the proportion of more toxic NH_3, the pKa of the NH_3/NH_4^+ system can be presumed to increase as temperature decreases; a pKa of ~10.1 at 0 °C has been approximated[76]. The pKa of the NH_3/NH_4^+ equilibrium is also influenced by ionic strength[21]. Thus, with oceanic temperatures estimated at 0 °C[28] and ionic strength at 0.333 molal[31], it can be calculated that the Enceladus ocean would require a pH of < 10.6 to satisfy a relative abundance of NH_3 at < 62% suggested as a habitability boundary in this sstudy. This is in the range of the lower pH estimations currently modelled for Enceladus, where phosphate speciation in the waters constrains the ocean to pH 10.1 to 11.6, with a most consistent value of pH 10.6[31].

On Earth, up to 78 tetragrams of ammonia per annum are expelled globally from agricultural processes[35,36]. Individual livestock buildings show ammonia concentrations up to 30 ppm (0.002 M)[77,78], which is lower than the habitability limit indicated in this study, yet, it should be noted a water volume of 1 L would require just 1 gram of ammonia to exceed an ammonia concentration of 0.05 M. In alkaline environments, this may alter bacterial community structures and biodiversity once the molarity and relative abundance of NH_3 exceeds thresholds for survival, as has been observed in Mono Lake[22]. Bactericidal effects from NH_3 may be transient, unless NH_3 deposition is continuous, due to the open-air volatilization and dispersal of NH_3 – repopulation of *H. meridiana* in an open-air ammonia system was observed at concentrations above 0.05 M ammonia. However, it is not without mention that localised and recurrent "point sources" of ammonia deposition have been identified in both agriculture and industrial processes that may consistently disturb bacterial habitats despite volatilization and dispersal[79].

Without field-based environmental surveys, the effects of NH_3 on terrestrial and extraterrestrial habitability are only estimated. Additionally, without isolation and biological characterisation of metabolites i and ii, we can only speculate the contribution of these molecules in ammonia toxicity. However, we have shown that bacterial growth and viability may become impacted when molar concentrations of ammonia are above 0.05 M, where NH_3 exceeds NH_4^+. Moreover, we deduce that ammonia and pH toxicity are distinct, suggesting a need to modify the current understanding of NH_3 toxicity in bacteria. Together, these findings can be integrated into the current knowledge regarding the impact of ammonia on terrestrial geomicrobiology and may inform future habitability assessments of NH_3-rich extraterrestrial environments.

Materials and methods

Solution Preparation

Solutions of liquid ammonia were made to the required molar concentrations—0.01, 0.025, 0.05, 0.1, 0.25, 0.5, 1 M ammonia in yeast media using 35% NH_3 (Fisher Scientific, CAS Number: 1336-21-6). The pH of the solutions was determined with a Jenway 3510 benchtop pH meter. pH-matched sodium hydroxide solutions (NaOH; Fisher Scientific, CAS Number: 1310-73-2) were prepared by gradual addition of 1 M NaOH into yeast media. To compare growth in different basic solutions at a pH equivalent to that of 0.25 M ammonia (pH 10.18), several bases were selected that have a natural pH at or greater than pH 10.18 and high solubility in water. Thus, yeast media was made to pH 10.18 ± 0.01 using gradual addition of 1 M NaOH, 1 M potassium hydroxide (KOH), 1 M sodium metasilicate (Na_2SiO_3), 1 M potassium carbonate (K_2CO_3) or 1 M sodium carbonate (Na_2CO_3). Growth experiments proceeded as outlined below. pH was matched to within ± 0.01 pH units. All solutions were filter-sterilised through a 0.22-micron pore before use.

NH_3/NH_4^+ percentage abundance

The percentage concentration of ammonia was determined by indirect calculation based on commonly utilised equations developed by Hampson[19]. Firstly, the ionic strength of the prepared solutions based on known salinity (0.2 M NaCl) was determined by Eq. 1.

$$I = 19.9273\,(S)\,/(1000 - 1.005109\,(S)) \tag{1}$$

Where I = molar ionic strength; S = salinity (parts per thousand, ppt).

The stoichiometric acid hydrolysis constant of ammonium ions, pKa^s, based on I, was then calculated. pKa^s values for given ionic strengths were provided by Hampson[19]. These values were plotted to obtain a linear regression for calculating pKa (Supplementary Fig. 1). pKa^s was calculated from Eq. 2.

$$pKa^s = 0.1179\,(I) + 9.246 \tag{2}$$

Percentage abundance of NH_3 at given salinity, pH and temperature was then calculated from Eq. 3. As salinity, temperature, pressure and pKa^s are constant in the experiment, only pH was modified to give percentage abundance of NH_3 at each pH value (Supplementary Table 8).

$$\%\,NH_3 = 100/[1 + 10^{(pKa^s + 0.0324(298 - T) + 0.0415(P/T) - pH)}] \tag{3}$$

Where P = 1 atm pressure; T = temperature (K).

Oxygen measurements
Oxygen concentrations (µmol/L) of unamended yeast media, ammonia solutions and pH-matched solutions, prepared as described above, were recorded using an oxygen microsenser with tip diameter of < 2 mm (OX-500, Unisense, Denmark). Solutions were equilibrated for 0.5 h before reading at 28 °C in 96-well plates sealed with aluminium foil to prevent gas loss.

Water activity
Unamended yeast media, ammonia solutions and pH-matched solutions were prepared as described above. Solutions were equilibrated for 1.5 h and water activities measured at 28 °C with a Rotronic HP23-AW water activity meter (Rotoronic AG, Bassersdorf, Switzerland).

Bacterial strain selection
Halomonas meridiana Slthf1 (DSM 15724; Gram negative) was obtained from the German Collection of Microorganisms and Cell Cultures (DSMZ). The organism was originally isolated at a depth of 2000 m from low temperature hydrothermal fluid in the East Pacific Rise. The strain exhibits halophilic growth up to 22% NaCl, and shows tolerance up to pH 12[50]. The strain is therefore representative of the physiological attributes that could be necessary to grow in saline, alkaline fluids. A complete genome sequence is available for this strain[50]. This organism is not known to have specific adaptations to ammonia; this was a deliberate choice. The purpose of this study was not to study microbial biochemical adaptation to high ammonia, but rather to study whether NH_3 can act as an abiotic factor influencing bacterial growth, survival and physiology.

Bacterial culture
An aerobic culture of *H. meridiana* was grown in glass conical Erlenmeyer flasks at 28 °C in an orbital benchtop shaking incubator set to rotate at 150 RPM. We assume ammonia-rich environments present optimal nutrient conditions (i.e., available organic debris) with a salinity < 2% for the purpose of this study. Thus, *H. meridiana* Slthf1 was grown in a yeast media consisting of 1 g/100 mL Bacto™ yeast extract (Becton, Dickinson and Company), 0.2 M NaCl (1.17% salinity) (Thermo Fisher Scientific, CAS Number: 7647-14-5) and distilled water (dH_2O).

Growth experiments
Two growth systems were implemented: 'closed' growth experiments were conducted in sealed air-tight 15 mL falcon tubes with sufficient headspace (14 mL) to allow aerobic metabolism but prevent ammonia evaporation; 'open-air' growth experiments were conducted in 96-well plates to permit ammonia evaporation and to monitor growth dynamics. Growth in closed-air system experiments were assessed by colony forming units (CFU) after 72 h incubation at 28 °C and 150 RPM. Growth in open-air systems were assessed in 96-well plates by optical density (OD) readings in a BMG SPECTROstar Nano Microplate Reader at 600 nm with reading taken every half an hour for 48 h at 28 °C. Plates were shaken at 200 RPM before each reading. Plate wells were prepared with 190 µL of a selected solution and seeded with 10 µL overnight *H. meridiana* culture to $OD_{600} = 0.05$. Positive control wells were 190 µL unamended yeast media inoculated with 10 µL overnight *H. meridiana* culture to $OD_{600} = 0.05$. Negative controls had no inoculation. To avoid condensation, plate lids were coated with Triton X-100 (0.05%) in 20% ethanol.

Growth parameters
Experiments were conducted to yield three standard microbiological growth parameters: lag phase duration, doubling time (T_d), and final OD_{600}. The lag phase was calculated with a web-based microbial lag phase calculator[80], with the following parameters: algorithm = parameter fitting to a model; pre-processing applied: cut data at some time = yes, max time = 24–48 h; smooth data = no; initial biomass = first observation; model to fit = logistic; NLS fitting algorithm = auto; max number of iterations = 1000. T_d was calculated by first determining the growth rate in the exponential growth phase (μ) as per Eq. 4, followed by calculation of T_d as per Eq. 5.

$$\mu = (Log_{10}(N) - Log_{10}(N_0))\, 2.303/(t - t_0) \tag{4}$$

Where $N_0 = OD_{600}$ at the beginning of a selected time interval (t_0) in the exponential growth phase; $N = OD_{600}$ at the end of a selected time interval (t) in the exponential growth phase. t and t_0 are recorded in minutes.

$$T_d = ln2/\mu \tag{5}$$

The final OD_{600} reached after 48 h was recorded and used to represent the final cell concentration reached. Cell viability versus OD_{600} over 24 h was assessed by PrestoBlue™ cell viability reagent (Thermo Fisher Scientific, Massachusetts, USA). Calibration curves confirm changes to observed OD_{600} corresponds to increasing number of viable cells (Supplementary Fig. 2). Growth or lack of growth was determined by the presence or absence of a defined lag phase, exponential phase, and stationary phase within a 48 h growth period.

Ammonia evaporation and cell viability
In separate 96-well plates, overnight culture of *H. meridiana* was inoculated to $OD_{600} = 0.05$ in 0.1 M and 0.25 ammonia solutions. Plates were incubated at 28 °C on an orbital shaker continuously shaken at 150 RPM and tested as described below at 0, 4, and 8 h for 0.1 M ammonia solutions, and 0, 4, 8, and 16 h for 0.25 M ammonia solutions. Separate 96-well plates were used for each time point. The viability of cells in the culture wells at these time points was assessed by CFU on yeast media agar plates incubated at 28 °C. Ammonia content of culture

wells at these time intervals was recorded using the CHEMetrics High Range VACUette Ammonia test kit (K-1510 C) by direct nesslerization. The parts per million (ppm) of ammonia in the sample was determined by colorimetric analysis of the Nessler reaction product at 420 nm[81]. Molarity (M) of ammonia was calculated by conversion of ppm to molarity using the molar mass of ammonia (Eq. 6)

$$M = \frac{(ppm/1000\ )}{17.031\ g/mol} \tag{6}$$

Transmission electron microscopy

An overnight culture of *H. meridiana* was pelleted, resuspended and exposed for 2 h to the following solutions: unamended yeast media (control), 1 M ammonia and a pH-matched solution (pH 10.78). The matched pH solution was created by gradual addition of 1 M NaOH to yeast media. Following incubation, cells were washed and resuspended in phosphate buffered saline (PBS). Samples were fixed in 3% glutaraldehyde in 0.1 M Sodium Cacodylate buffer, pH 7.3, for 2 h then washed in three 10-minute changes of 0.1 M Sodium Cacodylate. Specimens were then post-fixed in 1% Osmium Tetroxide in 0.1 M Sodium Cacodylate for 45 min, then washed in three 10-minute changes of 0.1 M Sodium Cacodylate buffer. These samples were then dehydrated in 50%, 70%, 90% and 100% ethanol (X3) for 15 min each, then in two 10-minute changes in Propylene Oxide. Samples were then embedded in TAAB 812 resin. Sections, 1 µm thick were cut on a Leica Ultracut ultramicrotome, stained with Toluidine Blue, and viewed in a light microscope to select suitable areas for investigation. Ultrathin sections, 60 nm thick were cut from selected areas, stained in Uranyl Acetate and Lead Citrate then viewed in a JEOL JEM-1400 Plus TEM. Representative images were collected on a GATAN OneView camera at 4 K resolution. Images were processed using ImageJ[58].

Metabolomics sampling and extraction

An overnight culture of *H. meridiana* was inoculated to $OD_{600} = 0.05$ within 0.25 M ammonia, pH-matched yeast media (pH 10.18) or unamended yeast media (control) within a 24-well plate. The pH-matched solution was created by gradual addition of 1 M NaOH to yeast media. Growth occurred within plates at 28 °C and was assessed by OD_{600} reading every half an hour using a BMG SPECTROstar Nano Microplate Reader. Samples were harvested during the log phase of growth at $OD_{600} = 0.5$. All the following procedures occurred at 4 °C. Samples were aliquoted into microcentrifuge tubes and quenched by rapid cooling through submersion in a dry ice/70% (v/v) ethanol bath after brief incubation on ice. During cooling, samples were mixed vigorously to prevent freezing. Cells were separated from spent medium by centrifugation at 1,000 *g* for 10 min and supernatant discarded. Metabolite extraction occurred by addition of ice-cold chloroform/methanol/water (1:3:1 ratio). Cell lysis was encouraged by sonication with ice for 5 min at 37 kHz within an ultrasonication bath (Elmasonic S 60 H). Extraction mixtures were mixed vigorously at 1,200 rpm on an orbital shaker for 1 h. Following mixing, samples were centrifuged at 13,000 *g* for 3 min. The supernatant, containing metabolites, was collected into sterile microcentrifuge tubes. A pooled quality control sample was generated by combining equal volumes of metabolites from each sample. All samples were stored at − 80 °C until analysis.

Untargeted metabolomics analysis

The untargeted metabolomics analysis was performed using liquid chromatography (LC) coupled to ion mobility (IM) quadrupole time-of-flight (qTOF) mass spectrometry (MS). The instrumentation consisted of an Agilent 1290 Infinity II series UHPLC system hyphenated with an Agilent 6560 IM-qTOF with a Dual Agilent Jet Stream Electron Ionization source. LC separation was performed on an InfinityLab Poroshell 120 HILIC-Z, 2.1 mm × 50 mm, 2.7 µm UHPLC column (Agilent Technologies 689775–924) coupled to an InfinityLab Poroshell 120 HILIC-Z, 3.0 mm × 2.7 µm UHPLC guard column (Agilent Technologies 823750–948). A 3.5 min gradient was run using organic buffer (acetonitrile) combined with an aqueous buffer with low pH (10 mM ammonium formate, pH 3) or high pH (10 mM ammonium acetate, pH 9) for positive and negative ionization modes, respectively. Data was acquired using MassHunter Data Acquisition 10.0 software on 1 µL of sample separated on the column with a flow rate of 800 µL/min. The quality control sample was injected five times at the beginning of the experiment to condition the column and after every five test samples to monitor the instrument state throughout data acquisition. Data were acquired in the 50 to 1700 m/z range, with an MS acquisition rate of 0.8 scans/s. The metabolomics analyses were carried out by the EdinOmics research facility (RRID: SCR_021838) at the University of Edinburgh.

Metabolomics data processing and statistical analysis

The raw data files were processed using the Agilent MassHunter software suite. Briefly, ion multiplexed data files and calibration files were demultiplexed using the PNNL PreProcessor v2020.03.23 (the default settings for demultiplexing, moving average smoothing, saturation repair and spike removal were applied to the data). The data files were recalibrated for accurate mass and drift time using the AgtTofReprocessUi and the IM-MS Browser 10.0, respectively. Molecular features were extracted in Mass Profiler 10.0 with a retention time tolerance of ± 0.3 min, drift time tolerance of ± 1.5% and accurate mass tolerance of ± (5 ppm + 2 mDa). Features were annotated based on accurate mass and collision cross section (CCS) values using McLean CCS Compendium PCDL library[82]. Multivariate and univariate statistical analysis was performed using the MetaboAnalyst 6.0 web-based platform[83]. The input data were log-transformed and Pareto-scaled. The results were visualised using principal component analysis (PCA), box and whisker plots, volcano plots and heatmaps. Further aesthetic adjustments, including font changes and line thickness modifications, were made using Inkscape (version 1.0.1). Chemical structures were drawn using ChemDraw (version 23.1.2) and exported in SVG format for inclusion in the figures. The raw data associated with this dataset is available to view in the Supplementary Dataset. This

study focuses on metabolomic changes in ammonia, pH and control samples, but the broader metabolomics profiling also included samples exposed to $(NH_4)_2SO_4$. For analysis, only ammonia, pH and control samples were included in this study. The metabolomics of $(NH_4)_2SO_4$ exposed samples are to be addressed in a separate analysis.

Statistics and reproducibility

All data were compiled from a minimum of three different cultures inoculated on different days with new media ($n = 3$–4 biological replicates). The normality of data was assessed with the Shapiro-Wilk test. For comparison of two groups, unpaired two-tailed t-tests were used. The Mann Whitney U test was used for unpaired groups where the assumption of normality was violated. An unpaired t-test with Welch's correction was applied for groups with unequal variance as assessed by an F test. For comparison of two or more groups, equal variance was assessed with the Brown-Forsythe test. Samples of equal variance were examined by analysis of variance (ANOVA) followed by Tukey's post-hoc test. For samples where variance was not equal, Welch's ANOVA test with Games-Howell's post-hoc test was used. Statistical tests are specified in figure legends. Significance was considered when $p < 0.05$. All statistical analyses were performed using GraphPad Prism version 8.0.2 (GraphPad Software Inc.).

Data availability

All data generated or analysed during this study are included in this published article within the Supplementary Dataset, except when specified as part of the Supplementary Material.

Received: 7 March 2025; Accepted: 22 May 2025
Published online: 04 June 2025

References

1. Doherty, M. J. et al. Ammonia in the interstellar medium of a starbursting disc at z = 2.6. *Mon not R Astron. Soc. Lett.* **517**, L60–L64 (2022).
2. Henderson-Sellers, A. & Schwartz, A. W. Chemical evolution and ammonia in the early Earth's atmosphere. *Nature* **287**, 526–528 (1980).
3. Woodman, J. H., Trafton, L. & Owen, T. The abundances of ammonia in the atmospheres of Jupiter, Saturn, and Titan. *Icarus* **32**, 314–320 (1977).
4. Nagatani, H., Shimizu, M. & Valentine, R. C. The mechanism of ammonia assimilation in nitrogen fixing bacteria. *Arch. Für Mikrobiol.* **79**, 164–175 (1971).
5. Burris, R. H. & Roberts, G. P. Biological nitrogen fixation. *Annu. Rev. Nutr.* **13**, 317–335 (1993).
6. Stein, L. Y. & Klotz, M. G. The nitrogen cycle. *Curr. Biol.* **26**, R94–R98 (2016).
7. Fowler, D. et al. The global nitrogen cycle in the twenty-first century. *Philos. Trans. R Soc. B Biol. Sci.* **368**, 20130164 (2013).
8. Vines, H. M. & Wedding, R. T. Some effects of ammonia on plant metabolism and a possible mechanism for ammonia toxicity. *Plant. Physiol.* **35**, 820–825 (1960).
9. Kelly, L. C., Cockell, C. S. & Summers, S. Diverse microbial species survive high ammonia concentrations. *Int. J. Astrobiol.* **11**, 125–131 (2012).
10. Dasarathy, S. et al. Ammonia toxicity: From head to toe? *Metab. Brain Dis.* **32**, 529–538 (2017).
11. Jurcă, A. D. et al. Clinical and genetic diversity of congenital hyperammonemia. *Romanian J. Morphol. Embryol. Rev. Roum Morphol. Embryol.* **59**, 945–948 (2018).
12. Walter, A. & Gutknecht, J. Permeability of small nonelectrolytes through lipid bilayer membranes. *J. Membr. Biol.* **90**, 207–217 (1986).
13. Brazier, B. W. Membrane transport of ammonia. *Am. J. Food Nutr.* **4**, 135–137 (2016).
14. Ritchie, R. J. & Gibson, J. Permeability of ammonia and amines in *Rhodobacter sphaeroides* and *Bacillus firmus*. *Arch. Biochem. Biophys.* **258**, 332–341 (1987).
15. Ritchie, R. J. & Gibson, J. Permeability of ammonia, methylamine and ethylamine in the Cyanobacterium *Synechococcus* R-2 (*Anacystis nidulans*) PCC 7942. *J. Membr. Biol.* **95**, 131–142 (1987).
16. Weng, X. et al. Biofilm formation during wastewater treatment: Motility and physiological response of aerobic denitrifying bacteria under ammonia stress based on surface plasmon resonance imaging. *Bioresour Technol.* **361**, 127712 (2022).
17. Fischer, M. A. et al. Immediate effects of ammonia shock on transcription and composition of a biogas reactor Microbiome. *Front. Microbiol.* **10**, 2064 (2019).
18. Wang, F. et al. Effects of ammonia on apoptosis and oxidative stress in bovine mammary epithelial cells. *Mutagenesis* **33**, 291–299 (2018).
19. Hampson, B. L. Relationship between total ammonia and free ammonia in terrestrial and ocean waters. *ICES J. Mar. Sci.* **37**, 117–122 (1977).
20. Whitfield, M. The hydrolysis of ammonium ions in sea water - a theoretical study. *J. Mar. Biol. Assoc. U K.* **54**, 565–580 (1974).
21. Bower, C. E. & Bidwell, J. P. Ionization of ammonia in seawater: Effects of temperature, pH, and salinity. *J. Fish. Res. Board. Can.* **35**, 1012–1016 (1978).
22. Humayoun, S. B., Bano, N. & Hollibaugh, J. T. Depth distribution of microbial diversity in mono lake, a meromictic soda lake in California. *Appl. Environ. Microbiol.* **69**, 1030–1042 (2003).
23. Ward, B. B., Martino, D. P., Diaz, M. C. & Joye, S. B. Analysis of ammonia-oxidizing bacteria from hypersaline mono lake, California, on the basis of 16s rRNA sequences. *Appl. Environ. Microbiol.* **66**, 2873–2881 (2000).
24. Waite, J. H. Jr et al. Liquid water on enceladus from observations of ammonia and 40Ar in the plume. *Nature* **460**, 487–490 (2009).
25. Waite, J. H. et al. Cassini finds molecular hydrogen in the enceladus plume: Evidence for hydrothermal processes. *Science* **356**, 155–159 (2017).
26. Hay, H. C. F. C. & Matsuyama, I. Nonlinear tidal dissipation in the subsurface oceans of enceladus and other icy satellites. *Icarus* **319**, 68–85 (2019).
27. Roberts, J. H. & Nimmo, F. Tidal heating and the long-term stability of a subsurface ocean on enceladus. *Icarus* **194**, 675–689 (2008).
28. Matson, D. L., Castillo-Rogez, J. C., Davies, A. G., Johnson, T. V. & Enceladus A hypothesis for bringing both heat and chemicals to the surface. *Icarus* **221**, 53–62 (2012).
29. Hsu, H. W. et al. Ongoing hydrothermal activities within enceladus. *Nature* **519**, 207–210 (2015).

30. Fifer, L. M., Catling, D. C. & Toner, J. D. Chemical fractionation modeling of plumes indicates a gas-rich, moderately alkaline enceladus ocean. *Planet. Sci. J.* **3**, 191 (2022).
31. Glein, C. R. & Truong, N. Phosphates reveal high pH ocean water on Enceladus. *Icarus* **441**, 116717 (2025).
32. McKay, C. P., Porco, C. C., Altheide, T., Davis, W. L. & Kral, T. A. The possible origin and persistence of life on enceladus and detection of biomarkers in the plume. *Astrobiology* **8**, 909–919 (2008).
33. Taubner, R. S. et al. Biological methane production under putative Enceladus-like conditions. *Nat. Commun.* **9**, 748 (2018).
34. Taubner, R. S., Schleper, C., Firneis, M. G. & Rittmann, S. K.-M. R. Assessing the ecophysiology of methanogens in the context of recent Astrobiological and planetological studies. *Life* **5**, 1652–1686 (2015).
35. Luo, Z. et al. Estimating global ammonia (NH_3) emissions based on IASI observations from 2008 to 2018. *Atmospheric Chem. Phys.* **22**, 10375–10388 (2022).
36. Yang, Y. et al. Improved global agricultural crop- and animal-specific ammonia emissions during 1961–2018. *Agric. Ecosyst. Environ.* **344**, 108289 (2023).
37. Erisman, J. W. & Draaijers, G. P. J. *Atmospheric Deposition: in Relation To Acidification and Eutrophication*vol. 63 (Elsevier, 1995).
38. Krupa, S. V. Effects of atmospheric ammonia (NH_3) on terrestrial vegetation: a review. *Environ. Pollut.* **124**, 179–221 (2003).
39. Duce, R. A. et al. The atmospheric input of trace species to the world ocean. *Glob Biogeochem. Cycles.* **5**, 193–259 (1991).
40. Powlson, D. S. & Dawson, C. J. Use of ammonium sulphate as a sulphur fertilizer: implications for ammonia volatilization. *Soil. Use Manag.* **38**, 622–634 (2022).
41. Wang, X. et al. Effect of *Trichoderma viride* biofertilizer on ammonia volatilization from an alkaline soil in Northern China. *J. Environ. Sci.* **66**, 199–207 (2018).
42. Wang, X. et al. Ammonia volatilization, greenhouse gas emissions and Microbiological mechanisms following the application of nitrogen fertilizers in a saline-alkali paddy ecosystem. *Geoderma* **433**, 116460 (2023).
43. Leejeerajumnean, A., Ames, J. M. & Owens, J. D. Effect of ammonia on the growth of *Bacillus* species and some other bacteria. *Lett. Appl. Microbiol.* **30**, 385–389 (2000).
44. Jahns, T. Ammonium/urea-dependent generation of a proton electrochemical potential and synthesis of ATP in *Bacillus pasteurii*. *J. Bacteriol.* **178**, 403–409 (1996).
45. Wiley, W. R. & Stokes, J. L. Effect of pH and ammonium ions on the permeability of *Bacillus pasteurii*. *J. Bacteriol.* **86**, 1152–1156 (1963).
46. Wiley, W. R. & Stokes, J. L. Requirement of an alkaline pH and ammonia for substrate oxidation by *Bacillus pasteurii*. *J. Bacteriol.* **84**, 730–734 (1962).
47. Vejmelkova, D. et al. Analysis of ammonia-oxidizing bacteria dominating in lab-scale bioreactors with high ammonium bicarbonate loading. *Appl. Microbiol. Biotechnol.* **93**, 401–410 (2012).
48. Hayatsu, M. et al. An acid-tolerant ammonia-oxidizing γ-proteobacterium from soil. *ISME J.* **11**, 1130–1141 (2017).
49. Deal, P. H., Souza, K. A. & Mack, H. M. High pH, ammonia toxicity, and the search for life on the Jovian planets. *Orig Life.* **6**, 561–573 (1975).
50. Takahashi, Y., Takahashi, H., Galipon, J. & Arakawa, K. Complete genome sequence of *Halomonas meridiana* strain Slthf1, isolated from a deep-sea thermal vent. *Microbiol. Resour. Announc.* https://doi.org/10.1128/MRA.00292-20 (2020).
51. Kaye, J. Z., Márquez, M. C., Ventosa, A. & Baross, J. A. Y. *Halomonas neptunia* sp. nov., *Halomonas sulfidaeris* sp. nov., *Halomonas axialensis* sp. nov. and *Halomonas hydrothermalis* sp. nov.: halophilic bacteria isolated from deep-sea hydrothermal-vent environments. *Int. J. Syst. Evol. Microbiol.* 54, 499–511 (2004). (2004).
52. Baharoglu, Z. & Mazel, D. SOS, the formidable strategy of bacteria against aggressions. *FEMS Microbiol. Rev.* **38**, 1126–1145 (2014).
53. Boutte, C. C. & Crosson, S. Bacterial lifestyle shapes stringent response activation. *Trends Microbiol.* **21**, 174–180 (2013).
54. Fernandez, L., Rosvall, M., Normark, J., Fällman, M. & Avican, K. Co-PATHOgenex web application for assessing complex stress responses in pathogenic bacteria. *Microbiol. Spectr.* **12**, e02781–e02723 (2023).
55. Fuentes, D. E., Acuña, L. G. & Calderón, I. L. Stress response and virulence factors in bacterial pathogens relevant for Chilean aquaculture: current status and outlook of our knowledge. *Biol. Res.* **55**, 21 (2022).
56. Langer, G., Nehrke, G., Probert, I., Ly, J. & Ziveri, P. Strain-specific responses of *Emiliania huxleyi* to changing seawater carbonate chemistry. *Biogeosciences* **6**, 2637–2646 (2009).
57. Moreno-Galván, A., Romero-Perdomo, F. A., Estrada-Bonilla, G., Meneses, C. H. S. G. & Bonilla, R. R. Dry-caribbean *Bacillus* spp. Strains ameliorate drought stress in maize by a strain-specific antioxidant response modulation. *Microorganisms* **8**, 823 (2020).
58. Agency for Toxic Substances and Disease Registry (ATSDR). *Toxicological Profile for Ammonia* (U.S. Department of Health and Human Services, Public Health Service, 2004).
59. Liu, S. & Cheng, X. Insertion of ammonia into alkenes to build aromatic N-heterocycles. *Nat. Commun.* **13**, 425 (2022).
60. Nielsen, A. T., Moore, D. W., Ogan, M. D. & Atkins, R. L. Structure and chemistry of the aldehyde ammonias. 3. Formaldehyde-ammonia reaction. 1,3,5-Hexahydrotriazine. *J. Org. Chem.* **44**, 1678–1684 (1979).
61. Yao, J. & Rock, C. O. Exogenous fatty acid metabolism in bacteria. *Biochimie* **141**, 30–39 (2017).
62. Leonardi, R., Zhang, Y. M., Rock, C. O., Jackowski, S. & Coenzyme, A. Back in action. *Prog Lipid Res.* **44**, 125–153 (2005).
63. Shi, L. & Tu, B. P. Acetyl-CoA and the regulation of metabolism: mechanisms and consequences. *Curr. Opin. Cell. Biol.* **33**, 125 (2015).
64. Tomita, T. Structure, function, and regulation of enzymes involved in amino acid metabolism of bacteria and archaea. *Biosci. Biotechnol. Biochem.* **81**, 2050–2061 (2017).
65. Lam, H. et al. D-amino acids govern stationary phase cell wall remodeling in bacteria. *Science* **325**, 1552–1555 (2009).
66. Aharonowitz, Y. & Friedrich, C. G. Alanine dehydrogenase of the β-lactam antibiotic producer *Streptomyces clavuligerus*. *Arch. Microbiol.* **125**, 137–142 (1980).
67. Li, Q. et al. Alanine synthesized by alanine dehydrogenase enables ammonium-tolerant nitrogen fixation in *Paenibacillus sabinae* T27. *Proc. Natl. Acad. Sci.* 119, e2215855119 (2022).
68. Yoshida, A. & Freese, E. Enzymic properties of Alanine dehydrogenase of *Bacillus subtilis*. *Biochim. Biophys. Acta BBA - Nucleic Acids Protein Synth.* **96**, 248–262 (1965).
69. Miyamoto, T. et al. Identification of a novel d-amino acid aminotransferase involved in d-glutamate biosynthetic pathways in the hyperthermophile *Thermotoga maritima*. *FEBS J.* **289**, 5933–5946 (2022).
70. Trivedi, R. R. et al. Mechanical genomic studies reveal the role of d-alanine metabolism in *Pseudomonas aeruginosa* cell stiffness. *mBio* **9**, e01340–e01318 (2018).
71. Liu, D. et al. Knockout of the Alanine racemase gene in *Aeromonas hydrophila* HBNUAh01 results in cell wall damage and enhanced membrane permeability. *FEMS Microbiol. Lett.* **362**, fnv089 (2015).
72. Palumbo, E. et al. Knockout of the Alanine racemase gene in *Lactobacillus plantarum* results in septation defects and cell wall perforation. *FEMS Microbiol. Lett.* **233**, 131–138 (2004).
73. Stadtman, E. R. Regulation of glutamine synthetase activity. *EcoSal Plus.* **1** https://doi.org/10.1128/ecosalplus.3.6.1.6 (2004).
74. Hubbard, J. S. & Stadtman, E. R. Regulation of glutamine synthetase II. Patterns of feedback Inhibition in microorganisms. *J. Bacteriol.* **93**, 1045–1055 (1967).
75. Liaw, S. H., Pan, C. & Eisenberg, D. Feedback Inhibition of fully unadenylylated glutamine synthetase from Salmonella typhimurium by Glycine, Alanine, and Serine. *Proc. Natl. Acad. Sci.* **90**, 4996–5000 (1993).

76. Bates, R. G. & Pinching, G. D. Acidic dissociation constant of ammonium ion at 0 to 50 °C, and the base strength of ammonia. *J. Res. Natl. Bur. Stan.* **42**, 419 (1949).
77. Groot Koerkamp, P. W. G. et al. Concentrations and emissions of ammonia in livestock buildings in Northern Europe. *J. Agric. Eng. Res.* **1**, 79–95 (1998).
78. Seedorf, J. & Hartung, J. Survey of ammonia concentrations in livestock buildings. *J. Agric. Sci.* **133**, 433–437 (1999).
79. Van Damme, M. et al. Industrial and agricultural ammonia point sources exposed. *Nature* **564**, 99–103 (2018).
80. Smug, B. J., Opalek, M., Necki, M. & Wloch-Salamon, D. Microbial lag calculator: A shiny-based application and an R package for calculating the duration of microbial lag phase. *Methods Ecol. Evol.* **15**, 301–307 (2024).
81. Jeong, H., Park, J. & Kim, H. Determination of NH_4^+ in environmental water with interfering substances using the modified nessler method. *J. Chem.* e359217 (2013). (2013).
82. Nichols, C. M. et al. Untargeted molecular discovery in primary metabolism: collision cross section as a molecular descriptor in ion mobility-mass spectrometry. *Anal. Chem.* **90**, 14484–14492 (2018).
83. Pang, Z. et al. MetaboAnalyst 6.0: towards a unified platform for metabolomics data processing, analysis and interpretation. *Nucleic Acids Res.* **52**, W398–W406 (2024).

Acknowledgements

This work was supported by a Natural Environmental Research Council (NERC) Doctoral Training Partnership grant (NE/S007407/1). C.H. and C.S.C thanks the Science and Technology Facilities Council (STFC) for support under grant ST/V000586/1 and ST/Y001788/1. We also acknowledge the support of the Wellcome Trust Multiuser Equipment Grant (WT104915MA) for use of the JEOL JEM-1400 Plus TEM. We acknowledge the EdinOmics research facility at the University of Edinburgh where the metabolomics analyses were carried out.

Author contributions

C.M.H. conducted the experiments, data analysis and paper writing. C.S.C. and P.N. jointly supervised this work and provided input in the writing of the paper. C.S.C. provided instruments and materials for experiments.

Declarations

Competing interests

The authors declare no competing interests.

Additional information

Supplementary Information The online version contains supplementary material available at https://doi.org/10.1038/s41598-025-03858-z.

Correspondence and requests for materials should be addressed to C.M.H.

Reprints and permissions information is available at www.nature.com/reprints.

Publisher's note Springer Nature remains neutral with regard to jurisdictional claims in published maps and institutional affiliations.

4.3 Conclusion

The research presented in this chapter characterises the limits of extremophile life in ammoniacal solutions where there is a high relative abundance of NH_3. The concentrations utilised are relevant to icy moon oceans but also have implications for polluted Earth habitats of high pH. Survival thresholds of 0.05 M ammonia in a closed-air system and 0.25 M ammonia in an open-air system for *H. meridiana* were characterised. Increased lag time, increased doubling time and decreased cell density were evident as ammonia concentrations increased from 0.01 to 1 M ammonia. These effects were not mimicked when *H. meridiana* was grown in solutions of matching pH made by sodium hydroxide. In probing the possible toxicity mechanisms and internal reaction of ammonia on *H. meridiana*, intracellular aggregation, loss of intracellular structures, and complete cell disfigurement and lysis was observed. These changes were again not found when applying a pH-matched sodium hydroxide solution. Ammonia toxicity was thus found to be distinct from pH toxicity, indicating ammonia toxicity in this case was not determined by an external rise in pH. It is likely the distinction between ammonia and sodium hydroxide toxicity was underpinned by the unregulated, passive diffusion of NH_3 into cells. Charged species such as Na^+ and OH^- in sodium hydroxide diffuse into cells by regulated, active transport (Rosen and Silver, 2014, Henriquez et al., 2021). Thus, internal concentrations are limited and toxic effects avoided.

The subsequent impact of NH_3 on metabolites and molecular pathways as NH_3 diffused into a cellular environment was assessed by untargeted metabolomics. Despite that ammonia and pH toxicity was found to be distinct, the metabolomic response to ammonia was highly similar to that of high pH exposure. This indicated the primary response to ammonia by *H. meridiana* was a response to its properties as a weak base. However, a few ammonia-specific alterations were observed. These hinted at cell wall modifications and possible consequences of internal NH_3-driven reactions, suggesting possible adaptation mechanisms or manifestations of internal toxicity.

To the best of my knowledge, this is the first time an extremophile with astrobiology-relevant physiologies has been used to characterise habitability limits in ammonia. I also believe this is the first study to characterise bacterial survival in up to 0.05 M ammonia in a solution where the relative abundance of NH_3 was greater than NH_4^+. This is significant as the Enceladus environment, as well as Titan, likely bears an ocean with a high NH_3 to NH_4^+ ratio. Additionally, the habitability threshold for *H. meridiana* of 0.05 M established here is above the lower concentration limit of ammonia modelled within the ocean of Enceladus (0.01 M) (Fifer et al., 2022, Glein and Truong, 2025). This indicates the presence of ammonia in the ocean of Enceladus may not constrain the existence of viable bacterial life. Terrestrially, the concentration of NH_3 deposited onto Earth environments by agricultural and industrial processes is not explicitly estimated, but is known to commonly occur. The results of this study show that, in the open-air system, 0.1 M and 0.25 M ammonia reduced cell number upon immediate exposure and also reduced doubling time. There was no viability in solutions at or above 0.5 M ammonia. These thresholds can be utilised as a basis for considering how ammonia polluted into the environment at particular concentrations could impact the bacteriology of high pH soils treated with or exposed to ammonia fertilizer.

During the course of this research, it was evident NH_3 could disperse from the growth system as part of the open-air system. Atmospheric transport and deposition of NH_3 into surrounding environments is plausible. This posed a significant question as to whether NH_3 gas dispersed from a highly concentrated source could impact *H. meridiana* habitability over a spatial and temporal range, impacting not just local but also distant environments. This question was addressed next in Chapter 5.

5

Spatiotemporal cultivation of extremophile *Halomonas meridiana* impacted by Enceladus- and Earth-relevant ammonia gas

Since the submission of this thesis, the following chapter has been published in *Microbial Ecology* (DOI: 10.1007/s00248-025-02621-1). A copy of this publication can be found in the appendix.

5.1 Introduction

The habitability of an environment is influenced by its physicochemical conditions, the accessibility of chemical elements, nutrients and energy, and, distinctly, the availability of liquid water. Equally, the habitability of an environment can become constrained or limited by the presence of detrimental environmental components (Cockell et al., 2016, 2024). One class of detrimental compounds is volatile toxic gases, which can be transported through the atmosphere. One such gas is ammonia (hereafter, the term "ammonia" is utilised to denote the total concentration of unionized ammonia, NH_3, and the ammonium ion, NH_4^+, in an environment). Ammonia is a bioavailable nitrogen source and metabolic input for many living organisms including bacteria (Nagatani et al., 1971, Burris and Roberts, 1993, Stein and Klotz, 2016). However, the toxicity of ammonia has been demonstrated across a number of species, from bacteria to humans (Vines and Wedding, 1960, Kelly et al., 2012, Dasarathy et al., 2017, Jurcă et al., 2018). Notably, NH_3 possesses certain properties (e.g., small size, uncharged) which facilitates passive permeation through biological membranes. As a weak proton (H^+) acceptor, NH_3 readily reacts with H^+ to raise pH, disrupt proton motive force and form NH_4^+ which impacts ionic balance (Rose et al., 2005, Bosoi and Rose, 2009, Shi et al., 2020, Angelova et al., 2022). The presence of NH_3 gas in the environment is therefore an important consideration when assessing habitability.

In aqueous environments, NH_3 exists in equilibrium with NH_4^+. The proportion of each species of ammonia is determined primarily by pH, but also temperature, pressure, and salinity (Whitfield, 1974, Hampson, 1977, Bower and Bidwell, 1978). Under standard Earth conditions (temperate, standard pressure) and pH exceeding 9.25, over half of ammonia is present as NH_3 gas. NH_3 is thus commonly released into the terrestrial atmosphere following application of ammonium fertilizer to high pH soils. The process of release is known as volatilization, a phenomenon whereby ammonia transitions to the gas phase ($_{(g)}NH_3$) and escapes into the atmosphere. Due to volatilization, long-range dispersion and deposition of NH_3 has been well demonstrated (Sutton et al., 1998, Bouet et al., 2005, Leytem et al., 2024, Lô et al., 2025). Ammonia has been detected up to 3 kilometres from a source pollution site, and could be detected at a level of 5.1 $\mu g/m^3$ in natural reserves (Lô et al., 2025). Despite the relatively short atmospheric lifetime of NH_3 which is in the order of hours to days (Pinder et al., 2008, Behera et al., 2013, Xie et al., 2024), atmospheric transport can thus deposit ammonia into surrounding environments (Duce et al., 1991, Erisman and Draaijers, 1995, Krupa, 2003). It is therefore possible for NH_3 to disperse from a concentrated, local source to distant environments. Such deposition may impact the habitability of afflicted environments.

As one of the simplest organisms on Earth, bacteria can provide a valuable foundation to examine growth limitations when considering habitability. Growth limitations in ammonia have been established for *Bacillus subtilis* (Deal et al., 1975, Leejeerajumnean et al., 2000), *Escherichia coli* (Deal et al., 1975), *B. pasteurii*, *B. pumilus* (Leejeerajumnean et al., 2000), sulphate-reducing bacteria (Dai et al., 2017) and the extremophile *Halomonas meridiana* (Hopton et al., 2025). Increasing concentrations of atmospheric NH_3 has been found to reduce the number of viable bacteria (Eno et al., 1955). Through studies such as these, NH_3 gas dissolved into environments from a distant source could be presumed to elicit one of two distinct effects. At low concentrations, the deposition of dispersed NH_3 could support the growth of organisms by providing essential nitrogen (Kleiner, 1981, Raven et al., 1992, Britto

et al., 2001, Reitzer, 2003, Li et al., 2013). Alternatively, at high concentrations, NH_3 could exert adverse effects on the biodiversity of aquatic life, plants, invertebrates and bacteria (Sutton et al., 2009, Bobbink and Hicks, 2014, García-Gómez et al., 2014, Paoli et al., 2014, Hou et al., 2018). However, this binary effect of NH_3 has not been explicitly demonstrated in research. Additionally, due to atmospheric dispersion, NH_3 can presumably alter growth over a wider spatial range than direct deposition but may be less toxic due to diminished concentration. The effects of NH_3 are also likely to be temporary as ammonia disperse into air over time. These facets of atmospheric NH_3 gas generate questions, such as what this spatial effect on bacterial growth could look like, and whether bacteria could recover from NH_3 gas exposure after complete dispersal. Such fundamentals are important when considering how terrestrial bacteria may be impacted by anthropogenic ammonia pollution.

Crucially, these fundamentals could also inform extraterrestrial habitability. Icy moons of our solar system feature liquid water subsurface oceans encased below thick ice shells (Khurana et al., 1998, Tobie et al., 2008, Nimmo and Pappalardo, 2016). The liquid state of the oceans has been thought to be preserved by anti-freeze components such as ammonia (Lewis, 1971, Spohn and Schubert, 2003). Supporting this, mass spectrometry analysis by the Cassini-Huygens mission of the material ejected from the Southern plume of Saturn's icy moon Enceladus, presumed to originate from the subsurface ocean, measured ammonia at a volume mixing ratio of 0.4-1.3% (Waite et al., 2009, 2017). Enceladus features an availability of heat (Nimmo et al., 2007, Roberts and Nimmo, 2008), energy (Hsu et al., 2015, Matson et al., 2007, Zolotov, 2007), nutrients (Waite et al., 2009, 2017, Postberg et al., 2023, Xu et al., 2025) and organics (Waite et al., 2009, Postberg et al., 2018), as well as liquid water, essential for prebiotic chemistry. Enceladus is thus a prominent target in astrobiology and the search for habitable environments beyond Earth.

On Enceladus, the spatial and temporal impact of NH_3 gas could be relevant to habitability prospects in the brine channels, veins, pockets and fractures presumed to feature in the ice shell. These networks have been hypothesised as potentially habitable environments (Kargel et al., 2000, Wettlaufer, 2009, Buffo et al., 2021, Wolfenbarger et al., 2022). NH_3 gas may permeate into these environments through multiple pathways. In one pathway, NH_3 gas may be released and adsorbed into the ice shell following exsolution from the ocean (Fifer et al., 2022, Richter et al., 2025) and migrate to the fluid networks by surface diffusion. Alternatively, ice fractures that are open to the surface may enable NH_3 volatilization on icy moons. This would dependent on local temperature (-23 to 0 °C or higher) and pH (greater than pH 9) (Bates and Pinching, 1949), as well as pressure. NH_3 can easily volatilize on Earth; the air contains trace amounts of ammonia, creating a strong gradient driving ammonia from environments to the air. On icy moons, NH_3 escape is governed by Henry's Law and vapor pressure equilibrium: colder temperatures reduce NH_3 volatility, and thus near-zero pressures are needed for NH_3 to escape, volatilize, from liquid. Such conditions could exist in ice shell fractures connected to the surface of Enceladus which is under near vacuum pressure. Volatilized NH_3 could then migrate along the fracture system and potentially solubilise into intersecting brine networks within the ice shell. As with exsolved NH_3, volatilized NH_3 may also absorb onto ice walls of the fracture and enter brine networks through ice diffusion (Richter et al., 2025). It is not without mention that other prominent astrobiology targets, the icy moons Titan, Europa, Callisto and Ganymede, are also modelled with an internal ocean of NH_3 where spatial and

temporal effects of NH_3 gas could be relevant (Khurana et al., 1998, Sohl et al., 2003, Spohn and Schubert, 2003). However, the presence of NH_3 in these oceans has yet to be confirmed by direct measurements.

To characterise the habitability impacts exerted by volatilized and dispersed NH_3 gas, this work investigates the cultivation of *Halomonas meridiana* (*n*omenclature synonym: H. aquamarina) circumjacent to NH_3 gas. *H. meridiana* is a deep-sea bacterium with no specialised ammonia adaptations (Takahashi et al., 2020), but has extremophilic adaptations relevant to the physicochemical characteristics of the Enceladus ocean (Kaye et al., 2004). Indeed, I have previously shown *H. meridiana* can grow in concentrations of ammonia above the lower putative ammonia concentration threshold (0.01 M (Fifer et al., 2022)) expected on Enceladus (Hopton et al., 2025). I utilised optical density readings to characterise the spatial impact of incrementally increasing concentrations of ammonia from 0.1 M to 1 M on growth. I also analyse temporal recovery of cell density following exposure. Using growth kinetic and cell viability assays, I compare the growth kinetics of *H. meridiana* cultured adjacent to an ammonia source ("adjacently exposed") to those directly exposed to ammonia ("directly exposed"). Through this, I assess implications for the habitability of environmental niches susceptible to NH_3 gas exposure on the icy moon Enceladus as well as Earth.

5.2 Methods

5.2.1 Bacterial strain selection and culture

The gram-negative bacterium *Halomonas meridiana* Slfth1 (DSM 15724) was obtained from the German Collection of Microorganisms and Cell Cultures (DSMZ). *H. meridiana* remains validly published as a heterotypic synonym according to the International Code of Nomenclature of Prokaryotes (ICNP). However, it should be noted this strain has been synonymized with H. aquamarina based on phylogenomic classifications (Dobson and Franzmann, 1996). *H. meridiana* was isolated from low temperature hydrothermal fluid at a depth of 2000 m. As such, *H. meridiana* presents physiological traits necessary for growth in this environment. This includes halophilic adaptations (growth in up to 22% NaCl), alkalitolerance (tolerance up to pH 12), psychrotolerant traits (growth at -1 °C and cold shock protein genes), and piezotolerance (growth at 550 bar) (Kaye et al., 2004, Kaye and Baross, 2004, Takahashi et al., 2020). Evidence of hydrothermal systems are present on Enceladus (Hsu et al., 2015, Waite et al., 2017). The isolation location and physiological adaptations exhibited by this organism therefore make it a suitable model for establishing the limits of life on Earth and potential for habitability on icy moons where cold, saline, high pH, and high-pressure waters would be expected. Additionally, the strain genome hosts no known ammonia adaptations (Takahashi et al., 2020) [DDBJ, accession no. AP022821]. This was an intentional choice. The estimated ammonia concentrations within icy moons oceans are low and may preclude the need for distinct ammonia adaptations. Additionally, the intention of this study was not to assess an already established ammonia adaptation, but to assess whether NH_3 gas acts as a chemical parameter that can affect habitability of organisms without ammonia adaptations. Pure cultures of *H. meridiana* were maintained in a simplistic yeast media consisting of 1g/100 mL Bacto™yeast extract (Becton, Dickinson and Company), 0.2 M NaCl (1.17% salinity) (Thermo Fisher Scientific, CAS Number: 7647-14-5) and distilled water (dH2O) at pH 6.

Cultures were cultivated aerobically in conical Erlenmeyer flasks with orbital agitation at 150 RPM and 28 °C.

5.2.2 Ammonia preparation

All ammonia solutions were prepared from a stock solution of 35% liquid ammonia (Fisher Scientific, CAS Number: 1336-21-6). Stock ammonia was diluted in yeast media to molar concentrations of 0.1 M, 0.25 M, 0.5 M and 1 M ammonia and maintained in air-tight falcon tubes to prevent gaseous escape. Control solutions of 0 M ammonia consisted of yeast media with no ammonia supplementation. The pH of all solutions was unaltered to preserve incrementally higher concentrations of NH_3 gas. The pH of each solution was recorded as follows: control (0 M), pH 6.06 $\pm$ 0.07; 0.1 M, pH 9.73 $\pm$ 0.01; 0.25 M, pH 10.18 $\pm$ 0.03; 0.5 M, pH 10.49 $\pm$ 0.01; and 1 M, pH 10.78 $\pm$ 0.02. The pH of solutions was determined with a Jenway 3510 benchtop pH meter.

5.2.3 Spatiotemporal analysis of ammonia toxicity

Experiments were conducted in polystyrene 96-well plates. These plates were not air-tight and thus permitted ammonia to travel from wells to the exterior atmosphere. All wells, with exception of four central wells (D6, D7, E6, E7), were plated with 190 µL yeast media inoculated with 10 µL overnight *H. meridiana* culture to an optical density at 600 nm (OD_{600}) of 0.05. A blank plate was created identically but without inoculation. The four central wells (D6, D7, E6, E7) were plated with 200 µL ammonia at concentrations of either 0 M (control), 0.1 M, 0.25 M, 0.5 M or 1 M, prepared as described above. Plates were incubated at 28 °C in a table-top orbital shaker at 150 RPM with OD_{600} readings taken at 24 and 48 h using a BMG SPECTROstar Nano Microplate Reader. Plates were shaken at 200 RPM before each reading. All plates were blank corrected against the blank plate before reading. Plate lids were utilised during incubation and analysis to ensure planar spread of NH_3 gas across the plate. The liquid culture depth was approximately 6 mm in a total well depth of 10.67 mm. An open space of 1 mm was between the well top and the plate lid.

5.2.4 Growth experiments of direct and adjacent ammonia exposure

Growth experiments were conducted within polystyrene 96-well plates utilising two distinct culture conditions: direct and adjacent ammonia exposure. In the direct ammonia condition, ammonia concentrations of 0 M (control), 0.1 M, 0.25 M, 0.5 M and 1 M in yeast media were prepared as outlined above and dispensed into five wells. Ammonia solutions were inoculated with 10 µL overnight culture of *H. meridiana* to OD_{600} = 0.05 in a final volume of 200 µL (Figure 5.1A). In the adjacent ammonia condition, five wells of yeast media were inoculated with 10 µL overnight culture of *H. meridiana* to OD_{600} = 0.05 in a final volume of 200 µL. Five wells directly adjacent to these culture wells were supplemented with ammonia in yeast media to concentrations of 0 M (control), 0.1 M, 0.25 M, 0.5 M or 1 M ammonia (Figure 5.1B). In both growth conditions, separate 96-well plates were used for each ammonia concentration. Negative controls had no inoculation.

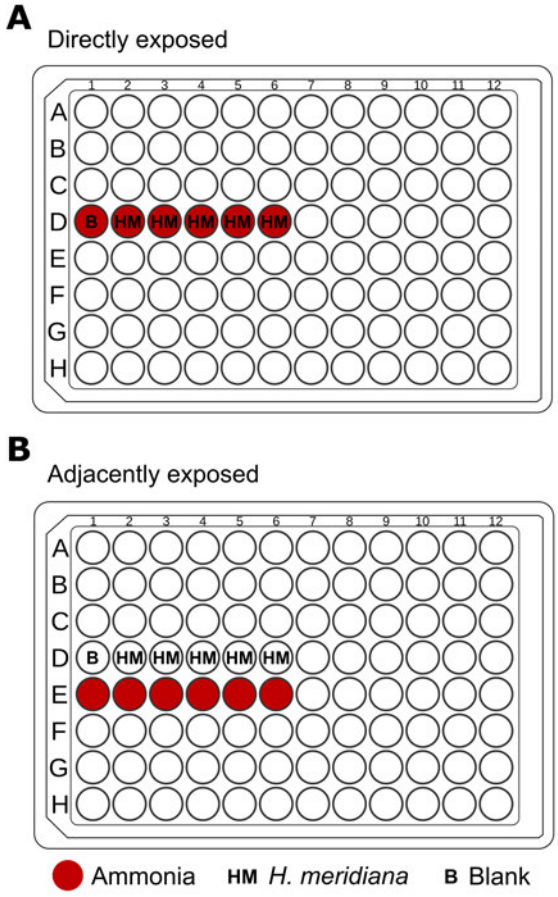

Figure 5.1: Diagram of "directly" and "adjacently" exposed cultures to ammonia. (A) Depiction of *H. meridiana* cultures directly exposed to ammonia (red circles). *H. meridiana* (HM) is cultivated in yeast media with ammonia to concentrations of 0.1 M, 0.25 M, 0.5 M or 1 M ammonia. (B) Depiction of *H. meridiana* cultures adjacently exposed to ammonia. *H. meridiana* is cultivated in yeast media without ammonia. Ammonia at concentrations of either 0.1 M, 0.25 M, 0.5 M or 1 M ammonia is placed in the wells directly below these cultures. Blank (B) solutions are identical but are without inoculation of *H. meridiana*.

5.2.5 Kinetic growth assays and parameters

Growth over time was assessed using OD_{600} readings over 48 h in a BMG SPECTROstar Nano Microplate Reader. Plates were shaken at 200 RPM before each reading. Growth parameters of lag phase duration, doubling time and final OD_{600} at 48 h were extrapolated from the OD_{600} growth curve. Lag phase duration was determined using the online microbial lag phase calculator developed by Smug et al (2024) (Smug et al., 2024). The following parameters were applied: algorithm=parameter fitting to a model; pre-processing applied: cut data at some time=yes, max time=24 or 48 hours; smooth data=no; initial biomass=first observation; model to fit=logistic; NLS fitting algorithm=auto; max number of iterations=100. Doubling time was derived from the growth rate, μ, by the equation ln2/μ. Calculation of μ is presented in Eq. 5.1. N_0 is the OD_{600} at a beginning time interval (t_0) in the exponential growth phase. N is the OD_{600} at the end of a selected time interval (t) in the exponential growth phase. t and t_0 were recorded in minutes.

$$\mu = (Log_{10}(N) - Log_{10}(N_0))2.303/(t - t_0) \tag{5.1}$$

The OD_{600} at 48 h determined final cell density. No growth was defined as any analysis where there was no defined lag or exponential phase after 48 h. Increases to OD_{600} were found to correspond to increases in cell viability (Supplementary Figure S1).

5.2.6 Cell count

Cell viability of *H. meridiana* was assessed in cultures directly and adjacently exposed to ammonia. The experimental set-up of the two conditions occurred analogously to that described in the growth experiments. 96-well plates were incubated for 4 h at 28 °C on a table-top orbital shaker at 150 RPM. This incubation period was found to be a suitable length of time to allow volatilization of NH_3 from the central ammonia wells and complete dispersal across adjacent wells utilised for testing. The duration is also within the doubling time range of *H. meridiana* (i.e., 1 to 2 h). Following incubation, cell numbers were determined using colony forming units (CFU) on yeast media agar plates incubated at 28 °C.

5.2.7 Evaluation of ammonia concentration

Volatilization and permeation of NH_3 from and into cultures that were directly and adjacently exposed to ammonia was assessed by using the CHEMetrics High Range VACUette Ammonia test kit (K-1510C). The K-1510C kit features a detection range of 0-10,000 ppm ammonia and a detection limit of 100 ppm. Precision data is not available for this kit. However, a related kit, K-1513, has shown precision of ± 11 ppm at 112 ppm. This kit measures ammonia by a direct nesslerization reaction. Direct nesslerization determines ammonia concentration by a reaction of ammonia with potassium mercuric iodide. This produces a yellow-coloured complex, the Nessler reaction product, which can be measured at 420 nm (Jeong et al., 2013). The experimental set-up of the two conditions occurred as described in the growth experiments. A 4 h incubation period was identified as a suitable length of time that could allow NH_3 volatilization, dispersal and dissolution into adjacent cultures. Plates were incubated for 4 h at 28 °C on a table-top orbital shaker at 150 RPM. The parts per million (ppm) of ammonia in each culture was determined by colorimetric analysis of the Nessler reaction product at 420 nm. Ammonia content in ppm was determined by linear regression; the absorbance of the culture sample at 420 nm was compared against a calibration curve created by absorbance of known concentrations of ammonia at 420 nm (Supplementary Figure S2). Molarity was derived from ppm as shown in Eq. 5.2, where 1 ppm≈1 mg/L, and molar mass refers to the molar mass of ammonia expressed in g/mol.

$$M = \frac{ppm \div 1000}{Molar\ mass} \tag{5.2}$$

5.2.8 Statistics and reproducibility

All data was compiled from a minimum of three biological replicates (n = 3 to 4). The Shapiro-Wilk test was utilised to assess normality of data. Where the assumption of normality was violated, two groups were analysed by the Mann Whitney test or, for three or more groups, by the Kruskal-Wallis test. Multiple comparison correction was applied using Dunn's test. Where normality was not violated, sample variance was assessed by an F-test for two groups. Samples of equal variance were analysed by two-tailed unpaired t-test. If the assumption of variance was violated, a two-tailed unpaired t-test with Welch's correction was applied. For three or more groups, the Brown-Forsythe test was utilised to assess equal variance. Samples of equal variance were analysed by analysis of variance (ANOVA) followed by Tukey's post-hoc test. Samples of unequal variance were assessed by Welch's ANOVA test with Tamhane's T2 post-hoc test. Data is presented as the mean ± standard deviation (SD). Significance

was considered when $p < 0.05$. Statistical tests are specified in figure legends as well as the supplementary material when indicated. All figures and statistical analyses were produced using GraphPad Prism version 8.0.2 (GraphPad Software Inc.).

5.3 Results

5.3.1 Spatiotemporal toxicity of ammonia

NH_3 is a gas under temperate conditions and standard pressure. The spatiotemporal impact of NH_3 on bacterial cultures was assessed using 96-well plates. Plates were prepared with four central wells containing either yeast media (0 M ammonia, control) or ammonia at concentrations of 0.1 M, 0.25 M, 0.5 M, and 1 M. The peripheral wells were filled with yeast media inoculated with *H. meridiana*. Figure 5.2A-E is a heatmap illustrating the cell density of wells surrounding ammonia concentrations of 0 M (Control, Figure 5.2A), 0.1 M (Figure 5.2B), 0.25 M (Figure 5.2C), 0.5 M (Figure 5.2D) and 1 M (Figure 5.2E) at 24 h and 48 h post-inoculation. Cell density is given by optical density values at 600 nm (OD_{600}). Values of cell density are characterised as follows: 0 – red, 0.5 – orange, 1 – yellow, 1.5 – green, ≥ 2 – dark green. Figure 5.2F and Figure 5.2G indicate the total number of wells, as a percentage of the total number of culture wells (92), that reached cell densities between 0-0.5, $>$ 0.5-1, $>$ 1-2 and $>$ 2 OD_{600} at 24 h and 48 h, respectively, for each control and ammonia treatment condition.

Figure 5.2 demonstrates a pronounced suppression of cell density which was most severe in proximity to the ammonia source as ammonia concentration increases. Culture wells circumjacent to the control solution at 24 h and 48 h, with exception of a single well in each case, showed an average cell density at or exceeding 2 (Figure 5.2A). At 24 h, 43.12% of culture wells in the control condition were at a cell density between $OD_{600} >$ 1-2 and 55.8% of wells at a cell density $OD_{600} \geq 2$ (Figure 5.2F). At 48 h, 89.86% wells exhibited a cell density of $OD_{600} \geq 2$ (Figure 5.2G). The control represents typical growth densities that would be expected of *H. meridiana* when cultivated in optimal conditions. In culture wells circumjacent to 0.1 M ammonia, all wells with exception of one exceeded a cell density of $OD_{600} = 1$ (Figure 5.2B). At 48 h, 57.97% of wells were $OD_{600} \geq 2$. This was lower than the number of wells at or exceeding a cell density of $OD_{600} \geq 2$ at 48 h in the control condition ($p < 0.01$), but higher than the number of wells at a cell density of $OD_{600} \geq 2$ when compared against the 0.25 M ($p < 0.05$) and 0.5 M ($p < 0.01$) ammonia conditions at 48 h (Figure 5.2G).

The majority of cultures wells circumjacent to ammonia at a concentration of 0.25 M exhibited a cell density between $OD_{600} = 1$ and $OD_{600} = 2$ at both 24 h and 48 h (Figure 5.2C). In this culture system, 19.93% of wells exhibited cell density values of $OD_{600} \geq 2$ at 24 h (Figure 5.2F). This increased to 37.32% at 48 h (Figure 5.2G). The number of wells at a cell density of $OD_{600} \geq 2$ was found to be non-significantly different from the 0.1 M ($p = 0.0664$), 0.5 M ($p = 0.808$) and 1 M ammonia ($p = 0.101$) conditions but lower than the control condition at 48 h ($p < 0.0001$) (Figure 5.2G).

In the 0.5 M ammonia condition, 9.78% of wells exhibited a cell density of $OD_{600} \geq 2$ at 24 h. The number of wells at this level increased to 30.07% at 48 h but was still lower than that

observed in control ($p < 0.0001$) and 0.1 M ammonia ($p < 0.05$) conditions (Figure 5.2G). A cell density of OD_{600} <0.5 at 24 was observed in 6.52% of wells (Figure 5.2F), but none were observed at this level at 48 h (Figure 5.2G). Comparatively, 7.97% of wells exhibited a cell density of $OD_{600} \geq 2$ when surrounding 1 M ammonia at 24 h, while 33.7% of wells exhibited an OD_{600} <0.5 (Figure 5.2F). At 48 h, the number of wells at a cell density of OD_{600} ≥ 2 increased to 18.48%, but the majority of wells were between OD_{600} = 1-2 (63.77%) and 3.62% of wells were at a cell density of OD_{600} <0.5 (Figure 5.2F). Notably, there was no significant difference found between the mean percentage of wells between > 0.5-1, > 1-2 and > 2 OD_{600} compared across all treatment concentrations at 24 h, but treatment with 1 M ammonia significantly increased the number of wells between OD_{600} = 0-0.5 compared to control ($p < 0.05$) and 0.1 M conditions ($p < 0.05$) (Figure 5.2F).

For *H. meridiana* cultivated proximal to 0.25 M, 0.5 M and 1 M ammonia, lower cell density values (OD_{600} <1) were nearer to the ammonia source at both 24 h and 48 h, while the horizontal and vertical perimeter wells showed higher cell densities (OD_{600} > 1) (Figure 5.2C-E). In addition, the radial distribution of NH_3 was reflected in cell density alterations; the spatial zone of alterations became larger as ammonia concentration increased.

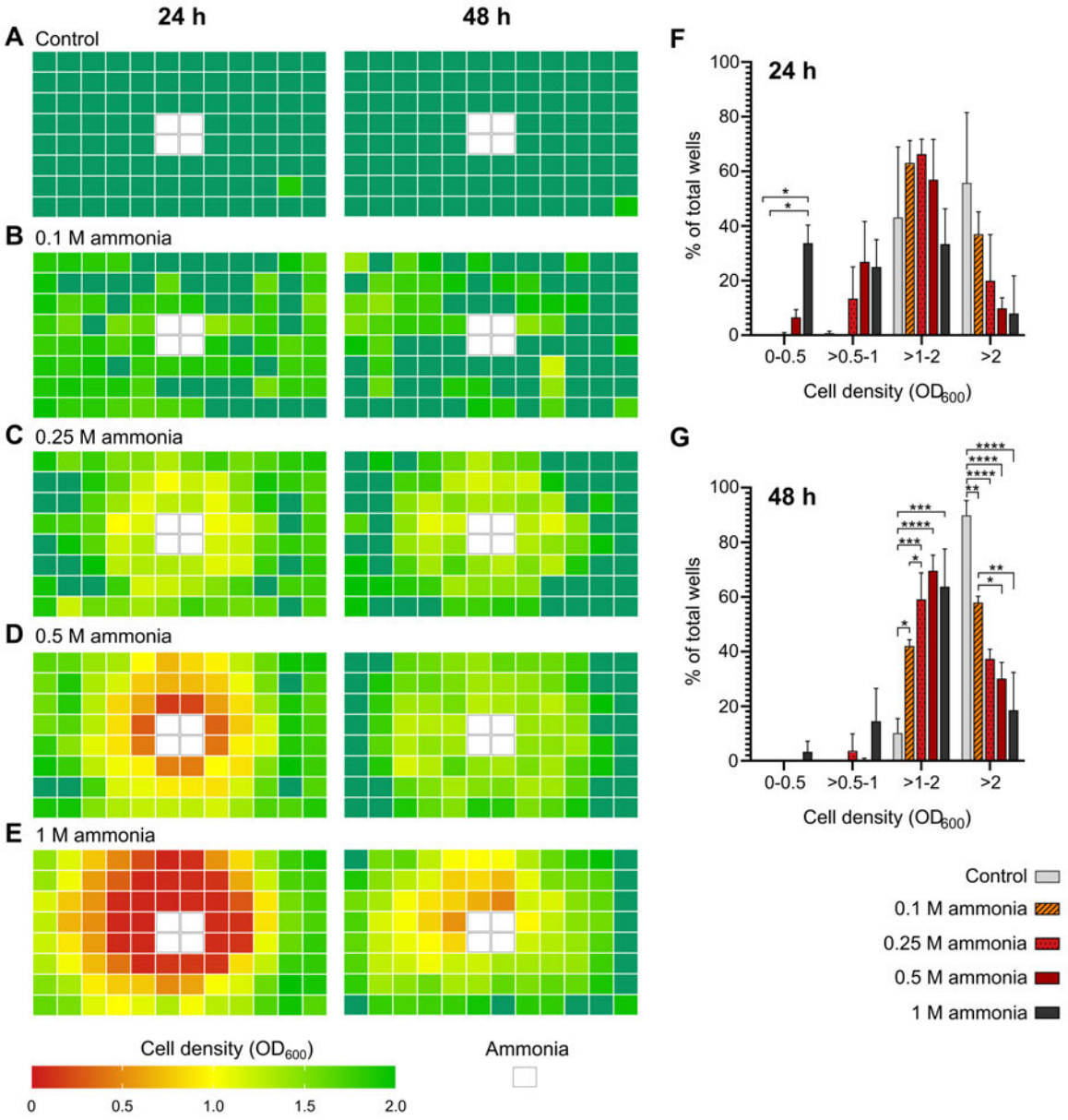

Figure 5.2: Spatiotemporal effect of ammonia on growth of *H. meridiana*. (A-E) Heatmaps representing the mean OD_{600} of wells in a 96-well plate ($n = 3$). Central wells (D6, D7, E6, E7) were filled with either 0 M (control), 0.1 M, 0.25 M, 0.5 M or 1 M ammonia as indicated by white squares. Surrounding wells were yeast media inoculated with *H. meridiana*. OD_{600} values were recorded 24 h and 48 h post-inoculation to ammonia. OD_{600} values were coloured as follows: 0, red; 1, yellow; 2, green; $>$ 2, dark green. (F, G) Cell density changes with increasing ammonia concentrations. For each concentration of ammonia, the number of wells between OD_{600} 0-0.5, $>$ 0.5-1, $>$ 1-2 and $>$ 2 at 24 h (F) and 48 h (G) post-inoculation was determined and calculated as a percentage of the total number of inoculated wells (92). The results are represented as a column graph with column heights and error bars indicating the mean $\pm$ S.D ($n = 3$). Statistical significance in (F) and (G) is given by the Kruskal-Wallis's test using Dunn's multiple comparison test for optical density groups 0-0.05 and $>$ 0.5-1, and one-way ANOVA using Tukey's multiple comparison test for optical density groups $>$ 1-2 and $>$ 2. ns, no significance; *, $p < 0.05$; **, $p < 0.01$; ***, $p < 0.001$; ****, $p < 0.0001$.

5.3.2 Kinetics of *H. meridiana* cultivated directly and adjacently to ammonia

Wells immediately adjacent to the ammonia source showed a lower cell density than those farther from the ammonia source. The lower cell density suggests an alteration to growth kinetics. Given the small (9 mm) distance from the ammonia source, the impact to growth kinetics could be similarly observed in *H. meridiana* directly exposed to ammonia. To explore this possibility, the growth dynamics of *H. meridiana* directly exposed to ammonia and adjacently exposed to an ammonia source were investigated and lag phase duration (Figure 5.3A-C), doubling time (Figure 5.3D-F) and final cell density (OD_{600}) at 48 h (Figure 5.3G-I) extrapolated. The growth curves utilised to extrapolate these growth parameters are available in Supplementary Figure S3.

H. meridiana exhibited an extension to lag phase duration when directly cultivated in all concentrations of ammonia. Adjacent cultivation to ammonia increased the duration of the lag phase at concentrations of 0.25 M and 0.5 M ammonia, but not 0.1 M ammonia (Figure 5.3A-D). *H. meridiana* cultivated adjacent to 0.1 M ammonia wells assumed a lag phase time of 0.2 ± 0.141 (Figure 5.3A). This was a shorter duration than those cultivated directly in 0.1 M ammonia (6.13 ± 1.55). Differences between lag phase duration of *H. meridiana* cultivated adjacently to 0.1 M ammonia was found to be non-significant from cells cultivated directly in ammonia ($p = 2.00$) and in control conditions ($p = 0.665$). Similarly, *H. meridiana* cultivated adjacent to 0.25 M ammonia wells assumed a lag phase time of 18.15 ± 4.62 (Figure 5.3B). This was a shorter duration than those cultivated directly in 0.25 M ammonia (25.65 ± 1.72). Differences between lag phase duration of *H. meridiana* cultivated adjacently to ammonia were found to be non-significant from cells directly exposed to ammonia ($p = 0.485$) and to control conditions ($p = 0.267$).

In Figure 5.3D, the doubling time of cells cultivated adjacently to 0.1 M was comparable to growth in control conditions ($p = 0.989$), and faster than cells cultivated directly in 0.1 M ammonia ($p < 0.001$). Conversely, as ammonia concentration increased, cells adjacent to 0.25 M ammonia showed comparable doubling time to cells cultivated directly in 0.25 M ammonia ($p = 0.271$). This was longer when compared to control conditions ($p < 0.05$) (Figure 5.3E). *H. meridiana* adjacently exposed to ammonia showed comparable final OD_{600} to cells cultivated directly in ammonia at concentrations of 0.1 M ($p = 0.991$) (Figure 5.3G) and 0.25 M ($p = 0.999$) (Figure 5.3H).

Notably, the cell density at 48 h was significantly higher in cells cultivated adjacently to ammonia than those in control conditions at 0.1 M ammonia ($p < 0.05$) (Figure 5.3G) and 0.25 M ammonia ($p < 0.05$) (Figure 5.3H). *H. meridiana* did not show an observable lag, log or stationary phase when cultivated directly in 0.5 M ammonia but did show onset of growth at 30 h post-inoculation when cultivated adjacently to a 0.5 M ammonia source (Supplementary Figure S3). Consequently, cultures adjacent to 0.5 M ammonia exhibited a higher final cell density compared to cells cultivated directly in 0.5 M ammonia ($p < 0.0001$) (Figure 5.3C). *H. meridiana* cultivated adjacently to 0.5 M were found to have a longer lag phase duration ($p < 0.1$) (Figure 5.3C), slower doubling time ($p < 0.05$) (Figure 5.3F) and lower final cell density ($p < 0.01$) (Figure 5.3I) than *H. meridiana* in control conditions.

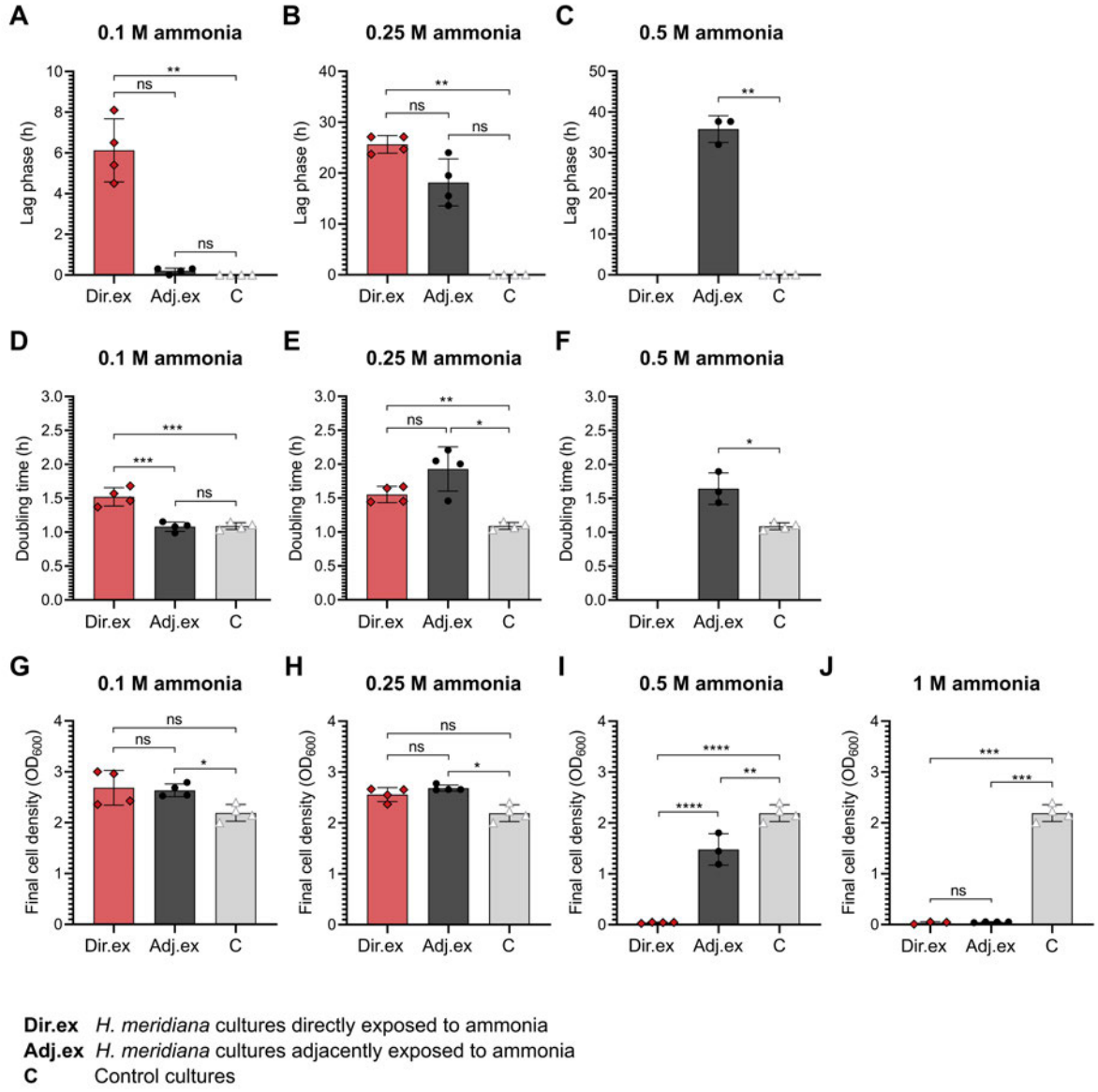

Figure 5.3: Growth kinetics of *H. meridiana* cultivated directly and adjacently to ammonia. (A-C) Lag phase time, (D-F) doubling time, and (G-J) final OD_{600} of *H. meridiana* at 48 h extrapolated from growth curves of Supplementary Figure S3. Column heights indicate the mean ± S.D. (n = 3 to 4). Statistical significance was calculated by one-way ANOVA, Welch's ANOVA, Kruskal-Wallis test and Welch's unpaired t-test. The individual tests utilised are outlined in Supplementary Table S1. ns, no significance; *, $p < 0.05$; **, $p < 0.01$; ***, $p < 0.001$; ****, $p < 0.0001$.

No growth was recorded in *H. meridiana* cultivated directly in or adjacently to 1 M ammonia (Supplementary Figure S3). OD_{600} at 48 h in both conditions thus remained at 0.05 (Figure 5.3J).

5.3.3 Cell viability and ammonia content in *H. meridiana* cultures directly and adjacently exposed to ammonia

Lag phase duration of *H. meridiana* increased incrementally when cultivated adjacently to higher concentrations of ammonia. I have previously shown this extension to lag phase duration is a result of reduced viable cell populations correlating with ammonia concentration (Hopton et al., 2025). Figure 5.4 shows cell number of *H. meridiana* and ammonia content in cultures following 4 h of direct and adjacent exposure to ammonia. Control conditions without ammonia are also shown. Across all directly exposed ammonia cultures, the concentration of ammonia was diminished from original inoculation concentration at 4 h confirming ammonia volatilization from wells over time. Gaseous NH_3 solubilised into adjacent cultures from an ammonia source was indicated by detectable levels of ammonia in these wells.

Differences in cell number were non-significant between control cultures and cultures adjacent to 0.1 M ($p = 0.794$) (Figure 5.4A). This aligned with a non-significant change in lag phase between this condition and control conditions in Figure 5.3A. The ammonia content in 0.1 M ammonia adjacently exposed cultures at 0.0308 M $\pm$ 0.0002, however, was significantly higher than those in the control condition ($p < 0.0001$). This indicates 0.1 M was not a concentration that detrimentally impacts cell number, and in turn, lag phase duration. Cell number was lower in cultures directly exposed to 0.1 M ammonia compared to adjacently exposed to ammonia ($p < 0.01$) and control conditions ($p < 0.01$). In correlation with this, ammonia content in directly exposed cultures at 0.0538 M $\pm$ 0.004 was higher than those in adjacently exposed ammonia cultures ($p < 0.001$) or control cultures ($p < 0.0001$) (Figure 5.4A). This correlates with the results of Figure 5.3A that demonstrate direct exposure of *H. meridiana* to 0.1 M ammonia increases lag phase duration compared with control.

Differences in cell number were significant between control cultures and cultures adjacent to 0.25 M ammonia ($p < 0.01$) (Figure 5.4B). Cultures adjacently exposed to 0.25 M showed a concentration of ammonia at 0.0677 M $\pm$ 0.000 which was significantly higher than control cultures ($p < 0.0001$). This level of ammonia may account for cell number reduction in ammonia-adjacent cultures. However, the level of viable cell loss was not found to impact lag phase duration significantly between ammonia-adjacent and control cultures, as indicated in Figure 5.3B. As a result of viable cell loss, cell number changes in cultures adjacently exposed to 0.25 M were found to be non-significant from cultures directly exposed to 0.25 M ($p = 0.999$) (Figure 5.4B). The non-significant change in cell number between directly and adjacently exposed cultures did not correlate with ammonia. Cultures adjacently exposed to 0.25 M showed a lower ammonia concentration than cultures directly exposed to 0.25 M, which were found to be 0.108 M $\pm$ 0.01 ($p < 0.001$). These results indicate, while not as cytotoxic as direct ammonia exposure, adjacent exposure to 0.25 M ammonia demonstrates detrimental effects on viability. This may account for the longer doubling time observed in cultures adjacently exposed to 0.25 M (Figure 5.3E) which was not observable in cultures adjacently exposed to 0.1 M (Figure 5.3D).

There was no growth in *H. meridiana* cultures cultivated directly in 0.5 M (Figure 5.4C) and 1 M ammonia (Figure 5.4D). These solutions also demonstrated the highest ammonia content compared to adjacent and control cultures, with concentrations of 0.146 M $\pm$ 0.02 and

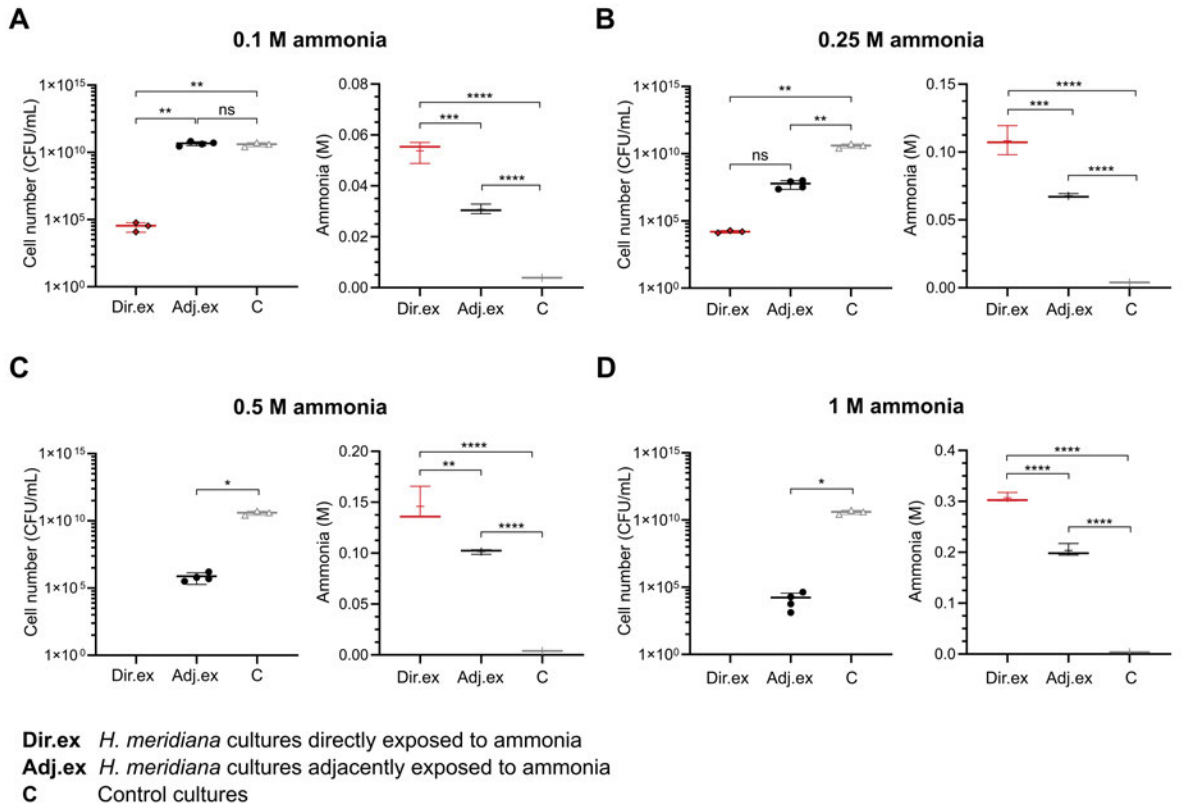

Figure 5.4: Cell number and ammonia content of *H. meridiana* exposed to ammonia. Cell number and ammonia content at 4 h in *H. meridiana* cultures following direct and adjacent exposure to ammonia concentrations of 0.1 M (A), 0.25 M (B), 0.5 M (C) and 1 M (D). Comparison to cell number and ammonia content in 0 M (control) cultures for each concentration is illustrated. Cell number is given by CFU/mL in individual value scatter plots. Mean is indicated by the central line between individual points ($n = 3$). Error bars are ± S.D. Statistical significance was calculated by one-way ANOVA with Tukey's post hoc test (0.1 M and 0.25 M) or two-tailed unpaired t-test with Welch's correction (0.5 M and 1 M). Ammonia concentration is depicted in box plots that show molar concentrations of ammonia measured in culture solutions 4 h post direct and adjacent exposure to ammonia. Box plots represent the median as well as the 25% and 75% interquartile ranges. The whiskers represent 1.5× the interquartile ranges. Plus sign (+) indicates the mean and the middle line indicate the median ($n = 3$). All statistical tests here correspond to one-way ANOVA with Tukey's post hoc test. ns, no significance; *, $p < 0.05$; **, $p < 0.01$; ***, $p < 0.001$; ****, $p < 0.0001$.

0.307 M ± 0.009, respectively. These concentrations were deleterious to *H. meridiana*. There were viable cells in cultures adjacent to 0.5 M and 1 M ammonia. This indicated adjacent cultures did not acquire ammonia to the concentrations observed in direct cultures at any point. Indeed, the ammonia content of ammonia-adjacent cultures was significantly lower than those in directly exposed cultures at 0.5 M (0.102 M ± 0.002, $p < 0.01$) and 1 M ammonia (0.203 M ± 0.01, $p < 0.0001$). Compared to control, the cell number in cultures adjacently exposed to 0.5 M ($p < 0.05$) (Figure 5.4C) and 1 M ($p < 0.05$) (Figure 5.4D) were lower. In accordance with this, the ammonia content was found to be significantly higher in cultures adjacent to 0.5 M ($p < 0.0001$) and 1 M ammonia ($p < 0.0001$) solutions compared to control.

5.4 Discussion

The aim of this work was to characterise the spatiotemporal effect of NH_3 gas on the cultivation of an extremophile, *H. meridiana*. Although the habitability of extraterrestrial environments is speculative, ammonia is known to be a component of extraterrestrial oceans (Fortes, 2000, Spohn and Schubert, 2003, Waite et al., 2009). Thus, our findings have relevance to the potential for habitability in these environments. Additionally, NH_3 volatilization, resulting from agricultural and industrial pollution (Van Damme et al., 2018, Luo et al., 2022), can deposit ammonia at great distances and may alter habitability in environments on Earth beyond the local site of release (Sutton et al., 1998, Bouet et al., 2005, Leytem et al., 2024, Lô et al., 2025). These results therefore advance the current understanding on how the gaseous state of NH_3 may permeate into environments and impact the potential for a habitat to become or remain inhabited.

Although previous studies have investigated the effects of toxic gases on microbial growth, none of these studies have examined the spatial effects of gas on microbial growth. In literature, the growth of a diverse range of bacteria has shown to be disturbed most closely to a pollutant source. For example, as in the case of soils nearby tailing ponds of seepage pollution (Geng et al., 2022) or soils with crude oil contamination (Jiao et al., 2016). In accordance with this, I observed reduction of cell density nearest to an ammonia source. I also identified that increased concentrations of NH_3 gas increased the spatial size of the zone affecting cell density. The effects I observed in the gas phase are analogous to diffuse-limited effects observed in agar plates. An increasing zone of inhibition with increasing concentration of a toxic substance has been demonstrated in agar diffusion assays using non-gas substances such as propolis extract (Boyanova et al., 2005), lauric acid-KOH Hinton Jr and Ingram (2011), chromium (Diaz-Baez and Roldan, 1996), and a range of organics, inorganics and organometallics (Liu et al., 1989). Likewise, an increasing spatial zone of antibacterial activity has been observed for application of increasing concentrations of reactive oxygen species on *Pseudomonas aeruginosa* (Dwivedi et al., 2014) and *E. coli* (Goswami et al., 2006). Our findings show how microbial growth can also be influenced by compounds traversing through the atmosphere as well as through liquid media.

NH_3 dispersal within the system was not instantaneous, and the timing at which NH_3 reached *H. meridiana* would have depended on spatial position within the plate. For wells located further from the NH_3 source, it is likely that NH_3 exposure occurred after cells had already transitioned from lag phase into exponential growth. This is significant, as bacteria are generally more sensitive during exponential phase, owing to more frequent cell wall remodeling, more permeable envelopes, and a lesser focus on the stress response (Mueller and Levin, 2020, Ughy et al., 2023, Keller and Dörr, 2023). Consequently, NH_3 exposure during this phase may have had a more pronounced inhibitory effect compared to exposure during lag phase. In these wells, *H. meridiana* may have initially exhibited growth dynamics similar to the control (i.e., progression through lag and early exponential phase), but then observed disruption of exponential growth and premature transition into stationary or death phase. Proportionally, a greater number of cell deaths may have occurred than cells exposed to NH_3 in the lag phase. In contrast, wells closer to the NH_3 source experienced earlier exposure, resulting in a prolonging of the observed lag phage due to cell death, but overall cell deaths may have been propor-

tionally lower. Despite this potential disruption, wells at the periphery remained at densities above OD_{600} = 1. It is reasonable to presume that cells at the periphery could reach a greater density as the initial growth phase was already started, while a lower density was reached in wells adjacent to the NH_3 source due to a delayed growth response. This phase-dependent and spatially variable exposure likely contributed to the heterogeneity observed in growth levels across the plate, and should be considered when interpreting differences between wells.

A notable alteration was that *H. meridiana* cultivated adjacently to ammonia at concentrations of 0.1 M and 0.25 M were able to establish a higher density at 48 h compared to control conditions. It is possible these concentrations were low enough, particularly following evaporation, that diffusion of NH_3 across the cytoplasmic membrane into the cell in equilibrium with NH_4^+ were sufficient to promote growth by providing additional nitrogen (Müller et al., 2006). NH_4^+ is assimilated by either the glutamine synthetase-glutamate synthase (GS-GOGAT) or glutamate dehydrogenase (GDH) pathway. In enzymology, K_m is the substrate concentration at which an enzyme's reaction is half of its maximal velocity, Vmax. K_m values for GS, GOGAT, and GDH have been reported at 0.033 M (Tachiki et al., 1978, Shatters et al., 1993), 0.0002 M(Hemmilä and Mäntsälä, 1978), and 0.029 M in bacteria (Kanamori et al., 1987a). At 4 h, the ammonia concentration in wells adjacent to 0.1 M were 0.0308 M ammonia, and adjacent to 0.25 M ammonia were 0.0678 M ammonia. These concentrations are thus suitable for GS and GDH to achieve 50% velocity or higher according to Michaelis-Menten kinetics and may account for enhanced cell density compared to control.

In *Halomonas*, ammonia nitrogen removal, and thus assimilation, rates have been reported at 5 mg N L^{-1} h^{-1} in species *H. salifodinae* (Hu et al., 2022), 9.10 mg N L^{-1} h^{-1} for *H. piezotolerans* strain HN2 (Dong et al., 2022) and 22 mg N L-1 h-1 in *Halomonas* sp. strain B01 (Wang et al., 2017). This approximately corresponds to the removal, and possible assimilation, of NH_4^+ at ≈0.00036 M h^{-1}, ≈0.00064 M h^{-1}, and ≈0.0016 M h^{-1}. As aforementioned, cultures adjacent to 0.1 M and 0.25 M ammonia sources were found to accumulate ammonia at 4 h to concentrations of 0.0308 M and 0.0677 M, respectively. This indicates the ammonia provided into the wells were near 20-fold and 42-fold higher than the concentration utilised in assimilation per hour. Such abundance may have stimulated higher growth than the control which featured limited amounts of ammonia.

Such abundance of ammonia could also be deleterious to growth, however. While enhanced cell density was observed in cultures adjacent to 0.25 M ammonia, lag phase duration was higher, doubling time was slower and cell viability also lower compared to control. In contrast to 0.1 M ammonia, cultures adjacent to 0.25 M showed ammonia values that were substantially higher than the Km values required for 50% Vmax in nitrogen assimilation enzymes and typical rates of nitrogen assimilation. Ammonia at 0.25 M ammonia thus reflects a transition concentration whereby excess ammonia becomes deleterious to growth. It is notable adjacent exposure to NH_3 gas at a concentration of $\geq$ 0.5 M is the limit at which the following effects were observed: i) reduced cell density surrounding the ammonia source (OD_{600} <0.5): ii) increased lag phase duration and doubling time; and, iii) reduced cell number of *H. meridiana* from control conditions. Cultures adjacent to 0.5 and 1 M solutions may have experienced enhanced nitrogen assimilation but likely experienced an overriding toxicity effect including internal alkalization and disruption to the internal H^+ pool that ultimately led to the deleterious

growth effects described. This is a function of ammonia concentration; I have previously demonstrated 0.05 M ammonia as a habitable limit for *H. meridiana* (Hopton et al., 2025). It is thus in accordance with this that cultures adjacent to 0.1 M ammonia showed an ammonia content below this limit. Concentrations above this limit were observed in 0.25 M, 0.5 M and 1 M cultures where growth or viability was significantly impacted. Our findings indicating a correlation between increased concentrations of NH_3 gas and reduced cell growth has also been demonstrated using other forms of toxic gas (Gee and Duane Brown, 1981, Porter et al., 1983, Coyne and Hardy, 1997, Cheng and Hu, 2021, Mendes et al., 2021, Seregina et al., 2022, Couvert et al., 2023).

In extraterrestrial icy worlds, ammonia is a primordial component incorporated into subsurface oceans. Fluid networks are expected within the overlying ice shells and could function as potential habitats (Kargel et al., 2000, Wettlaufer, 2009, Buffo et al., 2021, Wolfenbarger et al., 2022). It is probable fluids within the ice shell networks closely mimic, or are identical to, the composition of the ocean below and thus contain ammonia. However, it is feasible NH_3 gas may also be formed in these environments and thus influence habitability in addition to solubilised ammonia. For example, NH_3 gas may be produced by a process of exsolution at the plume vent region of Enceladus. NH_3 gas adsorbed onto the plume vent ice walls may then migrate through the ice shell to fluid networks. Alternatively, fractures through the ice shell that connect to the near vacuum surface could provide the pressure to facilitate NH_3 volatilization from connected fluid networks or the ocean if also permitted by pH and temperature. Volatilized NH_3 migrating up a fracture shaft may then disperse and dissolve into other fluid networks that intersect with the fracture region, impacting the potential for habitability in these environments.

The work presented here mimics an NH_3 exposure scenario. I show the spatial migration of ammonia impacts the concentration of ammonia dissolved into a solution and thus the growth of *H. meridiana*. I provide proof-of-principle evidence that the concentration of ammonia solubilised determines whether growth is facilitated or hindered. At low concentrations, addition of bioavailable nitrogen in the form of ammonia can facilitate growth, while higher concentrations can exert toxic cellular effects. On Enceladus, a hypothetical scenario can be argued; NH_3 volatilized at the base of a fracture site may be more harmful at this site and less harmful as the gas migrates up, absorbs into ice walls and fluid networks and deceases in concentration.

I show also show that environments neighbouring an ammonia concentration of 0.1 M demonstrate improved growth, while environments adjacent to concentrations exceeding 0.1 M can become detrimental to growth and viability. This would indicate environments adjacent to such concentrations may be habitable but display an altered bacterial community structure. For example, alkaliphilic bacteria may survive and propagate with greater abundance than alkali-tolerant bacteria, such as *H. meridiana*, that may grow slower. It is notable 0.1 M ammonia is the upper concentration boundary approximated for the ocean of Enceladus (Fifer et al., 2022). These thresholds are specific to *H. meridiana*; generalised habitability thresholds in NH_3 gas could be further constrained using a diversity of bacterial species. Indeed, comparisons with literature show that direct exposure to 0.1 M ammonia has been found toxic to neutrophilic *E. coli* and *B. subtilis* under icy moon conditions (Deal et al., 1975). In accordance with our

results, solutions where the NH_3 concentration exceeds 0.1 M can be survived by a diverse array of bacteria under standard terrestrial conditions including: *B. subtilis* T5 (0.15 M NH_3) (Leejeerajumnean et al., 2000), isolated sulphate-reducing bacteria (0.2 M NH_3) (Dai et al., 2017), Staphylococcus aureus (0.3 M NH_3), Enterococcus faecium (0.3 M NH_3), Micrococcus luteus (0.3 M NH_3), Salmonella typhimurium (0.3 M NH_3), B. cereus T41 (0.3 M NH_3), Proteus pumilus (0.5 M NH_3), B. pumilus ($>$ 0.5 M NH_3), and B. pasteurii ($>$ 0.5 M NH_3) (Leejeerajumnean et al., 2000). Thus, there is reason to believe such concentrations of NH_3 gas volatilized from an ammonia source could be survived by a range of species, although growth may not be optimal.

The temporal effects of NH_3 gas were also demonstrated. Due to the use of an open-air system, cultures of *H. meridiana* exhibited cell density recovery with time when adjacently exposed to ammonia at all concentrations. This is comparable to our previous study which demonstrated *H. meridiana* cell numbers recovered over time with ammonia evaporation from culture media (Hopton et al., 2025). The spatial toxicity imposed by ammonia is therefore transient and suggests ecosystems exposed to NH_3 would only be temporarily affected if there is a pathway to ammonia dispersal into the bulk atmosphere. This may occur on Enceladus if NH_3 outgassing from the ocean is infrequent. Presumably, continuous exposure would exert a continuous deleterious effect on growth. It is crucial to note these results do not infer an increased or decreased likelihood of life existing on icy moons. Indeed, many other factors will influence habitability. It may be found these environments are habitable but not inhabited. Rather, these results show that NH_3 gas is a chemical parameter that could influence the potential for habitability in a spatiotemporal manner. The presence of NH_3 gas should thus be considered when constraining targets for astrobiological exploration.

Our results also have implications for Earth habitability. In terrestrial environments, localised "point sources" of ammonia pollution have been identified in both agriculture and industry (Van Damme et al., 2018). This would suggest long-term spatial effects on nearby bacterial communities according to the results of this study. *H. meridiana* was selected as an organism that could survive in cold, saline and high pH fluids under pressure. However, *H. meridiana* is also a mesophile, grows optimally at standard pressure and can grow at neutral pH. This organism, and the growth results presented, can thus represent bacteria without extremophilic adaptations and indeed our results are in accordance with other, diverse bacteria as outlined.

5.5 Limitations and future work

A natural extension of this work would be to consider evaporation rate of NH_3. The importance of evaporation rate in temporal toxicity may account for a discrepancy observed between the cell density achieved at 48 h in cultures surrounding 1 M ammonia (Figure 5.2E) compared to the cell density reached at 48 h in cultures adjacent to 1 M ammonia in Figure 5.3J. The evaporation rate of essential oils has been shown to effect the minimal inhibitory dose (MID) against Staphylococcus aureus and *E. coli*, with rapid evaporation producing a higher vapour concentration that reduces the MID required (Inouye et al., 2001). This research indicates discrepancies between experiments could be attributed to altered rate of ammonia evaporation, and thus delivery of NH_3, driven by differences in the culture instrumentation and shaking speed. A continuation of this work would be to alter atmospheric pressure or incorporate an

air flow system. The incorporation of such measures could more accurately replicate in situ environments relevant to icy worlds and in anthropogenic NH_3 pollution.

5.6 Conclusion

NH_3 is a gas that can supply essential nitrogen but also exert cellular toxicity. NH_3 volatilized from a concentrated source into surrounding environments is therefore a crucial consideration when assessing the capacity of environments to support life, such as within terrestrial environments polluted with ammonia, or the ice crusts above ammonia-water oceans of icy moons. In this chapter, it was evident that lower cell densities (OD_{600} = 0-1) occurred nearest an NH_3 source. At 24 h, wells exhibited an OD_{600} = 0-0.5 when ammonia concentrations were $\geq$ 0.5 M. *H. meridiana* in proximity to 0 M, 0.1 M, 0.25 M, 0.5 M and 1 M ammonia exhibited an $OD_{600} > 2$ in 89.86%, 57.97%, 37.32%, 30.07% and 18.48% of culture wells at 48 h, respectively. Alteration to growth kinetics and viability of *H. meridiana* cultivated adjacently to an NH_3 source were not as severe compared to direct culture in ammonia. Compared to control, adjacent exposure to 0.1 M ammonia exhibited no significant detrimental effect on growth kinetics and enhanced cell density, but adjacent exposure to $\geq$ 0.5 M ammonia greatly extended lag time, doubling time, reduced cell density and reduced viability. When considering the habitability of terrestrial and extraterrestrial environments, it can be surmised from these results that NH_3 volatilized from 0.1 M sources may thus minimally affect, if not improve, habitability. However, environments exposed to NH_3 volatilized from sources at $\geq$ 0.5 M could constrain habitability and may preclude the growth or viability of biological organisms.

6

Growth, physiology and metabolism of *Halomonas meridiana* in aqueous ammonium sulphate with implications for icy moon astrobiology

This publication appeared in *Frontiers in Microbiology*, 19th September 2025.
DOI: 10.3389/fmicb.2025.1642998

6.1 Introduction

Chapters 4 and Chapter 5 demonstrated that NH_3 can impose certain habitability limits and physiological effects on *Halomonas meridiana* in high pH environments, where the relative abundance of NH_3 is high. Near neutral environments will observe higher proportions of NH_4^+. It has been shown NH_4^+, while "less toxic", can also exert a distinct toxicological effect (Gorissen et al., 1993, Witter et al., 1993, Goude et al., 2004, Toljander et al., 2008, Zorz et al., 2018). Near neutral or acidic oceanic environments may occur on the icy moon Europa (Johnson et al., 2019, Pasek and Greenberg, 2012, Tan et al., 2021), and $(NH_4)_2SO_4$ has been tentatively recorded on the surface (Mermy et al., 2023). In an alternative model of Titan's ocean environment, it is possible NH_4^+ in the form of $(NH_4)_2SO_4$ could also constitute a major portion of the ocean (Fortes et al., 2007, Grindrod et al., 2008). On Earth, $(NH_4)_2SO_4$ is a common fertilizer (Randive et al., 2021, Tyagi et al., 2022). Thus, to fully characterise the bacteriological impacts of aqueous ammonia for both icy moon and Earth environments, it was pertinent in Chapter 6 to define the limits of habitability and physiological effect of aqueous $(NH_4)_2SO_4$ on *H. meridiana*. To the best of my knowledge, this was the first study to explore growth limits and physiology of an aerobic, extremophile bacteria without specified ammonia adaptations in $(NH_4)_2SO_4$. Concentration thresholds of $(NH_4)_2SO_4$ on icy moon environments have not been estimated, thus a concentration scale from sub-molar (0.1 M) to molar (1 M) was chosen to examine limits. The study begins by assessing growth dynamics, kinetics and viable cell number in these increasing concentrations of $(NH_4)_2SO_4$. As $(NH_4)_2SO_4$ is a salt, the impact of individual ions, salinity, osmotic pressure, pH, and water activity on the observed response of *H. meridiana* in $(NH_4)_2SO_4$ were explored by comparatively assessing growth in a range of common ammonium and sulphate salts. In addition to this, phenotypic changes in cell structure were examined by transmission electron microscopy, and internal molecular changes were explored using untargeted metabolomics. It should be noted that ionic strength values reported for the brines were calculated as stoichiometric ionic strengths. This approach provides a consistent metric for comparing the ionic environments generated by the different ammonium salts used in this study.

frontiers | Frontiers in Microbiology

TYPE Original Research
PUBLISHED 19 September 2025
DOI 10.3389/fmicb.2025.1642998

OPEN ACCESS

EDITED BY
Cristian Randieri,
University of eCampus, Italy

REVIEWED BY
Satya P. Singh,
Saurashtra University, India
Ram Karan,
University of Delhi, India
Jia-Hui Wu,
Macau University of Science and Technology, China

*CORRESPONDENCE
Cassie M. Hopton
✉ c.m.hopton@sms.ed.ac.uk

RECEIVED 07 June 2025
ACCEPTED 25 August 2025
PUBLISHED 19 September 2025

CITATION
Hopton CM, Nienow P and Cockell CS (2025) Growth, physiology, and metabolism of *Halomonas meridiana* in aqueous ammonium sulfate with implications for icy moon astrobiology. *Front. Microbiol.* 16:1642998. doi: 10.3389/fmicb.2025.1642998

Growth, physiology, and metabolism of *Halomonas meridiana* in aqueous ammonium sulfate with implications for icy moon astrobiology

Cassie M. Hopton[1]*, Peter Nienow[2] and Charles S. Cockell[1]

[1]UK Centre for Astrobiology, School of Physics and Astronomy, University of Edinburgh, Edinburgh, United Kingdom, [2]School of Geosciences, University of Edinburgh, Edinburgh, United Kingdom

The discovery of extraterrestrial reservoirs of liquid water has motivated missions to icy moons Europa and Titan. Tentative evidence of ammonium sulfate ($(NH_4)_2SO_4$) has been detected on the surface of Europa, and $(NH_4)_2SO_4$ could be a prominent constituent of the Titan subsurface ocean. While NH_4^+ acts as a nitrogen source for many organisms, detrimental impacts of $(NH_4)_2SO_4$ fertilizer have been documented in bacteria. Consequently, the presence of $(NH_4)_2SO_4$ within icy moon environments may constrain the capacity of these environments to support life. In this study, the bacterial survival limits and physiological response to aqueous $(NH_4)_2SO_4$ were assessed using the extremophile *Halomonas meridiana* SIthf1. Growth assays demonstrated concentrations exceeding 0.25 M $(NH_4)_2SO_4$ led to a measurable slowing of the growth rate. Cell density remained comparable to control conditions up to 0.75 M $(NH_4)_2SO_4$ at which a decline was observed. Contrary to existing hypotheses, alterations to cell density were not determined by pH, osmolarity, salinity, ionic strength, or water activity of the aqueous $(NH_4)_2SO_4$ solution. Furthermore, neither NH_4^+ nor SO_4^{2-} alone accounted for these alterations. Metabolite profiling revealed that exposure to $(NH_4)_2SO_4$ reduced the abundance of glutamine compared to control, indicating an alteration to nitrogen, carbon, and energy metabolism. Active catabolism was suggested by reduced levels of purine metabolites and amino acids. Metabolites within the methylaspartate cycle were detected. We discuss these results with regards to the potential for habitability in aqueous extraterrestrial $(NH_4)_2SO_4$ environments as well as terrestrial environments in which $(NH_4)_2SO_4$ fertilizer is applied.

KEYWORDS

ammonium, ammonium sulfate, icy moons, Europa, Titan, habitability, extremophiles, pollution

Introduction

Where there is liquid water, there is the prospect for habitable conditions—the liquid water subsurface oceans of icy moons orbiting Jupiter (Europa, Ganymede, Callisto) and Saturn (Enceladus, Titan) are prominent targets in the search for life. Recently launched missions to Europa—the Jupiter Icy Moons Explorer (Juice) (Grasset et al., 2013) and Europa Clipper (Howell and Pappalardo, 2020), and the confirmed launch of NASA's Dragonfly mission to Titan (Barnes et al., 2021)—will probe these environments for extraterrestrial habitability. For decades, Europa and Titan have been hypothesized as

environments that could support the emergence of life; there is availability of energy (Schulze-Makuch and Irwin, 2001; McKay and Smith, 2005; Hand et al., 2007; McKay, 2016) and many of the essential elements for life (CHNOPS: carbon, hydrogen, nitrogen, oxygen, phosphorus, sulfur) have been detected (Sagan et al., 1992; Hiscox, 2000; Owen, 2000; Nixon, 2024; Szalay et al., 2024).

A further compositional expectation for Europa and Titan is the presence of ammonia (Lewis, 1971; Engel et al., 1994; Spohn and Schubert, 2003; Tobie et al., 2005). Ammonia is a ubiquitous molecule found in a variety of celestial bodies (Wyckoff et al., 1989; Ao et al., 2011; Wong et al., 2018; Irwin et al., 2025). It can occur as the biologically toxic unionized ammonia (NH_3) or less toxic ammonium ion (NH_4^+). Under standard pressure and temperature, the speciation of ammonia (hereafter ammonia refers to the total NH_4^+ and NH_3 in a system) is dependent on pH; a pH above or below 9.25 dictates whether NH_3 (>pH 9.25) or NH_4^+ (<pH 9.25) predominates. In cold waters of 0 °C, this threshold increases to pH 10.1 (Bates and Pinching, 1949). While the ocean of Europa is predominantly magnesium sulfate ($MgSO_4$) (McCord et al., 1998; Kargel et al., 2000; Zolotov and Shock, 2001), or possibly chloride salts (Brown and Hand, 2013; Hand and Carlson, 2015; Ligier et al., 2016), ammonium sulfate ($(NH_4)_2SO_4$) could be a constituent at the surface of Europa (Mermy et al., 2023). Surface $(NH_4)_2SO_4$ could be of oceanic origin due to emplacement by cryovolcanic venting (Roth et al., 2014; Sparks et al., 2016; Jia et al., 2018) or convection of the ice shell (Howell and Pappalardo, 2018). Indeed, with oceanic waters at pH <8.4 (Johnson et al., 2019) and between −63 °C to 0 °C (Marion et al., 2003; Melosh et al., 2004), most ammonia within the internal ocean of Europa would be in the form of NH_4^+. On Titan, an ocean of aqueous $(NH_4)_2SO_4$ fits with the modeled density and could account for cryovolcanism at the surface (Fortes et al., 2007; Grindrod et al., 2008). Titan's ocean temperature has been estimated in excess of −18°C (Sohl et al., 2014). The oceanic pH of Titan remains undetermined; an alkaline pH is predicted in models where NH_3 is expected (∼pH 11) (Marion et al., 2012; Leitner and Lunine, 2019). However, for the purpose of this study, we consider the aqueous $(NH_4)_2SO_4$ ocean model.

The detection of NH_4^+ in the oceans of Europa and Titan would be a significant finding. NH_4^+ is one of the preferred nitrogen sources for many organisms on Earth (Kleiner, 1981; Raven et al., 1992; Britto et al., 2001; Reitzer, 2003; Li et al., 2013). Ammonia could have also acted as a nitrogen source for internal ocean prebiotic chemistry in early Earth (Martin et al., 2008; Sojo et al., 2016). The bioavailability of NH_4^+ on Earth underpins its widespread use as a nitrogen fertilizer, commonly in the form of ammonium nitrate (NH_4NO_3), diammonium phosphate ($(NH_4)_2HPO_4$) or $(NH_4)_2SO_4$ (Randive et al., 2021; Tyagi et al., 2022). However, there is a concentration limit at which NH_4^+ transitions from a vital nitrogen source to a cytotoxic compound. The toxicity of NH_4^+ in high concentrations has been well-documented in prokaryotes (Sprott and Patel, 1986; Hendriksen and Ahring, 1991; Leejeerajumnean et al., 2000), plants (Britto et al., 2001; Esteban et al., 2016; Hachiya et al., 2021) and aquatic eukaryotes (Ip et al., 2001; Randall and Tsui, 2002; Collos and Harrison, 2014).

In bacteria, the application of $(NH_4)_2SO_4$ has shown to reduce populations, impact diversity (Gorissen et al., 1993; Witter et al., 1993; Toljander et al., 2008) and alter metabolism (Goude et al., 2004; Zorz et al., 2018). However, few studies have examined the survival limits of bacterial life in $(NH_4)_2SO_4$. *Bacillus subtilis* and *Corynebacterium glutamicum* are capable of survival in up to, and possibly exceeding, 0.716 M (Leejeerajumnean et al., 2000) and 1 M $(NH_4)_2SO_4$ (Müller et al., 2006), respectively. However, the oceans of Europa and Titan are putatively saline, cold and under hydrostatic pressure. It is therefore appropriate to assess habitability using terrestrial organisms with appropriate physiological adaptations. Halophilic bacteria have been shown to grow in brines relevant to the sodium chloride (NaCl), magnesium chloride ($MgCl_2$) and $MgSO_4$ content of Europa (Wilks et al., 2019; Cesur et al., 2022; Parker et al., 2023). Yet, the molar thresholds for survival and physiological impacts of $(NH_4)_2SO_4$ on halophilic bacteria are poorly represented in the literature. Such information could allow us to assess the habitability of aqueous extraterrestrial environments and hypothesize suitable signatures that could be captured by life-detection machinery in $(NH_4)_2SO_4$-bearing environments.

We have previously demonstrated that ammonia, predominantly speciated as NH_3, can constrain growth and alter the physiology of *Halomonas meridiana* Slfth1 (Sltfh1) (nomenclature synonym: *H. aquamarina*). This had implications for the habitability of Enceladus and alkaline terrestrial environments (Hopton et al., 2025). These results could also be applicable to models of the Titan subsurface ocean where ammonia is NH_3 (Lunine and Stevenson, 1987; Tobie et al., 2012; Sohl et al., 2014). Here, we aim to understand the survival limits and physiological response of Sltfh1 to $(NH_4)_2SO_4$, with implications for the habitability of Europa and Titan that could bear solubilised oceanic $(NH_4)_2SO_4$, as well as environments on Earth polluted with $(NH_4)_2SO_4$ fertilizer. Sltfh1 is a deep-sea extremophile with physiological adaptations relevant to conditions presented within the oceans of Europa and Titan. We assessed cultivation of Sltfh1 in increasing concentrations of $(NH_4)_2SO_4$ and other ammonium and sulfate salts. Using microscopy and an untargeted metabolomics approach, we determined physiological changes upon $(NH_4)_2SO_4$ exposure. We draw conclusions on the habitability of extraterrestrial and terrestrial environments.

Materials and methods

Bacterial strain selection and cultivation

Halomonas meridiana Slthf1 (DSM 15724; Gram negative bacterium) was obtained from the German Collection of Microorganisms and Cell Cultures (DSMZ). It should be noted this strain has been synonymized with *H. aquamarina* based on phylogenomic classifications (Dobson and Franzmann, 1996), but *H. meridiana* remains validly published as a heterotypic synonym according to the International Code of Nomenclature of Prokaryotes (ICNP). Due to constantly evolving taxonomy, we refer to *H. meridiana* Slthf1 as "Slthf1" in the proceeding text. Slthf1 was isolated in a deep-sea hydrothermal environment. Such environments could have supported prebiotic chemistry on Earth (Martin et al., 2008; Sojo et al., 2016) and may occur within icy moon oceans (Vance et al., 2007; Hsu et al., 2015; Russell et al., 2017). Typical phenotypic characteristics of the hydrothermal-vent habitat of origin are exhibited by Slthf1 (Kaye and Baross, 2004;

Kaye et al., 2004; Takahashi et al., 2020). This includes not only adaptability to high salinity (growth in up to 22% (w/v) NaCl) and high alkalinity (tolerance up to pH 12), but also, genomic adaptations to the cold (possessing three cold shock protein genes, growth at −1 °C) and high-pressure deep-sea environment (growth at 550 bar). This combination of polyextremophilic adaptations makes Slthf1 a superior model organism compared to halophilic archaea for studying potential life in cold, saline-alkaline environments similar to those presented in icy moon subsurface oceans. Additionally, Slthf1 has no known specialised adaptations to ammonium. This was an intentional choice. Ammonium content in the oceans of icy moons is such that adaptation to ammonium may not be required for survival. The intention of this study was to assess survival in ammonium, not to study an already established ammonium adaptation. The complete genome sequence for this organism is also available [DDBJ, accession no. AP022821] (Takahashi et al., 2020). Aerobic culture of Slthf1 was performed in glass conical Erlenmeyer flasks in an orbital benchtop shaking incubator set to rotate at 150 RPM, 28 °C. Slthf1 was cultivated in a yeast media consisting of 1 g/100 mL Bacto^{TM} yeast extract (Becton, Dickinson and Company), 0.2 M NaCl (Thermo Fisher Scientific, CAS Number: 7647-14-5) and distilled water.

Brine preparation

Solutions of ammonium and sulfate salts were prepared to 0.1 M, 0.25 M, 0.5 M, 0.75 M and 1 M from 2 M stock solutions diluted into yeast media. Ammonium salts included: $(NH_4)_2SO_4$; Fisher Scientific, CAS Number: 7783-20-2, ammonium nitrate (NH_4NO_3; Scientific Laboratory Supplies, CAS Number: 6484-52-2) and ammonium chloride (NH_4Cl; Honeywell Research Chemicals, CAS Number: 12125-02-9). In addition to $(NH_4)_2SO_4$, sulfate salts included sodium sulfate (Na_2SO_4; Sigma Aldrich CAS number: 7757-82-6), and potassium sulfate (K_2SO_4; Acros Organics, CAS number: 7778-80-5). Owing to limited solubility of K_2SO_4, molarities beyond 0.5 M were not tested. $(NH4)_2SO_4$ was also prepared in yeast media at concentrations of 0.05 M, 0.125 M and 0.375 M to achieve equivalent NH_4^+ concentrations of 0.1 M, 0.25 M and 0.75 M, respectively, in accordance with the stoichiometry of NH_4^+ ions in other ammonium brines. The pH of solutions was determined with a Jenway 3510 benchtop pH meter. All solutions were between pH 5.5 and pH 6.5. Solution pH remained unmodified in order to preserve a high NH_4^+/NH_3 ratio at acidic pH. Solutions of matching pH were created by addition of HCl or NaOH into yeast media. Solutions were matched to within ± 0.01 pH units. All solutions were filter-sterilized through a 0.22-micron pore before use.

Growth conditions

The growth kinetics of Slthf1 cultivated in ammonium and sulfate salts was determined by recorded optical density (OD) measurements at 600 nm (OD_{600}). Overnight Slthf1 culture was inoculated to OD_{600} = 0.05 into the selected brines. Controls were prepared by Slthf1 inoculation into unamended yeast media. Negative controls had no inoculation. Samples were seeded into a 96-well plate with a low evaporation lid and measurements taken with a BMG SPECTROstar Nano Microplate Reader over 48 h (h) at 28 °C. For cell viability assays, $(NH_4)_2SO_4$ solutions were prepared to 1 M in yeast media. Brines were inoculated with overnight culture of Slthf1 to OD_{600} = 0.05 in a 96-well plate. Cultures were incubated in a tabletop shaker at 28 °C for 72 h. Cell viability was examined using colony forming units (CFU) on yeast media agar and incubated at 28 °C for 3 days prior to enumeration. To prevent condensation, 96-well plate lids were treated with a solution of Triton X-100 (0.05%) in 20% ethanol in all growth experiments.

Growth kinetics

Growth curves were analyzed to determine growth rate and final cell density at 600 nm. Growth rate, μ, was calculated as per Equation 1, where N_0 is the OD_{600} at the beginning of a selected time interval (t_0) in the exponential growth phase; N is the OD_{600} at the end of a selected time interval (t) in the exponential growth phase. t and t_0 were recorded in minutes.

$$\mu = \left(Log_{10}(N) - Log_{10}(N_0)\right) 2.303/(t - t_0) \quad (1)$$

Final cell concentration was indicated by the final OD_{600} reached after 48 h. Measurement of OD_{600} vs. cell viability confirms that an increase in OD_{600} reflects increased viability and proliferation of cells (Supplementary Figure S1).

Water activity

Water activities were measured in the laboratory with a Rotronic HP23-AW water activity meter (Rotoronic AG, Bassersdorf, Switzerland). Solutions were prepared and measured after a time interval of 1.5 h to allow equilibration.

Metabolomics sampling and extraction

Slthf1 was cultivated overnight and inoculated to OD_{600} = 0.05 into 0.5 M $(NH_4)_2SO_4$ or unamended yeast media (control) within a 24-well plate. Growth at 28 °C was assessed by OD_{600} readings every 30 min using a BMG SPECTROstar Nano Microplate Reader. Slfth1 was harvested at OD_{600} = 0.5 following 28 h growth. An aliquot of each sample was placed into a microcentrifuge tube and briefly incubated on ice. Samples were retained for transmission electron microscopy (TEM) as described in the TEM preparation section. The remaining samples were quenched by rapid cooling in a dry ice-ethanol bath (70% v/v ethanol). Samples were vigorously mixed to prevent freezing. Any spent medium was discarded by centrifugation at 1,000 × g for 10 min at 4 °C followed by removal of supernatant. Metabolites were extracted by application of ice-cold chloroform/methanol/water (1:3:1). During metabolite extraction, cell lysis was encouraged by sonication of samples in water for 5 min at 37 kHz in an ultrasonication bath (Elmasonic S 60 H) maintained at 4 °C with ice. Extraction mixtures were shaken

at 1,200 RPM for 1 h at 4 °C and centrifuged at 13,000 × *g* for 3 min at 4 °C. The metabolite-rich supernatant was harvested into sterile microcentrifuge tubes and maintained at −80 °C until analysis. A quality control sample was created by pooling equal volumes of metabolites from all samples, which was also maintained at −80 °C until analysis.

Metabolomics

Global metabolomic profiling was conducted using liquid chromatography (LC) coupled with ion mobility (IM) quadrupole time-of-flight (qTOF) mass spectrometry (MS). The system consisted of an Agilent 1290 Infinity II series ultra-high-performance liquid chromatography (UHPLC) setup interfaced with an Agilent 6560 IM-qTOF mass spectrometer equipped with a Dual Agilent Jet Stream Electron Ionization source. Chromatographic separation was achieved using an InfinityLab Poroshell 120 HILIC-Z UHPLC column (2.1 mm × 50 mm, 2.7 μm) coupled to an InfinityLab Poroshell 120 HILIC-Z guard column (3.0 mm × 2.7 μm), both sourced from Agilent Technologies (689775–924 and 823750–948, respectively). A gradient elution was performed over 3.5 min, utilizing an organic solvent (acetonitrile) in combination with an aqueous buffer, either low-pH (10 mM ammonium formate, pH 3) for positive ionization or high-pH (10 mM ammonium acetate, pH 9) for negative ionization. Data were collected using MassHunter Data Acquisition 10.0 software, with 1 μL of each sample injected at a flow rate of 800 μL/min. A pooled quality control (QC) sample, comprising equal volumes of all experimental samples, was injected five times at the beginning of the experiment to equilibrate the column and after every subsequent set of five test samples to monitor system stability during data acquisition. Mass spectrometry data were acquired over a m/z range of 50–1,700, with a scan rate of 0.8 scans per second. The metabolomic analysis was performed at the EdinOmics research facility (RRID: SCR_021838) at the University of Edinburgh.

Data processing and statistical analysis of the metabolomics dataset

Analysis of the raw data files was performed by the Agilent MassHunter software suite. Specifically, ion multiplexed and calibration files underwent demultiplexing with the PNNL PreProcessor v2020.03.23, utilizing default settings for tasks such as demultiplexing, moving average smoothing, saturation correction, and spike removal. For recalibration, accurate mass and drift time adjustments were made using AgtTofReprocessUi and IM-MS Browser 10.0, respectively. Molecular features were extracted using Mass Profiler 10.0, with parameters set for retention time tolerance (±0.3 min), drift time tolerance (±1.5%), and accurate mass tolerance (± 5 ppm + 2 mDa). Feature annotation was carried out by matching accurate mass and collision cross-section (CCS) values to the McLean CCS Compendium PCDL library (Nichols et al., 2018). Statistical analyses was performed via the MetaboAnalyst 6.0 online platform (Pang et al., 2024), with data log-transformed and Pareto-scaled before analysis. Annotated molecular features were used to generate principal component analysis (PCA), volcano analysis, unpaired *t*-test and box plots. For pathway analysis, compound names were first converted to ID labels according to the human metabolome database (HMDB). Compound HMDB ID with relative intensities were submitted to the MetaboAnalyst 6.0 online platform pathway analysis tool. Data was log-transformed, auto-scaled and examined against the *H. meridiana* SCSIO 43005 KEGG pathway library using global test and relative betweenness centrality methods. Altered pathways with a p-value < 0.05 and FDR < 0.05 were considered significant. Significantly altered metabolites in the unpaired *t*-test that were also identified as altered in the pathway analysis are depicted in box and whisker plots. The plots were retrieved following *t*-test analysis on the MetaboAnalyst 6.0 online platform. Normalized values are presented. The raw data associated with this study is available in the Supplementary Data Sheet. This study focuses on metabolomic changes in $(NH_4)_2SO_4$, but the broader metabolomic profiling also included samples cultivated in NH_3 and NaOH. For the purpose of this study, only $(NH_4)_2SO_4$ and control samples were included. The metabolomics of NH_3 and NaOH exposed samples were addressed in a separate analysis (Hopton et al., 2025).

Transmission electron microscopy

Cultures of Slthf1 cultivated in 0.5 M $(NH_4)_2SO_4$ were harvested during metabolomics sampling, prior to extraction. Cells were pelleted by centrifugation at 5,000 × *g* and supernatant removed. The pellet was washed and resuspended in phosphate-buffered saline (PBS). Following centrifugation at 5,000 × *g* and supernatant removal, the cell pellets were fixed in 3% glutaraldehyde prepared in 0.1 M sodium cacodylate buffer (pH 7.3) for 2 h, followed by three 10 min washes in 0.1 M sodium cacodylate. Post-fixation was carried out using 1% osmium tetroxide in 0.1 M sodium cacodylate for 45 min, followed by a series of three 10 min washes in 0.1 M sodium cacodylate. The samples were dehydrated sequentially in ethanol solutions at 50%, 70%, 90%, and 100% for 15 min each. This was repeated in triplicate and followed by two 10 min washes in propylene oxide. The samples were embedded in TAAB 812 resin. Sections of 1 μm thickness were prepared using a Leica Ultracut ultramicrotome, stained with Toluidine Blue, and examined under a light microscope to identify regions of interest. Ultrathin sections (60 nm thick) were cut from these selected regions, stained with uranyl acetate and lead citrate, and observed using a JEOL JEM-1400 Plus TEM. Representative images were acquired with a GATAN OneView camera at 4K resolution and subsequently processed using ImageJ software (version 57).

Statistics and reproducibility

Normality of data was assessed with the Shapiro-Wilk test. For comparison of two groups, equal variance was assessed with an F-test. Groups of equal variances were analyzed by unpaired two-tailed *t*-test. Groups of unequal variances were assessed by

unpaired two-tailed *t*-test with Welch's correction. For analysis of three or more groups, equal variance was assessed by the Brown-Forsythe test. Samples of equal variance were analyzed by analysis of variance (ANOVA) followed by Tukey's *post-hoc* test. For samples where variance was not equal, Welch's ANOVA test with Tamhane's T2 *post-hoc* test was applied. For datasets with non-normal distribution, means were compared using the Kruskal–Wallis test with Dunn's multiple comparisons test. Statistical tests are specified in figure legends. Results where $p < 0.05$ were considered significant. All data was compiled from at least three biological replicates ($n = 3$–5). Data is presented as the mean ± standard deviation (SD). All figures and statistical analyses were produced using GraphPad Prism version 8.0.2 (GraphPad Software Inc.).

Results

Concentration thresholds for growth of Slthf1 in $(NH_4)_2SO_4$

Growth of Slthf1 over 48 h in increasing concentrations of $(NH_4)_2SO_4$ was investigated to assess concentration thresholds of growth in $(NH_4)_2SO_4$. Concentrations of 0.1 M, 0.25 M, 0.5 M, 0.75 M and 1 M were utilized, with unamended yeast media, 0 M $(NH_4)_2SO_4$, as a control. The resulting growth curves are depicted in Figure 1A. Growth progressively declined with increasing $(NH_4)_2SO_4$, with minimal cell density observed at 1 M $(NH_4)_2SO_4$. Cell viability assay confirmed that Slthf1 remained viable at 1 M $(NH_4)_2SO_4$ after 72 h incubation (Figure 1B). Growth rate and final cell density at 48 h are shown in Figures 1C, D, respectively. Overall, growth of Slthf1 was limited by increasing concentrations of $(NH_4)_2SO_4$. Growth rate was non-significant from control at concentrations of 0.1 M ($p = 0.599$). Successive reduction in growth rate compared to control was observed in 0.25 M ($p < 0.05$), 0.5 M ($p < 0.01$), 0.75 M ($p < 0.01$) and 1 M ($p < 0.01$) brines. However, reduction in growth rate does not affect final cell density when grown up to 0.5 M $(NH_4)_2SO_4$; at 48 h, there was no significant difference between the OD_{600} in control solutions compared to 0.1 M ($p = 0.766$), 0.25 M ($p = 0.825$) and 0.5 M ($p = 0.815$). Cell density was lower compared to control in 0.75 M ($p < 0.01$) and 1 M $(NH_4)_2SO_4$ ($p < 0.01$). Cell density remained above $OD_{600} = 2.00$ when cultivated in the control, 0.1 M, 0.25 M and 0.5 M $(NH_4)_2SO_4$. Cell density was below $OD_{600} = 1.00$ in 0.75 M $(NH_4)_2SO_4$ ($OD_{600} = 0.847 \pm 0.448$). The average cell density of Slthf1 after 48 h incubation in 1 M $(NH_4)_2SO_4$ was 0.2 OD_{600} ± 0.029.

Comparative growth and water activity analysis in ammonium and sulfate salts

The established survival limits of Slthf1 in increasing concentrations of $(NH_4)_2SO_4$ could be due to altered water availability, salinity, osmotic pressure, ion induced toxicity or pH changes. To investigate these possibilities, Slthf1 was cultivated in ammonium (NH_4Cl, NH_4NO_3) and sulfate salts (Na_2SO_4, K_2SO_4) at concentrations of 0.1 M (Figure 2A), 0.5 M (Figure 2B) and 1 M (Figure 2C), in addition to $(NH_4)_2SO_4$. Growth was assessed by OD_{600} after 48 h incubation. For comparison against ammonium salts, $(NH_4)_2SO_4$ was prepared to concentrations of 0.05 M, 0.25 M and 0.5 M to ensure ionic levels of NH_4^+ were equivalent to NH_4Cl and NH_4NO_3 at 0.1 M, 0.5 M, 1 M, respectively. Salinity, osmolarity and ionic strength of each brine is displayed in Table 1. Slthf1 was also grown in unamended yeast media pH-matched to $(NH_4)_2SO_4$ brines using NaOH or HCl. Slthf1 reached an $OD_{600} > 2$ in all brines at 0.1 M (Figure 2A). The OD_{600} at 48 h of Slthf1 in 0.05 M $(NH_4)_2SO_4$ (0.1 M NH_4^+) was found to be not significantly different in 0.1 M NH_4Cl ($p = 0.380$) and the pH-matched solution at pH 6.38 ($p > 0.999$) (Figure 2A). There was a higher OD_{600} in 0.1 M NH_4NO_3 compared to 0.05 M $(NH_4)_2SO_4$ ($p < 0.01$). When matching the molar concentration of SO_4^{2-} ion, the OD_{600} at 48 h was lower in 0.1 M $(NH_4)_2SO_4$ compared to 0.1 M Na_2SO_4 ($p < 0.01$) and 0.1 M K_2SO_4 ($p < 0.05$). Growth in the pH-matched solution at pH 6.38 was not significantly different from growth in 0.1 M $(NH_4)_2SO_4$. At 0.5 M, there was no significant difference between the OD_{600} at 48 h for any of the tested brines compared to growth in 0.25 M (0.5 M NH_4^+) and 0.5 M $(NH_4)_2SO_4$ (Figure 2B) (p-values in Supplementary Table S1), despite differential salinity, osmolarity and ionic strengths between certain brines.

Alterations to cell density became evident when brine concentrations reached 1 M (Figure 2C). Slthf1 grew in 1 M NH_4Cl ($p = 0.883$) and a pH-matched solution at pH 5.8 ($p = 0.933$) with a non-significant change to OD_{600} at 48 h compared to 0.5 M $(NH_4)_2SO_4$ (1 M NH_4^+). Cell density was maintained above $OD_{600} = 1.8$ in these solutions. OD_{600} in 1 M NH_4NO_3 was lower compared to $(NH_4)_2SO_4$ ($p < 0.05$), with a final $OD_{600} < 0.05$ indicating severely limited growth. Thus, the molarity of NH_4^+ ion alone does not determine growth outcomes. Growth in 1 M $(NH_4)_2SO_4$ was significantly lowered compared to growth in 1 M Na_2SO_4 ($p < 0.01$) and a pH-matched solution at pH 5.7 ($p < 0.01$), despite the fact that Na_2SO_4 displayed higher salinity, and equal osmolarity and ionic strength compared to $(NH_4)_2SO_4$ (Table 1). This confirms molarity of SO_4^{2-} alone does not determine growth outcomes. The difference between the OD_{600} at 48 h in 1 M Na_2SO_4 and the pH-matched solution at 5.7 was found to be non-significant ($p = 0.108$). Water availability was assessed by water activity measurements of the brines at each concentration −0.1 M (Figure 2D), 0.5 M (Figure 2E) and 1 M (Figure 2F). The water activity of all brines was found to be above 0.9 a_w (Figures 2D–F). There was a non-significant difference between the a_w of ammonium salts and the a_w of sulfate salts (p-values in Supplementary Table S2). The results of these tests suggest that neither toxicity by individual ions, osmotic stress, ionic strength, salinity nor pH were contributing factors that limit growth at higher concentrations of $(NH_4)_2SO_4$.

Altered metabolites of Slthf1 cultivated in $(NH_4)_2SO_4$

Metabolites can indicate stress (Avci, 2024; Sharma et al., 2025), and can additionally be utilized as biomarkers in the search

10.3389/fmicb.2025.1642998

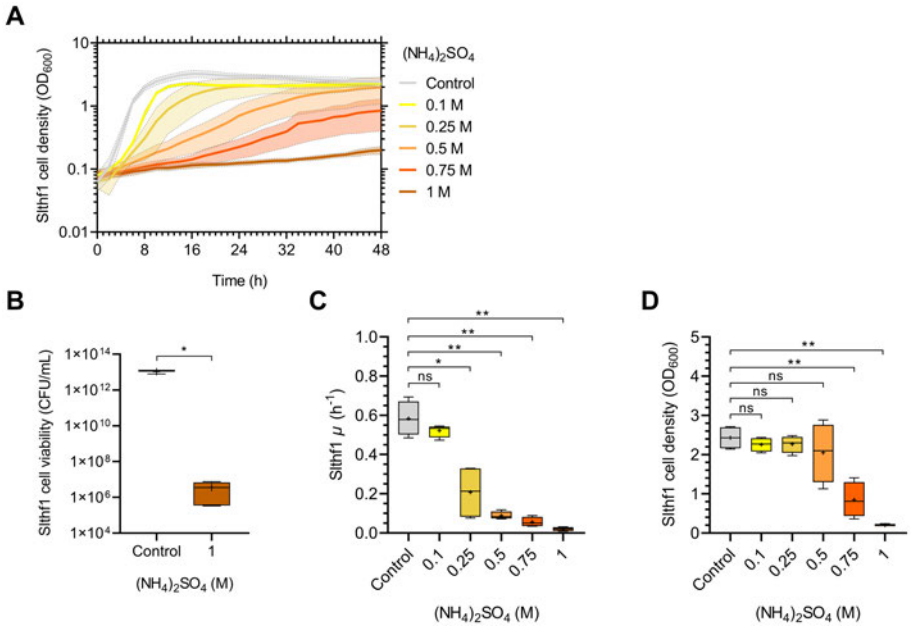

FIGURE 1
Growth dynamics of Slfth1 in increasing molar concentrations of $(NH_4)_2SO_4$. **(A)** OD_{600} growth curve of Slthf1 cultivated in 0 M (control), 0.1 M, 0.25 M, 0.5 M, 0.75 M, and 1 M $(NH_4)_2SO_4$ over 48 h. Growth curves represent mean OD_{600} values over time ± s.d. ($n = 4$). Error is indicated by area fill within error bands. **(B)** CFU of Slfth1 following 72 h cultivation in 0 M $(NH_4)_2SO_4$ (control, $n = 3$) and 1 M $(NH_4)_2SO_4$ ($n = 5$). **(C)** Growth rate (μ) and **(D)** final OD_{600} at 48 h extrapolated from **(A)** in increasing molar concentrations of $(NH_4)_2SO_4$. Statistics in **(B)** correspond to a two-tailed unpaired *t*-test with Welch's correction. Statistics in **(C)** and **(D)** correspond to Welch's ANOVA using Tamhane's T2 multiple comparisons test. ns, no significance; *$p < 0.05$; **$p < 0.01$.

for life (Fairén et al., 2020; Weber et al., 2023). To examine the stress response and adaptations in $(NH_4)_2SO_4$, comparative untargeted metabolomics was performed in Slthf1 cultivated under two conditions: 0.5 M $(NH_4)_2SO_4$ and unamended yeast media (0 M $(NH_4)_2SO_4$, hereafter denoted "control"). The annotated molecular features with relative intensities underwent multivariate and univariate statistical analysis, the results of which are shown in a PCA scores plot (Figure 3A), volcano plot (Figure 3B), and unpaired *t*-test (Supplementary Table S3). The PCA scores plot shows clear separation of the 0.5 M $(NH_4)_2SO_4$ group from control group with no overlap. The metabolites attributed to this group differentiation were identified using univariate volcano analysis, using a fold change greater than 2 and a *p*-value < 0.05 (adjusted using FDR correction). Volcano analysis revealed significant elevation of 17 molecular features ($p < 0.05$, FDR corrected), and significant reduction of 24 molecular features ($p < 0.05$, FDR corrected) in 0.5 M $(NH_4)_2SO_4$ cultivated samples compared to control samples. The complete volcano analysis dataset for this comparison is shown in Supplementary Table S4. The altered metabolites included amino acids and derivatives; there was an enrichment of aspartate (FC = 7.24, $p < 0.05$) and D-allo-isoleucine (FC = 8.42, $p < 0.0001$), and a reduction to the levels of serine (FC = 1.2×10^{-8}, $p < 0.0001$), glutamine (FC=1.15×10^{-8}, $p < 0.0001$) and N-acetyl-L-aspartate (FC = 0.159, $p < 0.05$) in 0.5 M $(NH_4)_2SO_4$ cultivated samples compared to control samples.

Morphological changes in $(NH_4)_2SO_4$ cultivated Slfth1

Lipids were also found to be significantly altered in the volcano analysis. Figure 4A depicts lipid alterations as Log2(FC) from control sample. The levels of unsaturated phosphatidylcholine (PC) 36:05 (FC = 1.6×10^9, $p < 0.0001$), PC (18:1/18:1) (del9-trans) (FC = 4.83, $p < 0.01$), PC [16:1(9Z)/16:1(9Z)] (FC = 11.35, $p < 0.05$) and phosphatidylethanolamine (PE) 37:01 (FC = 3.16×10^7, $p < 0.001$) and PE (O-34:03) (FC = 46.15, $p < 0.05$) were higher in $(NH_4)_2SO_4$ cultivated Slthf1. There were lower levels of unsaturated 40-carbon phosphatidylserine (FC = 3.16×10^{-7}, $p < 0.001$), and a small but significant elevation in the levels of saturated stearic acid (FC = 2.43, $p < 0.01$) in Slthf1 cultivated in $(NH_4)_2SO_4$ compared to the control. These alterations suggest cell wall modulation; morphological changes in Slthf1 cultivated in control and 0.5 M $(NH_4)_2SO_4$ solutions are shown in Figures 4B, C, respectively. Cells in both conditions exhibited irregular, undulating outer membrane morphology with an enlarged periplasm between inner and outer membrane. Cytoplasm showed an abundance of ribosomes and nucleoids in both conditions. PHA-like granules were also apparent in both conditions but significantly greater in number in the control condition. This possibly suggested nitrogen limitation in the growth media that was satisfied by addition of NH_4^+ in cells cultivated in 0.5 M $(NH_4)_2SO_4$. Cells without membranes, indicating cell lysis events, were evident with greater occurrence in

10.3389/fmicb.2025.1642998

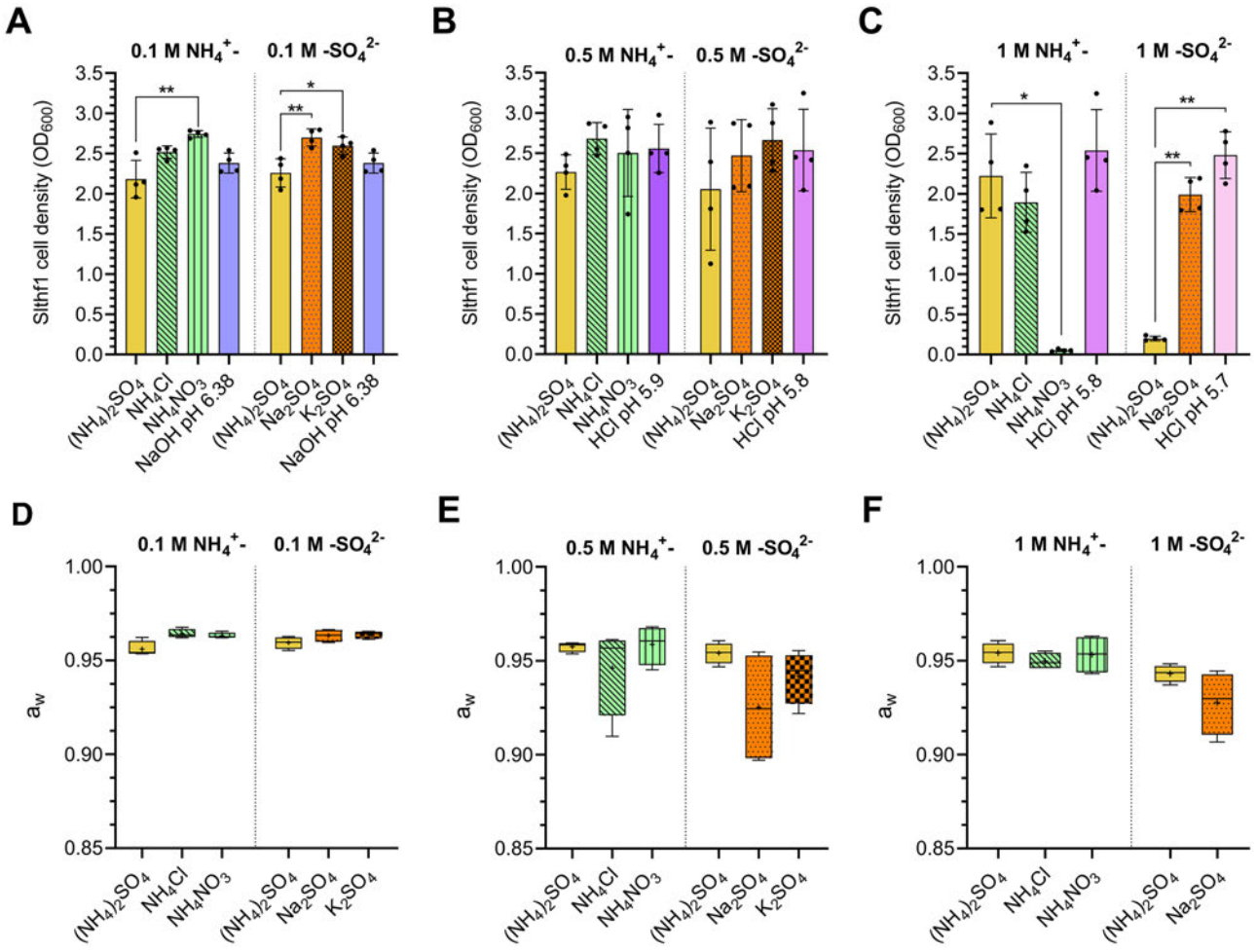

FIGURE 2
Cell density and water activity of Slfth1 cultivated in ammonium and sulfate salts of matched molar concentrations of NH_4^+ and SO_4^{2-}. **(A–F)** Aqueous solutions are represented by the following patterns: $(NH_4)_2SO_4$–solid yellow; NH_4Cl–green with diagonal stripes; NH_4NO_3–green with vertical stripes; Na_2SO_4–dotted orange; K_2SO_4–checkered orange; pH–solid purple to pink scaling with alkaline to acidic pH. **(A–C)** Final OD_{600} following 48 h incubation of Slfth1 in salts with matched molar concentrations of NH_4^+ and SO_4^{2-} ions at concentrations of **(A)** 0.1 M, **(B)** 0.5 M, and **(C)** 1 M, as well as solutions of matched pH made by NaOH and HCl. Statistical tests employed: one-way ANOVA with Tukey's *post-hoc* test for 0.1 M $(NH_4)_2SO_4$ vs. 0.1 M sulfate salts **(A)** and 0.25 M $(NH_4)_2SO_4$ vs. 0.5 M ammonium salts **(B)**; the Kruskal–Wallis test using Dunn's multiple comparisons test for 0.05 M $(NH_4)_2SO_4$ vs. 0.1 M ammonium salts **(A)** and 0.5 M $(NH_4)_2SO_4$ vs. 0.5 M sulfate salts **(B)**; iii) all comparisons in **(C)** were made by Welch's ANOVA using Tamhane's T2 multiple comparisons test. **(D–F)** Water activities of salts with matched molar concentrations of NH_4^+ and SO_4^{2-} ions at **(D)** 0.1 M, **(E)** 0.5 M, and **(F)** 1 M. Statistical comparison of ammonium and sulfate salts occurred separately. Statistical tests employed: one-way ANOVA with Tukey's *post-hoc* test for 0.1 M $(NH_4)_2SO_4$ vs. 0.1 M sulfate salts **(D)**; Kruskal–Wallis test using Dunn's multiple comparisons test for 0.05 M $(NH_4)_2SO_4$ vs. 0.1 M ammonium salts **(D)** and 0.25 M $(NH_4)_2SO_4$ vs. 0.5 M ammonium salts **(E)**; Welch's ANOVA using Tamhane's T2 multiple comparisons test for 0.5 M $(NH_4)_2SO_4$ vs. 0.5 M sulfate salts **(E)** and 0.5 M $(NH_4)_2SO_4$ vs. 1 M ammonium salts **(F)**; unpaired two-tailed *t*-test for comparison of 1 M $(NH_4)_2SO_4$ vs. 1 M Na_2SO_4 **(F)**. All a_w comparisons were found to be non-significant. ns, no significance; $*p < 0.05$; $**p < 0.01$.

the $(NH_4)_2SO_4$ cultivated cells. There was electron-dense material observed between cells cultivated in $(NH_4)_2SO_4$ that may indicate microbial interactions with $(NH_4)_2SO_4$.

$(NH_4)_2SO_4$ cultivation reduces abundance of the nitrogen metabolism metabolite glutamine

To identify pathways altered upon 0.5 M $(NH_4)_2SO_4$ exposure, a pathway enrichment analysis of the annotated metabolites was conducted using the MetaboAnalyst 6.0 platform. Significantly altered metabolites in the unpaired *t*-test (Supplementary Table S3) that were also identified as altered in the pathway analysis are depicted in box and whisker plots in the following sections. Pathway analysis identified 12 significantly ($p < 0.05$) altered pathways. Figure 5A depicts the altered pathways. Associated significance values are in Supplementary Table S5. The altered pathways correspond to sphingolipid, nitrogen, purine, glyoxylate and dicarboxylic, amino acid, folate, pyruvate, butanoate metabolism and the citric acid cycle. The levels of serine were found to be lower in 0.5 M $(NH_4)_2SO_4$ cultivated cells relative to control samples ($p < 0.0001$). This resulted in the pathway of sphingolipid

metabolism to appear significantly altered. However, based on the complete genome of Slthf1, we do not believe this organism to be capable of sphingolipid metabolism. The next most significantly altered pathway corresponded to nitrogen metabolism, attributed to the significant reduction to glutamine ($p < 0.0001$) in $(NH_4)_2SO_4$ samples compared to control samples. Glutamate was not identified as significantly altered. The reduced levels of glutamine could suggest, in NH_4^+ surplus, nitrogen assimilation shifted from utilizing glutamine. The proposed alternative pathway for nitrogen metabolism is presented in Figure 5B.

$(NH_4)_2SO_4$ lowers purine levels in Slthf1

Numerous metabolites involved in purine metabolism were identified as altered (22/70) following 0.5 M $(NH_4)_2SO_4$ cultivation (Figure 5A). Figure 6 depicts boxplots of the metabolites within purine metabolism that were found to be significantly altered in both the pathway and volcano analysis—glutamine ($p < 0.0001$), deoxyguanosine ($p < 0.001$), guanosine ($p < 0.0001$), hypoxanthine ($p < 0.0001$) and inosine ($p < 0.0001$). The KEGG pathway for purine metabolism attributes these molecules to purine biosynthesis (glutamine) (Figure 6A), guanine metabolism (deoxyguanosine, guanosine) (Figure 6B) and adenine ribonucleotide degradation (hypoxanthine, inosine) (Figure 6C). Pathway analysis also identified 3′,5′-cyclic-GMP as significantly elevated ($p < 0.05$) and adenine as significantly reduced ($p < 0.05$) in 0.5 M $(NH_4)_2SO_4$ cultivated samples compared to control, further suggesting reduced turnover of 3′,5′-cyclic-GMP for production of guanine and reduced adenine biosynthesis.

TABLE 1 Osmolarity, salinity and ionic strength of 0.05 M $(NH_4)_2SO_4$ and 0.1 M $(NH_4)_2SO_4$, NH_4Cl, NH_4NO_3, Na_2SO_4, and K_2SO_4 solutions utilized in this study.

Solution	Osmolarity (Osm/L)	Salinity (ppt)	Ionic strength (M)
0.1 M NH_4Cl	0.20	0.0054	0.10
0.1 M NH_4NO_3	0.20	0.0080	0.10
0.1 M $(NH_4)_2SO_4$	0.30	0.0132	0.30
0.05 M $(NH_4)_2SO_4$	0.15	0.0066	0.15
0.1 M Na_2SO_4	0.30	0.0142	0.30
0.1 M K_2SO_4	0.30	0.0174	0.30

Changes to amino acids detected in $(NH_4)_2SO_4$ cultivated Slthf1

Pathway analysis indicated four amino acid pathways altered in response to 0.5 M $(NH_4)_2SO_4$ cultivation (Figure 5A). Box plots of the altered metabolites identified in the pathway analysis related to amino acid metabolism that were also found to be altered in the volcano analysis are depicted in Figure 7. These correspond to the metabolism of glycine, serine and threonine ($p < 0.001$) (Figure 7A), D-amino acids ($p < 0.01$) (Figure 7B) and alanine, aspartate and glutamate ($p < 0.001$) (Figure 7C). All comparisons made below reference metabolites altered in samples cultivated in 0.5 M $(NH_4)_2SO_4$ compared to control samples. Five metabolites out of 33 total metabolites were found to be altered in glycine, serine and threonine metabolism. Of these, two were found to be significantly reduced: serine ($p < 0.0001$) and dimethylglycine ($p < 0.0001$). Reduction of serine may account for the reduction to PS.

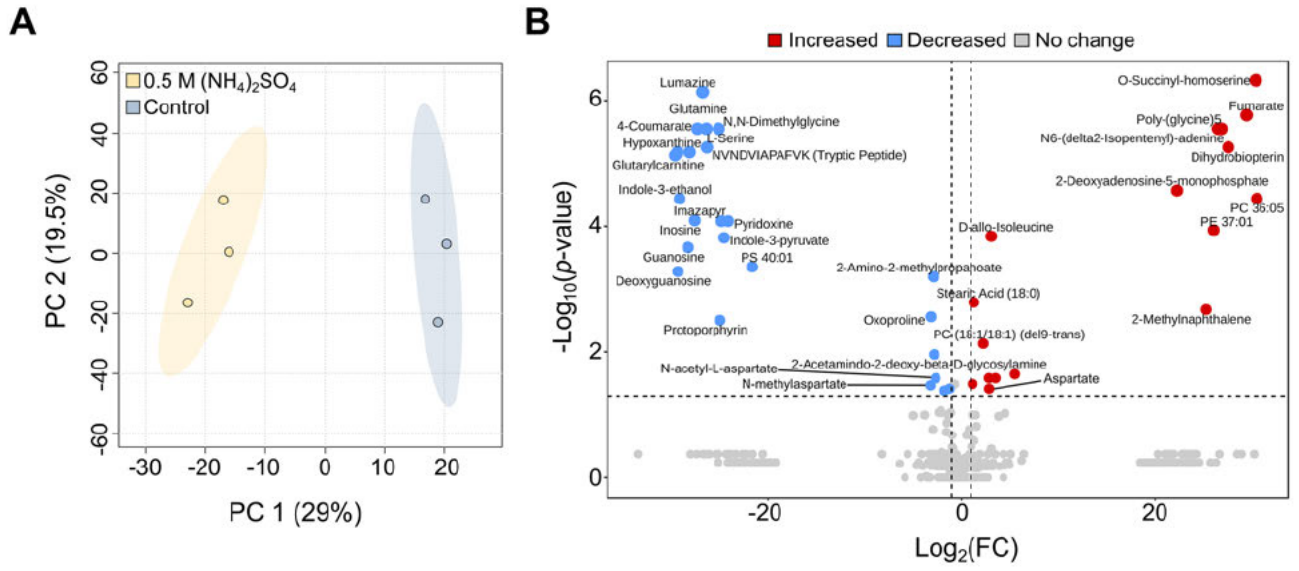

FIGURE 3
Metabolite changes of Slfth1 cultivated in 0.5 M $(NH_4)_2SO_4$. **(A)** Principal component analysis (PCA) scores plot depicting clear separation of the control (0 M $(NH_4)_2SO_4$) from 0.5 M $(NH_4)_2SO_4$ cultivated samples. **(B)** Volcano plot depicting metabolites with a fold change >2 and a p-value lower than 0.05 (adjusted using FDR correction) for 0.5 M $(NH_4)_2SO_4$/control. Comparatively elevated metabolites (red) and reduced metabolites (blue) are depicted. Metabolites without significant change are shown in gray.

10.3389/fmicb.2025.1642998

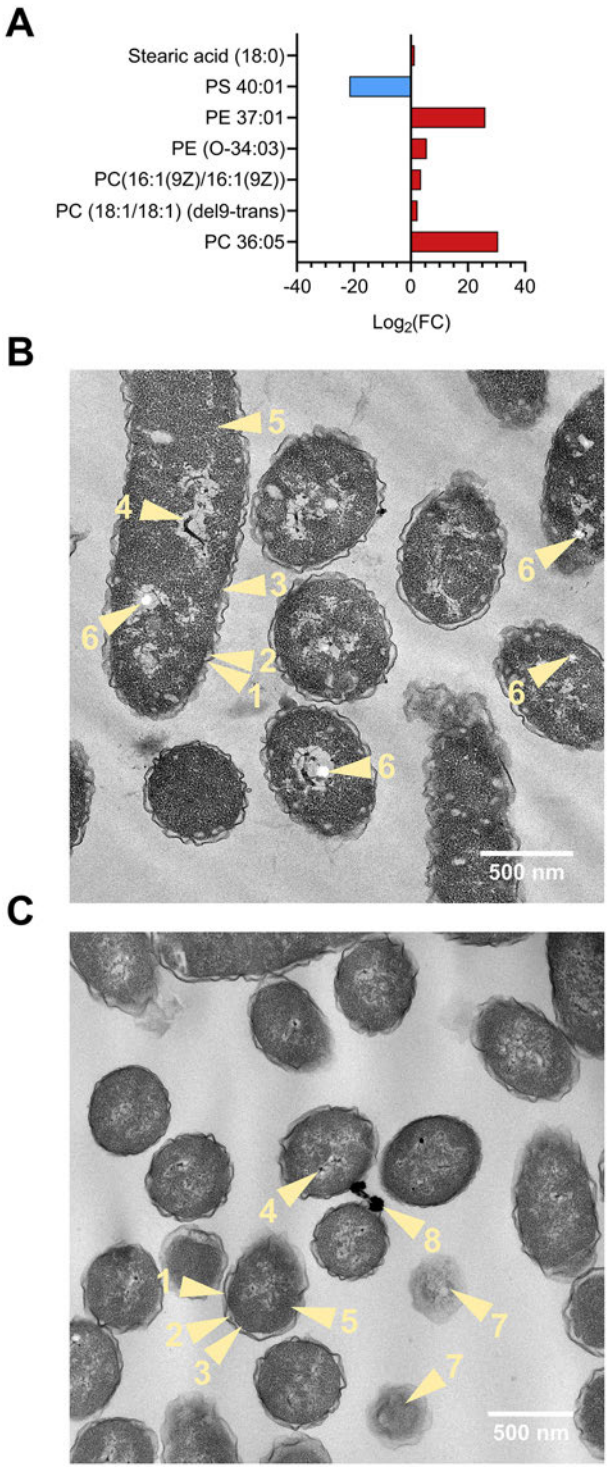

FIGURE 4
Lipid analysis and morphology of Slthf1 growth in $(NH_4)_2SO_4$. **(A)** Phospholipid alterations of Sltfh1 cultivated in 0.5 M $(NH_4)_2SO_4$. Alterations are depicted as Log_2 fold-change (FC) from control samples (0 M $(NH_4)_2SO_4$). Lipids depicted had a FC greater than 2 and were also identified as significantly altered (p-value < 0.05) in the volcano analysis. PC, phosphatidylcholine; PE, phosphatidylethanolamine; PS, phosphatidylserine. **(B, C)** Transmission electron microscopy (TEM) micrographs depicting morphology of Slfth1 harvested for metabolomics when OD_{600} = 0.5 at 28 h in **(B)** 0 M $(NH_4)_2SO_4$ (control) **(C)** 0.5 M $(NH_4)_2SO_4$. Light

(Continued)

FIGURE 4 (Continued)
yellow numbered items and arrows refer to the following biological components: 1, undulating outer membrane; 2, periplasmic space; 3, inner membrane; 4, nucleoid; 5, cytoplasm; 6, PHA-like granule; 7, lysed cell; 8, electron-dense material.

Four metabolites related to D-amino acid biosynthesis were found to be altered. These included significantly lower levels of serine ($p < 0.0001$). It is notable that D-allo-isoleucine was also found to be significantly elevated in the volcano analysis ($p < 0.001$). In alanine, aspartate and glutamate metabolism, 11/28 metabolites were found to be altered. These included significantly higher levels of aspartate ($p < 0.01$), fumarate ($p < 0.0001$), and significantly lower levels of N-acetyl-L-aspartate ($p < 0.01$), glutamate ($p < 0.05$), glutamine ($p < 0.0001$) and succinate ($p < 0.05$). Not depicted in Figure 7, the significant reduction to the levels of glutamate ($p < 0.05$) and glutamine ($p < 0.0001$), and significant elevation to the levels of aspartate ($p < 0.01$) and fumarate ($p < 0.0001$), were also relevant to arginine metabolism.

Differential metabolite abundance indicates modulations to energy and carbon metabolism

The citric acid cycle was found to be significantly altered ($p < 0.05$) in the pathway analysis (Figure 5A). Pathway analysis revealed significant reduction to succinate ($p < 0.05$) and elevation to fumarate ($p < 0.0001$) in the 0.5 M $(NH_4)_2SO_4$ cultivated sample compared to control. It is notable that elevated levels of O-succinyl-homoserine (FC = 1.44×10^9, $p < 0.0001$), a succinate precursor, and reduced levels of 4-Guanidinobutanoate (FC = 0.431, $p < 0.05$), a product of arginine degradation which is subsequently converted to succinate, were also identified in the volcano analysis. Figure 8A depicts box plots of significantly altered metabolites in the citric acid cycle identified in both the pathway and volcano analysis. Pyruvate metabolism was also found to be significantly altered ($p < 0.01$) with significant alteration to fumarate ($p < 0.0001$), and non-significant alteration of (S)-lactate ($p = 0.269$) and pyruvate ($p = 0.116$). Reduced levels of glutamate ($p < 0.05$), succinate ($p < 0.05$), and acetoacetate ($p = 0.119$) in the 0.5 M $(NH_4)_2SO_4$ cultivated cells compared to control also caused butanoate metabolism to be found as significantly altered ($p < 0.01$). The most significantly altered pathway was that of glyoxylate and dicarboxylate metabolism ($p < 0.001$). Three metabolites of this pathway were found to be significantly reduced in the 0.5 M $(NH_4)_2SO_4$ cultivated cells compared to control: glutamate ($p < 0.05$), glutamine ($p < 0.0001$) and serine ($p < 0.0001$). Figure 8B depicts box plots of significantly altered metabolites in the glyoxylate cycle identified in both the pathway and volcano analysis. Notably, we additionally found the methylaspartate cycle intermediate N-methylaspartate to be reduced in the volcano analysis (FC = 0.108, $p < 0.05$) in $(NH_4)_2SO_4$ cultivated cells (Figure 3B).

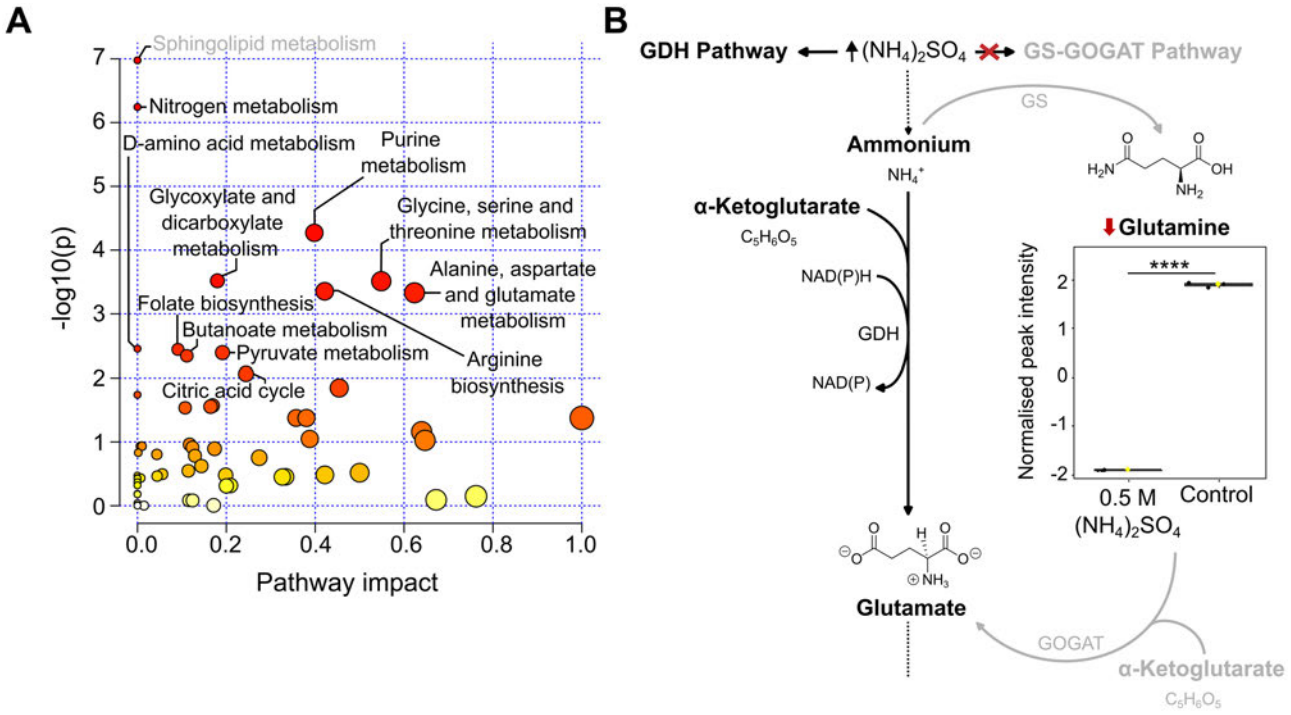

FIGURE 5
Altered pathways in Slfth1 cultivated in 0.5 M $(NH_4)_2SO_4$. **(A)** Scatter plot of KEGG pathways identified in the metabolomics dataset. Altered pathways with a p-value < 0.05 and FDR < 0.05 were considered significant. The size of each node is relative to the pathway impact values (i.e., the importance of the identified metabolite to the depicted pathway), while the color of nodes is indicative of p-value, with a darker red coloring indicating a more significant change to the pathway indicated. **(B)** Proposed altered nitrogen metabolism in $(NH_4)_2SO_4$ cultivated Slfth1. The box and whiskers summarize the normalized values with mean indicated by a yellow diamond and the central line indicating the median black dots representing the values from all samples ($n = 3$). Box and whiskers were generated using MetaboAnalyst 6.0 and edited for visual clarity in Inkscape. Diagram depicts high concentrations of $(NH_4)_2SO_4$ altering ammonium assimilation by having an inhibitory effect on the glutamine synthetase (GS)-glutamate synthase (GOGAT) pathway, thus reducing glutamine relative to control samples. Nitrogen assimilation occurs preferentially by the glutamate dehydrogenase (GDH) pathway. Chemical structures were created using ChemDraw. ****$p < 0.0001$.

Discussion

To assess the habitability of environments on other celestial bodies, it is valuable to first establish the known limits of life on Earth. $(NH_4)_2SO_4$ could be a constituent of the surface of Europa (Mermy et al., 2023) delivered from the ocean below, and a major salt within the subsurface ocean of Titan (Fortes et al., 2007; Grindrod et al., 2008). These icy moons have strong astrobiological interest due to the presence of liquid water (Carr et al., 1998; Pappalardo et al., 1998; Bills and Nimmo, 2011; Nimmo and Pappalardo, 2016) and putative physicochemical properties suitable for the emergence of life. In this work, we provide insights into the relationship between $(NH_4)_2SO_4$ and environmental habitability by investigating molar thresholds for growth, alterations to morphology and the metabolite profile of a hydrothermal vent extremophile, Slthf1, cultivated in $(NH_4)_2SO_4$.

Our work showed that concentrations at and exceeding 0.25 M $(NH_4)_2SO_4$ caused a distinct alteration to growth rate, while concentrations at and exceeding 0.75 M reduced final cell density. The molar limits established agree with that determined in *B. subtilis,* in which optical density when cultivated in $(NH_4)_2SO_4$ remained unchanged until 0.76 M (Hamill et al., 2020). However, reduction to growth rate has been recorded at a higher molar limit in *B. subtilis*—0.375 M (Müller et al., 2006) and 0.5 M $(NH_4)_2SO_4$ (Hamill et al., 2020), as well as in *Escherichia coli* (0.375 M $(NH_4)_2SO_4$), and *C. glutamicum* (1 M $(NH_4)_2SO_4$) (Müller et al., 2006). Slthf1 did not exhibit complete cell death at 1 M $(NH_4)_2SO_4$, as also observed for *C. glutamicum* at this concentration (Müller et al., 2006). Thus, we propose concentrations up to 1 M $(NH_4)_2SO_4$ do not limit habitability for Slthf1 but do affect cell density and growth rate.

In agriculture, application of $(NH_4)_2SO_4$ fertilizer is found to alter bacterial community structure and diversity; these effects are attributed to intrinsic changes in pH (Khonje et al., 1989; Toljander et al., 2008; Zhang et al., 2017). Our results show pH-independent influence of $(NH_4)_2SO_4$ on bacterial density. In *B. subtilis*, *E. coli*, and *C. glutamicum*, changes to growth kinetics upon treatment with $(NH_4)_2SO_4$ or Na_2SO_4 have been found to be near identical, indicating toxicity by osmolarity or ionic strength as opposed to the specific effects of $(NH_4)_2SO_4$ (Müller et al., 2006). We advance the current understanding of the limits of life in $(NH_4)_2SO_4$ by presenting a new perspective on ammonium salt toxicity in Slthf1 – we indicate the presence of both NH_4^+ and SO_4^{2-} ions, as opposed to individual ionic toxicity, salinity, osmotic or ionic strength, as the source of reduction to growth rate and cell density. Our experiments show that when ionic concentrations of NH_4^+ were equal to 1 M (0.5 M $(NH_4)_2SO_4$), there was no statistical difference between growth in 0.5 M $(NH_4)_2SO_4$ and 1 M NH_4Cl, but growth

10.3389/fmicb.2025.1642998

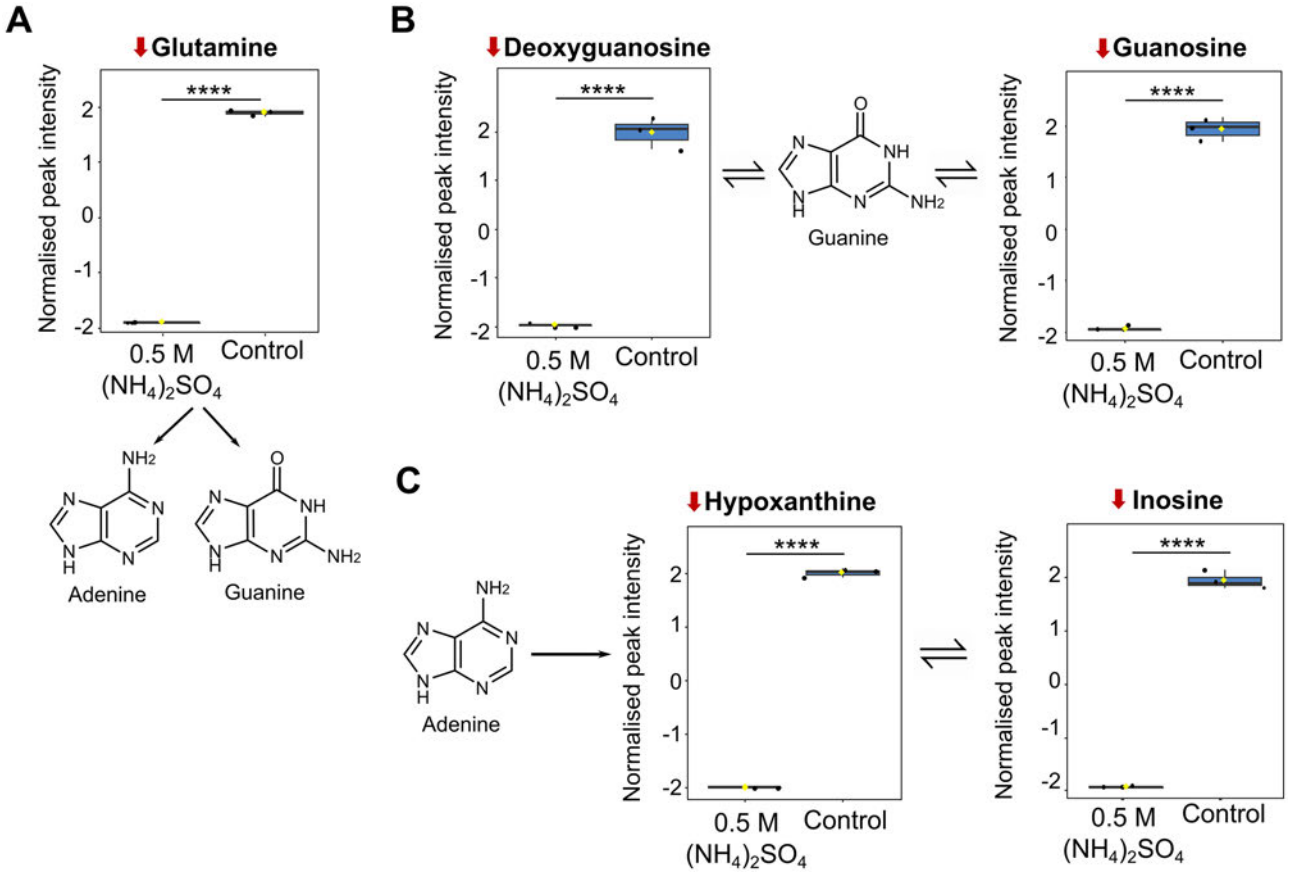

FIGURE 6
Metabolite changes associated with purine metabolism. Box plots showing significantly altered metabolites involved in **(A)** purine biosynthesis **(B)** guanine metabolism and **(C)** adenine ribonucleotide degradation. Reduction from control is indicated by a downward red arrow. Downstream and upstream metabolites according to the KEGG pathway for purine metabolism are indicated. The box and whiskers summarize the normalized values with mean indicated by a yellow diamond and the central line indicating the median black dots representing the values from all samples ($n = 3$). Box and whiskers were generated using MetaboAnalyst 6.0 and edited for visual clarity in Inkscape. Figure contains diagrams contextualizing the role of the metabolites in purine biosynthesis and adenine ribonucleotide degradation. Chemical structures were created using ChemDraw. ****$p < 0.0001$.

was comparatively reduced in 1 M NH_4NO_3. Likewise, when SO_4^{2-} concentrations were equal to 1 M (1 M $(NH_4)_2SO_4$, 2 M NH_4^+) the levels of cell density were significantly less compared to those in 1 M Na_2SO_4 brines also containing 1 M SO_4 (2 M Na^+). There was no correlation between NH_4 and SO_4^{2-} toxicity separately, and changes in cell density were also not accounted for by differences in pH, water activity, osmolarity, ionic strength or salinity.

$(NH_4)_2SO_4$ is the most kosmotropic salt utilized in this study, while NH_4NO_3 and Na_2SO_4 represent the most chaotropic salts (Cacace et al., 1997; Zhang and Cremer, 2006). However, chaotropic and kosmotropic properties alone are not typically predictors of habitability (Stevens and Cockell, 2020). We propose $(NH_4)_2SO_4$ may repress cell density due to altered NH_4^+ assimilation promoted by the metabolism of SO_4^{2-}, the effects of which become apparent when concentrations of NH_4^+ exceed 1 M. Indeed, untargeted metabolomics revealed O-succinyl-homoserine was found to be significantly elevated in $(NH_4)_2SO_4$ cultivated Slthf1. This metabolite is part of the sulfur assimilation pathway (Vermeij and Kertesz, 1999; Ferla and Patrick, 2014; Kim et al., 2024).

Significantly lowered levels of glutamine, a nitrogen assimilation metabolite, were also detected in Slthf1 cultivated in $(NH_4)_2SO_4$. This reduction coincides with other studies of NH_4^+ stress, whereby genes in nitrogen assimilation have been found to be altered in *Nitrobacter winogradskyi* (Sayavedra-Soto et al., 2015), and nitrogen reduction reactions reduced in *Methylomonas sp.* ZR1 (Guo W. et al., 2024). Under low NH_4^+ conditions nitrogen metabolism occurs by the glutamine synthetase-glutamate synthase (GS-GOGAT) pathway, whereby NH_4^+ is converted to glutamine and subsequently to glutamate, the primary nitrogen reservoir (Nagatani et al., 1971; Bravo and Mora, 1988; Schreier et al., 1993). Under high NH_4^+ conditions, the glutamate dehydrogenase (GDH) pathway predominates, whereby α-ketoglutarate and NH_4^+ are converted to glutamate (Kanamori et al., 1987; Reitzer, 2003; Legendre et al., 2020). We propose Slthf1 utilized the GDH pathway under high $(NH_4)_2SO_4$. The GDH pathway produces glutamate, but does not rely on glutamine, which coincides with the *t*-test results showing non-significant change in glutamate and significant reduction to glutamine in $(NH_4)_2SO_4$ cultivated Slthf1 compared to the control sample without $(NH_4)_2SO_4$. Similarly, a downregulation to transcripts in the GS-GOGAT pathway has been observed in *Enterobacter cloacae* HNR under NH_4^+ stress (Weng et al., 2022), but conversely upregulated in *Nitrobacter winogradsky*

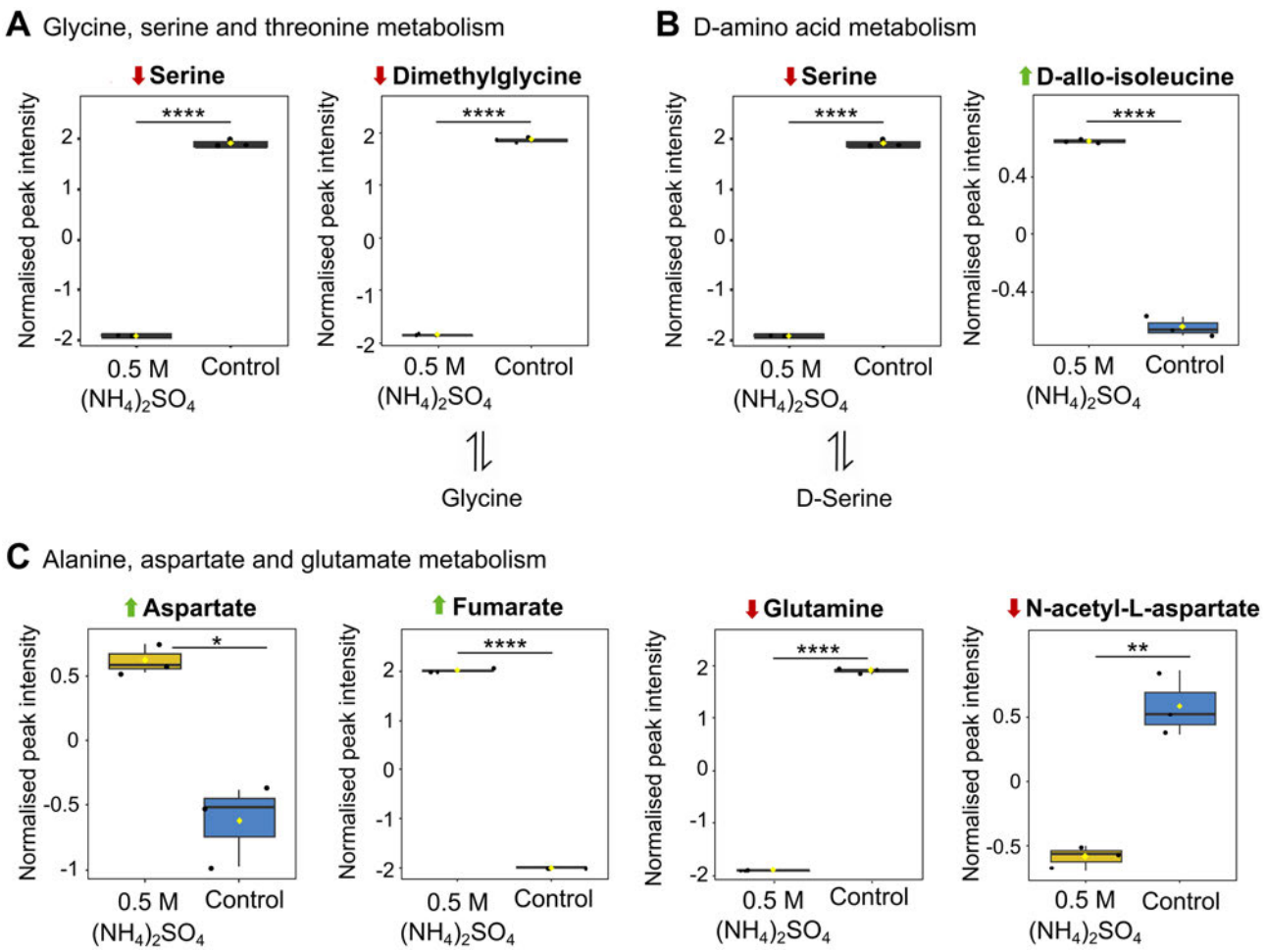

FIGURE 7
Altered metabolites of amino acid metabolism. Box plots showing significantly altered metabolites involved in **(A)** glycine, serine and threonine metabolism **(B)** D-amino acid metabolism and **(C)** alanine, aspartate and glutamate metabolism. Reduction and elevation from control is indicated by a downward red arrow and upward green arrow, respectively. Downstream and upstream metabolites according to the relevant KEGG pathway are indicated. The box and whiskers summarize the normalized values with mean indicated by a yellow diamond and the central line indicating the median black dots representing the values from all samples ($n = 3$). Box and whiskers were generated using MetaboAnalyst 6.0 and edited for visual clarity in Inkscape. *$p < 0.05$; **$p < 0.01$; ****$p < 0.0001$.

Nb-255 (Sayavedra-Soto et al., 2015). Due to a lower affinity for NH_4^+, GDH is less efficient in producing glutamate than GS (Wakisaka et al., 1989; Yan et al., 1996), which may contribute to the observed reduction in growth rate of $(NH_4)_2SO_4$ cultivated Slthf1. The underlying cause for GDH-dependent synthesis of glutamate is beyond the scope of this study but can be speculated. GS may be regulated by the Na^+/K^+ pump or Ca^{2+} (Benjamin, 1987), and is linked to an intracellular K^+ pool (Yan et al., 1996). Given that NH_4^+ can compete with K^+ transport through ion channels (Moser, 1987) and has also been implicated in disrupting Ca^{2+} homeostasis (Wang et al., 2018), it is possible the presence of NH_4^+ could disrupt the internal K^+ and Ca^{2+} balance that regulates GS activity. Notably, no GS or GOGAT activity has been detected in *B. pasteurii* grown in 0.04 M NH_4^+ (Mörsdorf and Kaltwasser, 1989), an organism that has shown ammonia-dependent oxidation of glutamate (Wiley and Stokes, 1962, 1963).

Transamination reactions with glutamate generate amino acids, purines and pyrimidines, and catabolism of glutamate provides intermediates for the citric acid cycle (Commichau et al., 2006; Walker and van der Donk, 2016). We observed reduced levels of amino acids (serine and N-acetyl-L-aspartate) and reduced metabolites in guanine synthesis, adenine synthesis and adenine degradation (guanosine, inosine, hypoxanthine) in Slthf1 under $(NH_4)_2SO_4$ cultivation. These changes could indicate: (i) implementation of energy saving adaptations such as reducing amino acid and nucleotide biosynthesis, (ii) a shift to catabolism for energy production as suggested by an inferred reduction to amino acid pools and nucleotides, and (iii) increased turnover of guanosine, inosine and hypoxanthine for synthesis of energy carrier molecules guanosine triphosphate (GTP) and adenosine triphosphate (ATP).

Lower levels of amino acids and purine metabolites have also been identified in *Pseudomonas* RCH2 when grown in media without ammonia (Kurczy et al., 2016). Nutrient-limiting conditions promote catabolic processes. Under stress, cells require more energy to sustain protective and adaptive responses. It is

10.3389/fmicb.2025.1642998

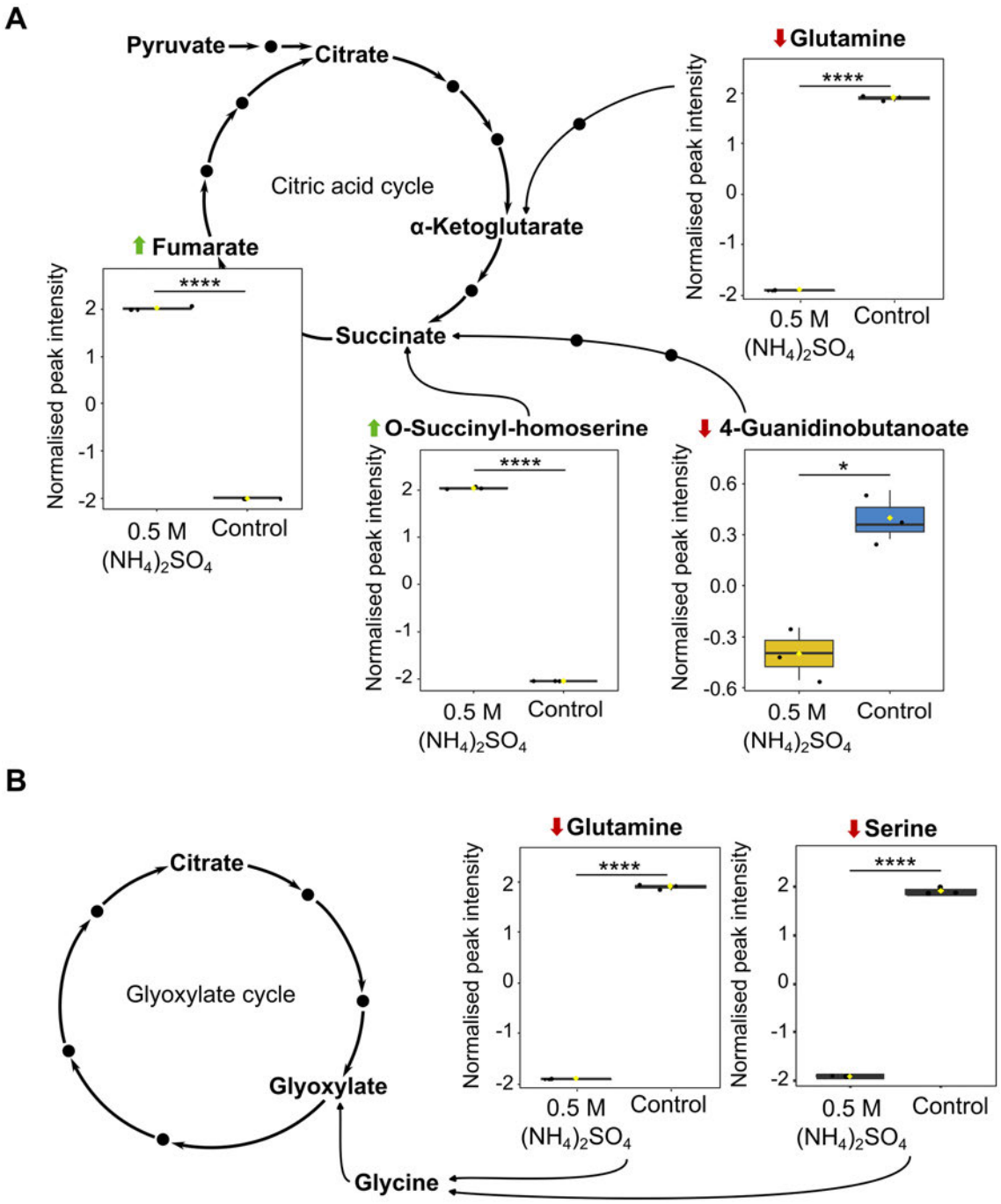

FIGURE 8
Recognized metabolites of carbon and energy metabolism. Box plots showing significantly altered metabolites involved in **(A)** the citric acid cycle and **(B)** the glyoxylate cycle. Reduction and elevation from control is indicated by a downward red arrow and upward green arrow, respectively. Downstream and upstream metabolites according to the relevant KEGG pathway are depicted or indicated by a solid black dot. The box and whiskers summarize the normalized values with mean indicated by a yellow diamond and the central line indicating the median black dots representing the values from all samples ($n = 3$). Box and whiskers were generated using MetaboAnalyst 6.0 and edited for visual clarity in Inkscape. ns, no significance; *$p < 0.05$; ****$p < 0.0001$.

therefore plausible changes to guanosine, inosine, hypoxanthine levels were reflective of an internal stress response to meet energy demands in response to $(NH_4)_2SO_4$. In accordance with this, we observe the relative abundance of citric acid cycle intermediate fumarate to be elevated in $(NH_4)_2SO_4$ cultivated cells. However, we also observed reduced levels of citric acid cycle intermediate succinate. In the canonical citric acid cycle, succinate is oxidized to fumarate by succinate dehydrogenase. The differential alterations to these metabolites could indicate upregulation of the succinate to fumarate conversion, or reduced input from the glyoxylate cycle under stress conditions. In the latter case, succinate is liberated by cleavage of isocitrate and funneled into the citric acid cycle.

A reduction to metabolites in the glyoxylate cycle in Slthf1 was indicated by pathway analysis. We also found several precursor molecules to key intermediates in the citric acid cycle and butanoate metabolism were reduced. This is suggestive of altered carbon metabolism. Indeed, citric acid cycle genes have been found to be down regulated in *E. cloacae* HNR exposed to high NH_4^+ (Weng et al., 2022).

The reduced levels of metabolites in citric acid cycle, the glyoxylate cycle and butanoate cycle suggest utilization of an alternative mechanism of catabolism. Notably, fumarate also feeds the methylaspartate cycle. We find the methylaspartate cycle intermediate N-methylaspartate to be reduced in $(NH_4)_2SO_4$ cultivated cells. The methylaspartate cycle has been characterized in haloarchaea and involves the processing of acetyl-CoA by a series of reactions to malate, a starting substrate for anabolism. Within this process, methylaspartate is converted to N-methylaspartate and then mesaconate (Khomyakova et al., 2011; Borjian et al., 2016). Albeit reduced, the detection of N-methylaspartate could indicate an active methylaspartate cycle, in turn indicating a less active glyoxylate cycle. We can surmise these alterations to key intermediates and precursor molecules as an indication of altered energy and carbon metabolism induced by high concentrations of $(NH_4)_2SO_4$. This aligns with previous studies that show NH_4^+ exposed bacteria alter central carbon pathways and the citric acid cycle (Sugden et al., 2021; Guo L. et al., 2024).

Currently, the planetary habitability and compositions of extraterrestrial aqueous environments, until measured, can only be speculated. The ocean of Europa is estimated to be predominantly composed of $MgSO_4$ (McCord et al., 1998; Kargel et al., 2000; Zolotov and Shock, 2001) or chloride salts (Brown and Hand, 2013; Hand and Carlson, 2015; Ligier et al., 2016), and thus could have a lower concentration of ammonia and $(NH_4)_2SO_4$, if any, than Titan (Kargel, 1991). Titan is expected to have formed with up to 15% ammonia (Lunine and Stevenson, 1987; Engel et al., 1994; Tobie et al., 2005) and could contain an ocean of $(NH_4)_2SO_4$ (Fortes et al., 2007; Grindrod et al., 2008). Our results showed a reduction to growth rate and cell density with increasing $(NH_4)_2SO_4$. However, we found that Slthf1 cells remained viable at concentrations up to 1 M $(NH_4)_2SO_4$ (2 M NH_4^+). This data cannot suggest whether icy moons oceans are or have been inhabited but can suggest that substantial concentrations of $(NH_4)_2SO_4$ may not necessarily preclude survival of terrestrial bacteria in highly concentrated $(NH_4)_2SO_4$ aqueous environments. Such conditions could be relevant to the subsurface oceans hypothesized on icy moons like Europa and Titan. The findings reported in this study also have terrestrial applications. For instance, application of 35 g/m^2 of $(NH_4)_2SO_4$ fertilizer, as advised for some commercial fertilizers, could yield a molarity of 2.64 M when dissolved in 100 mL water. At concentrations equal to and below 1 M, our results showed that $(NH_4)_2SO_4$ slowed growth rate and reduced cell density, as well as altered metabolites associated with growth processes in nitrogen, carbon and energy metabolism, purine metabolism and amino acid metabolism. These cellular and molecular effects could correlate with alterations to bacterial populations, richness and diversity observed in literature when soil is treated with $(NH_4)_2SO_4$ (Gorissen et al., 1993; Witter et al., 1993; Toljander et al., 2008). This further establishes that $(NH_4)_2SO_4$ can affect susceptible terrestrial bacteria when applied.

Stress responses and metabolites in bacteria can act as potential biomarkers for life (Kort et al., 2008; Goordial et al., 2017; Moreno-Paz et al., 2023). For this reason, instruments capable of metabolite detection have been considered for life-detection missions (Weber et al., 2023; Wronkiewicz et al., 2024). Under $(NH_4)_2SO_4$ cultivation, we detected higher levels of phospholipids PC and PE with monounsaturated 16:1 and 18:1 lipids in Slthf1 cultivated in $(NH_4)_2SO_4$. Similar biomarkers have been reported in heterotrophic nitrification-aerobic denitrification (HN-AD) bacteria and *E. cloacae* HNR exposed to high NH_4^+ (Weng et al., 2022; Guo L. et al., 2024). In halophiles, this modification may support survival under salt stress by enhancing membrane fluidity (Lopalco et al., 2013). Fatty acids are also synthesized by halophiles under salt stress (Liu et al., 2015); we observed a small elevation to stearic acid in Slthf1. However, given the low salinity of the $(NH_4)_2SO_4$ solution, Sltfh1 did not demonstrate many other metabolomic markers characteristic of osmotic stress (e.g., accumulation of compatible solutes) (Saum and Müller, 2008). We recognize the $(NH_4)_2SO_4$ media utilized in this study was simplistic. This was intentional, as we aimed to probe the specific effect of $(NH_4)_2SO_4$ on life. A natural progression of this work would be to investigate survival limits and physiology under multi-extremes. Brines simulating the putative composition of fluids in the oceans of Europa and Titan (such as the incorporation of $MgSO_4$ or sodium ions) would be particularly valuable in identifying physiological markers of life in aqueous $(NH_4)_2SO_4$ environments.

Data availability statement

The original contributions presented in the study are included in the article/Supplementary material, further inquiries can be directed to the corresponding author.

Author contributions

CH: Conceptualization, Investigation, Methodology, Data curation, Validation, Formal analysis, Writing – original draft, Writing – review & editing. PN: Writing – review & editing, Supervision. CC: Writing – review & editing, Supervision, Methodology, Resources, Funding acquisition, Project administration.

Funding

The author(s) declare that financial support was received for the research and/or publication of this article. Funding for this research was provided by the Natural Environmental Research Council (NERC) through an E4 Doctoral Training Partnership (DTP) studentship (NE/S007407/1) and the Science and Technology Facilities Council (STFC) through grants ST/V000586/1 and ST/Y001788/1. Access to the JEOL JEM-1400 Plus transmission electron microscope was supported by the Wellcome Trust Multiuser Equipment Grant (WT104915MA).

Acknowledgments

The metabolomics analyses were carried out by the EdinOmics research facility at the University of Edinburgh, and we particularly acknowledge the assistance of Tessa Moses. The authors would like to acknowledge Steve Mitchell from the School of Biological Sciences' TEM facility, University of Edinburgh, for assistance with TEM.

Conflict of interest

The authors declare that this research was carried out without any commercial or financial affiliations that could be perceived as a potential conflict of interest.

Generative AI statement

The author(s) declare that no Gen AI was used in the creation of this manuscript.

Any alternative text (alt text) provided alongside figures in this article has been generated by Frontiers with the support of artificial intelligence and reasonable efforts have been made to ensure accuracy, including review by the authors wherever possible. If you identify any issues, please contact us.

Publisher's note

All claims expressed in this article are solely those of the authors and do not necessarily represent those of their affiliated organizations, or those of the publisher, the editors and the reviewers. Any product that may be evaluated in this article, or claim that may be made by its manufacturer, is not guaranteed or endorsed by the publisher.

Supplementary material

The Supplementary Material for this article can be found online at: https://www.frontiersin.org/articles/10.3389/fmicb.2025.1642998/full#supplementary-material

References

Ao, Y., Henkel, C., Braatz, J. A., Weiß, A., Menten, K. M., and Mühle, S. (2011). Ammonia (*J,K*)=(1,1) to (4,4) and (6,6) inversion lines detected in the Seyfert 2 galaxy NGC 1068. *Astron. Astrophys.* 529:A154. doi: 10.1051/0004-6361/201116595

Avci, F. G. (2024). Unraveling bacterial stress responses: implications for next-generation antimicrobial solutions. *World J. Microbiol. Biotechnol.* 40:285. doi: 10.1007/s11274-024-04090-z

Barnes, J. W., Turtle, E. P., Trainer, M. G., Lorenz, R. D., MacKenzie, S. M., Brinckerhoff, W. B., et al. (2021). Science goals and objectives for the Dragonfly Titan rotorcraft relocatable lander. *Planet. Sci. J.* 2:130. doi: 10.3847/PSJ/abfdcf

Bates, R. G., and Pinching, G. D. (1949). Acidic dissociation constant of ammonium ion at 0 to 50 °C, and the base strength of ammonia. *J. Res. Natl. Bur. Stand.* 42:419. doi: 10.6028/jres.042.037

Benjamin, A. M. (1987). Influence of Na^+, K^+, and Ca^{2+} on glutamine synthesis and distribution in rat brain cortex slices: a possible linkage of glutamine synthetase with cerebral transport processes and energetics in the astrocytes. *J. Neurochem.* 48, 1157–1164. doi: 10.1111/j.1471-4159.1987.tb05641.x

Bills, B. G., and Nimmo, F. (2011). Rotational dynamics and internal structure of Titan. *Icarus* 214, 351–355. doi: 10.1016/j.icarus.2011.04.028

Borjian, F., Han, J., Hou, J., Xiang, H., and Berg, I. A. (2016). The methylaspartate cycle in *Haloarchaea* and its possible role in carbon metabolism. *ISME J.* 10, 546–557. doi: 10.1038/ismej.2015.132

Bravo, A., and Mora, J. (1988). Ammonium assimilation in *Rhizobium phaseoli* by the glutamine synthetase-glutamate synthase pathway. *J. Bacteriol.* 170, 980–984. doi: 10.1128/jb.170.2.980-984.1988

Britto, D. T., Siddiqi, M. Y., Glass, A. D. M., and Kronzucker, H. J. (2001). Futile transmembrane NH_4^+ cycling: a cellular hypothesis to explain ammonium toxicity in plants. *Proc. Natl. Acad. Sci. U. S. A.* 98, 4255–4258. doi: 10.1073/pnas.061034698

Brown, M. E., and Hand, K. P. (2013). Salts and radiation products on the surface of Europa. *Astron. J.* 145:110. doi: 10.1088/0004-6256/145/4/110

Cacace, M. G., Landau, E. M., and Ramsden, J. J. (1997). The Hofmeister series: salt and solvent effects on interfacial phenomena. *Q. Rev. Biophys.* 30, 241–277. doi: 10.1017/S0033583597003363

Carr, M. H., Belton, M. J. S., Chapman, C. R., Davies, M. E., Geissler, P., Greenberg, R., et al. (1998). Evidence for a subsurface ocean on Europa. *Nature* 391, 363–365. doi: 10.1038/34857

Cesur, R. M., Ansari, I. M., Chen, F., Clark, B. C., and Schneegurt, M. A. (2022). Bacterial growth in brines formed by the deliquescence of salts relevant to cold arid worlds. *Astrobiology* 22, 104–115. doi: 10.1089/ast.2020.2336

Collos, Y., and Harrison, P. J. (2014). Acclimation and toxicity of high ammonium concentrations to unicellular algae. *Mar. Pollut. Bull.* 80, 8–23. doi: 10.1016/j.marpolbul.2014.01.006

Commichau, F. M., Forchhammer, K., and Stülke, J. (2006). Regulatory links between carbon and nitrogen metabolism. *Curr. Opin. Microbiol.* 9, 167–172. doi: 10.1016/j.mib.2006.01.001

Dobson, S. J., and Franzmann, P. D. (1996). Unification of the genera *Deleya* (Baumann et al. 1983), *Halomonas* (Vreeland et al. 1980), and *Halovibrio* (Fendrich 1988) and the species *Paracoccus halodenitrificans* (Robinson and Gibbons 1952) into a single genus, *Halomonas*, and placement of the genus *Zymobacter* in the family *Halomonadaceae*. *Int. J. Syst. Evol. Microbiol.* 46, 550–558. doi: 10.1099/00207713-46-2-550

Engel, S., Lunine, J. I., and Norton, D. L. (1994). Silicate interactions with ammonia-water fluids on early Titan. *J. Geophys. Res. Planets* 99, 3745–3752. doi: 10.1029/93JE03433

Esteban, R., Ariz, I., Cruz, C., and Moran, J. F. (2016). Review: mechanisms of ammonium toxicity and the quest for tolerance. *Plant Sci.* 248, 92–101. doi: 10.1016/j.plantsci.2016.04.008

Fairén, A. G., Gómez-Elvira, J., Briones, C., Prieto-Ballesteros, O., Rodríguez-Manfredi, J. A., López Heredero, R., et al. (2020). The Complex Molecules Detector (CMOLD): a fluidic-based instrument suite to search for (bio)chemical complexity on Mars and icy moons. *Astrobiology* 20, 1076–1096. doi: 10.1089/ast.2019.2167

Ferla, M. P., and Patrick, W. M. (2014). Bacterial methionine biosynthesis. *Microbiology* 160, 1571–1584. doi: 10.1099/mic.0.077826-0

Fortes, A. D., Grindrod, P. M., Trickett, S. K., and Vočadlo, L. (2007). Ammonium sulfate on Titan: possible origin and role in cryovolcanism. *Icarus* 188, 139–153. doi: 10.1016/j.icarus.2006.11.002

Goordial, J., Altshuler, I., Hindson, K., Chan-Yam, K., Marcolefas, E., and Whyte, L. G. (2017). *In situ* field sequencing and life detection in remote (79°26′N) Canadian high arctic permafrost ice wedge microbial communities. *Front. Microbiol.* 8:2594. doi: 10.3389/fmicb.2017.02594

Gorissen, A., Jansen, A. E., and Olsthoorn, A. F. M. (1993). Effects of a two-year application of ammonium sulphate on growth, nutrient uptake, and rhizosphere microflora of juvenile Douglas-fir. *Plant Soil* 157, 41–50. doi: 10.1007/BF02390226

Goude, R., Renaud, S., Bonnassie, S., Bernard, T., and Blanco, C. (2004). Glutamine, glutamate, and α-glucosylglycerate are the major osmotic solutes accumulated by *Erwinia chrysanthemi* strain 3937. *Appl. Environ. Microbiol.* 70, 6535–6541. doi: 10.1128/AEM.70.11.6535-6541.2004

Grasset, O., Dougherty, M. K., Coustenis, A., Bunce, E. J., Erd, C., Titov, D., et al. (2013). JUpiter ICy moons Explorer (JUICE): an ESA mission to orbit Ganymede and to characterise the Jupiter system. *Planet. Space Sci.* 78, 1–21. doi: 10.1016/j.pss.2012.12.002

Grindrod, P., Fortes, A., Nimmo, F., Feltham, D., Brodholt, J. P., and Vočadlo, L. (2008). The long-term stability of a possible aqueous ammonium sulfate ocean inside Titan. *Icarus* 197, 137–151. doi: 10.1016/j.icarus.2008.04.006

Guo, L., Li, L., Zhou, S., Xiao, P., and Zhang, L. (2024). Metabolomic insight into regulatory mechanism of heterotrophic bacteria nitrification-aerobic denitrification bacteria to high-strength ammonium wastewater treatment. *Bioresour. Technol.* 394:130278. doi: 10.1016/j.biortech.2023.130278

Guo, W., He, R., Zhao, Y., and Li, D. (2024). Imbalanced metabolism induced NH_4^+ accumulation and its effect on the central metabolism of *Methylomonas* sp. ZR1. *Int. Microbiol.* 27, 49–66. doi: 10.1007/s10123-023-00457-8

Hachiya, T., Inaba, J., Wakazaki, M., Sato, M., Toyooka, K., Miyagi, A., et al. (2021). Excessive ammonium assimilation by plastidic glutamine synthetase causes ammonium toxicity in *Arabidopsis thaliana*. *Nat. Commun.* 12:4944. doi: 10.1038/s41467-021-25238-7

Hamill, P. G., Stevenson, A., McMullan, P. E., Williams, J. P., Lewis, A. D. R., Sudharsan, S., et al. (2020). Microbial lag phase can be indicative of, or independent from, cellular stress. *Sci. Rep.* 10:5948. doi: 10.1038/s41598-020-62552-4

Hand, K. P., and Carlson, R. W. (2015). Europa's surface color suggests an ocean rich with sodium chloride. *Geophys. Res. Lett.* 42, 3174–3178. doi: 10.1002/2015GL063559

Hand, K. P., Carlson, R. W., and Chyba, C. F. (2007). Energy, chemical disequilibrium, and geological constraints on Europa. *Astrobiology* 7, 1006–1022. doi: 10.1089/ast.2007.0156

Hendriksen, H. V., and Ahring, B. K. (1991). Effects of ammonia on growth and morphology of thermophilic hydrogen-oxidizing methanogenic bacteria. *FEMS Microbiol. Lett.* 85, 241–245. doi: 10.1111/j.1574-6968.1991.tb04730.x

Hiscox, J. A. (2000). Outer solar system, Europa, Titan and the possibility of life. *Astron. Geophys. 41* 5.23–5.24. doi: 10.1046/j.1468-4004.2000.41523.x

Hopton, C. M., Nienow, P., and Cockell, C. S. (2025). Ammonia sets limit to life and alters physiology independently of pH in *Halomonas meridiana*. *Sci. Rep.* 15, 1–16. doi: 10.1038/s41598-025-03858-z

Howell, S. M., and Pappalardo, R. T. (2018). Band formation and ocean-surface interaction on Europa and Ganymede. *Geophys. Res. Lett.* 45, 4701–4709. doi: 10.1029/2018GL077594

Howell, S. M., and Pappalardo, R. T. (2020). NASA's Europa Clipper—a mission to a potentially habitable ocean world. *Nat. Commun.* 11, 1311. doi: 10.1038/s41467-020-15160-9

Hsu, H.-W., Postberg, F., Sekine, Y., Shibuya, T., Kempf, S., Horányi, M., et al. (2015). Ongoing hydrothermal activities within Enceladus. *Nature* 519, 207–210. doi: 10.1038/nature14262

Ip, Y. K., Chew, S. F., Randall, D. J., Patricia, W., and Paul, A. (2001). "Ammonia toxicity, tolerance, and excretion," in *Fish Physiology*, eds P. Wright and P. Anderson (Academic *Press*), 109–148. doi: 10.1016/S1546-5098(01)20005-3

Irwin, P. G. J., Hill, S. M., Fletcher, L. N., Alexander, C., and Rogers, J. H. (2025). Clouds and ammonia in the atmospheres of Jupiter and Saturn determined from a band-depth analysis of VLT/MUSE observations. *J. Geophys. Res. Planets* 130:e2024JE008622. doi: 10.1029/2024JE008622

Jia, X., Kivelson, M. G., Khurana, K. K., and Kurth, W. S. (2018). Evidence of a plume on Europa from Galileo magnetic and plasma wave signatures. *Nat. Astron.* 2, 459–464. doi: 10.1038/s41550-018-0450-z

Johnson, P. V., Hodyss, R., Vu, T. H., and Choukroun, M. (2019). Insights into Europa's ocean composition derived from its surface expression. *Icarus* 321, 857–865. doi: 10.1016/j.icarus.2018.12.009

Kanamori, K., Weiss, R. L., and Roberts, J. D. (1987). Role of glutamate dehydrogenase in ammonia assimilation in nitrogen-fixing *Bacillus macerans*. *J. Bacteriol.* 169, 4692–4695. doi: 10.1128/jb.169.10.4692-4695.1987

Kargel, J. S. (1991). Brine volcanism and the interior structures of asteroids and icy satellites. *Icarus* 94, 368–390. doi: 10.1016/0019-1035(91)90235-L

Kargel, J. S., Kaye, J. Z., Head, J. W., Marion, G. M., Sassen, R., Crowley, J. K., et al. (2000). Europa's crust and ocean: origin, composition, and the prospects for life. *Icarus* 148, 226–265. doi: 10.1006/icar.2000.6471

Kaye, J. Z., and Baross, J. A. (2004). Synchronous effects of temperature, hydrostatic pressure, and salinity on growth, phospholipid profiles, and protein patterns of four *Halomonas* species isolated from deep-sea hydrothermal-vent and sea surface environments. *Appl. Environ. Microbiol.* 70, 6220–6229. doi: 10.1128/AEM.70.10.6220-6229.2004

Kaye, J. Z., Márquez, M. C., Ventosa, A., and Baross, J. A. Y., (2004). Halomonas neptunia sp. *nov., Halomonas sulfidaeris* sp. nov., *Halomonas axialensis* sp. nov. and *Halomonas hydrothermalis* sp. nov.: halophilic bacteria isolated from deep-sea hydrothermal-vent environments. *Int. J. Syst. Evol. Microbiol.* 54, 499–511. doi: 10.1099/ijs.0.02799-0

Khomyakova, M., Bükmez, Ö., Thomas, L. K., Erb, T. J., and Berg, I. A. (2011). A methylaspartate cycle in haloarchaea. *Science* 331, 334–337. doi: 10.1126/science.1196544

Khonje, D. J., Varsa, E. C., and Klubek, B. (1989). The acidulation effects of nitrogenous fertilizers on selected chemical and microbiological properties of soil. *Commun. Soil Sci. Plant Anal.* 20, 1377–1395. doi: 10.1080/00103628909368156

Kim, Y.-T., Kwon, J.-G., O'Sullivan, D. J., and Lee, J.-H. (2024). Regulatory mechanism of cysteine-dependent methionine biosynthesis in *Bifidobacterium longum*: insights into sulfur metabolism in gut microbiota. *Gut Microbes* 16:2419565. doi: 10.1080/19490976.2024.2419565

Kleiner, D. (1981). The transport of NH_3 and NH_4^+ across biological membranes. *Biochim. Biophys. Acta BBA - Rev. Bioenerg.* 639, 41–52. doi: 10.1016/0304-4173(81)90004-5

Kort, R., Keijser, B. J., Caspers, M. P., Schuren, F. H., and Montijn, R. (2008). Transcriptional activity around bacterial cell death reveals molecular biomarkers for cell viability. *BMC Genomics* 9:590. doi: 10.1186/1471-2164-9-590

Kurczy, M. E., Forsberg, E. M., Thorgersen, M. P., Poole, F. L. I., Benton, H. P., Ivanisevic, J., et al. (2016). Global isotope metabolomics reveals adaptive strategies for nitrogen assimilation. *ACS Chem. Biol.* 11, 1677–1685. doi: 10.1021/acschembio.6b00082

Leejeerajumnean, A., Ames, J. M., and Owens, J. D. (2000). Effect of ammonia on the growth of *Bacillus* species and some other bacteria. *Lett. Appl. Microbiol.* 30, 385–389. doi: 10.1046/j.1472-765x.2000.00734.x

Legendre, F., MacLean, A., Appanna, V. P., and Appanna, V. D. (2020). Biochemical pathways to α-ketoglutarate, a multi-faceted metabolite. *World J. Microbiol. Biotechnol.* 36:123. doi: 10.1007/s11274-020-02900-8

Leitner, M. A., and Lunine, J. I. (2019). Modeling early Titan's ocean composition. *Icarus* 333, 61–70. doi: 10.1016/j.icarus.2019.05.008

Lewis, J. S. (1971). Satellites of the outer planets: their physical and chemical nature. *Icarus* 15, 174–185. doi: 10.1016/0019-1035(71)90072-8

Li, S.-X., Wang, Z.-H., and Stewart, B. A. (2013). "Chapter five - responses of crop plants to ammonium and nitrate N," in *Advances in Agronomy*, ed. D. L. Sparks (Academic Press), 205–397. doi: 10.1016/B978-0-12-405942-9.00005-0

Ligier, N., Poulet, F., Carter, J., Brunetto, R., and Gourgeot, F. (2016). VLT/SINFONI observations of Europa: new insights into the surface composition. *Astron. J.* 151:163. doi: 10.3847/0004-6256/151/6/163

Liu, L., Si, L., Meng, X., and Luo, L. (2015). Comparative transcriptomic analysis reveals novel genes and regulatory mechanisms of *Tetragenococcus halophilus* in response to salt stress. *J. Ind. Microbiol. Biotechnol.* 42, 601–616. doi: 10.1007/s10295-014-1579-0

Lopalco, P., Angelini, R., Lobasso, S., Köcher, S., Thompson, M., Müller, V., et al. (2013). Adjusting membrane lipids under salt stress: the case of the moderate halophilic organism *Alobacillus halophilus*. *Environ. Microbiol.* 15, 1078–1087. doi: 10.1111/j.1462-2920.2012.02870.x

Lunine, J. I., and Stevenson, D. J. (1987). Clathrate and ammonia hydrates at high pressure: application to the origin of methane on Titan. *Icarus* 70, 61–77. doi: 10.1016/0019-1035(87)90075-3

Marion, G. M., Fritsen, C. H., Eicken, H., and Payne, M. C. (2003). The search for life on Europa: limiting environmental factors, potential habitats, and earth analogues. *Astrobiology* 3, 785–811. doi: 10.1089/153110703322736105

Marion, G. M., Kargel, J. S., Catling, D. C., and Lunine, J. I. (2012). Modeling ammonia–ammonium aqueous chemistries in the Solar System's icy bodies. *Icarus* 220, 932–946. doi: 10.1016/j.icarus.2012.06.016

Martin, W., Baross, J., Kelley, D., and Russell, M. J. (2008). Hydrothermal vents and the origin of life. *Nat. Rev. Microbiol.* 6, 805–814. doi: 10.1038/nrmicro1991

McCord, T. B., Hansen, G. B., Fanale, F. P., Carlson, R. W., Matson, D. L., Johnson, T. V., et al. (1998). Salts on Europa's surface detected by Galileo's near infrared mapping spectrometer. *Science* 280, 1242–1245. doi: 10.1126/science.280.5367.1242

McKay, C. P. (2016). Titan as the abode of life. *Life* 6:8. doi: 10.3390/life6010008

McKay, C. P., and Smith, H. D. (2005). Possibilities for methanogenic life in liquid methane on the surface of Titan. *Icarus* 178, 274–276. doi: 10.1016/j.icarus.2005.05.018

Melosh, H. J., Ekholm, A. G., Showman, A. P., and Lorenz, R. D. (2004). The temperature of Europa's subsurface water ocean. *Icarus* 168, 498–502. doi: 10.1016/j.icarus.2003.11.026

Mermy, G. C., Schmidt, F., Andrieu, F., Cornet, T., Belgacem, I., and Altobelli, N. (2023). Selection of chemical species for Europa's surface using Galileo/NIMS. *Icarus* 394:115379. doi: 10.1016/j.icarus.2022.115379

Moreno-Paz, M., dos Santos Severino, R. S., Sánchez-García, L., Manchado, J. M., García-Villadangos, M., Aguirre, J., et al. (2023). Life detection and microbial biomarker profiling with Signs of Life Detector-Life Detector Chip during a Mars drilling simulation campaign in the hyperarid core of the Atacama Desert. *Astrobiology* 23, 1259–1283. doi: 10.1089/ast.2021.0174

Mörsdorf, G., and Kaltwasser, H. (1989). Ammonium assimilation in *Proteus vulgaris*, *Bacillus pasteurii*, and *Sporosarcina ureae*. *Arch. Microbiol.* 152, 125–131. doi: 10.1007/BF00456089

Moser, H. (1987). Electrophysiological evidence for ammonium as a substitute for potassium in activating the sodium pump in a crayfish sensory neuron. *Can. J. Physiol. Pharmacol.* 65, 141–145. doi: 10.1139/y87-028

Müller, T., Walter, B., Wirtz, A., and Burkovski, A. (2006). Ammonium toxicity in bacteria. *Curr. Microbiol.* 52, 400–406. doi: 10.1007/s00284-005-0370-x

Nagatani, H., Shimizu, M., and Valentine, R. C. (1971). The mechanism of ammonia assimilation in nitrogen fixing bacteria. *Arch. Für Mikrobiol.* 79, 164–175. doi: 10.1007/BF00424923

Nichols, C. M., Dodds, J. N., Rose, B. S., Picache, J. A., Morris, C. B., Codreanu, S. G., et al. (2018). Untargeted molecular discovery in primary metabolism: collision cross section as a molecular descriptor in ion mobility-mass spectrometry. *Anal. Chem.* 90, 14484–14492. doi: 10.1021/acs.analchem.8b04322

Nimmo, F., and Pappalardo, R. T. (2016). Ocean worlds in the outer solar system. *J. Geophys. Res. Planets* 121, 1378–1399. doi: 10.1002/2016JE005081

Nixon, C. A. (2024). The composition and chemistry of Titan's atmosphere. *ACS Earth Space Chem.* 8, 406–456. doi: 10.1021/acsearthspacechem.2c00041

Owen, T. C. (2000). On the origin of Titan's atmosphere. *Planet. Space Sci.* 48, 747–752. doi: 10.1016/S0032-0633(00)00040-4

Pang, Z., Lu, Y., Zhou, G., Hui, F., Xu, L., Viau, C., et al. (2024). MetaboAnalyst 6.0: towards a unified platform for metabolomics data processing, analysis and interpretation. *Nucleic Acids Res.* 52, W398–W406. doi: 10.1093/nar/gkae253

Pappalardo, R. T., Head, J. W., Greeley, R., Sullivan, R. J., Pilcher, C., Schubert, G., et al. (1998). Geological evidence for solid-state convection in Europa's ice shell. *Nature* 391, 365–368. doi: 10.1038/34862

Parker, C. W., Vu, T. H., Kim, T., and Johnson, P. V. (2023). Vitreous magnesium sulfate hydrate as a potential mechanism for preservation of microbial viability on Europa. *Planet. Sci. J.* 4:178. doi: 10.3847/PSJ/aceefa

Randall, D. J., and Tsui, T. K. N. (2002). Ammonia toxicity in fish. *Mar. Pollut. Bull.* 45, 17–23. doi: 10.1016/S0025-326X(02)00227-8

Randive, K., Raut, T., and Jawadand, S. (2021). An overview of the global fertilizer trends and India's position in 2020. *Miner. Econ.* 34, 371–384. doi: 10.1007/s13563-020-00246-z

Raven, J. A., Wollenweber, B., and Handley, L. L. (1992). A comparison of ammonium and nitrate as nitrogen sources for photolithotrophs. *New Phytol.* 121, 19–32. doi: 10.1111/j.1469-8137.1992.tb01088.x

Reitzer, L. (2003). Nitrogen assimilation and global regulation in *Escherichia coli*. *Annu. Rev. Microbiol.* 57, 155–176. doi: 10.1146/annurev.micro.57.030502.090820

Roth, L., Saur, J., Retherford, K. D., Strobel, D. F., Feldman, P. D., McGrath, M. A., et al. (2014). Transient water vapor at Europa's south pole. *Science* 343, 171–174. doi: 10.1126/science.1247051

Russell, M. J., Murray, A. E., and Hand, K. P. (2017). The possible emergence of life and differentiation of a shallow biosphere on irradiated icy worlds: the example of Europa. *Astrobiology* 17, 1265–1273. doi: 10.1089/ast.2016.1600

Sagan, C., Thompson, W. R., and Khare, B. N. (1992). Titan: a laboratory for prebiological organic chemistry. *Acc. Chem. Res.* 25, 286–292. doi: 10.1021/ar00019a003

Saum, S. H., and Müller, V. (2008). Regulation of osmoadaptation in the moderate halophile *Halobacillus halophilus*: chloride, glutamate and switching osmolyte strategies. *Saline Syst.* 4:4. doi: 10.1186/1746-1448-4-4

Sayavedra-Soto, L., Ferrell, R., Dobie, M., Mellbye, B., Chaplen, F., Buchanan, A., et al. (2015). *Nitrobacter winogradskyi* transcriptomic response to low and high ammonium concentrations. *FEMS Microbiol. Lett.* 362, 1–7. doi: 10.1093/femsle/fnu040

Schreier, H. J., Abraham, L. S., James, A. H., and Richard, L. (1993). "Biosynthesis of glutamine and glutamate and the assimilation of ammonia," in *Bacillus subtilis and Other Gram-Positive Bacteria*, eds A. L. Sonenshein and J. A. Hoch (Washington, DC: American Society for Microbiology), 281–298. doi: 10.1128/9781555818388.ch20

Schulze-Makuch, D., and Irwin, L. N. (2001). Alternative energy sources could support life on Europa. *Eos Trans. Am. Geophys. Union* 82, 150–150. doi: 10.1029/EO082i013p00150

Sharma, A., Tayal, S., and Bhatnagar, S. (2025). Analysis of stress response in multiple bacterial pathogens using a network biology approach. *Sci. Rep.* 15:15342. doi: 10.1038/s41598-025-91269-5

Sohl, F., Solomonidou, A., Wagner, F. W., Coustenis, A., Hussmann, H., and Schulze-Makuch, D. (2014). Structural and tidal models of Titan and inferences on cryovolcanism. *J. Geophys. Res. Planets* 119, 1013–1036. doi: 10.1002/2013JE004512

Sojo, V., Herschy, B., Whicher, A., Camprubí, E., and Lane, N. (2016). The origin of life in alkaline hydrothermal vents. *Astrobiology* 16, 181–197. doi: 10.1089/ast.2015.1406

Sparks, W. B., Hand, K. P., McGrath, M. A., Bergeron, E., Cracraft, M., and Deustua, S. E. (2016). Probing for evidence of plumes on Europa with HST/STIS. *Astrophys. J.* 829:121. doi: 10.3847/0004-637X/829/2/121

Spohn, T., and Schubert, G. (2003). Oceans in the icy Galilean satellites of Jupiter? *Icarus* 161, 456–467. doi: 10.1016/S0019-1035(02)00048-9

Sprott, G. D., and Patel, G. B. (1986). Ammonia toxicity in pure cultures of methanogenic bacteria. *Syst. Appl. Microbiol.* 7, 358–363. doi: 10.1016/S0723-2020(86)80034-0

Stevens, A. H., and Cockell, C. S. (2020). A systematic study of the limits of life in mixed ion solutions: physicochemical parameters do not predict habitability. *Front. Microbiol.* 11:1478. doi: 10.3389/fmicb.2020.01478

Sugden, S., Lazic, M., Sauvageau, D., and Stein, L. Y. (2021). Transcriptomic and metabolomic responses to carbon and nitrogen sources in *Methylomicrobium album BG8*. *Appl. Environ. Microbiol.* 87, e00385–e00321. doi: 10.1128/AEM.00385-21

Szalay, J. R., Allegrini, F., Ebert, R. W., Bagenal, F., Bolton, S. J., Fatemi, S., et al. (2024). Oxygen production from dissociation of Europa's water-ice surface. *Nat. Astron.* 8, 567–576. doi: 10.1038/s41550-024-02206-x

Takahashi, Y., Takahashi, H., Galipon, J., and Arakawa, K. (2020). Complete genome sequence of *Halomonas meridiana* strain Slthf1, isolated from a deep-sea thermal vent. *Microbiol. Resour. Announc.* 9, e00292–20. doi: 10.1128/MRA.00292-20

Tobie, G., Gautier, D., and Hersant, F. (2012). Titan's bulk composition constrained by Cassini-Huygens: implication for internal outgassing. *Astrophys. J.* 752:125. doi: 10.1088/0004-637X/752/2/125

Tobie, G., Grasset, O., Lunine, J. I., Mocquet, A., and Sotin, C. (2005). Titan's internal structure inferred from a coupled thermal-orbital model. *Icarus* 175, 496–502. doi: 10.1016/j.icarus.2004.12.007

Toljander, J. F., Santos-González, J. C., Tehler, A., and Finlay, R. D. (2008). Community analysis of arbuscular mycorrhizal fungi and bacteria in the maize mycorrhizosphere in a long-term fertilization trial. *FEMS Microbiol. Ecol.* 65, 323–338. doi: 10.1111/j.1574-6941.2008.00512.x

Tyagi, J., Ahmad, S., and Malik, M. (2022). Nitrogenous fertilizers: impact on environment sustainability, mitigation strategies, and challenges. *Int. J. Environ. Sci. Technol.* 19, 11649–11672. doi: 10.1007/s13762-022-04027-9

Vance, S., Harnmeijer, J., Kimura, J., Hussmann, H., deMartin, B., and Brown, J. M. (2007). Hydrothermal systems in small ocean planets. *Astrobiology* 7, 987–1005. doi: 10.1089/ast.2007.0075

Vermeij, P., and Kertesz, M. A. (1999). Pathways of assimilative sulfur metabolism in *Pseudomonas putida*. *J. Bacteriol.* 181, 5833–5837. doi: 10.1128/JB.181.18.5833-5837.1999

Wakisaka, S., Sung, H.-C., Aikawa, T., Tachiki, T., and Tochikura, T. (1989). Glutamate formation by a new *In vitro* enzyme system consisting of purified glutamine synthetase and glutamate synthase. *J. Ferment. Bioeng.* 67, 395–398. doi: 10.1016/0922-338X(89)90047-0

Walker, M. C., and van der Donk, W. A. (2016). The many roles of glutamate in metabolism. *J. Ind. Microbiol. Biotechnol.* 43, 419–430. doi: 10.1007/s10295-015-1665-y

Wang, F., Chen, S., Jiang, Y., Zhao, Y., Sun, L., Zheng, B., et al. (2018). Effects of ammonia on apoptosis and oxidative stress in bovine mammary epithelial cells. *Mutagenesis* 33, 291–299. doi: 10.1093/mutage/gey023

Weber, J. M., Marlin, T. C., Prakash, M., Teece, B. L., Dzurilla, K., and Barge, L. M. (2023). A review on hypothesized metabolic pathways on Europa and Enceladus: space-flight detection considerations. *Life* 13:1726. doi: 10.3390/life13081726

Weng, X., Mao, Z., Fu, H.-M., Chen, Y.-P., Guo, J.-S., Fang, F., et al. (2022). Biofilm formation during wastewater treatment: motility and physiological response of aerobic denitrifying bacteria under ammonia stress based on surface plasmon resonance imaging. *Bioresour. Technol.* 361:127712. doi: 10.1016/j.biortech.2022.127712

Wiley, W. R., and Stokes, J. L. (1962). Requirement of an alkaline pH and ammonia for substrate oxidation by *Bacillus pasteurii*. *J. Bacteriol.* 84, 730–734. doi: 10.1128/jb.84.4.730-734.1962

Wiley, W. R., and Stokes, J. L. (1963). Effect of pH and ammonium ions on the permeability of *Bacillus pasteurii*. *J. Bacteriol.* 86, 1152–1156. doi: 10.1128/jb.86.6.1152-1156.1963

Wilks, J. M., Chen, F., Clark, B. C., and Schneegurt, M. A. (2019). Bacterial growth in saturated and eutectic solutions of magnesium sulphate and potassium chlorate with relevance to Mars and the ocean worlds. *Int. J. Astrobiol.* 18, 502–509. doi: 10.1017/S1473550418000502

Witter, E., Mårtensson, A. M., and Garcia, F. V. (1993). Size of the soil microbial biomass in a long-term field experiment as affected by different N-fertilizers and organic manures. *Soil Biol. Biochem.* 25, 659–669. doi: 10.1016/0038-0717(93)90105-K

Wong, K. T., Menten, K. M., Kamiński, T., Wyrowski, F., Lacy, J. H., and Greathouse, T. K. (2018). Circumstellar ammonia in oxygen-rich evolved stars. *Astron. Astrophys.* 612:A48. doi: 10.1051/0004-6361/201731873

Wronkiewicz, M., Lee, J., Mandrake, L., Lightholder, J., Doran, G., Mauceri, S., et al. (2024). Onboard science instrument autonomy for the detection of microscopy biosignatures on the Ocean Worlds Life Surveyor. *Planet. Sci. J.* 5:19. doi: 10.3847/PSJ/ad0227

Wyckoff, S., Tegler, S., and Engel, L. (1989). Ammonia abundances in comets. *Adv. Space Res.* 9, 169–176. doi: 10.1016/0273-1177(89)90257-3

Yan, D., Ikeda, T. P., Shauger, A. E., and Kustu, S. (1996). Glutamate is required to maintain the steady-state potassium pool in *Salmonella typhimurium*. *Proc. Natl. Acad. Sci. U. S. A.* 93, 6527–6531. doi: 10.1073/pnas.93.13.6527

Zhang, Y., and Cremer, P. S. (2006). Interactions between macromolecules and ions: the Hofmeister series. *Curr. Opin. Chem. Biol.* 10, 658–663. doi: 10.1016/j.cbpa.2006.09.020

Zhang, Y., Shen, H., He, X., Thomas, B. W., Lupwayi, N. Z., Hao, X., et al. (2017). Fertilization shapes bacterial community structure by alteration of soil pH. *Front. Microbiol.* 8:1325. doi: 10.3389/fmicb.2017.01325

Zolotov, M. Y., and Shock, E. L. (2001). Composition and stability of salts on the surface of Europa and their oceanic origin. *J. Geophys. Res. Planets* 106, 32815–32827. doi: 10.1029/2000JE001413

Zorz, J. K., Kozlowski, J. A., Stein, L. Y., Strous, M., and Kleiner, M. (2018). Comparative proteomics of three species of ammonia-oxidizing bacteria. *Front. Microbiol.* 9:938. doi: 10.3389/fmicb.2018.00938

6.3 Conclusion

While the habitability of extraterrestrial habitats can only be defined by direct sampling of these environments, the potential for habitability and biology as we know it can be explored using Earth bacteria. The results presented in this chapter characterise the habitability thresholds, underlying toxicological impacts, and physiological changes of *H. meridiana* within concentrated aqueous $(NH_4)_2SO_4$ relevant to icy moon and Earth environments. *H. meridiana* was first exposed to increasing concentrations of $(NH_4)_2SO_4$ to establish the limits of life. The habitability thresholds of *H. meridiana* in $(NH_4)_2SO_4$ were high; cultures remained viable in up 1 M $(NH_4)_2SO_4$. However, while cells were viable, toxic effects were evident as cell number was reduced compared to control conditions (0 M $(NH_4)_2SO_4$), and growth rate and final cell density decreased onward from 0.25 M and 0.75 M $(NH_4)_2SO_4$, respectively.

Comparative assessment of *H. meridiana* cell density in ammonium salts (ammonium chloride, ammonium nitrate) and sulphate salts (sodium sulphate, potassium sulphate), where ionic concentrations were matched to $(NH_4)_2SO_4$ revealed that changes to the proportion of dissolved NH_4^+ or SO_4^{2-}, salinity, osmotic pressure, pH, or water activity did not account for the cell density changes observed. In aqueous solution, $(NH_4)_2SO_4$ dissociates into NH_4^+ and SO_4^{2-} ions. This indicated that toxicity in $(NH_4)_2SO_4$ may have been driven by a combined effect of NH_4^+ and SO_4^{2-} on the cell, as opposed to intact $(NH_4)_2SO_4$ molecules.

However, the relative behaviour of NH_4^+ and SO_4^{2-} may vary with environmental parameters such as pH, temperature, and salinity. Therefore, we must also consider that the differential effects on growth may have arisen from changes to these parameters. Temperature was constant, so any effects on solubility or temperature-dependent alterations to pK_a should have remained stabilised across each condition. Salinity and ionic strength increased with increasing concentration of $(NH_4)_2SO_4$. This is significant as increasing salinity can alter ion activities and favour ion pairing, where weak and transient electrostatic interactions would occur between ions such as NH_4^+ and SO_4^{2-} (Raeispour Shirazi et al., 2025). Ion pairing can improve permeation of compounds across lipid membranes (Cristofoli et al., 2021), a possible mechanism accounting for the elevated toxicity of $(NH_4)_2SO_4$ with concentration. Likewise, pH must be considered. As concentrations of $(NH_4)_2SO_4$ increased, pH became more acidic. Lower pH can promote partial protonation of SO_4^{2-} to HSO_4^- (Vielma and Hefter, 2022). It is plausible the creation of this molecule may have contributed to the greater toxicity observed with increasing concentration, although literature demonstrating HSO_4^- as a toxic ion is limited.

Similarly, the effect of water activity (a_w) could also be discussed. While there appeared to be no correlation between the a_w of a solution and the level of growth observed by *H. meridiana* within the ammonium and sulphate salt solutions, a_w would lower as concentrations of $(NH_4)_2SO_4$ increased. Indeed, it can be observed that the a_w of the 0.1 M $(NH_4)_2SO_4$ (0.1 M SO_4^{2-}) solution is 0.96, while the a_w of the 1 M $(NH_4)_2SO_4$ (1 M SO_4^{2-}) solution is 0.94. The lower limit of a_w, where cell division is permitted, extends to 0.6 a_w (Stevenson et al., 2015, Grant, 2004). However, even small changes in a_w can impact growth. Predictive models that depict growth rate versus a_w show a smooth but non-linear decline in growth rate as a_w decreases. In some bacteria, decreasing a_w from 0.96 to 0.94 can result in an almost two-fold reduction in growth rate (Peleg, 2022). This means that even a small decrease in a_w by 0.02

has the potential to result in noticeable growth limitations, and may account for, or at least contribute to, the lower growth levels of *H. meridiana* observed at 0.1 M $(NH_4)_2SO_4$ versus 1 M $(NH_4)_2SO_4$.

An additional physicochemical factor that may contribute to the observed physiological responses of *H. meridiana* in $(NH_4)_2SO_4$ solutions is the kosmotropic or chaotropic nature of dissolved ions. Kosmotropic ions stabilise hydrogen-bonding networks in water and promote macromolecular stability, whereas chaotropic ions weaken water structure and destabilise biomolecules such as proteins, membranes and nucleic acids (Collins and Washabaugh, 1985, Ball and Hallsworth, 2015). SO_4^{2-} is widely recognised as a strongly kosmotropic anion within the Hofmeister series, while NH_4^+ occupies a comparatively weaker kosmotropic position and can exert destabilising effects at elevated concentrations (Zhang and Cremer, 2006). In microbial systems, chaotropic or strongly hydrated ionic environments have been shown to influence protein folding, membrane integrity and metabolic activity, ultimately constraining growth once critical thresholds are exceeded (Cray et al., 2013). Consequently, the combined ionic effects present in solutions of increasing $(NH_4)_2SO_4$ may generate physicochemical stresses that extend beyond simple osmotic, salinity, ionic strength, or pH effects, and could account for the greater toxicity observed. While kosmotropicity and chaotropicity are usually not indicators of habitability by themselves (Cockell et al., 2020), these findings highlight that the habitability of $(NH_4)_2SO_4$-rich oceans may also depend on kosmotropic and chaotropic balance, which could influence the stability of biomolecules and the functionality of cells.

Subsequent analysis of cellular changes indicated that cell morphology was unaffected by the presence of $(NH_4)_2SO_4$. Internal structures were comparable to that of the control at 0 M $(NH_4)_2SO_4$. However, molecular alterations were evident. Most prominently, lowered levels of the metabolite glutamine were observed in *H. meridiana* exposed to $(NH_4)_2SO_4$. This is significant as glutamine forms a vital part of many essential metabolic pathways. As such, purine metabolites were found to be reduced, with major alteration to amino acids, and there were also changes to metabolites within nitrogen, carbon, and energy metabolism pathways. Reduced levels of glutamine could be a clear mechanism of toxicity by $(NH_4)_2SO_4$.

When assessing the potential for habitability, the presence of ammonia within Europa is not currently known. Europa is often modelled with an ammonia-water ocean, however, it is likely the heat of the Jovian nebula would have precluded significant incorporation of ammonia into this satellite. It is therefore unlikely that the ocean of Europa hosts an ocean that exceeds 1 M NH_4^+, a concentration in which *H. meridiana* was found to remain viable. On Titan, ammonia incorporation is thought to be more significant and could possibly exceed 1 M NH_4^+. Application of $(NH_4)_2SO_4$ fertilizer could in some instances raise the concentration of $(NH_4)_2SO_4$ to above this level. This is significant as, even in concentrations below 1 M $(NH_4)_2SO_4$, it is evident that $(NH_4)_2SO_4$ can slow growth rate and diminish cell density of *H. meridiana*, in addition to altering vital metabolisms. The presence of $(NH_4)_2SO_4$ in terrestrial environments and extraterrestrial oceans may not preclude the existence of life but may constrain the rate at which biology such as this could emerge or be sustained, or altogether change the typical metabolisms we might expect to observe.

7

Conclusion

Contents

7.1 Thesis outcomes

The motivation for this thesis was to answer key knowledge gaps that limited the current understanding of bacterial habitability in aqueous ammonia. Dissolved NH_3/NH_4^+, volatilized NH_3, and $(NH_4)_2SO_4$ salt were utilised. The first knowledge gap addressed was in regard to the survival thresholds of a bacteria in aqueous ammonia, particularly for an extremophile bacteria. The contribution of external changes in pH to observed ammonia toxicity was also considered. The second knowledge gap investigated was the physiological response to aqueous ammonia. The final knowledge gap explored pertained to the influence of dispersed gaseous NH_3 on habitability in local and distant bacterial cultures. By exploring these facets, this thesis aimed to contribute to a wider understanding of habitability in ammoniacal waters. This should provide a foundation in which to better estimate the potential for habitability in icy moon oceans that contain ammonia, as well as to better understand the implications of ammonia pollution on terrestrial ecosystems.

Most substances exert a deleterious effect on microbial growth once a certain concentration threshold is exceeded, either by altering the chemical environment or by eliciting biological disruptions. In Chapter 4, I showed that there is a distinct habitability limit of 0.05 M ammonia

for the extremophile *H. meridiana* in an aqueous, closed-air ammonia system where the relative proportion of NH_3 to NH_4^+ was high. In opposition to literature utilising neutrophilic bacteria, these growth alterations were shown to be distinct from an external rise in pH and were thus conferred through specific ammonia-driven reactions. A higher survival threshold of 0.25 M ammonia was established in ammonia solutions where NH_3 gas escape was permitted. Not only was there distinct survival thresholds, but ammonia could also exert morphological changes on the cell that were not observed in high pH conditions. The molecular response to ammonia was primarily that of high pH adaptations, however, some unique ammonia-driven reactions were observed. This suggested that, if ammonia concentrations are above the survival thresholds established, ammoniacal waters may limit the habitability potential in a pH-independent manner for organisms with similar physiologies to *H. meridiana*. This is important when considering appropriate celestial targets and biosignatures in the search for life, as well as how ammonia pollution may shape bacterial community structure and diversity in afflicted terrestrial environments.

Some toxic substances are relatively immobile in the environment and tend to remain where they are deposited. Others can migrate through the atmosphere, water or solid environments. NH_3 is a gas at standard pressure and temperatures above -33.3 °C. On icy moons, ice shell environments may accommodate these parameters, and entrain or adsorb NH_3 gas as it is expelled from the ocean below. On Earth, such conditions are common in the environment, and NH_3 escape was recorded in Chapter 4. Thus, in Chapter 5, I considered ammonia dispersal from an aqueous source to surrounding environments without ammonia. The implications for *H. meridiana* habitability in local and distant environments were assessed. I found that NH_3 gas dispersed from a central source and dissolved into surrounding aqueous cultures of *H. meridiana*. Exposed cultures observed extended lag phase duration, slowed doubling time, reduced cell density, and reduced cell viability. The effect was both spatial and temporal. At lower concentrations (i.e., 0.1 M, 0.25 M), ammonia elicited a smaller radius of effect on cell density. Cell density could recover over time as ammonia dispersed. The opposite was true for higher concentrations (i.e., 0.5 M, 1 M). The radius of effect was larger and cell density did not recover completely over time. A nuanced discovery was also made; adjacent exposure to lower concentrations of ammonia enhanced final cell density. When adjacent to 0.1 M ammonia, ammonia concentrations were below 0.04 M at 4 h and cultures exhibited a higher cell density and similar growth rate to control conditions without ammonia. This further supported the finding in Chapter 4 that concentrations at and below 0.05 M ammonia are habitable. Ammonia can therefore benefit growth as a nitrogen source as well as have a detrimental effect on bacterial propagation, depending on concentration.

NH_3 is frequently characterised as the toxic component of ammonia, but it is known NH_4^+ can also independently elicit toxic cellular effects. Near neutral aqueous environments are theorised on Europa, and are common in terrestrial environments. To fully characterise the impacts of aqueous ammonia, it was therefore pertinent in Chapter 6 to define the limits of habitability in NH_4^+ as well as the physiological effects. Namely, $(NH_4)_2SO_4$ was investigated. $(NH_4)_2SO_4$ is a salt that could feature within the oceans of Europa and Titan, and is a common fertilizing agent on Earth. I found that the habitability threshold for NH_4^+ habitability was high. Cultures of *H. meridiana* remained viable up to 1 M $(NH_4)_2SO_4$. However, in accordance to literature indicating $(NH_4)_2SO_4$ can alter bacterial diversity, I found growth rate

and cell density declined as concentrations of $(NH_4)_2SO_4$ increased. Disruption to pathways in nitrogen, carbon, and energy metabolism were also evident. This suggested that $(NH_4)_2SO_4$ could constrain the proliferation and metabolism of bacteria with physiologies similar to *H. meridiana* if at a growth limiting concentrations. However, ammoniacal waters with a high relative abundance of NH_4^+ may not eliminate viability, and thus habitability, altogether at molar level concentrations.

7.2 Implications for habitability: icy moons

Icy moons Enceladus, Titan, and Europa could present conditions favourable for prebiotic chemistry; there is availability of liquid water, energy, heat, nutrients, and organics. Hydrothermal vent systems could be present on Enceladus and Europa, similar to those on Earth that are believed to have supported the origin of life (Glein et al., 2007, Matson et al., 2007, Hand et al., 2007, Vance et al., 2007). On Titan, there are extensive hydrocarbon systems that mirror the hydrological cycle on Earth (Stofan et al., 2007, Turtle et al., 2009, Poggiali et al., 2024). For these reasons, icy moons are prominent targets in the search for life beyond Earth. But, not all conditions on these moons are favourable for life as we know it. There are extremes of temperature and pressure exceeding those even possible on Earth, such as near -200 °C icy surfaces (Brown et al., 2006, Jennings et al., 2019, Ashkenazy, 2019) and oceanic pressures of 8000 bar (Journaux et al., 2020). There are also the extremes of ammonia. Due to a lack of natural environments on Earth where ammonia is present beyond trace levels, there is in turn a lack of organisms that can survive in higher concentrations of ammonia and the limits of life in ammonia are not properly defined.

The results presented in this thesis have immediate implications for astrobiology. The *in vitro* experiments presented suggest that the concentrations of ammonia present on Enceladus would not constrain the viability of terrestrial bacteria. *H. meridiana* could remain viable up to 0.05 M ammonia in a closed-air system where 62% of ammonia was present as NH_3. On Enceladus, the molar concentration of ammonia is estimated at ≈0.0188 M, with a dominance of NH_3. Within the ice shell of Enceladus, ammonia may migrate from the ocean or via ice adsorption into brine channels. This thesis presents results that indicate ammonia can disperse from a concentrated source and dissolve into nearby aqueous habitats. This was shown to either aid bacterial propagation (< 0.05 M NH_3) or limit bacterial propagation (> 0.05 M NH_3) based on the concentration of ammonia that remains following transport. Several scenarios are plausible on Enceladus: (i) ammonia is not delivered to ice shell brine networks and thus is at trace or null levels, (ii) ammonia in brine networks may be directly derived from the ocean and thus equal to that in the ocean, or, (iii) ammonia may concentrate in the ice shell networks, exceeding the levels in the ocean due to exclusion from ice. Whether one, or none, of these scenarios are possible is beyond the scope of this thesis as well as current data regarding Enceladus. However, the molar threshold of 0.05 M ammonia established in this thesis, and the spatial toxicity of transported ammonia, provides a basis for which to make assumptions on whether the concentration of ammonia within the brines could support life.

This thesis also suggests that the concentrations of ammonia currently estimated in the ocean of Europa would not be limiting to life as we know it. *H. meridiana* remained viable up to 1 M $(NH_4)_2SO_4$. If ammonia is present in the ocean of Europa, it is likely to be below this

threshold. The warmth of the Jovian nebula would have prevented significant incorporation of NH_3 into Europa during it's formation. It may therefore be deduced that at current concentration estimates and speciation expectations, ammonia may not act as a chemical parameter that could constraint habitability in this extraterrestrial ocean. The presence and physicochemical conditions of potential ice shell brine networks on Europa are not known, however for the purpose of this thesis I assume brine networks would present a similar pH, and thus speciation of ammonia, as the ocean. Thus, the habitability assumptions of the ocean can also be applied to brine networks. However, it is likely that solutes such as $(NH_4)_2SO_4$ or other ammonium salts would become excluded from ice as it forms. It is therefore plausible brine networks of Europa may contain concentrations of NH_4^+ that exceed concentrations in the ocean. Yet, given the small amount of ammonia that is expected to have accreted with Europa, it is more likely to assume this concentration could remain below 1 M NH_4^+.

Habitability limitations may not be imposed by lower concentrations of ammonia, but the higher concentrations of ammonia utilised in this thesis exert a deleterious effect on life. On Titan, the ocean could exceed 0.5 M, with a high relative abundance of NH_3 to NH_4^+ (Brassé et al., 2017). *H. meridiana* did not remain viable in up to 0.5 M (95.4% NH_3) whether in a closed-air or open-air system. Concentrations at and above 0.5 M were also identified as the threshold at which cultures of *H. meridiana* adjacently exposed to NH_3 showed the most detrimental and significant change to growth dynamics and viability. The ammonia concentration within the Titan ocean, and any potential ice shell networks, may not be suitable for the development of life as we know. However, habitable pockets may exist; for example, if ammonia is unevenly distributed or excluded from ice shell brine networks. Ammonia may also be retained in non-toxic ammonia hydrates if permitted by specified temperatures and pressures.

Titan could also consist of an ocean of $(NH_4)_2SO_4$. In this scenario, concentrations exceeding 0.5 M may not be limiting for habitability; as aforementioned, *H. meridiana* remained viable up to 1 M $(NH_4)_2SO_4$. The prospect for habitable environments on Titan as a function of ammonia can only be clarified by further oceanic physicochemical characterisations of this moon.

It is not without mention that the findings of this thesis expand beyond icy moons. Ceres may also host an internal liquid layer that is ammonia-rich. Surface observations of Ceres shows carbonate-rich bright deposits that are interpreted as residues from subsurface brines. Spectral measurements additionally show that the crust of Ceres is enriched in ammoniated phyllosilicates, indicating that NH_3 was incorporated into the dwarf planet. Surface brines on Ceres are NH_4^+-bearing, but internal brines within Ceres could be NH_3-bearing under the correct conditions. We cannot speculate on ammonia speciation as the physicochemical properties (i.e., pH, temperature, pressure) of the subsurface brines of Ceres are not yet known. However, the experimental results presented here indicate that NH_3 and NH_4^+ toxicity is concentration dependent, with bacterial growth remaining possible below defined molar thresholds. If the NH_4^+-bearing brines, or NH_3-bearing brines, on Ceres fall within comparable concentration ranges, the subsurface brines may remain chemically permissive for microbial life. This suggests that ammoniacal brines on Ceres could represent potentially habitable aqueous niches despite the presence of ammonia. It is also reasonable to speculate that even

if ammonia concentrations did exceed habitable levels, mobilisation of brines may generate transient aqueous environments with ammonia gradients that could create microhabitats in which ammonia concentrations fall within biologically tolerable ranges, similar to the spatial ammonia exposure gradients explored experimentally in this thesis.

It must be reiterated that habitability is not intrinsically linked with the presence of life. Conditions in icy moons may be found to be habitable, but not inhabited. There are also many other factors that dictate whether an environment has the potential to be habitable. This habitability discussion does not indicate whether there is or is not life within the oceans of icy moons. Rather, this thesis and discussion should be used as a basis to constrain environments that could be valuable candidates in missions of astrobiology, based on the limits of habitability established for terrestrial life in ammonia.

7.3 Implications for habitability: Earth

Terrestrially, ammonia occurs in trace concentrations in the natural atmosphere (Roney et al., 2004). Larger accumulations of ammonia are often a by-product of anthropogenic activities. 78 tetragrams of NH_3 are deposited into the terrestrial environment per year at a global scale (Luo et al., 2022, Yang et al., 2023). Much of this pollution is deposited into the environment from fertilizers in the form of ammonium, but ammonia fertilizer is also utilised (Randive et al., 2021, Tyagi et al., 2022). As $(NH_4)_2SO_4$ can acidify soil while also providing nitrogen in the form of NH_4^+, $(NH_4)_2SO_4$ a commonly utilised fertilizer to stimulate plant growth in high pH soils. In such soils, application of $(NH_4)_2SO_4$ fertilizer has led to appreciable nitrogen losses of up to 66% by NH_3 volatilization (Powlson and Dawson, 2022). Subsequently, long-range dispersion and deposition of volatilized NH_3 has been demonstrated (Sutton et al., 1998, Bouet et al., 2005, Leytem et al., 2024, Lô et al., 2025). The results of this thesis are therefore also highly applicable to Earth environments when considering the bacteriology in areas afflicted with ammonia pollution.

Firstly, this thesis indicates that, in an open-air system as on Earth, concentrations of ammonia exceeding 0.25 M are likely to impose immediate alterations to bacterial diversity and community structure. Growth dynamics and viability of *H. meridiana* were affected above this concentration even with ammonia dispersal. As ammonia concentrations resulting from pollution are seldom measured and lack representation in literature, it is not possible to estimate whether such concentrations occur in any environments on Earth. However, it can be assumed concentrations even below this limit would likely have detrimental effects. Many bacteria are not adapted to high pH as *H. meridiana* is. Thus, these bacteria would likely exhibit an even lower survival threshold in ammonia. At and below 0.25 M, detrimental growth effects were apparent in *H. meridiana* but recovered through time as NH_3 dispersed from the system.

Physiological changes were also apparent. Some environments may not be continually exposed to ammonia, and therefore only exhibit transient detrimental effects to bacterial life and physiology. However, in many environments there are continuous "point sources" of pollution. The Clarbeston Stream in south-west Wales has shown consistently high concentrations of ammonia as a result of discharge and field run-off by rainfall events from a nearby farmyard

(Schofield et al., 1990). Similarly, Onondaga Lake, New York, United States, has exhibited high concentrations of ammonia over a 10-year period as a consequence of discharge from a wastewater treatment plant (Matthews et al., 2000). Sites such as these would be expected to observe near permanent changes to bacterial biology and populations as a function of ammonia concentration.

This thesis also demonstrates that volatilized and dispersed NH_3 from a nearby source is not as toxic as direct deposition, but may still have detrimental effects. While the effect of dispersed and deposited NH_3 on life has been assumed, it has been little demonstrated by proof-of-concept experiments. This thesis provides evidence that, depending on concentration, NH_3 could alter bacterial ecosystems by either providing a source of nitrogen or acting as a toxicological agent. These effects would be transient due to open-air dispersal, unless NH_3 is supplemented continuously. However, continuous NH_3 pollution and thus ecosystem changes are possible from regular "point sources" of ammonia as aforementioned.

Likewise, the results of this thesis indicate application of $(NH_4)_2SO_4$ is likely detrimental to the wider bacterial ecosystem. Some commercial fertilizers advise an application of 35 g/m^2 $(NH_4)_2SO_4$ fertilizer to soils. This could yield a molarity of 2.64 M when dissolved in 100 mL water. It is therefore plausible that applied $(NH_4)_2SO_4$ fertilizer could accumulate in some environments to beyond 1 M $(NH_4)_2SO_4$. While I show that *H. meridiana* could remain viable at this concentration, growth dynamics and cell number were negatively affected and physiology was altered. These effects are likely to be only exemplified in bacteria without halophilic adaptations. In an ecosystem, the results of this thesis suggest that $(NH_4)_2SO_4$ application may cause a major shift to bacterial biology, diversity and structure. This is only supported by experiments in literature showing changes to soil biology following treatment with $(NH_4)_2SO_4$.

7.4 Limitations and future work

The work in this thesis aimed to establish fundamentals in the limits of life in aqueous ammonia. As such, other parameters and extremes were not considered. Multi-extremes are present on icy moons; extremes of temperature, pressure, and salinity. All of these factors also affect the potential for habitability as well as the phase behaviour and speciation of ammonia. The use of ammonia in combination with multi-extremes could be a valuable avenue of future research now that some fundamental habitability principles have been established. Additionally, this thesis utilised aqueous ammonia within which NH_3 gas was dissolved in solution. While dissolved NH_3 gas may be present in some scenarios of icy moons (i.e., plume sites), liquid NH_3 would be the predominant phase due to pressure and temperature. It would not be possible to utilise liquid ammonia without also altering temperature to extremes levels (-33.3 °C), thus negating the thesis mission of understanding the basic effects of ammonia on bacteria. However, both phases of NH_3 are membrane permeable and alkaline. This thesis therefore assumes toxicity between the phases is comparable and the results obtained applicable nonetheless.

In terms of habitability beyond Earth, the implications of this thesis are also purely hypothetical. This thesis works on the assumption that any life that may develop beyond Earth

would do so in a similar framework to early Earth. However, it is possible, if not likely, that any life that would develop beyond Earth would be adapted to it's habitat. In essence, life may be alien to that of which we know. However, we can only explore habitability based on the knowledge and resources available on Earth, and therefore this thesis explores the constraints imposed by ammonia on life as we know it. Similarly, this thesis is based upon the current data available for icy moons. Due to physical and technical limitations, it is not yet possible to sample icy moon oceans and thus ammonia concentrations, ammonia speciation, and habitability implications are based upon the most current knowledge; this may change.

Future work could explore the growth, viability and physiology of other diverse bacteria grown in ammonia. In theory, the results of a diverse range of bacteria, with distinct physiologies, to ammonia could provide a valuable basis to make generalisations regarding ammonia tolerance and adaptation. However, it is likely that each individual species, if not strains, would have a unique response to ammonia. This would make it challenging to define an absolute habitability limit across bacteria. There is also the difficulty that each bacteria would have a specified growth temperature, optimal salinity level and pH range. These factors can alter the proportion of NH_3 and NH_4^+ and thus the toxicity of an ammonia solution. Nonetheless, such a study could drive a better, generalised understanding of the limits of habitability in aqueous ammonia environments. As the ocean of Enceladus has been recently constrained to pH 10.6 and an ammonia concentration of $\approx$0.0181 M (Glein and Truong, 2025), such habitability investigations could utilise these parameters.

A notable avenue of research would be to employ directed evolution. Artificial evolution can be used to create an organism that is ammonia adapted under multi-extremes. The type of adaptations and tolerance mechanisms observed could correspond to strategies that would be suitable for survival in an ammonia-rich, extreme aqueous environments. However, the applicability of an organism created by directed evolution to extraterrestrial habitability is slim. These organisms are often evolved over decades, as opposed to billions of years, and the adaptations evolved may not necessarily parallel adaptations that could develop in icy moon oceans. For example, an organism may incorporate ammonia as an energy source, as in AOB, or simply evolve an efficient mechanism of ammonia exclusion from the intracellular space. Either of these scenarios provide a mechanism to survive in ammonia, but the incorporation of either adaptation in a bacteria made by directed evolution does not mean this adaptation could or would occur in icy moon oceans. However, in lieu of extremophile bacteria that observe adaptations to high ammonia on Earth, such a strategy could be valuable in defining the limits of habitability in ammonia further.

7.5 Final remarks

This body of work provides an *a posteriori* understanding of habitability in ammonia which is applicable to both icy moon environments as well as Earth environments. I found that there was a distinct habitability limit in aqueous ammonia for *H. meridiana*, an extremophile that has physiologies relevant to the physicochemical conditions within icy moons. Ammonia and external pH toxicity were found to be distinct drivers of bacterial demise. Thus, the impacts of ammonia were both concentration-dependent and pH-independent. In solutions with a high relative abundance of NH_3, physiological changes in *H. meridiana* corresponded to high pH

adaptations but also illuminated unique ammonia-driven changes. The habitability impacts of NH_3 were found to be both spatial and temporal. Volatilized NH_3 could impact the growth of *H. meridiana* in nearby, exposed growth systems. In solutions with a high NH_4^+ abundance, key changes to physiology suggested internal toxicity mechanisms that included disruption to the three metabolisms that pillar the survival of terrestrial organisms: nitrogen, carbon, and energy metabolism. Together, the results of this thesis correspond to a single conclusion: ammonia, whether as dissolved NH_3/NH_4^+, volatilized NH_3, or $(NH_4)_2SO_4$ salt, is a chemical parameter that must be considered when evaluating the prospects for life within ocean worlds and polluted environments on Earth alike.

“ *Nothing happens in contradiction to nature, only in contradiction to what we know of it.* ”

- Dana Scully, *The X Files*

References

Alarico, S., Costa, M., Sousa, M. S., Maranha, A., Lourenço, E. C., Faria, T. Q., Ventura, M. R., and Empadinhas, N. (2014). Mycobacterium hassiacum recovers from nitrogen starvation with up-regulation of a novel glucosylglycerate hydrolase and depletion of the accumulated glucosylglycerate. *Scientific Reports*, 4(1):6766.

Alexander, M. (1965). Denitrifying bacteria. In *Methods of Soil Analysis*, chapter 103, pages 1484–1486. John Wiley & Sons, Ltd.

Anderson, J. D., Schubert, G., Jacobson, R. A., Lau, E. L., Moore, W. B., and Sjogren, W. L. (1998). Europa's differentiated internal structure: Inferences from four Galileo encounters. *Science*, 281(5385):2019–2022.

Angelova, P. R., Kerbert, A. J. C., Habtesion, A., Hall, A., Abramov, A. Y., and Jalan, R. (2022). Hyperammonaemia induces mitochondrial dysfunction and neuronal cell death. *JHEP reports: innovation in hepatology*, 4(8):100510.

Antunes, J., Leão, P., and Vasconcelos, V. (2019). Marine biofilms: Diversity of communities and of chemical cues. *Environmental Microbiology Reports*, 11(3):287–305.

Ao, Y., Henkel, C., Braatz, J. A., Weiß, A., Menten, K. M., and Mühle, S. (2011). Ammonia (*J,K*)=(1,1) to (4,4) and (6,6) inversion lines detected in the Seyfert 2 galaxy NGC 1068. *Astronomy & Astrophysics*, 529:A154.

Ashkenazy, Y. (2019). The surface temperature of Europa. *Heliyon*, 5(6):e01908.

Bai, G., Rama Rao, K., Murthy, Ch.R.K., Panickar, K., Jayakumar, A., and Norenberg, M. (2001). Ammonia induces the mitochondrial permeability transition in primary cultures of rat astrocytes. *Journal of Neuroscience Research*, 66(5):981–991.

Baland, R.-M., Hoolst, T. V., Yseboodt, M., and Karatekin, O. (2011). Titan's obliquity as evidence of a subsurface ocean? *Astronomy & Astrophysics*, 530:A141.

Baland, R.-M., Tobie, G., Lefèvre, A., and Van Hoolst, T. (2014). Titan's internal structure inferred from its gravity field, shape, and rotation state. *Icarus*, 237:29–41.

Ball, P. and Hallsworth, J. E. (2015). Water structure and chaotropicity: Their uses, abuses and biological implications. *Physical Chemistry Chemical Physics*, 17(13):8297–8305.

Barnes, J. W., Turtle, E. P., Trainer, M. G., Lorenz, R. D., MacKenzie, S. M., Brinckerhoff, W. B., Cable, M. L., Ernst, C. M., Freissinet, C., Hand, K. P., Hayes, A. G., Hörst, S. M., Johnson, J. R., Karkoschka, E., Lawrence, D. J., Gall, A. L., Lora, J. M., McKay, C. P., Miller, R. S., Murchie, S. L., Neish, C. D., Newman, C. E., Núñez, J., Panning, M. P., Parsons, A. M., Peplowski, P. N., Quick, L. C., Radebaugh, J., Rafkin, S. C. R., Shiraishi, H., Soderblom, J. M., Sotzen, K. S., Stickle, A. M., Stofan, E. R., Szopa, C., Tokano, T., Wagner, T., Wilson, C., Yingst, R. A., Zacny, K., and Stähler, S. C. (2021). Science goals and objectives for the Dragonfly Titan rotorcraft relocatable lander. *The Planetary Science Journal*, 2(4):130.

Bates, R. G. and Pinching, G. D. (1949). Acidic dissociation constant of ammonium ion at 0 to 50 °C, and the base strength of ammonia. *Journal of Research of the National Bureau of Standards*, 42(5):419.

Beagle, S. D. and Lockless, S. W. (2021). Unappreciated Roles for K^+ Channels in Bacterial Physiology. *Trends in Microbiology*, 29(10):942–950.

Becker, T. M., Zolotov, M. Y., Gudipati, M. S., Soderblom, J. M., McGrath, M. A., Henderson, B. L., Hedman, M. M., Choukroun, M., Clark, R. N., Chivers, C., Wolfenbarger, N. S., Glein, C. R., Castillo-Rogez, J. C., Mousis, O., Scanlan, K. M., Diniega, S., Seelos, F. P., Goode, W., Postberg, F., Grima, C., Hsu, H.-W., Roth, L., Trumbo, S. K., Miller, K. E., Chan, K., Paranicas, C., Brooks, S. M., Soderlund, K. M., McKinnon, W. B., Hibbitts, C. A., Smith, H. T., Molyneux, P. M., Gladstone, G. R., Cable, M. L., Ulibarri, Z. E., Teolis, B. D., Horanyi, M., Jia, X., Leonard, E. J., Hand, K. P., Vance, S. D., Howell, S. M., Quick, L. C., Mishra, I., Rymer, A. M., Briois, C., Blaney, D. L., Raut, U., Waite, J. H., Retherford, K. D., Shock, E., Withers, P., Westlake, J. H., Jun, I., Mandt, K. E., Buratti, B. J., Korth, H., Pappalardo, R. T., and the Europa Clipper Composition Working Group (2024). Exploring the Composition of Europa with the Upcoming Europa Clipper Mission. *Space Science Reviews*, 220(5):49.

Behera, S. N., Sharma, M., Aneja, V. P., and Balasubramanian, R. (2013). Ammonia in the atmosphere: A review on emission sources, atmospheric chemistry and deposition on terrestrial bodies. *Environmental Science and Pollution Research*, 20(11):8092–8131.

Běhounková, M., Tobie, G., Choblet, G., Kervazo, M., Melwani Daswani, M., Dumoulin, C., and Vance, S. D. (2021). Tidally induced magmatic pulses on the oceanic floor of Jupiter's moon Europa. *Geophysical Research Letters*, 48(3):e2020GL090077.

Behrends, V., Williams, K. J., Jenkins, V. A., Robertson, B. D., and Bundy, J. G. (2012). Free Glucosylglycerate Is a Novel Marker of Nitrogen Stress in Mycobacterium smegmatis. *Journal of Proteome Research*, 11(7):3888–3896.

Benarroch, J. M. and Asally, M. (2020). The microbiologist's guide to membrane potential dynamics. *Trends in Microbiology*, 28(4):304–314.

Bender, D. A. (2012). *Amino Acid Metabolism*. John Wiley & Sons, third edition.

Billings, S. E. and Kattenhorn, S. A. (2005). The great thickness debate: Ice shell thickness models for Europa and comparisons with estimates based on flexure at ridges. *Icarus*, 177(2):397–412.

Bills, B. G. and Nimmo, F. (2011). Rotational dynamics and internal structure of Titan. *Icarus*, 214(1):351–355.

Bobbink, R. and Hicks, W. K. (2014). Factors affecting nitrogen deposition impacts on biodiversity: An overview. In Sutton, M. A., Mason, K. E., Sheppard, L. J., Sverdrup, H., Haeuber, R., and Hicks, W. K., editors, *Nitrogen Deposition, Critical Loads and Biodiversity*, pages 127–138. Springer Netherlands, Dordrecht.

Bollmann, A., Bär-Gilissen, M.-J., and Laanbroek, H. J. (2002). Growth at Low Ammonium Concentrations and Starvation Response as Potential Factors Involved in Niche Differentiation among Ammonia-Oxidizing Bacteria. *Applied and Environmental Microbiology*, 68(10):4751–4757.

Bosoi, C. R. and Rose, C. F. (2009). Identifying the direct effects of ammonia on the brain. *Metabolic Brain Disease*, 24(1):95–102.

Bouet, R., Duplantier, S., and Salvi, O. (2005). Ammonia large scale atmospheric dispersion experiments in industrial configurations. *Journal of Loss Prevention in the Process Industries*, 18(4-6):512–519.

Bower, C. E. and Bidwell, J. P. (1978). Ionization of ammonia in seawater: Effects of temperature, pH, and salinity. *Journal of the Fisheries Research Board of Canada*, 35(7):1012–1016.

Bowers, K. J., Mesbah, N. M., and Wiegel, J. (2009). Biodiversity of poly-extremophilic Bacteria: Does combining the extremes of high salt, alkaline pH and elevated temperature approach a physico-chemical boundary for life? *Saline Systems*, 5:9.

Boyanova, L., Gergova, G., Nikolov, R., Derejian, S., Lazarova, E., Katsarov, N., Mitov, I., and Krastev, Z. (2005). Activity of bulgarian propolis against 94 *Helicobacter pylori* strains *in vitro* by agar-well diffusion, agar dilution and disc diffusion methods. *Journal of Medical Microbiology*, 54(5):481–483.

Brandes, J. A., Boctor, N. Z., Cody, G. D., Cooper, B. A., Hazen, R. M., and Yoder, H. S. (1998). Abiotic nitrogen reduction on the early Earth. *Nature*, 395(6700):365–367.

Brassé, C., Buch, A., Coll, P., and Raulin, F. (2017). Low-temperature alkaline pH hydrolysis of oxygen-free Titan tholins: Carbonates' impact. *Astrobiology*, 17(1):8–26.

Brazier, B. W. (2016). Membrane transport of ammonia. *American Journal of Food and Nutrition*, 4(5):135–137.

Britto, D. T., Siddiqi, M. Y., Glass, A. D. M., and Kronzucker, H. J. (2001). Futile transmembrane NH_4^+ cycling: A cellular hypothesis to explain ammonium toxicity in plants. *Proceedings of the National Academy of Sciences*, 98(7):4255–4258.

Brown, M. E. (2012). The compositions of Kuiper Belt Objects. *Annual Review of Earth and Planetary Sciences*, 40(Volume 40, 2012):467–494.

Brown, M. E. and Calvin, W. M. (2000). Evidence for crystalline water and ammonia ices on Pluto's satellite Charon. *Science*, 287(5450):107–109.

Brown, M. V. and Bowman, J. P. (2001). A molecular phylogenetic survey of sea-ice microbial communities (SIMCO). *FEMS Microbiology Ecology*, 35(3):267–275.

Brown, R. H., Clark, R. N., Buratti, B. J., Cruikshank, D. P., Barnes, J. W., Mastrapa, R. M. E., Bauer, J., Newman, S., Momary, T., Baines, K. H., Bellucci, G., Capaccioni, F., Cerroni, P., Combes, M., Coradini, A., Drossart, P., Formisano, V., Jaumann, R., Langevin, Y., Matson, D. L., McCord, T. B., Nelson, R. M., Nicholson, P. D., Sicardy, B., and Sotin, C. (2006). Composition and physical properties of Enceladus' surface. *Science*, 311(5766):1425–1428.

Buffo, J. J., Meyer, C. R., Chivers, C. J., Walker, C. C., Huber, C., and Schmidt, B. E. (2023). Geometry of freezing impacts ice composition: Implications for icy satellites. *Journal of Geophysical Research: Planets*, 128(3):e2022JE007389.

Buffo, J. J., Schmidt, B. E., Huber, C., and Meyer, C. R. (2021). Characterizing the ice-ocean interface of icy worlds: A theoretical approach. *Icarus*, 360:114318.

Burckhardt, B.-C. and Frömter, E. (1992). Pathways of NH_3/NH_4^+ permeation across *Xenopus laevis* oocyte cell membrane. *Pflügers Archiv*, 420(1):83–86.

Burris, R. H. and Roberts, G. P. (1993). Biological nitrogen fixation. *Annual Review of Nutrition*, 13(1):317–335.

Bywaters, K., Stoker, C. R., Batista Do Nascimento, N., and Lemke, L. (2020). Towards determining biosignature retention in icy world plumes. *Life*, 10(4):40.

Čadek, O., Tobie, G., Van Hoolst, T., Massé, M., Choblet, G., Lefèvre, A., Mitri, G., Baland, R.-M., Běhounková, M., Bourgeois, O., and Trinh, A. (2016). Enceladus's internal ocean and ice shell constrained from Cassini gravity, shape, and libration data. *Geophysical Research Letters*, 43(11):5653–5660.

Cantera, J. J. L. and Stein, L. Y. (2007). Role of nitrite reductase in the ammonia-oxidizing pathway of Nitrosomonas europaea. *Archives of Microbiology*, 188(4):349–354.

Caranto, J. D. and Lancaster, K. M. (2017). Nitric oxide is an obligate bacterial nitrification intermediate produced by hydroxylamine oxidoreductase. *Proceedings of the National Academy of Sciences*, 114(31):8217–8222.

Carr, M. H., Belton, M. J. S., Chapman, C. R., Davies, M. E., Geissler, P., Greenberg, R., McEwen, A. S., Tufts, B. R., Greeley, R., Sullivan, R., Head, J. W., Pappalardo, R. T., Klaasen, K. P., Johnson, T. V., Kaufman, J., Senske, D., Moore, J., Neukum, G., Schubert, G., Burns, J. A., Thomas, P., and Veverka, J. (1998). Evidence for a subsurface ocean on Europa. *Nature*, 391(6665):363–365.

Castillo-Rogez, J., Weiss, B., Beddingfield, C., Biersteker, J., Cartwright, R., Goode, A., Melwani Daswani, M., and Neveu, M. (2023). Compositions and interior structures of the large moons of Uranus and implications for future spacecraft observations. *Journal of Geophysical Research. Planets*, 128(1):e2022JE007432.

Chen, E. M. A., Nimmo, F., and Glatzmaier, G. A. (2014). Tidal heating in icy satellite oceans. *Icarus*, 229:11–30.

Cheng, J. and Hu, J. (2021). Recent advances on carbon monoxide releasing molecules for antibacterial applications. *ChemMedChem*, 16(24):3628–3634.

Cheng, W. H., Lee, M. H., and Peale, S. J. (2014). Complete tidal evolution of Pluto–Charon. *Icarus*, 233:242–258.

Cheung, A. C., Rank, D. M., Townes, C. H., Thornton, D. D., and Welch, W. J. (1968). Detection of NH_3 Molecules in the Interstellar Medium by Their Microwave Emission. *Physical Review Letters*, 21(25):1701–1705.

Chua, B. H., Gloesener, E., Choukroun, M., Vu, T. H., Melwani Daswani, M., Journaux, B., Styczinski, M. J., and Vance, S. D. (2023). Low-temperature specific heat capacity of water–ammonia mixtures down to the eutectic. *ACS Earth and Space Chemistry*, 7(10):1971–1979.

Clegg, S. L. and Whitfield, M. (1995). A chemical model of seawater including dissolved ammonia and the stoichiometric dissociation constant of ammonia in estuarine water and seawater from -2 to 40 °C. *Geochimica et Cosmochimica Acta*, 59(12):2403–2421.

Cleland, C. E. and Rimmer, P. B. (2022). Ammonia and phosphine in the clouds of Venus as potentially biological anomalies. *Aerospace*, 9(12):752.

Clifford, I. I. and Hunter, E. (1933). The system ammonia–water at temperatures up to 150°C and at pressures up to twenty atmospheres. *The Journal of Physical Chemistry*, 37(1):101–118.

Cochrane, C. J., Vance, S. D., Castillo-Rogez, J. C., Styczinski, M. J., and Liuzzo, L. (2025). Stronger evidence of a subsurface ocean within callisto from a multifrequency investigation of its induced magnetic field. *AGU Advances*, 6(1):e2024AV001237.

Cochrane, C. J., Vance, S. D., Nordheim, T. A., Styczinski, M. J., Masters, A., and Regoli, L. H. (2021). In search of subsurface oceans within the Uranian moons. *Journal of Geophysical Research. Planets*, 126(12):e2021JE006956.

Cockell, C., Bush, T., Bryce, C., Direito, S., Fox-Powell, M., Harrison, J., Lammer, H., Landenmark, H., Martin-Torres, J., Nicholson, N., Noack, L., O'Malley-James, J., Payler, S., Rushby, A., Samuels, T., Schwendner, P., Wadsworth, J., and Zorzano, M. (2016). Habitability: A review. *Astrobiology*, 16(1):89–117.

Cockell, C. S. (2014). Habitable worlds with no signs of life. *Philosophical transactions. Series A, Mathematical, physical, and engineering sciences*, 372(2014):20130082.

Cockell, C. S. (2020). Persistence of Habitable, but Uninhabited, Aqueous Solutions and the Application to Extraterrestrial Environments. *Astrobiology*, 20(5):617–627.

Cockell, C. S., McLean, C.-M., Perera, L., Aka, S., Stevens, A., and Dickinson, A. W. (2020). Growth of non-halophilic bacteria in the sodium–magnesium–sulfate–chloride ion system: Unravelling the complexities of ion interactions in terrestrial and extraterrestrial aqueous environments. *Astrobiology*, 20(8):944–955.

Cockell, C. S., Simons, M., Castillo-Rogez, J., Higgins, P. M., Kaltenegger, L., Keane, J. T., Leonard, E. J., Mitchell, K. L., Park, R. S., Perl, S. M., and Vance, S. D. (2024). Sustained and comparative habitability beyond Earth. *Nature Astronomy*, 8(1):30–38.

Collins, K. D. and Washabaugh, M. W. (1985). The Hofmeister effect and the behaviour of water at interfaces. *Quarterly Reviews of Biophysics*, 18(4):323–422.

Cosciotti, B., Balbi, A., Ceccarelli, A., Fagliarone, C., Mattei, E., Lauro, S. E., Di Paolo, F., Pettinelli, E., and Billi, D. (2019). Survivability of anhydrobiotic cyanobacteria in salty ice: Implications for the habitability of icy worlds. *Life*, 9(4):86.

Coustenis, A. (2014). Chapter 38 - Titan. In Spohn, T., Breuer, D., and Johnson, T. V., editors, *Encyclopedia of the Solar System*, pages 831–849. Elsevier, Boston, third edition.

Couvert, O., Koullen, L., Lochardet, A., Huchet, V., Thevenot, J., and Le Marc, Y. (2023). Effects of carbon dioxide and oxygen on the growth rate of various food spoilage bacteria. *Food Microbiology*, 114:104289.

Coyne, F. P. and Hardy, W. B. (1997). The effect of carbon dioxide on bacteria growth. *Proceedings of the Royal Society of London. Series B, Containing Papers of a Biological Character*, 113(782):196–217.

Cray, J. A., Russell, J. T., Timson, D. J., Singhal, R. S., and Hallsworth, J. E. (2013). A universal measure of chaotropicity and kosmotropicity. *Environmental Microbiology*, 15(1):287–296.

Cristofoli, M., Kung, C.-P., Hadgraft, J., Lane, M. E., and Sil, B. C. (2021). Ion pairs for transdermal and dermal drug delivery: A review. *Pharmaceutics*, 13(6):909.

Croft, S. K., Lunine, J. I., and Kargel, J. (1988). Equation of state of ammonia-water liquid: Derivation and planetological applications. *Icarus*, 73(2):279–293.

Dai, X., Hu, C., Zhang, D., Dai, L., and Duan, N. (2017). Impact of a high ammonia-ammonium-pH system on methane-producing archaea and sulfate-reducing bacteria in mesophilic anaerobic digestion. *Bioresource Technology*, 245:598–605.

Dai, X., Yan, H., Li, N., He, J., Ding, Y., Dai, L., and Dong, B. (2016). Metabolic adaptation of microbial communities to ammonium stress in a high solid anaerobic digester with dewatered sludge. *Scientific Reports*, 6(1):28193.

Dalle Ore, C. M., Cruikshank, D. P., Protopapa, S., Scipioni, F., McKinnon, W. B., Cook, J. C., Grundy, W. M., Schmitt, B., Stern, S. A., Moore, J. M., Verbiscer, A., Parker, A. H., Singer, K. N., Umurhan, O. M., Weaver, H. A., Olkin, C. B., Young, L. A., and Ennico, K. (2019). Detection of ammonia on Pluto's surface in a region of geologically recent tectonism. *Science Advances*, 5(5):eaav5731.

Dasarathy, S., Mookerjee, R. P., Rackayova, V., Rangroo Thrane, V., Vairappan, B., Ott, P., and Rose, C. F. (2017). Ammonia toxicity: From head to toe? *Metabolic Brain Disease*, 32(2):529–538.

Dasgupta, P. K. and Dong, S. (1986). Solubility of ammonia in liquid water and generation of trace levels of standard gaseous ammonia. *Atmospheric Environment (1967)*, 20(3):565–570.

De Sanctis, M. C., Ammannito, E., Carrozzo, F. G., Ciarniello, M., De Angelis, S., Ferrari, M., Frigeri, A., and Raponi, A. (2024). Ammonium-rich bright areas on Ceres demonstrate complex chemical activity. *Communications Earth & Environment*, 5(1):131.

Deal, P. H., Souza, K. A., and Mack, H. M. (1975). High pH, ammonia toxicity, and the search for life on the Jovian planets. *Origins of Life*, 6(4):561–573.

Diaz-Baez, M. C. and Roldan, F. (1996). Evaluation of the agar plate method for rapid toxicity assessment with some heavy metals and environmental samples. *Environmental Toxicology and Water Quality*, 11(3):259–263.

Dieckmann, D. N. T. . G. S. (2002). Biogeochemistry of Antarctic sea ice. In *Oceanography and Marine Biology*. CRC Press.

Dobson, S. J. and Franzmann, P. D. (1996). Unification of the genera *Deleya* (Baumann et al. 1983), *Halomonas* (Vreeland et al. 1980), and *Halovibrio* (Fendrich 1988) and the species *Paracoccus halodenitrificans* (Robinson and Gibbons 1952) into a single genus, *Halomonas*, and placement of the genus *Zymobacter* in the family *Halomonadaceae*. *International Journal of Systematic and Evolutionary Microbiology*, 46(2):550–558.

Doherty, M. J., Geach, J. E., Ivison, R. J., Menten, K. M., Jacob, A. M., Forbrich, J., and Dye, S. (2022). Ammonia in the interstellar medium of a starbursting disc at z = 2.6. *Monthly Notices of the Royal Astronomical Society: Letters*, 517(1):L60–L64.

Dong, L., Ge, Z., Qu, W., Fan, Y., Dai, Q., and Wang, J. (2022). Characteristics and mechanism of heterotrophic nitrification/aerobic denitrification in a novel *Halomonas piezotolerans* strain. *Journal of Basic Microbiology*, 62(2):124–134.

Du, Y., Wang, T., Wang, C., Anane, P.-S., Liu, S., and Paz-Ferreiro, J. (2019). Nitrogen fertilizer is a key factor affecting the soil chemical and microbial communities in a Mollisol. *Canadian Journal of Microbiology*, 65(7):510–521.

Duce, R. A., Liss, P. S., Merrill, J. T., Atlas, E. L., Buat-Menard, P., Hicks, B. B., Miller, J. M., Prospero, J. M., Arimoto, R., Church, T. M., Ellis, W., Galloway, J. N., Hansen, L., Jickells, T. D., Knap, A. H., Reinhardt, K. H., Schneider, B., Soudine, A., Tokos, J. J., Tsunogai, S., Wollast, R., and Zhou, M. (1991). The atmospheric input of trace species to the world ocean. *Global Biogeochemical Cycles*, 5(3):193–259.

Dwivedi, S., Wahab, R., Khan, F., Mishra, Y. K., Musarrat, J., and Al-Khedhairy, A. A. (2014). Reactive oxygen species mediated bacterial biofilm inhibition via zinc oxide nanoparticles and their statistical determination. *PLOS One*, 9(11):e111289.

Emerson, K., Russo, R. C., Lund, R. E., and Thurston, R. V. (1975). Aqueous ammonia equilibrium calculations: Effect of pH and temperature. *Journal of the Fisheries Research Board of Canada*, 32(12):2379–2383.

Engel, S., Lunine, J. I., and Norton, D. L. (1994). Silicate interactions with ammonia-water fluids on early Titan. *Journal of Geophysical Research: Planets*, 99(E2):3745–3752.

Eno, C. F., Blue, W. G., and Good Jr., J. M. (1955). The effect of anhydrous ammonia on nematodes, fungi, bacteria, and nitrification in some Florida soils. *Soil Science Society of America Journal*, 19(1):55–58.

Erisman, J. W. and Draaijers, G. P. J. (1995). *Atmospheric Deposition: In Relation to Acidification and Eutrophication*, volume 63 of *Studies in Environmental Science*. Elsevier, Amsterdam.

Fanale, F. P., Li, Y.-H., De Carlo, E., Farley, C., Sharma, S. K., Horton, K., and Granahan, J. C. (2001). An experimental estimate of Europa's "ocean" composition independent of Galileo orbital remote sensing. *Journal of Geophysical Research: Planets*, 106(E7):14595–14600.

Feldman, P., Fournier, K., Grinin, V., and Zvereva, A. (1993). The abundance of ammonia in Comet P/Halley derived from ultraviolet spectrophotometry of NH by ASTRON and IUE | Semantic Scholar. *The Astrophysical Journal*, 404:348.

Fifer, L. M., Catling, D. C., and Toner, J. D. (2022). Chemical fractionation modeling of plumes indicates a gas-rich, moderately alkaline Enceladus ocean. *The Planetary Science Journal*, 3(8):191.

Fletcher, L. N., Cavalié, T., Grassi, D., Hueso, R., Lara, L. M., Kaspi, Y., Galanti, E., Greathouse, T. K., Molyneux, P. M., Galand, M., Vallat, C., Witasse, O., Lorente, R., Hartogh, P., Poulet, F., Langevin, Y., Palumbo, P., Gladstone, G. R., Retherford, K. D., Dougherty, M. K., Wahlund, J.-E., Barabash, S., Iess, L., Bruzzone, L., Hussmann, H., Gurvits, L. I., Santolik, O., Kolmasova, I., Fischer, G., Müller-Wodarg, I., Piccioni, G., Fouchet, T., Gérard, J.-C., Sánchez-Lavega, A., Irwin, P. G. J., Grodent, D., Altieri, F., Mura, A., Drossart, P., Kammer, J., Giles, R., Cazaux, S., Jones, G., Smirnova, M., Lellouch, E., Medvedev, A. S., Moreno, R., Rezac, L., Coustenis, A., and Costa, M. (2023). Jupiter science enabled by ESA's Jupiter icy moons explorer. *Space Science Reviews*, 219(7):53.

Fortes, A. D. (2000). Exobiological implications of a possible ammonia–water ocean inside Titan. *Icarus*, 146(2):444–452.

Fortes, A. D., Grindrod, P. M., Trickett, S. K., and Vočadlo, L. (2007). Ammonium sulfate on Titan: Possible origin and role in cryovolcanism. *Icarus*, 188(1):139–153.

Fouad, M. G. (1955). Die säurestärke des ammoniumions bei hohen salzkonzentrationen. *Monatshefte für Chemie und verwandte Teile anderer Wissenschaften*, 86(1):141–145.

Fowler, D., Coyle, M., Skiba, U., Sutton, M. A., Cape, J. N., Reis, S., Sheppard, L. J., Jenkins, A., Grizzetti, B., Galloway, J. N., Vitousek, P., Leach, A., Bouwman, A. F., Butterbach-Bahl, K., Dentener, F., Stevenson, D., Amann, M., and Voss, M. (2013). The global nitrogen cycle in the twenty-first century. *Philosophical Transactions of the Royal Society B: Biological Sciences*, 368(1621):20130164.

Franzmann, P. D., Springer, N., Ludwig, W., Conway De Macario, E., and Rohde, M. (1992). A Methanogenic Archaeon from Ace Lake, Antarctica: Methanococcoides burtonii sp. nov. *Systematic and Applied Microbiology*, 15(4):573–581.

Fredriksson, K. and Kerridge, J. F. (1988). Carbonates and sulfates in CI chondrites: Formation by aqueous activity on the parent body. *Meteoritics*, 23(1):35–44.

Fretwell, P., Pritchard, H. D., Vaughan, D. G., Bamber, J. L., Barrand, N. E., Bell, R., Bianchi, C., Bingham, R. G., Blankenship, D. D., Casassa, G., Catania, G., Callens, D., Conway, H., Cook, A. J., Corr, H. F. J., Damaske, D., Damm, V., Ferraccioli, F., Forsberg, R., Fujita, S., Gim, Y., Gogineni, P., Griggs, J. A., Hindmarsh, R. C. A., Holmlund, P., Holt, J. W., Jacobel, R. W., Jenkins, A., Jokat, W., Jordan, T., King, E. C., Kohler, J., Krabill, W., Riger-Kusk, M., Langley, K. A., Leitchenkov, G., Leuschen, C., Luyendyk, B. P., Matsuoka, K., Mouginot, J., Nitsche, F. O., Nogi, Y., Nost, O. A., Popov, S. V., Rignot, E., Rippin, D. M., Rivera, A., Roberts, J., Ross, N., Siegert, M. J., Smith, A. M., Steinhage, D., Studinger, M., Sun, B., Tinto, B. K., Welch, B. C., Wilson, D., Young, D. A., Xiangbin, C., and Zirizzotti, A.

(2013). Bedmap2: Improved ice bed, surface and thickness datasets for Antarctica. *The Cryosphere*, 7(1):375–393.

Furukawa, Y., Sekine, T., Oba, M., Kakegawa, T., and Nakazawa, H. (2009). Biomolecule formation by oceanic impacts on early Earth. *Nature Geoscience*, 2(1):62–66.

Gaeman, J., Hier-Majumder, S., and Roberts, J. H. (2012). Sustainability of a subsurface ocean within Triton's interior. *Icarus*, 220(2):339–347.

Gao, S., Zhao, M., Chen, Y., Yu, M., and Ruan, W. (2015). Tolerance response to *in situ* ammonia stress in a pilot-scale anaerobic digestion reactor for alleviating ammonia inhibition. *Bioresource Technology*, 198:372–379.

García-Gómez, H., Garrido, J. L., Vivanco, M. G., Lassaletta, L., Rábago, I., Àvila, A., Tsyro, S., Sánchez, G., González Ortiz, A., González-Fernández, I., and Alonso, R. (2014). Nitrogen deposition in Spain: Modeled patterns and threatened habitats within the Natura 2000 network. *Science of The Total Environment*, 485–486:450–460.

Gee, D. L. and Duane Brown, W. (1981). The effect of carbon monoxide on bacterial growth. *Meat Science*, 5(3):215–222.

Geng, Y., Peng, C., Wang, Z., Huang, S., Zhou, P., and Li, D. (2022). Insights into the spatiotemporal differences in tailings seepage pollution by assessing the diversity and metabolic functions of the soil microbial community. *Environmental Pollution*, 306:119408.

Gijsman, A. J. (1990). Nitrogen nutrition of Douglas-fir (Pseudotsuga menziesii) on strongly acid sandy soil. *Plant and Soil*, 126(1):53–61.

Glasser, L. (2009). Equations of state and phase diagrams of ammonia. *Journal of Chemical Education*, 86(12):1457.

Glavin, D. P., Dworkin, J. P., Alexander, C. M. O., Aponte, J. C., Baczynski, A. A., Barnes, J. J., Bechtel, H. A., Berger, E. L., Burton, A. S., Caselli, P., Chung, A. H., Clemett, S. J., Cody, G. D., Dominguez, G., Elsila, J. E., Farnsworth, K. K., Foustoukos, D. I., Freeman, K. H., Furukawa, Y., Gainsforth, Z., Graham, H. V., Grassi, T., Giuliano, B. M., Hamilton, V. E., Haenecour, P., Heck, P. R., Hofmann, A. E., House, C. H., Huang, Y., Kaplan, H. H., Keller, L. P., Kim, B., Koga, T., Liss, M., McLain, H. L., Marcus, M. A., Matney, M., McCoy, T. J., McIntosh, O. M., Mojarro, A., Naraoka, H., Nguyen, A. N., Nuevo, M., Nuth, J. A., Oba, Y., Parker, E. T., Peretyazhko, T. S., Sandford, S. A., Santos, E., Schmitt-Kopplin, P., Seguin, F., Simkus, D. N., Shahid, A., Takano, Y., Thomas-Keprta, K. L., Tripathi, H., Weiss, G., Zheng, Y., Lunning, N. G., Righter, K., Connolly, H. C., and Lauretta, D. S. (2025). Abundant ammonia and nitrogen-rich soluble organic matter in samples from asteroid (101955) Bennu. *Nature Astronomy*, 9(2):199–210.

Glein, C. R., Baross, J. A., and Waite, J. H. (2015). The pH of Enceladus' ocean. *Geochimica et Cosmochimica Acta*, 162:202–219.

Glein, C. R. and Truong, N. (2025). Phosphates reveal high pH ocean water on Enceladus. *Icarus*, 441:116717.

Glein, C. R., Zolotov, M. Yu., and Shock, E. L. (2007). Hydrothermal Geochemistry as the Source of Plume Gases on Enceladus: A Thermodynamic Evaluation. In *38th Lunar and Planetary Science Conference*, page 1251.

Golby, P., Carver, M., and Jackson, J. B. (1990). Membrane ionic currents in Rhodobacter capsulatus. *European Journal of Biochemistry*, 187(3):589–597.

Goldman, A. D. (2023). How did life become cellular? *Proceedings of the Royal Society B: Biological Sciences*, 290(1992):20222327.

Goles, G. G. (1971). A Review of the Apollo Project: A geochemical view of results of investigations of Apollo 11 and 12 lunar materials. *American Scientist*, 59(3):326–331.

Goossens, S., van Noort, B., Mateo, A., Mazarico, E., and van der Wal, W. (2024). A low-density ocean inside Titan inferred from Cassini data. *Nature Astronomy*, pages 1–10.

Gorissen, A., Jansen, A. E., and Olsthoorn, A. F. M. (1993). Effects of a two-year application of ammonium sulphate on growth, nutrient uptake, and rhizosphere microflora of juvenile Douglas-fir. *Plant and Soil*, 157(1):41–50.

Goswami, M., Mangoli, S. H., and Jawali, N. (2006). Involvement of reactive oxygen species in the action of ciprofloxacin against *Escherichia coli*. *Antimicrobial Agents and Chemotherapy*, 50(3):949–954.

Goude, R., Renaud, S., Bonnassie, S., Bernard, T., and Blanco, C. (2004). Glutamine, glutamate, and α-glucosylglycerate are the major osmotic solutes accumulated by *Erwinia chrysanthemi* strain 3937. *Applied and Environmental Microbiology*, 70(11):6535–6541.

Grant, W. D. (2004). Life at low water activity. *Philosophical Transactions of the Royal Society B: Biological Sciences*, 359(1448):1249–1267.

Grasset, O. and Sotin, C. (1996). The cooling rate of a liquid shell in Titan's interior. *Icarus*, 123(1):101–112.

Grasset, O., Sotin, C., and Deschamps, F. (2000). On the internal structure and dynamics of Titan. *Planetary and Space Science*, 48(7):617–636.

Greeley, R., Sullivan, R., Klemaszewski, J., Homan, K., Head, J. W., Pappalardo, R. T., Veverka, J., Clark, B. E., Johnson, T. V., Klaasen, K. P., Belton, M., Moore, J., Asphaug, E., Carr, M. H., Neukum, G., Denk, T., Chapman, C. R., Pilcher, C. B., Geissler, P. E., Greenberg, R., and Tufts, R. (1998). Europa: Initial Galileo geological observations. *Icarus*, 135(1):4–24.

Grindrod, P., Fortes, A., Nimmo, F., Feltham, D., Brodholt, J., and Vočadlo, L. (2008). The long-term stability of a possible aqueous ammonium sulfate ocean inside Titan. *Icarus*, 197:137–151.

Guthrie, S., Giles, S., Dunkerley, F., and Tabaqchali, H. (2016). *The Impact of Ammonia Emissions from Agriculture on Biodiversity*. RAND Corporation, Cambridge, UK.

Hachiya, T., Inaba, J., Wakazaki, M., Sato, M., Toyooka, K., Miyagi, A., Kawai-Yamada, M., Sugiura, D., Nakagawa, T., Kiba, T., Gojon, A., and Sakakibara, H. (2021). Excessive ammonium assimilation by plastidic glutamine synthetase causes ammonium toxicity in *Arabidopsis thaliana*. *Nature Communications*, 12(1):4944.

Hachiya, T. and Sakakibara, H. (2017). Interactions between nitrate and ammonium in their uptake, allocation, assimilation, and signaling in plants. *Journal of Experimental Botany*, 68(10):2501–2512.

Hales, J. M. and Drewes, D. R. (1979). Solubility of ammonia in water at low concentrations. *Atmospheric Environment (1967)*, 13(8):1133–1147.

Hamill, P. G., Stevenson, A., McMullan, P. E., Williams, J. P., Lewis, A. D. R., S, S., Stevenson, K. E., Farnsworth, K. D., Khroustalyova, G., Takemoto, J. Y., Quinn, J. P., Rapoport, A., and Hallsworth, J. E. (2020). Microbial lag phase can be indicative of, or independent from, cellular stress. *Scientific Reports*, 10(1):5948.

Hammond, N. P., Parmenteir, E. M., and Barr, A. C. (2018). Compaction and melt transport in ammonia-rich ice shells: Implications for the evolution of Triton. *Journal of Geophysical Research: Planets*, 123(12):3105–3118.

Hampson, B. L. (1977). Relationship between total ammonia and free ammonia in terrestrial and ocean waters. *ICES Journal of Marine Science*, 37(2):117–122.

Han, Q., Zhang, J., Sun, Q., Xu, Y., and Teng, X. (2020). Oxidative stress and mitochondrial dysfunction involved in ammonia-induced nephrocyte necroptosis in chickens. *Ecotoxicology and Environmental Safety*, 203:110974.

Hand, K. P., Carlson, R. W., and Chyba, C. F. (2007). Energy, chemical disequilibrium, and geological constraints on Europa. *Astrobiology*, 7(6):1006–1022.

Hand, K. P. and Chyba, C. F. (2007). Empirical constraints on the salinity of the europan ocean and implications for a thin ice shell. *Icarus*, 189(2):424–438.

Hao, D.-L., Zhou, J.-Y., Li, L., Qu, J., Li, X.-H., Chen, R.-R., Kong, W.-Y., Li, D.-D., Li, J.-J., Guo, H.-L., Liu, J.-X., Zong, J.-Q., and Chen, J.-B. (2023). An appropriate ammonium: Nitrate ratio promotes the growth of centipedegrass: Insight from physiological and micromorphological analyses. *Frontiers in Plant Science*, 14:1324820.

Hemmilä, I. A. and Mäntsälä, P. I. (1978). Purification and properties of glutamate synthase and glutamate dehydrogenase from Bacillus megaterium. *The Biochemical Journal*, 173(1):45–52.

Henderson-Sellers, A. and Schwartz, A. W. (1980). Chemical evolution and ammonia in the early Earth's atmosphere. *Nature*, 287(5782):526–528.

Henriquez, T., Wirtz, L., Su, D., and Jung, H. (2021). Prokaryotic Solute/Sodium Symporters: Versatile Functions and Mechanisms of a Transporter Family. *International Journal of Molecular Sciences*, 22(4):1880.

Hernández-Guzmán, M., Pérez-Hernández, V., Navarro-Noya, Y. E., Luna-Guido, M. L., Verhulst, N., Govaerts, B., and Dendooven, L. (2022). Application of ammonium to a N limited arable soil enriches a succession of bacteria typically found in the rhizosphere. *Scientific Reports*, 12:4110.

Hesse, M. A., Jordan, J. S., Vance, S. D., and Oza, A. V. (2022). Downward oxidant transport through Europa's ice shell by density-driven brine percolation. *Geophysical Research Letters*, 49(5):e2021GL095416.

Hinton Jr, A. and Ingram, K. D. (2011). Use of the agar diffusion assay to evaluate bactericidal activity of formulations of alkaline salts of fatty acids against bacteria associated with poultry processing. *Journal of Food Safety*, 31(3):357–364.

Hiscox, J. A. (2000). Outer solar system, Europa, Titan and the possibility of life. *Astronomy & Geophysics*, 41(5):5.23–5.24.

Hogenboom, D. L., Kargel, J. S., Consolmagno, G. J., Holden, T. C., Lee, L., and Buyyounouski, M. (1997). The ammonia–water system and the chemical differentiation of icy satellites. *Icarus*, 128(1):171–180.

Holler, B. J., Young, L. A., Buie, M. W., Grundy, W. M., Lyke, J. E., Young, E. F., and Roe, H. G. (2017). Measuring temperature and ammonia hydrate ice on Charon in 2015 from Keck/OSIRIS spectra. *Icarus*, 284:394–406.

Hopton, C. M., Nienow, P., and Cockell, C. S. (2025). Ammonia sets limit to life and alters physiology independently of pH in Halomonas meridiana. *Scientific Reports*, 15(1):19549.

Horie, S., Yano, S., and Watanabe, K. (1995). Intracellular alkalinization by NH_4Cl increases cytosolic Ca^{2+} level and tension in the rat aortic smooth muscle. *Life Sciences*, 56(21):1835–1843.

Hörst, S. M. (2017). Titan's atmosphere and climate. *Journal of Geophysical Research: Planets*, 122(3):432–482.

Hou, L., Zhou, Q., Wu, Q., Gu, Q., Sun, M., and Zhang, J. (2018). Spatiotemporal changes in bacterial community and microbial activity in a full-scale drinking water treatment plant. *Science of The Total Environment*, 625:449–459.

Howell, S. M. (2021). The Likely Thickness of Europa's Icy Shell. *The Planetary Science Journal*, 2(4):129.

Howell, S. M. and Pappalardo, R. T. (2020). NASA's Europa Clipper—a mission to a potentially habitable ocean world. *Nature Communications*, 11(1):1311.

Hsu, H.-W., Postberg, F., Sekine, Y., Shibuya, T., Kempf, S., Horányi, M., Juhász, A., Altobelli, N., Suzuki, K., Masaki, Y., Kuwatani, T., Tachibana, S., Sirono, S.-i., Moragas-Klostermeyer, G., and Srama, R. (2015). Ongoing hydrothermal activities within Enceladus. *Nature*, 519(7542):207–210.

Hu, J., Yan, J., Wu, L., Bao, Y., Yu, D., and Li, J. (2022). Insight into halotolerance of a robust heterotrophic nitrifying and aerobic denitrifying bacterium *Halomonas salifodinae*. *Bioresource Technology*, 351:126925.

Hu, S., He, R., He, X., Zeng, J., and Zhao, D. (2023). Niche-Specific Restructuring of Bacterial Communities Associated with Submerged Macrophyte under Ammonium Stress. *Applied and Environmental Microbiology*, 89(7):e00717–23.

Hubbard, G. S., Naderi, F. M., and Garvin, J. B. (2002). Following the water, the new program for Mars exploration. *Acta Astronautica*, 51(1):337–350.

Humayoun, S. B., Bano, N., and Hollibaugh, J. T. (2003). Depth distribution of microbial diversity in Mono Lake, a meromictic soda lake in California. *Applied and Environmental Microbiology*, 69(2):1030–1042.

Hussmann, H., Sohl, F., and Spohn, T. (2006). Subsurface oceans and deep interiors of medium-sized outer planet satellites and large trans-neptunian objects. *Icarus*, 185(1):258–273.

Idini, B. and Nimmo, F. (2024). Resonant Stratification in Titan's Global Ocean. *The Planetary Science Journal*, 5(1):15.

Inouye, S., Takizawa, T., and Yamaguchi, H. (2001). Antibacterial activity of essential oils and their major constituents against respiratory tract pathogens by gaseous contact. *Journal of Antimicrobial Chemotherapy*, 47(5):565–573.

Irwin, P. G. J., Hill, S. M., Fletcher, L. N., Alexander, C., and Rogers, J. H. (2025). Clouds and ammonia in the atmospheres of Jupiter and Saturn determined from a band-depth analysis of VLT/MUSE observations. *Journal of Geophysical Research: Planets*, 130(1):e2024JE008622.

Jahns, T. (1996). Ammonium/urea-dependent generation of a proton electrochemical potential and synthesis of ATP in *Bacillus pasteurii*. *Journal of Bacteriology*, 178(2):403–409.

Jennings, D. E., Tokano, T., Cottini, V., Nixon, C. A., Achterberg, R. K., Flasar, F. M., Kunde, V. G., Romani, P. N., Samuelson, R. E., Segura, M. E., Gorius, N. J. P., Guandique, E., Kaelberer, M. S., and Coustenis, A. (2019). Titan surface temperatures during the Cassini mission. *The Astrophysical Journal Letters*, 877(1):L8.

Jeong, H., Park, J., and Kim, H. (2013). Determination of NH_4^+ in environmental water with interfering substances using the modified nessler method. *Journal of Chemistry*, 2013:e359217.

Ji, B., Yang, K., Zhu, L., Jiang, Y., Wang, H., Zhou, J., and Zhang, H. (2015). Aerobic denitrification: A review of important advances of the last 30 years. *Biotechnology and Bioprocess Engineering*, 20(4):643–651.

Jiao, S., Liu, Z., Lin, Y., Yang, J., Chen, W., and Wei, G. (2016). Bacterial communities in oil contaminated soils: Biogeography and co-occurrence patterns. *Soil Biology and Biochemistry*, 98:64–73.

Johnson, M. L. and Nicol, M. (1987). The ammonia-water phase diagram and its implications for icy satellites. *Journal of Geophysical Research: Solid Earth*, 92(B7):6339–6349.

Johnson, P. V., Hodyss, R., Vu, T. H., and Choukroun, M. (2019). Insights into Europa's ocean composition derived from its surface expression. *Icarus*, 321:857–865.

Johnson, R., Vishwakarma, K., Hossen, M. S., Kumar, V., Shackira, A. M., Puthur, J. T., Abdi, G., Sarraf, M., and Hasanuzzaman, M. (2022). Potassium in plants: Growth regulation, signaling, and environmental stress tolerance. *Plant Physiology and Biochemistry*, 172:56–69.

Jolivet-Gougeon, A. and Bonnaure-Mallet, M. (2014). Biofilms as a mechanism of bacterial resistance. *Drug Discovery Today: Technologies*, 11:49–56.

Journaux, B., Kalousová, K., Sotin, C., Tobie, G., Vance, S., Saur, J., Bollengier, O., Noack, L., Rückriemen-Bez, T., Van Hoolst, T., Soderlund, K. M., and Brown, J. M. (2020). Large ocean worlds with high-pressure ices. *Space Science Reviews*, 216(1):7.

Jurcă, A. D., Jurcă, M. C., Bembea, M., Kozma, K., Budişteanu, M., and Gug, C. (2018). Clinical and genetic diversity of congenital hyperammonemia. *Romanian Journal of Morphology and Embryology = Revue Roumaine De Morphologie Et Embryologie*, 59(3):945–948.

Kanamori, K., Weiss, R. L., and Roberts, J. D. (1987a). Ammonia assimilation in Bacillus polymyxa. 15N NMR and enzymatic studies. *Journal of Biological Chemistry*, 262(23):11038–11045.

Kanamori, K., Weiss, R. L., and Roberts, J. D. (1987b). Role of glutamate dehydrogenase in ammonia assimilation in nitrogen-fixing *Bacillus macerans*. *Journal of Bacteriology*, 169(10):4692–4695.

Kargel, J. S. (1991). Brine volcanism and the interior structures of asteroids and icy satellites. *Icarus*, 94(2):368–390.

Kargel, J. S. (1992). Ammonia-water volcanism on icy satellites: Phase relations at 1 atmosphere. *Icarus*, 100(2):556–574.

Kargel, J. S., Kaye, J. Z., Head, J. W., Marion, G. M., Sassen, R., Crowley, J. K., Ballesteros, O. P., Grant, S. A., and Hogenboom, D. L. (2000). Europa's crust and ocean: Origin, composition, and the prospects for life. *Icarus*, 148(1):226–265.

Kato, S., Sasaki, K., Watanabe, K., Yumoto, I., and Kamagata, Y. (2014). Physiological and Transcriptomic Analyses of the Thermophilic, Aceticlastic Methanogen *Methanosaeta thermophila* Responding to Ammonia Stress. *Microbes and Environments*, 29(2):162–167.

Kaye, J. Z. and Baross, J. A. (2004). Synchronous effects of temperature, hydrostatic pressure, and salinity on growth, phospholipid profiles, and protein patterns of four *Halomonas* species isolated from deep-sea hydrothermal-vent and sea surface environments. *Applied and Environmental Microbiology*.

Kaye, J. Z., Márquez, M. C., Ventosa, A., and Baross, J. A. . (2004). *Halomonas Neptunia* sp. nov., *Halomonas sulfidaeris* sp. nov., *Halomonas axialensis* sp. nov. and *Halomonas hydrothermalis* sp. nov.: Halophilic bacteria isolated from deep-sea hydrothermal-vent environments. *International Journal of Systematic and Evolutionary Microbiology*, 54(2):499–511.

Keller, M. R. and Dörr, T. (2023). Bacterial metabolism and susceptibility to cell wall-active antibiotics. *Advances in microbial physiology*, 83:181–219.

Kelly, L. C., Cockell, C. S., and Summers, S. (2012). Diverse microbial species survive high ammonia concentrations. *International Journal of Astrobiology*, 11(2):125–131.

Khawaja, N., Postberg, F., Hillier, J., Klenner, F., Kempf, S., Nölle, L., Reviol, R., Zou, Z., and Srama, R. (2019). Low-mass nitrogen-, oxygen-bearing, and aromatic compounds in Enceladean ice grains. *Monthly Notices of the Royal Astronomical Society*, 489(4):5231–5243.

Khurana, K. K., Kivelson, M. G., Stevenson, D. J., Schubert, G., Russell, C. T., Walker, R. J., and Polanskey, C. (1998). Induced magnetic fields as evidence for subsurface oceans in Europa and Callisto. *Nature*, 395(6704):777–780.

Kilic, V., Kilic, G. A., Kutlu, H. M., and Martínez-Espinosa, R. M. (2017). Nitrate reduction in *Haloferax alexandrinus*: The case of assimilatory nitrate reductase. *Extremophiles*, 21(3):551–561.

Kim, M., Zhang, Z., Okano, H., Yan, D., Groisman, A., and Hwa, T. (2012). Need-based activation of ammonium uptake in *Escherichia coli*. *Molecular Systems Biology*, 8:616.

Kivelson, M. G., Khurana, K. K., and Volwerk, M. (2002). The permanent and inductive magnetic moments of Ganymede. *Icarus*, 157(2):507–522.

Kleiner, D. (1981). The transport of NH_3 and NH_4^+ across biological membranes. *Biochimica et Biophysica Acta (BBA) - Reviews on Bioenergetics*, 639(1):41–52.

Klenner, F., Bönigk, J., Napoleoni, M., Hillier, J., Khawaja, N., Olsson-Francis, K., Cable, M. L., Malaska, M. J., Kempf, S., Abel, B., and Postberg, F. (2024). How to identify cell material in a single ice grain emitted from Enceladus or Europa. *Science Advances*, 10(12):eadl0849.

Kong, L., Sun, M., Wang, F., Liu, J., Feng, B., Si, J., Zhang, B., Li, S., and Li, H. (2014). Effects of high NH_4^+ on K^+ uptake, culm mechanical strength and grain filling in wheat. *Frontiers in Plant Science*, 5.

Koops, H.-P. and Pommerening-Röser, A. (2001). Distribution and ecophysiology of the nitrifying bacteria emphasizing cultured species. *FEMS Microbiology Ecology*, 37(1):1–9.

Koops, H.-P., Purkhold, U., Pommerening-Röser, A., Timmermann, G., and Wagner, M. (2006). The lithoautotrophic ammonia-oxidizing bacteria. In Dworkin, M., Falkow, S., Rosenberg, E., Schleifer, K.-H., and Stackebrandt, E., editors, *The Prokaryotes: Volume 5: Proteobacteria: Alpha and Beta Subclasses*, pages 778–811. Springer, New York, NY.

Krupa, S. V. (2003). Effects of atmospheric ammonia (NH_3) on terrestrial vegetation: A review. *Environmental Pollution*, 124(2):179–221.

Kuiper, G. P. (1944). Titan: A satellite with an atmosphere. *The Astrophysical Journal*, 100:378.

Kunde, V. G., Aikin, A. C., Hanel, R. A., Jennings, D. E., Maguire, W. C., and Samuelson, R. E. (1981). C_4H_2, HC_3N and C_2N_2 in Titan's atmosphere. *Nature*, 292(5825):686–688.

Ladd, J. N. and Jackson, R. B. (1982). Biochemistry of ammonification. In *Nitrogen in Agricultural Soils*, pages 173–228. John Wiley & Sons, Ltd.

Lane, N. and Martin, W. F. (2012). The Origin of Membrane Bioenergetics. *Cell*, 151(7):1406–1416.

Leejeerajumnean, A., Ames, J., and Owens, J. (2000). Effect of ammonia on the growth of *Bacillus* species and some other bacteria. *Letters in Applied Microbiology*, 30(5):385–389.

Leitner, M. A. and Lunine, J. I. (2019). Modeling early Titan's ocean composition. *Icarus*, 333:61–70.

Leliwa-Kopystyński, J., Maruyama, M., and Nakajima, T. (2002). The water–ammonia phase diagram up to 300 MPa: Application to icy satellites. *Icarus*, 159(2):518–528.

Lellouch, E., Coustenis, A., Gautier, D., Raulin, F., Dubouloz, N., and Frère, C. (1989). Titan's atmosphere and hypothesized ocean: A reanalysis of the Voyager 1 radio-occultation and IRIS 7.7-μm data. *Icarus*, 79(2):328–349.

Leon, M. P. D., Montecillo, A. D., Pinili, D. S., Siringan, M. A. T., and Park, D.-S. (2018). Bacterial diversity of bat guano from Cabalyorisa Cave, Mabini, Pangasinan, Philippines: A first report on the metagenome of Philippine bat guano. *PLOS One*, 13(7):e0200095.

Levin, S. M., Zhang, Z., Bolton, S. J., Brown, S., Ermakov, A. I., Feng, J., Hand, K., Misra, S., Siegler, M., Stevenson, D., McKinnon, W., and Akiba, R. (2026). Europa's ice thickness and subsurface structure characterized by the Juno microwave radiometer. *Nature Astronomy*, 10(1):84–91.

Levinson, A. A. and Taylor, S. R. (1971). *Moon Rocks and Minerals: Scientific Results of the Study of the Apollo 11 Lunar Samples with Preliminary Data on Apollo 12 Samples*. Pergamon Press, New York.

Lewis, J. S. (1971). Satellites of the outer planets: Their physical and chemical nature. *Icarus*, 15(2):174–185.

Leytem, A. B., Walker, J. T., Wu, Z., Nouwakpo, K., Baublitz, C., Bash, J., and Beachley, G. (2024). Spatial distribution of ammonia concentrations and modeled dry deposition in an intensive dairy production region. *Atmosphere*, 15(1):15.

Li, S.-X., Wang, Z.-H., and Stewart, B. A. (2013). Chapter five - responses of crop plants to ammonium and nitrate N. In Sparks, D. L., editor, *Advances in Agronomy*, volume 118 of *Advances in Agronomy*, pages 205–397. Academic Press.

Liu, D., Chau, Y. K., and Dutka, B. J. (1989). Rapid toxicity assessment of water-soluble and water-insoluble chemicals using a modified agar plate method. *Water Research*, 23(3):333–339.

Lizotte, M. P. (2003). The microbiology of sea ice. In *Sea Ice: An Introduction to Its Physics, Chemistry, Biology and Geology*, chapter 6, pages 184–210. John Wiley & Sons, Ltd.

Lô, S., Dohmen, W., Heederik, D., Weijers, E., van Schothorst, I., Bleeker, A., Vermeulen, R., and Hoek, G. (2025). Spatial and temporal variability of atmospheric ammonia using a dense network in an area with livestock, residential and natural environments intertwined. *Atmospheric Environment*, page 121394.

Loose, B., Miller, L. A., Elliott, S., and Papakyriakou, T. (2011). Sea ice biogeochemistry and material transport across the frozen interface. *Oceanography*, 24(3):202–218.

Lopes, R. M. C., Mitchell, K. L., Stofan, E. R., Lunine, J. I., Lorenz, R., Paganelli, F., Kirk, R. L., Wood, C. A., Wall, S. D., Robshaw, L. E., Fortes, A. D., Neish, C. D., Radebaugh, J., Reffet, E., Ostro, S. J., Elachi, C., Allison, M. D., Anderson, Y., Boehmer, R., Boubin, G., Callahan, P., Encrenaz, P., Flamini, E., Francescetti, G., Gim, Y., Hamilton, G., Hensley, S., Janssen, M. A., Johnson, W. T. K., Kelleher, K., Muhleman, D. O., Ori, G., Orosei, R., Picardi, G., Posa, F., Roth, L. E., Seu, R., Shaffer, S., Soderblom, L. A., Stiles, B., Vetrella, S., West, R. D., Wye, L., and Zebker, H. A. (2007). Cryovolcanic features on Titan's surface as revealed by the Cassini Titan Radar Mapper. *Icarus*, 186(2):395–412.

Lorenz, R. D., Stiles, B. W., Kirk, R. L., Allison, M. D., Del Marmo, P. P., Iess, L., Lunine, J. I., Ostro, S. J., and Hensley, S. (2008). Titan's rotation reveals an internal ocean and changing zonal winds. *Science*, 319(5870):1649–1651.

Lorenz, R. D., Turtle, E. P., Barnes, J. W., and Trainer, M. G. (2018). Dragonfly: A rotorcraft lander concept for scientific exploration at Titan. *Johns Hopkins APL Technical Digest*, 34(3):14.

Lowe, C. U., Rees, M. W., and Markham, R. (1963). Synthesis of complex organic compounds from simple precursors: Formation of amino-acids, amino-acid polymers, fatty acids and purines from ammonium cyanide. *Nature*, 199(4890):219–222.

Lu, S., Liu, X., Liu, C., Cheng, G., Zhou, R., and Li, Y. (2021). A Review of Ammonia-Oxidizing Archaea and Anaerobic Ammonia-Oxidizing Bacteria in the Aquaculture Pond Environment in China. *Frontiers in Microbiology*, 12.

Lucchetti, A., Pozzobon, R., Mazzarini, F., Cremonese, G., and Massironi, M. (2017). Brittle ice shell thickness of Enceladus from fracture distribution analysis. *Icarus*, 297:252–264.

Ludwig, H. (2022). Seawater: Composition and properties. In Ludwig, H., editor, *Reverse Osmosis Seawater Desalination Volume 1: Planning, Process Design and Engineering – A Manual for Study and Practice*, pages 73–203. Springer International Publishing, Cham.

Lunine, J. I. and Stevenson, D. J. (1987). Clathrate and ammonia hydrates at high pressure: Application to the origin of methane on Titan. *Icarus*, 70(1):61–77.

Luo, Z., Zhang, Y., Chen, W., Van Damme, M., Coheur, P.-F., and Clarisse, L. (2022). Estimating global ammonia (NH_3) emissions based on IASI observations from 2008 to 2018. *Atmospheric Chemistry and Physics*, 22(15):10375–10388.

MacKenzie, S. M., Neveu, M., Davila, A. F., Lunine, J. I., Craft, K. L., Cable, M. L., Phillips-Lander, C. M., Hofgartner, J. D., Eigenbrode, J. L., Waite, J. H., Glein, C. R., Gold, R., Greenauer, P. J., Kirby, K., Bradburne, C., Kounaves, S. P., Malaska, M. J., Postberg, F.,

Patterson, G. W., Porco, C., Núñez, J. I., German, C., Huber, J. A., McKay, C. P., de Vera, J.-P., Brucato, J. R., and Spilker, L. J. (2021). The Enceladus Orbilander Mission Concept: Balancing Return and Resources in the Search for Life. *The Planetary Science Journal*, 2(2):77.

Maguire, W. C., Hanel, R. A., Jennings, D. E., Kunde, V. G., and Samuelson, R. E. (1981). C_3H_8 and C_3H_4 in Titan's atmosphere. *Nature*, 292(5825):683–686.

Maranger, R., Bird, D. F., and Juniper, S. K. (1994). Viral and bacterial dynamics in Arctic sea ice during the spring algal bloom near Resolute, N.W.T., Canada. *Marine Ecology Progress Series*, 111(1/2):121–127.

Marion, G. M., Fritsen, C. H., Eicken, H., and Payne, M. C. (2003). The search for life on Europa: Limiting environmental factors, potential habitats, and earth analogues. *Astrobiology*, 3(4):785–811.

Marion, G. M., Kargel, J. S., Catling, D. C., and Lunine, J. I. (2012). Modeling ammonia–ammonium aqueous chemistries in the Solar System's icy bodies. *Icarus*, 220(2):932–946.

Martin, A. and McMinn, A. (2018). Sea ice, extremophiles and life on extra-terrestrial ocean worlds. *International Journal of Astrobiology*, 17(1):1–16.

Martin, W., Baross, J., Kelley, D., and Russell, M. J. (2008). Hydrothermal vents and the origin of life. *Nature Reviews Microbiology*, 6(11):805–814.

Martin, W. and Russell, M. J. (2006). On the origin of biochemistry at an alkaline hydrothermal vent. *Philosophical Transactions of the Royal Society B: Biological Sciences*, 362(1486):1887–1926.

Matson, D. L., Castillo, J. C., Lunine, J., and Johnson, T. V. (2007). Enceladus' plume: Compositional evidence for a hot interior. *Icarus*, 187(2):569–573.

Matson, D. L., Castillo-Rogez, J. C., Davies, A. G., and Johnson, T. V. (2012). Enceladus: A hypothesis for bringing both heat and chemicals to the surface. *Icarus*, 221(1):53–62.

Matthews, D. A., Effler, S. W., and Matthews, C. M. (2000). Ammonia and toxicity criteria in polluted Onondaga Lake, New York. *Water Environment Research*, 72(6):731–741.

McCord, T. B., Hansen, G. B., Clark, R. N., Martin, P. D., Hibbitts, C. A., Fanale, F. P., Granahan, J. C., Segura, M., Matson, D. L., Johnson, T. V., Carlson, R. W., Smythe, W. D., and Danielson, G. E. (1998). Non-water-ice constituents in the surface material of the icy Galilean satellites from the Galileo near-infrared mapping spectrometer investigation. *Journal of Geophysical Research: Planets*, 103(E4):8603–8626.

McFarlane, D. A., Keeler, R. C., and Mizutani, H. (1995). Ammonia volatilization in a Mexican bat cave ecosystem. *Biogeochemistry*, 30(1):1–8.

McKay, C. P. (2016). Titan as the abode of life. *Life*, 6(1):8.

McKay, C. P., Porco, C. C., Altheide, T., Davis, W. L., and Kral, T. A. (2008). The possible origin and persistence of life on Enceladus and detection of biomarkers in the plume. *Astrobiology*, 8(5):909–919.

McKay, C. P. and Smith, H. D. (2005). Possibilities for methanogenic life in liquid methane on the surface of Titan. *Icarus*, 178(1):274–276.

McLean, R. M. and Wang, N. X. (2021). Potassium. In Eskin, N. A. M., editor, *Advances in Food and Nutrition Research*, volume 96 of *The Latest Research and Development of Minerals in Human Nutrition*, pages 89–121. Academic Press.

Meier, R., Eberhardt, P., Krankowsky, D., and Hodges, R. R. (1994). Ammonia in comet P/Halley. *Astronomy and Astrophysics*, 287:268–278.

Meinzer, M., Ahmad, N., and Nielsen, B. L. (2023). Halophilic plant-associated bacteria with plant-growth-promoting potential. *Microorganisms*, 11(12):2910.

Melosh, H. J., Ekholm, A. G., Showman, A. P., and Lorenz, R. D. (2004). The temperature of Europa's subsurface water ocean. *Icarus*, 168(2):498–502.

Melwani Daswani, M., Vance, S. D., Mayne, M. J., and Glein, C. R. (2021). A Metamorphic Origin for Europa's Ocean. *Geophysical Research Letters*, 48(18):e2021GL094143.

Mendes, S. S., Miranda, V., and Saraiva, L. M. (2021). Hydrogen sulfide and carbon monoxide tolerance in bacteria. *Antioxidants*, 10(5):729.

Mermy, G. C., Schmidt, F., Andrieu, F., Cornet, T., Belgacem, I., and Altobelli, N. (2023). Selection of chemical species for Europa's surface using Galileo/NIMS. *Icarus*, 394:115379.

Miflin, B. J. and Lea, P. J. (1982). Ammonia assimilation and amino acid metabolism. In Boulter, D. and Parthier, B., editors, *Nucleic Acids and Proteins in Plants I: Structure, Biochemistry and Physiology of Proteins*, Encyclopedia of Plant Physiology, pages 5–64. Springer, Berlin, Heidelberg.

Miller, S. L. (1955). Production of Some Organic Compounds under Possible Primitive Earth Conditions[1]. *Journal of the American Chemical Society*, 77(9):2351–2361.

Mills, E. A. C. and Morris, M. R. (2013). Detection of widespread hot ammonia in the galactic center. *The Astrophysical Journal*, 772(2):105.

Mitri, G., Meriggiola, R., Hayes, A., Lefevre, A., Tobie, G., Genova, A., Lunine, J. I., and Zebker, H. (2014). Shape, topography, gravity anomalies and tidal deformation of Titan. *Icarus*, 236:169–177.

Mitri, G., Showman, A. P., Lunine, J. I., and Lopes, R. M. C. (2008). Resurfacing of Titan by ammonia-water cryomagma. *Icarus*, 196(1):216–224.

Moeckel, C., de Pater, I., and DeBoer, D. (2023). Ammonia abundance derived from Juno MWR and VLA observations of Jupiter. *The Planetary Science Journal*, 4(2):25.

Molton, P. and Ponnamperuma, C. (1972). Survival of common terrestrial microorganisms under simulated Jovian conditions. *Nature*, 238(5361):217–218.

Monnard, P.-A. and Walde, P. (2015). Current ideas about prebiological compartmentalization. *Life*, 5(2):1239–1263.

Moriwaki, T., Terawaki, S., and Otomo, T. (2024). Impaired lysosomal acidity maintenance in acid lipase-deficient cells leads to defective autophagy. *The Journal of Biological Chemistry*, 300(3):105743.

Moser, H. (1987). Electrophysiological evidence for ammonium as a substitute for potassium in activating the sodium pump in a crayfish sensory neuron. *Canadian Journal of Physiology and Pharmacology*, 65(2):141–145.

Moulanier, A. A., Mousis, O., Bouquet, A., and Glein, C. R. (2025). The Role of Ammonia in the Distribution of Volatiles in the Primordial Hydrosphere of Europa. *The Planetary Science Journal*, 6(1):1.

Mousis, O. and Alibert, Y. (2006). Modeling the Jovian subnebula - II. Composition of regular satellite ices. *Astronomy & Astrophysics*, 448(2):771–778.

Mousis, O. and Gautier, D. (2004). Constraints on the presence of volatiles in Ganymede and Callisto from an evolutionary turbulent model of the Jovian subnebula. *Planetary and Space Science*, 52(5):361–370.

Mousis, O., Lunine, J. I., Thomas, C., Pasek, M., Marbœuf, U., Alibert, Y., Ballenegger, V., Cordier, D., Ellinger, Y., Pauzat, F., and Picaud, S. (2009). Clathration of volatiles in the solar nebula and implications for the origin of Titan's atmosphere. *The Astrophysical Journal*, 691(2):1780.

Mousis, O., Pargamin, J., Grasset, O., and Sotin, C. (2002). Experiments in the NH_3-H_2O system in the [0, 1 GPa] pressure range - implications for the deep liquid layer of large icy satellites. *Geophysical Research Letters*, 29(24):45–1–45–4.

Muñoz-Iglesias, V. and Prieto-Ballesteros, O. (2021). Thermal properties of the H_2O–CO_2–Na_2CO_3/CH_3OH/NH_3 systems at low temperatures and pressures up to 50 MPa. *ACS Earth and Space Chemistry*, 5(10):2626–2637.

Mueller, D. R., Vincent, W. F., Bonilla, S., and Laurion, I. (2005). Extremotrophs, extremophiles and broadband pigmentation strategies in a high arctic ice shelf ecosystem. *FEMS Microbiology Ecology*, 53(1):73–87.

Mueller, E. A. and Levin, P. A. (2020). Bacterial Cell Wall Quality Control during Environmental Stress. *mBio*, 11(5):e02456–20.

Müller, T., Walter, B., Wirtz, A., and Burkovski, A. (2006). Ammonium toxicity in bacteria. *Current Microbiology*, 52(5):400–406.

Mullin, J. W., Chakraborty, M., and Mehta, K. (1970). Nucleation and growth of ammonium sulphate crystals from aqueous solution. *Journal of Applied Chemistry*, 20(12):367–371.

Murray, A. E., Kenig, F., Fritsen, C. H., McKay, C. P., Cawley, K. M., Edwards, R., Kuhn, E., McKnight, D. M., Ostrom, N. E., Peng, V., Ponce, A., Priscu, J. C., Samarkin, V., Townsend, A. T., Wagh, P., Young, S. A., Yung, P. T., and Doran, P. T. (2012). Microbial life at minus 13 °C in the brine of an ice-sealed Antarctic lake. *Proceedings of the National Academy of Sciences*, 109(50):20626–20631.

Nagatani, H., Shimizu, M., and Valentine, R. C. (1971). The mechanism of ammonia assimilation in nitrogen fixing bacteria. *Archiv für Mikrobiologie*, 79(2):164–175.

Nathues, A., Hoffmann, M., Schmedemann, N., Sarkar, R., Thangjam, G., Mengel, K., Hernandez, J., Hiesinger, H., and Pasckert, J. H. (2022). Brine residues and organics in the Urvara basin on Ceres. *Nature Communications*, 13(1):927.

Neijssel, O. M., Buurman, E. T., and de Mattos, M. J. T. (1990). The role of futile cycles in the energetics of bacterial growth. *Biochimica et Biophysica Acta (BBA) - Bioenergetics*, 1018(2):252–255.

Neish, C. D., Somogyi, Á., Lunine, J. I., and Smith, M. A. (2009). Low temperature hydrolysis of laboratory tholins in ammonia-water solutions: Implications for prebiotic chemistry on Titan. *Icarus*, 201(1):412–421.

Neish, C. D., Somogyi, Á., and Smith, M. A. (2010). Titan's primordial soup: Formation of amino acids via low-temperature hydrolysis of tholins. *Astrobiology*, 10(3):337–347.

Nelson, R. M., Kamp, L. W., Matson, D. L., Irwin, P. G. J., Baines, K. H., Boryta, M. D., Leader, F. E., Jaumann, R., Smythe, W. D., Sotin, C., Clark, R. N., Cruikshank, D. P., Drossart, P., Pearl, J. C., Hapke, B. W., Lunine, J., Combes, M., Bellucci, G., Bibring, J. P., Capaccioni, F., Cerroni, P., Coradini, A., Formisano, V., Filacchione, G., Langevin, R. Y., McCord, T. B., Mennella, V., Nicholson, P. D., and Sicardy, B. (2009). Saturn's Titan: Surface change, ammonia, and implications for atmospheric and tectonic activity. *Icarus*, 199(2):429–441.

Neuhausen, B. S. and Patrick, W. A. (1921). A Study of the System Ammonia–Water as a Basis for a Theory of the Solution of Gases in Liquids. *The Journal of Physical Chemistry*, 25(9):693–720.

Neveu, M., Anbar, A. D., Davila, A. F., Glavin, D. P., MacKenzie, S. M., Phillips-Lander, C. M., Sherwood, B., Takano, Y., Williams, P., and Yano, H. (2020). Returning samples from Enceladus for life detection. *Frontiers in Astronomy and Space Sciences*, 7.

Newman, M. M., Kloepper, L. N., Duncan, M., McInroy, J. A., and Kloepper, J. W. (2018). Variation in Bat Guano Bacterial Community Composition With Depth. *Frontiers in Microbiology*, 9.

Niemann, H. B., Atreya, S. K., Bauer, S. J., Carignan, G. R., Demick, J. E., Frost, R. L., Gautier, D., Haberman, J. A., Harpold, D. N., Hunten, D. M., Israel, G., Lunine, J. I., Kasprzak, W. T., Owen, T. C., Paulkovich, M., Raulin, F., Raaen, E., and Way, S. H. (2005). The abundances of constituents of Titan's atmosphere from the GCMS instrument on the Huygens probe. *Nature*, 438(7069):779–784.

Nimmo, F. and Bills, B. G. (2010). Shell thickness variations and the long-wavelength topography of Titan. *Icarus*, 208(2):896–904.

Nimmo, F., Hamilton, D. P., McKinnon, W. B., Schenk, P. M., Binzel, R. P., Bierson, C. J., Beyer, R. A., Moore, J. M., Stern, S. A., Weaver, H. A., Olkin, C. B., Young, L. A., and Smith, K. E. (2016). Reorientation of Sputnik Planitia implies a subsurface ocean on Pluto. *Nature*, 540(7631):94–96.

Nimmo, F. and Pappalardo, R. T. (2016). Ocean worlds in the outer solar system. *Journal of Geophysical Research: Planets*, 121(8):1378–1399.

Nimmo, F., Spencer, J. R., Pappalardo, R. T., and Mullen, M. E. (2007). Shear heating as the origin of the plumes and heat flux on Enceladus. *Nature*, 447(7142):289–291.

Nishizawa, M., Saito, T., Makabe, A., Ueda, H., Saitoh, M., Shibuya, T., and Takai, K. (2021). Stable abiotic production of ammonia from nitrate in komatiite-hosted hydrothermal systems in the Hadean and Archean oceans. *Minerals*, 11(3):321.

Nixon, C. A. (2024). The composition and chemistry of Titan's atmosphere. *ACS Earth and Space Chemistry*, 8(3):406–456.

Owen, T. C. (2000). On the origin of Titan's atmosphere. *Planetary and Space Science*, 48(7):747–752.

Palmer, P., Wootten, A., Butler, B., Bockelee-Morvan, D., Crovisier, J., Despois, D., and Yeomans, D. K. (1996). Comet Hyakutake: First secure detection of ammonia in a comet. In *American Astronomical Society, 188th AAS Meeting*, volume 28, page 927.

Paoli, L., Benesperi, R., Proietti Pannunzi, D., Corsini, A., and Loppi, S. (2014). Biological effects of ammonia released from a composting plant assessed with lichens. *Environmental Science and Pollution Research*, 21(9):5861–5872.

Pappalardo, R. T., Head, J. W., Greeley, R., Sullivan, R. J., Pilcher, C., Schubert, G., Moore, W. B., Carr, M. H., Moore, J. M., Belton, M. J. S., and Goldsby, D. L. (1998). Geological evidence for solid-state convection in Europa's ice shell. *Nature*, 391(6665):365–368.

Parker, C. W., Vu, T. H., Kim, T., and Johnson, P. V. (2023). Vitreous magnesium sulfate hydrate as a potential mechanism for preservation of microbial viability on Europa. *The Planetary Science Journal*, 4(9):178.

Pasek, M. A. and Greenberg, R. (2012). Acidification of Europa's Subsurface Ocean as a Consequence of Oxidant Delivery. *Astrobiology*, 12(2):151–159.

Peleg, M. (2022). Models of the water activity effect on microbial growth rate and initiation. *Applied Microbiology and Biotechnology*, 106(4):1375–1382.

Pikuta, E. V., Hoover, R. B., and Tang, J. (2007). Microbial extremophiles at the limits of life. *Critical Reviews in Microbiology*, 33(3):183–209.

Pinder, R. W., Gilliland, A. B., and Dennis, R. L. (2008). Environmental impact of atmospheric NH_3 emissions under present and future conditions in the eastern United States. *Geophysical Research Letters*, 35(12).

Pizzarello, S., Williams, L., Lehman, J., Holland, G., and Yarger, J. (2011). Abundant ammonia in primitive asteroids and the case for a possible exobiology. *PNAS*, 108(11):4303–4306.

Poch, O., Istiqomah, I., Quirico, E., Beck, P., Schmitt, B., Theulé, P., Faure, A., Hily-Blant, P., Bonal, L., Raponi, A., Ciarniello, M., Rousseau, B., Potin, S., Brissaud, O., Flandinet, L., Filacchione, G., Pommerol, A., Thomas, N., Kappel, D., Mennella, V., Moroz, L.,

Vinogradoff, V., Arnold, G., Erard, S., Bockelée-Morvan, D., Leyrat, C., Capaccioni, F., De Sanctis, M. C., Longobardo, A., Mancarella, F., Palomba, E., and Tosi, F. (2020). Ammonium salts are a reservoir of nitrogen on a cometary nucleus and possibly on some asteroids. *Science*, 367(6483):eaaw7462.

Poggiali, V., Brighi, G., Hayes, A. G., Nicholson, P. D., MacKenzie, S., Lalich, D. E., Bonnefoy, L. E., Oudrhiri, K., Lorenz, R. D., Soderblom, J. M., Tortora, P., and Zannoni, M. (2024). Surface properties of the seas of Titan as revealed by Cassini mission bistatic radar experiments. *Nature Communications*, 15(1):5454.

Porco, C. C., Helfenstein, P., Thomas, P. C., Ingersoll, A. P., Wisdom, J., West, R., Neukum, G., Denk, T., Wagner, R., Roatsch, T., Kieffer, S., Turtle, E., McEwen, A., Johnson, T. V., Rathbun, J., Veverka, J., Wilson, D., Perry, J., Spitale, J., Brahic, A., Burns, J. A., DelGenio, A. D., Dones, L., Murray, C. D., and Squyres, S. (2006). Cassini observes the active south pole of enceladus. *Science*, 311(5766):1393–1401.

Porter, N., Drozd, J. W., and Linton, J. D. (1983). The effects of cyanide on the growth and respiration of *Enterobacter aerogenes* in continuous culture. *Microbiology*, 129(1):7–16.

Postberg, F., Kempf, S., Schmidt, J., Brilliantov, N., Beinsen, A., Abel, B., Buck, U., and Srama, R. (2009). Sodium salts in E-ring ice grains from an ocean below the surface of Enceladus. *Nature*, 459(7250):1098–1101.

Postberg, F., Khawaja, N., Abel, B., Choblet, G., Glein, C. R., Gudipati, M. S., Henderson, B. L., Hsu, H. W., Kempf, S., Klenner, F., Moragas-Klostermeyer, G., Magee, B., Nölle, L., Perry, M., Reviol, R., Schmidt, J., Srama, R., Stolz, F., Tobie, G., Trieloff, M., and Waite, J. H. (2018). Macromolecular organic compounds from the depths of Enceladus. *Nature*, 558(7711):564–568.

Postberg, F., Schmidt, J., Hillier, J., Kempf, S., and Srama, R. (2011). A salt-water reservoir as the source of a compositionally stratified plume on Enceladus. *Nature*, 474(7353):620–622.

Postberg, F., Sekine, Y., Klenner, F., Glein, C. R., Zou, Z., Abel, B., Furuya, K., Hillier, J. K., Khawaja, N., Kempf, S., Noelle, L., Saito, T., Schmidt, J., Shibuya, T., Srama, R., and Tan, S. (2023). Detection of phosphates originating from Enceladus's ocean. *Nature*, 618(7965):489–493.

Poulet, F., Piccioni, G., Langevin, Y., Dumesnil, C., Tommasi, L., Carlier, V., Filacchione, G., Amoroso, M., Arondel, A., D'Aversa, E., Barbis, A., Bini, A., Bolsée, D., Bousquet, P., Caprini, C., Carter, J., Dubois, J.-P., Condamin, M., Couturier, S., Dassas, K., Dexet, M., Fletcher, L., Grassi, D., Guerri, I., Haffoud, P., Larigauderie, C., Le Du, M., Mugnuolo, R., Pilato, G., Rossi, M., Stefani, S., Tosi, F., Vincendon, M., Zambelli, M., Arnold, G., Bibring, J.-P., Biondi, D., Boccaccini, A., Brunetto, R., Carapelle, A., Cisneros González, M., Hannou, C., Karatekin, O., Le Cle'ch, J.-C., Leyrat, C., Migliorini, A., Nathues, A., Rodriguez, S., Saggin, B., Sanchez-Lavega, A., Schmitt, B., Seignovert, B., Sordini, R., Stephan, K., Tobie, G., Zambon, F., Adriani, A., Altieri, F., Bockelée, D., Capaccioni, F., De Angelis, S., De Sanctis, M.-C., Drossart, P., Fouchet, T., Gérard, J.-C., Grodent, D., Ignatiev, N., Irwin, P., Ligier, N., Manaud, N., Mangold, N., Mura, A., Pilorget, C., Quirico, E., Renotte, E., Strazzulla, G., Turrini, D., Vandaele, A.-C., Carli, C., Ciarniello, M., Guerlet,

S., Lellouch, E., Mancarella, F., Morbidelli, A., Le Mouélic, S., Raponi, A., Sindoni, G., and Snels, M. (2024). Moons and Jupiter Imaging Spectrometer (MAJIS) on Jupiter Icy Moons Explorer (JUICE). *Space Science Reviews*, 220(3):27.

Powlson, D. S. and Dawson, C. J. (2022). Use of ammonium sulphate as a sulphur fertilizer: Implications for ammonia volatilization. *Soil Use and Management*, 38(1):622–634.

Qian, P.-Y., Cheng, A., Wang, R., and Zhang, R. (2022). Marine biofilms: Diversity, interactions and biofouling. *Nature Reviews. Microbiology*, 20(11):671–684.

Qian, W., Peng, Y., Li, X., Zhang, Q., and Ma, B. (2017). The inhibitory effects of free ammonia on ammonia oxidizing bacteria and nitrite oxidizing bacteria under anaerobic condition. *Bioresource Technology*, 243:1247–1250.

Radebaugh, J., Lorenz, R. D., Kirk, R. L., Lunine, J. I., Stofan, E. R., Lopes, R. M. C., and Wall, S. D. (2007). Mountains on Titan observed by Cassini Radar. *Icarus*, 192(1):77–91.

Raeispour Shirazi, A., Yang, F., Ngo, T. D., Bernard, O., Simonin, J.-P., and de Hemptinne, J.-C. (2025). Improved ion-pairing equation of state and its use for various property calculations. *Fluid Phase Equilibria*, 595:114396.

Rajta, A., Bhatia, R., Setia, H., and Pathania, P. (2020). Role of heterotrophic aerobic denitrifying bacteria in nitrate removal from wastewater. *Journal of Applied Microbiology*, 128(5):1261–1278.

Ramirez, M., Fernandez, R., and Malnic, G. (1999). Permeation of NH_3/NH_4^+ and cell pH in colonic crypts of the rat. *Pflügers Archiv*, 438(4):508–515.

Ramkissoon, N. K., Fox-Powell, M. G., Sym, L., Suttle, M. D., Del Moral, A., and Pearson, V. K. (2025). Accreted volatiles influence low-temperature rock equilibria on Europa. *Icarus*, 438:116631.

Randive, K., Raut, T., and Jawadand, S. (2021). An overview of the global fertilizer trends and India's position in 2020. *Mineral Economics*, 34(3):371–384.

Rathbun, J. A., Musser Jr., G. S., and Squyres, S. W. (1998). Ice diapirs on Europa: Implications for liquid water. *Geophysical Research Letters*, 25(22):4157–4160.

Raven, J. A., Wollenweber, B., and Handley, L. L. (1992). A comparison of ammonium and nitrate as nitrogen sources for photolithotrophs. *New Phytologist*, 121(1):19–32.

Ray, C., Glein, C. R., Waite, J. H., Teolis, B., Hoehler, T., Huber, J. A., Lunine, J., and Postberg, F. (2021). Oxidation processes diversify the metabolic menu on Enceladus. *Icarus*, 364:114248.

Raymond, C. A., Ermakov, A. I., Castillo-Rogez, J. C., Marchi, S., Johnson, B. C., Hesse, M. A., Scully, J. E. C., Buczkowski, D. L., Sizemore, H. G., Schenk, P. M., Nathues, A., Park, R. S., Prettyman, T. H., Quick, L. C., Keane, J. T., Rayman, M. D., and Russell, C. T. (2020). Impact-driven mobilization of deep crustal brines on dwarf planet Ceres. *Nature Astronomy*, 4(8):741–747.

Reitzer, L. (2003). Nitrogen assimilation and global regulation in *Escherichia coli*. *Annual Review of Microbiology*, 57:155–176.

Rhoden, A. R., Henning, W., Hurford, T. A., and Hamilton, D. P. (2015). The interior and orbital evolution of Charon as preserved in its geologic record. *Icarus*, 246:11–20.

Ribbe, M. W., editor (2011). *Nitrogen Fixation: Methods and Protocols*, volume 766 of *Methods in Molecular Biology*. Humana Press, Totowa, NJ.

Richter, C., Gholami, S., Manoharan, Y., Buttersack, T., Longetti, L., Artiglia, L., Ammann, M., Bartels-Rausch, T., and Bluhm, H. (2025). Uptake of ammonia by ice surfaces at atmospheric temperatures. *Faraday Discussions*, 258:532–545.

Ritchie, R. J. and Gibson, J. (1987a). Permeability of ammonia and amines in *Rhodobacter sphaeroides* and *Bacillus firmus*. *Archives of Biochemistry and Biophysics*, 258(2):332–341.

Ritchie, R. J. and Gibson, J. (1987b). Permeability of ammonia, methylamine and ethylamine in the cyanobacterium *Synechococcus* R-2 (*Anacystis nidulans*) PCC 7942. *The Journal of Membrane Biology*, 95(2):131–142.

Ritchie, R. J. and Islam, N. (2001). Permeability of methylamine across the membrane of a cyanobacterial cell. *New Phytologist*, 152(2):203–211.

Roberts, J. H. and Nimmo, F. (2008). Tidal heating and the long-term stability of a subsurface ocean on Enceladus. *Icarus*, 194(2):675–689.

Robuchon, G. and Nimmo, F. (2011). Thermal evolution of Pluto and implications for surface tectonics and a subsurface ocean. *Icarus*, 216(2):426–439.

Rogers, H. H. and Aneja, V. P. (1980). Uptake of atmospheric ammonia by selected plant species. *Environmental and Experimental Botany*, 20(3):251–257.

Roney, N., Llados, F., Little, S. S., and Knaebel, D. B. (2004). Toxicological profile for ammonia.

Rose, C., Kresse, W., and Kettenmann, H. (2005). Acute insult of ammonia leads to calcium-dependent glutamate release from cultured astrocytes, an effect of pH. *The Journal of Biological Chemistry*, 280(22):20937–20944.

Rosen, B. P. and Silver, S. (2014). *Ion Transport in Prokaryotes*. Academic Press.

Rothschild, L. J. and Mancinelli, R. L. (2001). Life in extreme environments. *Nature*, 409(6823):1092–1101.

Rovelli, C. (2023). *Anaximander: And the Nature of Science*. Allen Lane, London.

Russell, M. J., Hall, A. J., and Martin, W. (2010). Serpentinization as a source of energy at the origin of life. *Geobiology*, 8(5):355–371.

Sagan, C., Thompson, W. R., and Khare, B. N. (1992). Titan: A laboratory for prebiological organic chemistry. *Accounts of Chemical Research*, 25(7):286–292.

Sahai, N., LaRowe, D., and Senko, J. M. (2024). Bioenergetics of iron snow fueling life on Europa. *Proceedings of the National Academy of Sciences*, 121(17):e2316452121.

Samuelsen, L., Holm, R., Lathuile, A., and Schönbeck, C. (2019). Buffer solutions in drug formulation and processing: How pK_a values depend on temperature, pressure and ionic strength. *International Journal of Pharmaceutics*, 560:357–364.

Saur, J., Duling, S., Roth, L., Jia, X., Strobel, D. F., Feldman, P. D., Christensen, U. R., Retherford, K. D., McGrath, M. A., Musacchio, F., Wennmacher, A., Neubauer, F. M., Simon, S., and Hartkorn, O. (2015). The search for a subsurface ocean in Ganymede with Hubble Space Telescope observations of its auroral ovals. *Journal of Geophysical Research: Space Physics*, 120(3):1715–1737.

Sayavedra-Soto, L., Ferrell, R., Dobie, M., Mellbye, B., Chaplen, F., Buchanan, A., Chang, J., Bottomley, P., and Arp, D. (2015). *Nitrobacter Winogradskyi* transcriptomic response to low and high ammonium concentrations. *FEMS microbiology letters*, 362:1–7.

Schmidt, E. and Belser, L. (1983). Nitrifying bacteria. In *Methods of Soil Analysis*, chapter 48, pages 1027–1042. John Wiley & Sons, Ltd.

Schmidt, M. R., Neufeld, D. A., Szczerba, R., Yunnan, H. J., Siodmiak, N., and HIFISTARS Consortium (2011). Observations of the circumstellar ammonia 1_0–0_0 lines in carbon-rich AGB stars by the Herschel/HIFI. *Astronomy & Astrophysics*, 592:13.

Schoenfeld, A. M., Hawkins, E. K., Soderlund, K. M., Vance, S. D., Leonard, E., and Yin, A. (2023). Particle entrainment and rotating convection in Enceladus' ocean. *Communications Earth & Environment*, 4(1):1–8.

Schofield, K., Seager, J., and Merrlman, R. P. (1990). The impact of intensive dairy farming activities on river quality: The Eastern Cleddau catchment study. *Water and Environment Journal*, 4(2):176–186.

Schuldiner, S., Agmon, V., Brandsma, J., Cohen, A., Friedman, E., and Padan, E. (1986). Induction of SOS functions by alkaline intracellular pH in *Escherichia coli*. *Journal of Bacteriology*, 168(2):936–939.

Sedlacek, C. J., McGowan, B., Suwa, Y., Sayavedra-Soto, L., Laanbroek, H. J., Stein, L. Y., Norton, J. M., Klotz, M. G., and Bollmann, A. (2019). A Physiological and Genomic Comparison of Nitrosomonas Cluster 6a and 7 Ammonia-Oxidizing Bacteria. *Microbial Ecology*, 78(4):985–994.

Seregina, T. A., Lobanov, K. V., Shakulov, R. S., and Mironov, A. S. (2022). Enhancement of the bactericidal effect of antibiotics by inhibition of enzymes involved in production of hydrogen sulfide in bacteria. *Molecular Biology*, 56(5):638–648.

Shang, X., Huang, R., and Sun, W. (2023a). An ammonia-methane dominated atmosphere in the Hadean Eon. *Solid Earth Sciences*, 8(3):191–194.

Shang, X., Huang, R., and Sun, W. (2023b). Formation of ammonia through serpentinization in the Hadean Eon. *Science Bulletin*, 68(11):1109–1112.

Shatters, R. G., Liu, Y., and Kahn, M. L. (1993). Isolation and characterization of a novel glutamine synthetase from Rhizobium meliloti. *The Journal of Biological Chemistry*, 268(1):469–475.

Shi, S., Xu, F., Ge, Y., Mao, J., An, L., Deng, S., Ullah, Z., Yuan, X., Liu, G., Liu, H., and Wang, Q. (2020). NH_4^+ toxicity, which is mainly determined by the high NH_4^+/K^+ ratio, is alleviated by CIPK23 in *Arabidopsis*. *Plants*, 9(4):501.

Shin, W., Islam, R., Benson, A., Joe, M. M., Kim, K., Gopal, S., Samaddar, S., Banerjee, S., and Sa, T. (2016). Role of diazotrophic bacteria in biological nitrogen fixation and plant growth improvement. *Korean Journal of Soil Science and Fertilizer*, 49(1):17–29.

Showman, A. P., Mosqueira, I., and Head, J. W. (2004). On the resurfacing of Ganymede by liquid–water volcanism. *Icarus*, 172(2):625–640.

Simonelli, D., Baldelli, S., and Shultz, M. J. (1998). Ammonia–water complexes on the surface of aqueous solutions observed with sum frequency generation. *Chemical Physics Letters*, 298(4):400–404.

Singh, K. (2016). Microbial and enzyme activities of saline and sodic soils. *Land Degradation & Development*, 27(3):706–718.

Singh, S. K., Bergantini, A., Zhu, C., Ferrari, M., De Sanctis, M. C., De Angelis, S., and Kaiser, R. I. (2021). Origin of ammoniated phyllosilicates on dwarf planet Ceres and asteroids. *Nature Communications*, 12:2690.

Smith, B. A., Soderblom, L., Batson, R., Bridges, P., Inge, J., Masursky, H., Shoemaker, E., Beebe, R., Boyce, J., Briggs, G., Bunker, A., Collins, S. A., Hansen, C. J., Johnson, T. V., Mitchell, J. L., Terrile, R. J., Cook, A. F., Cuzzi, J., Pollack, J. B., Danielson, G. E., Ingersoll, A. P., Davies, M. E., Hunt, G. E., Morrison, D., Owen, T., Sagan, C., Veverka, J., Strom, R., and Suomi, V. E. (1982). A New Look at the Saturn System: The Voyager 2 Images. *Science*, 215(4532):504–537.

Smith, B. A., Soderblom, L. A., Beebe, R., Boyce, J., Briggs, G., Carr, M., Collins, S. A., Cook, A. F., Danielson, G. E., Davies, M. E., Hunt, G. E., Ingersoll, A., Johnson, T. V., Masursky, H., McCauley, J., Morrison, D., Owen, T., Sagan, C., Shoemaker, E. M., Strom, R., Suomi, V. E., and Veverka, J. (1979). The Galilean Satellites and Jupiter: Voyager 2 Imaging Science Results. *Science*, 206(4421):927–950.

Smith, C. J., Hespell, R. B., and Bryant, M. P. (1980). Ammonia assimilation and glutamate formation in the anaerobe Selenomonas ruminantium. *Journal of Bacteriology*, 141(2):593–602.

Soderblom, L. A. (1980). The Galilean moons of Jupiter. *Scientific American*, 242(1):88–101.

Sohl, F., Hussmann, H., Schwentker, B., Spohn, T., and Lorenz, R. D. (2003). Interior structure models and tidal Love numbers of Titan. *Journal of Geophysical Research: Planets*, 108(E12).

Sohl, F., Solomonidou, A., Wagner, F. W., Coustenis, A., Hussmann, H., and Schulze-Makuch, D. (2014). Structural and tidal models of Titan and inferences on cryovolcanism. *Journal of Geophysical Research: Planets*, 119(5):1013–1036.

Sojo, V., Herschy, B., Whicher, A., Camprubí, E., and Lane, N. (2016). The origin of life in alkaline hydrothermal vents. *Astrobiology*, 16(2):181–197.

Sorokin, D., Tourova, T., Schmid, M. C., Wagner, M., Koops, H.-P., Kuenen, G. J., and Jetten, M. (2001). Isolation and properties of obligately chemolithoautotrophic and extremely alkali-tolerant ammonia-oxidizing bacteria from Mongolian soda lakes. *Archives of Microbiology*, 176(3):170–177.

Soupene, E., He, L., Yan, D., and Kustu, S. (1998). Ammonia acquisition in enteric bacteria: Physiological role of the ammonium/methylammonium transport B (AmtB) protein. *Proceedings of the National Academy of Sciences*, 95(12):7030–7034.

Soupene, E., Lee, H., and Kustu, S. (2002). Ammonium/methylammonium transport (Amt) proteins facilitate diffusion of NH_3 bidirectionally. *Proceedings of the National Academy of Sciences*, 99(6):3926–3931.

Spitale, J. N. and Porco, C. C. (2007). Association of the jets of Enceladus with the warmest regions on its south-polar fractures. *Nature*, 449(7163):695–697.

Spohn, T. and Schubert, G. (2003). Oceans in the icy Galilean satellites of Jupiter? *Icarus*, 161(2):456–467.

Sprott, G. D. and Patel, G. B. (1986). Ammonia toxicity in pure cultures of methanogenic bacteria. *Systematic and Applied Microbiology*, 7(2):358–363.

Sprott, G. D., Shaw, K. M., and Jarrell, K. F. (1984). Ammonia/potassium exchange in methanogenic bacteria. *The Journal of Biological Chemistry*, 259(20):12602–12608.

Stein, L. Y. and Klotz, M. G. (2016). The nitrogen cycle. *Current Biology*, 26(3):R94–R98.

Stevenson, A., Burkhardt, J., Cockell, C. S., Cray, J. A., Dijksterhuis, J., Fox-Powell, M., Kee, T. P., Kminek, G., McGenity, T. J., Timmis, K. N., Timson, D. J., Voytek, M. A., Westall, F., Yakimov, M. M., and Hallsworth, J. E. (2015). Multiplication of microbes below 0.690 water activity: Implications for terrestrial and extraterrestrial life. *Environmental Microbiology*, 17(2):257–277.

Stofan, E. R., Elachi, C., Lunine, J. I., Lorenz, R. D., Stiles, B., Mitchell, K. L., Ostro, S., Soderblom, L., Wood, C., Zebker, H., Wall, S., Janssen, M., Kirk, R., Lopes, R., Paganelli, F., Radebaugh, J., Wye, L., Anderson, Y., Allison, M., Boehmer, R., Callahan, P., Encrenaz, P., Flamini, E., Francescetti, G., Gim, Y., Hamilton, G., Hensley, S., Johnson, W. T. K., Kelleher, K., Muhleman, D., Paillou, P., Picardi, G., Posa, F., Roth, L., Seu, R., Shaffer, S., Vetrella, S., and West, R. (2007). The lakes of Titan. *Nature*, 445(7123):61–64.

Storz, G. and Hengge, R., editors (2010). *Bacterial Stress Responses*. 1. American Society for Microbiolog, Washington (DC), USA, second edition.

Strock, J. S. (2008). Ammonification. In *Encyclopedia of Ecology*, pages 162–165. Elsevier Inc.

Studier, E. H. (1966). Studies on the mechanisms of ammonia tolerance of the guano bat. *Journal of Experimental Zoology*, 163(1):79–85.

Sutton, M. A., Milford, C., Dragosits, U., Place, C. J., Singles, R. J., Smith, R. I., Pitcairn, C. E. R., Fowler, D., Hill, J., Apsimon, H. M., Ross, C., Hill, R., Jarvis, S. C., Pain, B. F., Phillips, V. C., Harrison, R., Moss, D., Webb, J., Espenhahn, S. E., Lee, D. S., Hornung, M., Ullyett, J., Bull, K. R., Emmett, B. A., Lowe, J., and Wyers, G. P. (1998). Dispersion, deposition and impacts of atmospheric ammonia: Quantifying local budgets and spatial variability. *Environmental Pollution*, 102(S1):349–361.

Sutton, M. A., Reis, S., and Baker, S. M. H., editors (2009). *Atmospheric Ammonia*. Springer, Dordrecht; London.

Suzuki, S., Kuenen, J. G., Schipper, K., van der Velde, S., Ishii, S., Wu, A., Sorokin, D. Y., Tenney, A., Meng, X., Morrill, P. L., Kamagata, Y., Muyzer, G., and Nealson, K. H. (2014). Physiological and genomic features of highly alkaliphilic hydrogen-utilizing Betaproteobacteria from a continental serpentinizing site. *Nature Communications*, 5:3900.

Szalay, J. R., Allegrini, F., Ebert, R. W., Bagenal, F., Bolton, S. J., Fatemi, S., McComas, D. J., Pontoni, A., Saur, J., Smith, H. T., Strobel, D. F., Vance, S. D., Vorburger, A., and Wilson, R. J. (2024). Oxygen production from dissociation of Europa's water-ice surface. *Nature Astronomy*, 8(5):567–576.

Szczerba, M. W., Britto, D. T., Ali, S. A., Balkos, K. D., and Kronzucker, H. J. (2008). NH_4^+-stimulated and -inhibited components of K^+ transport in rice (*Oryza sativa* L.). *Journal of Experimental Botany*, 59(12):3415–3423.

Tachiki, T., Shirasu, Y., Haruna, M., and Tochikura, T. (1978). Occurrence of Glutamine Synthetase/Glutamate Synthase Pathway in *Gluconobacter suboxydans*. *Agricultural and Biological Chemistry*, 42(9):1689–1695.

Tada, S., Itoh, Y., Kiyoshi, K., and Yoshida, N. (2021). Isolation of ammonia gas-tolerant extremophilic bacteria and their application to the elimination of malodorous gas emitted from outdoor heat-treated toilets. *Journal of Bioscience and Bioengineering*, 131(5):509–517.

Taglicht, D., Padan, E., Oppenheim, A. B., and Schuldiner, S. (1987). An alkaline shift induces the heat shock response in *Escherichia coli*. *Journal of Bacteriology*, 169(2):885–887.

Takahashi, Y., Takahashi, H., Galipon, J., and Arakawa, K. (2020). Complete genome sequence of *Halomonas meridiana* strain Slthf1, isolated from a deep-sea thermal vent. *Microbiology Resource Announcements*.

Tan, S., Sekine, Y., Shibuya, T., Miyamoto, C., and Takahashi, Y. (2021). The role of hydrothermal sulfate reduction in the sulfur cycles within Europa: Laboratory experiments on sulfate reduction at 100 MPa. *Icarus*, 357:114222.

Taubner, R.-S., Schleper, C., Firneis, M. G., and Rittmann, S. K. M. R. (2015). Assessing the ecophysiology of methanogens in the context of recent astrobiological and planetological studies. *Life*, 5(4):1652–1686.

Teolis, B. D., Plainaki, C., Cassidy, T. A., and Raut, U. (2017). Water ice radiolytic O_2, H_2, and H_2O_2 yields for any projectile species, energy, or temperature: A model for icy astrophysical bodies. *Journal of Geophysical Research: Planets*, 122(10):1996–2012.

Tesch, M., de Graaf, A. A., and Sahm, H. (1999). *In Vivo* fluxes in the ammonium-assimilatory pathways in *Corynebacterium glutamicum* studied by 15N nuclear magnetic resonance. *Applied and Environmental Microbiology*, 65(3):1099–1109.

Thurston, R. V., Russo, R. C., and Vinogradov, G. A. (1981). Ammonia toxicity to fishes. Effect of pH on the toxicity of the unionized ammonia species. *Environmental Science & Technology*, 15(7):837–840.

Tobie, G., Čadek, O., and Sotin, C. (2008). Solid tidal friction above a liquid water reservoir as the origin of the south pole hotspot on Enceladus. *Icarus*, 196(2):642–652.

Tobie, G., Gautier, D., and Hersant, F. (2012). Titan's bulk composition constrained by Cassini-Huygens: Implication for internal outgassing. *The Astrophysical Journal*, 752(2):125.

Tobie, G., Grasset, O., Lunine, J. I., Mocquet, A., and Sotin, C. (2005). Titan's internal structure inferred from a coupled thermal-orbital model. *Icarus*, 175(2):496–502.

Toljander, J. F., Santos-González, J. C., Tehler, A., and Finlay, R. D. (2008). Community analysis of arbuscular mycorrhizal fungi and bacteria in the maize mycorrhizosphere in a long-term fertilization trial. *FEMS Microbiology Ecology*, 65(2):323–338.

Tourna, M., Stieglmeier, M., Spang, A., Könneke, M., Schintlmeister, A., Urich, T., Engel, M., Schloter, M., Wagner, M., Richter, A., and Schleper, C. (2011). *Nitrososphaera Viennensis*, an ammonia oxidizing archaeon from soil. *Proceedings of the National Academy of Sciences*, 108(20):8420–8425.

Turtle, E. P., Perry, J. E., McEwen, A. S., DelGenio, A. D., Barbara, J., West, R. A., Dawson, D. D., and Porco, C. C. (2009). Cassini imaging of Titan's high-latitude lakes, clouds, and south-polar surface changes. *Geophysical Research Letters*, 36(2).

Tyagi, J., Ahmad, S., and Malik, M. (2022). Nitrogenous fertilizers: Impact on environment sustainability, mitigation strategies, and challenges. *International Journal of Environmental Science and Technology*, 19(11):11649–11672.

Ughy, B., Nagyapati, S., Lajko, D. B., Letoha, T., Prohaszka, A., Deeb, D., Der, A., Pettko-Szandtner, A., and Szilak, L. (2023). Reconsidering dogmas about the growth of bacterial populations. *Cells*, 12(10):1430.

Van Damme, M., Clarisse, L., Whitburn, S., Hadji-Lazaro, J., Hurtmans, D., Clerbaux, C., and Coheur, P.-F. (2018). Industrial and agricultural ammonia point sources exposed. *Nature*, 564(7734):99–103.

Vance, S. and Brown, J. M. (2013). Thermodynamic properties of aqueous $MgSO_4$ to 800 MPa at temperatures from -20 to 100 °C and concentrations to 2.5 mol kg^{-1} from sound speeds, with applications to icy world oceans. *Geochimica et Cosmochimica Acta*, 110:176–189.

Vance, S., Harnmeijer, J., Kimura, J., Hussmann, H., deMartin, B., and Brown, J. M. (2007). Hydrothermal systems in small ocean planets. *Astrobiology*, 7(6):987–1005.

Vance, S. D., Craft, K. L., Shock, E., Schmidt, B. E., Lunine, J., Hand, K. P., McKinnon, W. B., Spiers, E. M., Chivers, C., Lawrence, J. D., Wolfenbarger, N., Leonard, E. J., Robinson, K. J., Styczinski, M. J., Persaud, D. M., Steinbrügge, G., Zolotov, M. Y., Quick, L. C., Scully, J. E. C., Becker, T. M., Howell, S. M., Clark, R. N., Dombard, A. J., Glein, C. R., Mousis, O., Sephton, M. A., Castillo-Rogez, J., Nimmo, F., McEwen, A. S., Gudipati, M. S., Jun, I., Jia, X., Postberg, F., Soderlund, K. M., and Elder, C. M. (2023). Investigating Europa's Habitability with the Europa Clipper. *Space Science Reviews*, 219(8):81.

Vance, S. D., Panning, M. P., Stähler, S., Cammarano, F., Bills, B. G., Tobie, G., Kamata, S., Kedar, S., Sotin, C., Pike, W. T., Lorenz, R., Huang, H.-H., Jackson, J. M., and Banerdt, B. (2018). Geophysical investigations of habitability in ice-covered ocean worlds. *Journal of Geophysical Research: Planets*, 123(1):180–205.

Vejmelkova, D., Sorokin, D. Y., Abbas, B., Kovaleva, O. L., Kleerebezem, R., Kampschreur, M. J., Muyzer, G., and van Loosdrecht, M. C. M. (2012). Analysis of ammonia-oxidizing bacteria dominating in lab-scale bioreactors with high ammonium bicarbonate loading. *Applied Microbiology and Biotechnology*, 93(1):401–410.

Vielma, T. and Hefter, G. (2022). Sulfate protonation in sodium chloride and sodium perchlorate media. *Journal of Solution Chemistry*, 51(8):962–969.

Vines, H. M. and Wedding, R. T. (1960). Some effects of ammonia on plant metabolism and a possible mechanism for ammonia toxicity. *Plant Physiology*, 35(6):820–825.

Vo, J., Inwood, W., Hayes, J. M., and Kustu, S. (2013). Mechanism for nitrogen isotope fractionation during ammonium assimilation by *Escherichia coli* K12. *Proceedings of the National Academy of Sciences*, 110(21):8696–8701.

Wacker, T., Garcia-Celma, J. J., Lewe, P., and Andrade, S. L. A. (2014). Direct observation of electrogenic NH_4^+ transport in ammonium transport (Amt) proteins. *Proceedings of the National Academy of Sciences*, 111(27):9995–10000.

Waite, J. H., Combi, M. R., Ip, W. H., Cravens, T. E., McNutt, R. L., Kasprzak, W., Yelle, R., Luhmann, J., Niemann, H., Gell, D., Magee, B., Fletcher, G., Lunine, J., and Tseng, W. L. (2006). Cassini ion and neutral mass spectrometer: Enceladus plume composition and structure. *Science*, 311(5766):1419–1422.

Waite, J. H., Glein, C. R., Perryman, R. S., Teolis, B. D., Magee, B. A., Miller, G., Grimes, J., Perry, M. E., Miller, K. E., Bouquet, A., Lunine, J. I., Brockwell, T., and Bolton, S. J. (2017). Cassini finds molecular hydrogen in the Enceladus plume: Evidence for hydrothermal processes. *Science*, 356(6334):155–159.

Waite, J. H., Lewis, W. S., Magee, B. A., Lunine, J. I., McKinnon, W. B., Glein, C. R., Mousis, O., Young, D. T., Brockwell, T., Westlake, J., Nguyen, M.-J., Teolis, B. D., Niemann, H. B., McNutt Jr, R. L., Perry, M., and Ip, W.-H. (2009). Liquid water on Enceladus from observations of ammonia and 40Ar in the plume. *Nature*, 460(7254):487–490.

Wakisaka, S., Sung, H.-C., Aikawa, T., Tachiki, T., and Tochikura, T. (1989). Glutamate formation by a new *In vitro* enzyme system consisting of purified glutamine synthetase and glutamate synthase. *Journal of Fermentation and Bioengineering*, 67(6):395–398.

Wallace, W. and Nicholas, D. J. D. (1969). The Biochemistry of Nitrifying Microorganisms. *Biological Reviews*, 44(3):359–389.

Wang, F., Chen, S., Jiang, Y., Zhao, Y., Sun, L., Zheng, B., Chen, L., Liu, Z., Zheng, X., Yi, K., Li, C., and Zhou, X. (2018). Effects of ammonia on apoptosis and oxidative stress in bovine mammary epithelial cells. *Mutagenesis*, 33(4):291–299.

Wang, T., Li, J., Zhang, L. H., Yu, Y., and Zhu, Y. M. (2017). Simultaneous heterotrophic nitrification and aerobic denitrification at high concentrations of NaCl and ammonia nitrogen by *Halomonas* bacteria. *Water Science and Technology*, 76(2):386–395.

Ward, B. B., Martino, D. P., Diaz, M. C., and Joye, S. B. (2000). Analysis of ammonia-oxidizing bacteria from hypersaline Mono Lake, California, on the basis of 16s rRNA sequences. *Applied and Environmental Microbiology*, 66(7):2873–2881.

Warner, J. X., Dickerson, R. R., Wei, Z., Strow, L. L., Wang, Y., and Liang, Q. (2017). Increased atmospheric ammonia over the world's major agricultural areas detected from space. *Geophysical Research Letters*, 44(6):2875–2884.

Weng, X., Mao, Z., Fu, H.-M., Chen, Y.-P., Guo, J.-S., Fang, F., Xu, X.-W., and Yan, P. (2022). Biofilm formation during wastewater treatment: Motility and physiological response of aerobic denitrifying bacteria under ammonia stress based on surface plasmon resonance imaging. *Bioresource Technology*, 361:127712.

Wettlaufer, J. S. (2009). Sea ice and astrobiology. In *Sea Ice*, chapter 15, pages 579–594. John Wiley & Sons, Ltd.

Whitfield, M. (1974). The hydrolysis of ammonium ions in sea water - a theoretical study. *Journal of the Marine Biological Association of the United Kingdom*, 54(3):565–580.

Wigley, T. M. L. and Brimblecombe, P. (1981). Carbon dioxide, ammonia and the origin of life. *Nature*, 291(5812):213–215.

Wiley, W. R. and Stokes, J. L. (1962). Requirement of an alkaline pH and ammonia for substrate oxidation by *Bacillus pasteurii*. *Journal of Bacteriology*, 84(4):730–734.

Wiley, W. R. and Stokes, J. L. (1963). Effect of pH and ammonium ions on the permeability of *Bacillus pasteurii*. *Journal of Bacteriology*, 86(6):1152–1156.

Witter, E., Mårtensson, A. M., and Garcia, F. V. (1993). Size of the soil microbial biomass in a long-term field experiment as affected by different N-fertilizers and organic manures. *Soil Biology and Biochemistry*, 25(6):659–669.

Wolfenbarger, N. S., Fox-Powell, M. G., Buffo, J. J., Soderlund, K. M., and Blankenship, D. D. (2022). Brine volume fraction as a habitability metric for Europa's ice shell. *Geophysical Research Letters*, 49(22):e2022GL100586.

Wong, K. T., Menten, K. M., Kamiński, T., Wyrowski, F., Lacy, J. H., and Greathouse, T. K. (2018). Circumstellar ammonia in oxygen-rich evolved stars. *Astronomy & Astrophysics*, 612:A48.

Wu, J.-H., McGenity, T. J., Rettberg, P., Simões, M. F., Li, W.-J., and Antunes, A. (2022). The archaeal class Halobacteria and astrobiology: Knowledge gaps and research opportunities. *Frontiers in Microbiology*, 13.

Wyckoff, S., Tegler, S., and Engel, L. (1989). Ammonia abundances in comets. *Advances in Space Research*, 9(3):169–176.

Xiao, J., Li, Q.-Y., Tu, J.-P., Chen, X.-L., Chen, X.-H., Liu, Q.-Y., Liu, H., Zhou, X.-Y., Zhao, Y.-Z., and Wang, H.-L. (2019). Stress response and tolerance mechanisms of ammonia exposure based on transcriptomics and metabolomics in *Litopenaeus vannamei*. *Ecotoxicology and Environmental Safety*, 180:491–500.

Xie, Y., Wang, W., Chen, Y., Qian, Z., Chen, J., Tong, J., Li, L., Yue, Y., Chen, K., Chu, Z., and Hu, X. (2024). NH_3 emissions and lifetime estimated by satellite observations with differential evolution algorithm. *Atmosphere*, 15(3):251.

Xu, W., Liu, C., Zhang, A., Lau, M., Cleaves, H. J., Huang, F., Glein, C. R., and Hao, J. (2025). Enough sulfur and iron for potential life make Enceladus's ocean fully habitable. *The Astrophysical Journal Letters*, 980(1):L10.

Yan, D., Ikeda, T. P., Shauger, A. E., and Kustu, S. (1996). Glutamate is required to maintain the steady-state potassium pool in *Salmonella typhimurium*. *Proceedings of the National Academy of Sciences*, 93(13):6527–6531.

Yang, Y., Liu, L., Liu, P., Ding, J., Xu, H., and Liu, S. (2023). Improved global agricultural crop- and animal-specific ammonia emissions during 1961–2018. *Agriculture, Ecosystems & Environment*, 344:108289.

Yi, Y., Dolfing, J., Jin, G., Fang, X., Han, W., Liu, L., Tang, Y., and Cheng, L. (2023). Thermodynamic restrictions determine ammonia tolerance of methanogenic pathways in Methanosarcina barkeri. *Water Research*, 232:119664.

Yin, H., Zhang, X., Li, X., He, Z., Liang, Y., Guo, X., Hu, Q., Xiao, Y., Cong, J., Ma, L., Niu, J., and Liu, X. (2014). Whole-genome sequencing reveals novel insights into sulfur oxidation in the extremophile *Acidithiobacillus thiooxidans*. *BMC Microbiology*, 14(1):179.

Young, T. F., Singleterry, C. R., and Klotz, I. M. (1978). Ionization constants and heats of ionization of the bisulfate ion from 5 to 55.degree.C. *The Journal of Physical Chemistry*, 82(6):671–674.

Zahn, D. (2017a). A molecular simulation study of the auto-protolysis of ammonia as a function of temperature. *Chemical Physics Letters*, 682:55–59.

Zahn, D. (2017b). On the solvation of metal ions in liquid ammonia: A molecular simulation study of $M(NH_2)_x(NH_3)_y$ complexes as a function of pH. *RSC Advances*, 7(85):54063–54067.

Zhang, C., Yuan, Q., and Lu, Y. (2014). Inhibitory effects of ammonia on methanogen mcrA transcripts in anaerobic digester sludge. *FEMS Microbiology Ecology*, 87(2):368–377.

Zhang, W., Ding, W., Li, Y.-X., Tam, C., Bougouffa, S., Wang, R., Pei, B., Chiang, H., Leung, P., Lu, Y., Sun, J., Fu, H., Bajic, V. B., Liu, H., Webster, N. S., and Qian, P.-Y. (2019). Marine biofilms constitute a bank of hidden microbial diversity and functional potential. *Nature Communications*, 10(1):517.

Zhang, Y. and Cremer, P. S. (2006). Interactions between macromolecules and ions: The Hofmeister series. *Current Opinion in Chemical Biology*, 10(6):658–663.

Zimmer, C., Khurana, K. K., and Kivelson, M. G. (2000). Subsurface oceans on Europa and Callisto: Constraints from Galileo magnetometer observations. *Icarus*, 147(2):329–347.

Zolotov, M. Y. (2007). An oceanic composition on early and today's Enceladus. *Geophysical Research Letters*, 34(23).

Zolotov, M. Y. (2017). Aqueous origins of bright salt deposits on Ceres. *Icarus*, 296:289–304.

Zolotov, M. Y. and Shock, E. L. (2001). Composition and stability of salts on the surface of Europa and their oceanic origin. *Journal of Geophysical Research: Planets*, 106(E12):32815–32827.

Zorz, J. K., Kozlowski, J. A., Stein, L. Y., Strous, M., and Kleiner, M. (2018). Comparative proteomics of three species of ammonia-oxidizing bacteria. *Frontiers in Microbiology*, 9:938.

Appendix

Chapter 4 appendix: Ammonia sets limit to life and alters physiology independently of pH in *Halomonas meridiana*

The following supplementary material originally appeared in *Scientific Reports*, 4th June 2025. DOI: 10.1038/s41598-025-03858-z.

Supplementary Figure 1: pKa^s of NH_4^+ at given ionic strengths. Scatter plot shows the relationship between the stoichiometric acid hydrolysis constant (pKa^s) of NH_4^+ at increasing ionic strengths (I). A linear regression (dotted line) was fitted to the data.

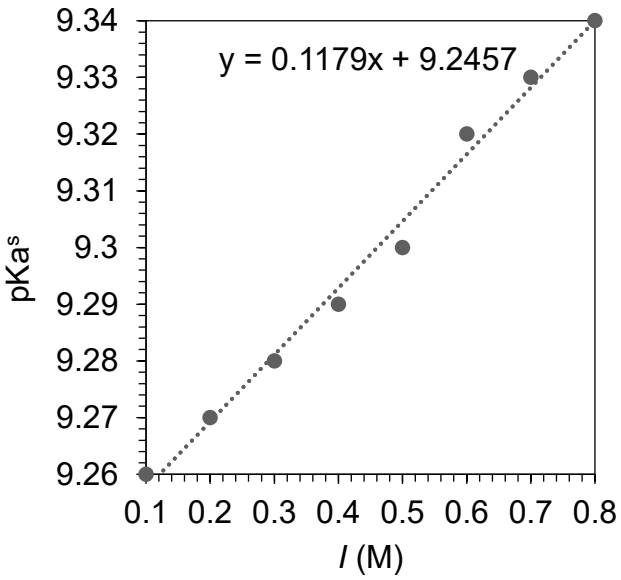

Supplementary Figure 2: Cell viability and optical density at 600 nm over 24 h. Marker and line plot show the PrestoBlue™ cell viability (closed black circles) against optical density at 600 nm (OD_{600}) readings (open white squares). Markers present the mean ± s.d. (n=3). The s.d. is smaller than the marker if error bar is not visible

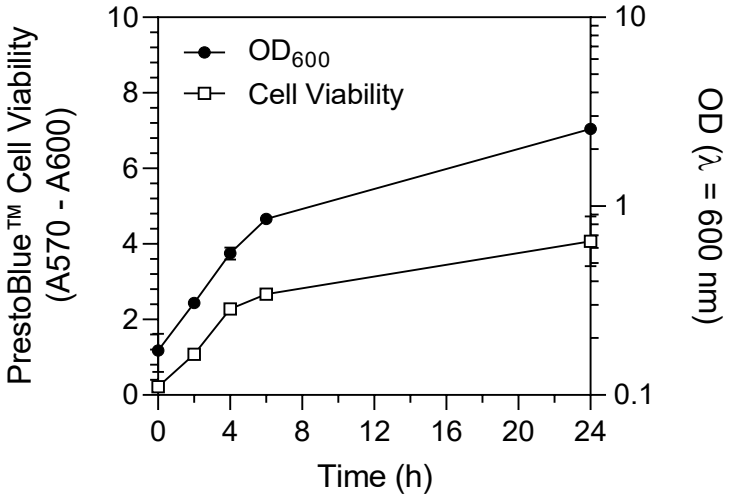

Supplementary Table 1: Outcome of statistical analysis by unpaired t-test and Mann-Whitney test comparing the oxygen measurements (Fig. 1c) and water activity (Fig. 1d) for ammonia and NaOH solutions at each pH value. The use of Mann-Whitney is specified by [MW]. All other tests are unpaired t-test. ns, no significance; *, $p < 0.05$; **, $p < 0.01$; ***, $p < 0.001$; ****, $p < 0.0001$.

Oxygen measurements

NaOH - ammonia	Significance	Test outcome
pH 8.05	ns	t=1.8, df=6, $p = 0.122$
pH 8.96	ns	t=0.150, df=6, $p = 0.886$
pH 9.38	ns	t=0.203, df=6, $p = 0.846$
pH 9.73	ns	t=0.257, df=6, $p = 0.806$
pH 10.18 [MW]	ns [MW]	U=4, $p = 0.343$ [MW]
pH 10.49	ns	t=2.053, df=6, $p = 0.0859$
pH 10.78	ns	t=0.272, df=6, $p = 0.795$

Water activity

NaOH - ammonia	Significance	Unpaired t-test outcome
pH 8.05	ns	t=0.768, df=6, $p = 0.472$
pH 8.96	ns	t=0.247, df=6, $p = 0.813$
pH 9.38	ns	t=0.396, df=6, $p = 0.706$
pH 9.73	ns	t=0.424, df=6, $p = 0.686$
pH 10.18	ns	t=0.533, df=6, $p = 0.613$
pH 10.49	ns	t=1.093, df=6, $p = 0.316$
pH 10.78	ns	t=0.415, df=6, $p = 0.693$

Supplementary Table 2: Statistical outcomes for one-way ANOVA with Tukey's post-hoc test comparing the mean cell number (CFU/mL) of *H. meridiana* grown in positive control (PC) solutions (0 M ammonia, no pH modification) and NaOH solutions pH-matched to ammonia solutions (Fig. 3a). ns, no significance; *, $p < 0.05$; **, $p < 0.01$; ***, $p < 0.001$; ****, $p < 0.0001$.

Comparison groups	Significance	*p*-value
PC - pH 8.05	ns	>0.9999
PC - pH 8.96	ns	0.4384
PC - pH 9.38	ns	0.9999
PC - pH 9.73	ns	0.9961
PC - pH 10.18	*	0.0410
PC - pH 10.49	ns	0.7936
PC - pH 10.78	ns	0.8097

Supplementary Table 3: Statistical tests utilised for the comparison of the data for lag phase (Fig. 3c), doubling time (*T*d) (Fig. 3d) and Final OD (Fig. 3e) of *H. meridiana* grown in ammonia vs. pH-matched NaOH solutions.

NaOH - ammonia	Lag Phase	*T*d	Final OD
pH 8.05	Mann-Whitney t-test,	Unpaired t-test	Unpaired t-test
pH 8.96	Unpaired t-test with Welch's correction	Unpaired t-test	Unpaired t-test with Welch's correction
pH 9.38	Unpaired t-test with Welch's correction	Unpaired t-test	Unpaired t-test
pH 9.73	Unpaired t-test with Welch's correction	Unpaired t-test	Unpaired t-test
pH 10.18	Unpaired t-test with Welch's correction	Mann-Whitney t-test,	Unpaired t-test
pH 10.49	n/a	n/a	Unpaired t-test with Welch's correction
pH 10.78	n/a	n/a	Unpaired t-test with Welch's correction

Supplementary Table 4: Volcano analysis comparing molecular features in the 0.25 M ammonia dataset against the control dataset (n=3) (Fig. 5c), where metabolites identified in the analysis exhibited a fold change (FC) greater than 2 and a *p*-value < 0.05 (adjusted using FDR correction). Volcano analysis was performed using the web-based software MetaboAnalyst 6.0.

Metabolite	FC	log2(FC)	p.ajusted	-log10(p)
CMP-Sialic acid	3.86E+07	25.202	1.20E-07	6.9196
9-OxoODE	1.89E-08	-25.654	2.79E-06	5.5541
N-Acetylserotonin	8.06E-08	-23.565	2.98E-06	5.5258
Glutarylcarnitine	1.23E-09	-29.595	1.62E-05	4.7898
Mevalonolactone	4.82E+08	28.845	1.62E-05	4.7898
Linolenic Acid	1.49E-08	-26	1.62E-05	4.7898
2,7-Dimethylnaphthalene	3.45E+07	25.038	1.68E-05	4.7747
Shikimic Acid	3.42E-07	-21.481	1.68E-05	4.7747
Glycerol-3-phosphate	8.34E+07	26.313	2.20E-05	4.6574
Bishomo-gamma-linolenic Acid (20:3)	2.43E-08	-25.293	2.47E-05	4.607
Indole-3-ethanol	1.72E-09	-29.115	5.33E-05	4.2733
Atrazine	4.19E+06	21.997	5.93E-05	4.2268
PA 36:02	5.80E+08	29.113	6.34E-05	4.1982
Sparfloxacin	1.39E+08	27.049	6.47E-05	4.1893
5-Hydroxyindoleacetate	4.53E+08	28.754	0.0002	3.6996
PS 37:04	2.48E+08	27.886	0.000412	3.385
PS 40:01	3.16E-07	-21.592	0.00063	3.2005
PE 38:02	8.20E-08	-23.539	0.002132	2.6712
GVLHAVK (Tryptic Peptide)	2.51E+07	24.582	0.002461	2.6088
D-allo-Isoleucine	3.79E+00	1.9222	0.020352	1.6914
Sorbitol	1.11E-01	-3.1706	0.039119	1.4076
Pantothenate	2.65E+00	1.4068	0.039119	1.4076
Alanine	2.89E+00	1.5335	0.045708	1.34

Supplementary Table 5: Volcano analysis comparing molecular features in the 0.25 M ammonia dataset against those in the NaOH pH 10.18 dataset (n=3) (Fig. 5d), where metabolites identified in the analysis exhibited a fold change (FC) greater than 2 and a *p*-value < 0.05 (adjusted using FDR correction). Volcano analysis was performed using the web-based software MetaboAnalyst 6.0.

Metabolite	FC	log2(FC)	p.ajusted	-log10(p)
ELR (Tryptic Peptide)	5.11E+08	28.928	2.52E-05	4.5991
2,7-Dimethylnaphthalene	3.45E+07	25.038	6.44E-05	4.191
Uric Acid	2.01E-07	-22.248	0.000134	3.8726
Atrazine	4.19E+06	21.997	0.000171	3.7681
3-Hydroxybenzaldehyde	1.97E-08	-25.597	0.000191	3.7186
PC (16:1/16:1) (del9-cis)	1.06E-07	-23.172	0.000191	3.7186
Tributylammonium	3.59E-07	-21.411	0.000191	3.7186
Astilbin	7.94E-08	-23.586	0.0002	3.6995
allo-Threonine	1.71E+07	24.03	0.000287	3.5424
3,4-Dihydroxy-L-phenylalanine	4.74E+06	22.175	0.000912	3.0399

Supplementary Table 6: Volcano analysis comparing molecular features in the NaOH pH 10.18 dataset against those in the control dataset (n=3) (Fig. 5e), where metabolites identified in the analysis exhibited a fold change (FC) greater than 2 and a *p*-value < 0.05 (adjusted using FDR correction). Volcano analysis was performed using the web-based software MetaboAnalyst 6.0.

Metabolite	FC	log2(FC)	p.ajusted	-log10(p)
PS 37:04	1.07E+09	29.99	5.76E-11	10.24
Fumarate	3.92E+08	28.546	2.03E-06	5.693
9-OxoODE	1.89E-08	-25.654	2.03E-06	5.693
N-Acetylserotonin	8.06E-08	-23.565	2.19E-06	5.6599
PS 41:06	1.80E+07	24.099	6.28E-06	5.202
1,2-Dimyristoyl-sn-glycero-3-phosphocholine	1.24E-07	-22.941	6.28E-06	5.202
NVNDVIAPAFVK (Tryptic Peptide)	3.55E-09	-28.07	1.02E-05	4.9923
Linolenic Acid	1.49E-08	-26	1.02E-05	4.9923
Glutarylcarnitine	1.23E-09	-29.595	1.06E-05	4.975
Adenosine-5'-monophosphate	8.12E-10	-30.198	1.09E-05	4.9635
Glycerol-3-phosphate	8.37E+07	26.319	1.68E-05	4.7746
5-Hydroxymethyluracil	1.65E-08	-25.852	1.68E-05	4.7746
ELR (Tryptic Peptide)	2.11E-09	-28.821	1.72E-05	4.7637
Bishomo-gamma-linolenic Acid (20:3)	2.43E-08	-25.293	1.72E-05	4.7637
Reserpine	3.77E+07	25.167	1.72E-05	4.7637
Indole-3-ethanol	1.72E-09	-29.115	3.59E-05	4.4451
allo-Threonine	6.04E-08	-23.981	4.15E-05	4.3815
CMP-Sialic acid	1.75E+07	24.058	4.37E-05	4.3599
Thiabendazole	6.62E+06	22.659	4.37E-05	4.3599
Terbutryn	4.61E+06	22.137	7.12E-05	4.1475
Imazapyr	3.46E-08	-24.784	7.31E-05	4.136
Astilbin	1.26E+07	23.586	7.42E-05	4.1295
N-(3-Phenylpropionyl)-glycine	9.76E-08	-23.288	0.000154	3.8122
PE 38:02	8.20E-08	-23.539	0.001566	2.8052
PE (O-34:03)	5.53E+01	5.788	0.022256	1.6526
N-Acetylglutamate	2.24E+00	1.1659	0.042834	1.3682
Riboflavin	4.18E-01	-1.259	0.04393	1.3572
LysoPC (13:0)	3.92E+00	1.9699	0.049445	1.3059

Supplementary Table 7: Metabolites significantly altered (*p*-value lower than 0.05 (FDR corrected) between the three treatment conditions assessed by ANOVA with Tukey's multiple comparison test (n=3) (Fig. 5f). *p*-values without FDR adjustment are also shown. ANOVA analysis was performed using the web-based software MetaboAnalyst 6.0.

Metabolite	f.value	p.value	-log10(p)	FDR	Tukey's HSD
9-OxoODE	23884	1.98E-12	11.703	1.11E-09	Ammonia-Control; PH-Control
N-Acetylserotonin	18876	4.01E-12	11.397	1.12E-09	Ammonia-Control; PH-Control
Linolenic Acid	6186.4	1.1387E-10	9.9436	2.0122E-08	Ammonia-Control; PH-Control
Glutarylcarnitine	5717.4	1.4424E-10	9.8409	2.0122E-08	Ammonia-Control; PH-Control
2,7-Dimethylnaphthalene	4865.6	2.34E-10	9.6309	2.61E-08	Ammonia-Control; PH-NH3
Bishomo-gamma-linolenic Acid (20:3)	3586.7	5.84E-10	9.2338	5.43E-08	Ammonia-Control; PH-Control
ELR (Tryptic Peptide)	2697.2	1.37E-09	8.8628	1.09E-07	PH-Control; PH-Ammonia
Indole-3-ethanol	2327.8	2.13E-09	8.6712	1.49E-07	Ammonia -Control; PH-Control
Atrazine	2112.3	2.8525E-09	8.5448	1.6497E-07	Ammonia -Control; PH- Ammonia
Glycerol-3-phosphate	2022.2	3.25E-09	8.488	1.65E-07	Ammonia -Control; PH-Control
CMP-Sialic acid	2021.9	3.25E-09	8.4878	1.65E-07	Ammonia -Control; PH-Control
Astilbin	1379.1	1.02E-08	7.9902	4.76E-07	PH-Control; PH-Ammonia
PS 37:04	765.86	5.9404E-08	7.2262	2.5498E-06	Ammonia -Control; PH-Control; PH-Ammonia
allo-Threonine	715.65	7.27E-08	7.1382	2.90E-06	PH-Control; PH-Ammonia
PE 38:02	284.79	1.1328E-06	5.9458	0.00004214	Ammonia -Control; PH-Control
PE (O-34:03)	45.702	0.00023373	3.6313	0.0081513	Ammonia -Control; PH-Control
Sorbitol	32.74	0.00059145	3.2281	0.019413	Ammonia -Control; PH-Control
N,N-Dimethylglycine	30.626	0.00071015	3.1487	0.022015	Ammonia -Control; PH-Control
Pantothenate	28.839	0.00083655	3.0775	0.022551	Ammonia -Control; PH- Ammonia
PC 34:02	28.822	0.000838	3.0768	2.26E-02	Ammonia -Control; PH-Control

D-allo-Isoleucine	28.686	0.000849	3.0712	2.26E-02	Ammonia -Control; PH-NH3
N-Acetylglutamate	25.653	0.0011478	2.9401	0.028623	Ammonia -Control; PH-Control
Alanine	25.391	0.0011798	2.9282	0.028623	Ammonia -Control; PH-NH3
N-Acetyl-L-aspartic Acid	24.091	0.0013579	2.8671	0.031572	Ammonia -Control; PH-Control
Stearic Acid (18:0)	22.984	0.001539	2.8128	0.033617	Ammonia -Control; PH-Control
Indoleacetaldehyde	22.832	0.0015664	2.8051	0.033617	Ammonia -Control; PH- Ammonia
Mannitol	20.965	0.0019616	2.7074	0.04054	Ammonia -Control; PH-Control
Riboflavin	19.872	0.0022566	2.6465	0.044971	PH-Control; PH-Ammonia
L-Tryptophanamide	19.588	0.0023426	2.6303	0.045076	Ammonia -Control; PH-Control
PE 36:05	18.741	0.0026273	2.5805	0.048867	Ammonia -Control; PH-Control

Supplementary Table 8: Relative abundance of NH_3 was calculated from equations Eq.1.0, 2.0 and 3.0 depicted in the main text. Table shows parameters and values for salinity (S), temperature (T), ionic strength (I), pKa^s and % NH_3 calculated. The pKa^s was calculated from the linear regression provided by Supplementary Figure 1.

Am (M)	Am (mg/L)	S (ppt)	pH	T (K)	I	pKa^s	NH_3 (mg/L)	% NH_3	% NH_4^+
0.010	170.31	11.688	8.05	301.15	0.236	9.274	11.96	7.0	93.0
0.025	425.78	11.688	8.96	301.15	0.236	9.274	161.97	38.0	62.0
0.050	851.55	11.688	9.38	301.15	0.236	9.274	525.89	61.8	38.2
0.100	1703.1	11.688	9.73	301.15	0.236	9.274	1334.08	78.3	21.7
0.250	4257.75	11.688	10.18	301.15	0.236	9.274	3877.22	91.1	8.9
0.500	8515.5	11.688	10.49	301.15	0.236	9.274	8124.94	95.4	4.6
1.000	17031	11.688	10.78	301.15	0.236	9.274	16621.2	97.6	2.4

Chapter 5 appendix: Spatiotemporal impacts of Enceladus- and Earth-relevant ammonia gas on cultivation of extremophile *Halomonas meridiana*

Supplementary Figure S1. Calibration curve of optical density readings at 600 nm coupled with cell viability. Column graph depicts optical density readings at 600 nm (OD_{600}) (left axis) and cell viability measured using the PrestoBlue™ cell viability assay (right axis) of *H. meridiana* over five time points within 24 h. Column heights present the mean ± s.d. (*n* = 3).

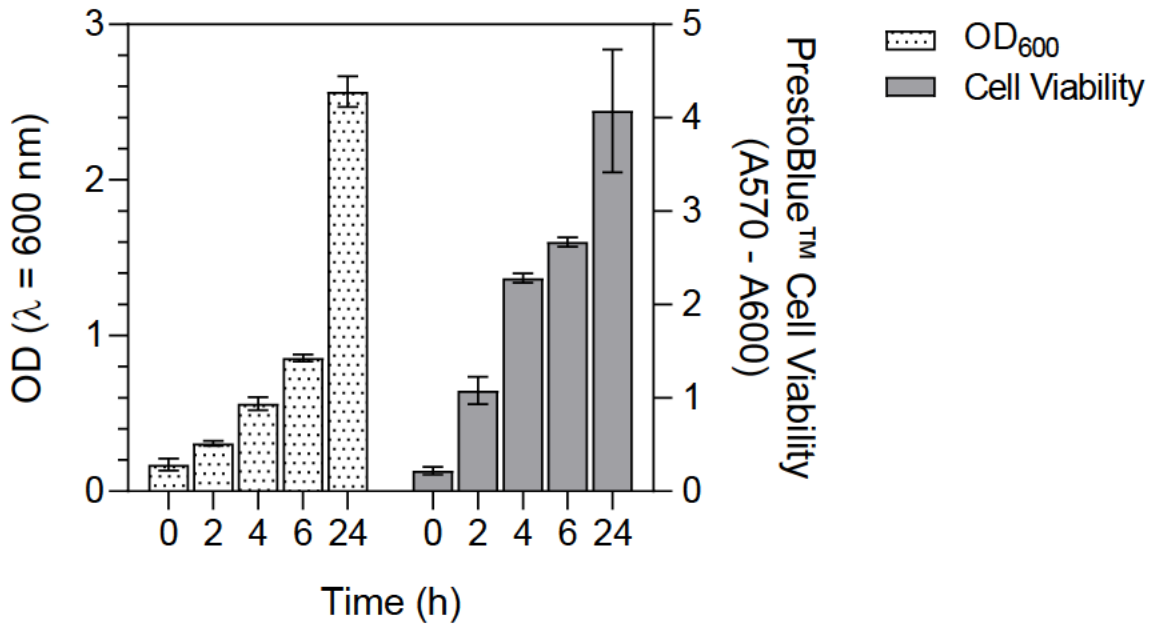

Supplementary Figure S2. Direct nesslerization calibration curve. Linear regression was created by measurement of known ammonia concentrations at 420 nm. Standard solutions of ammonia at known concentrations were provided by the CHEMetrics High Range VACUette Ammonia test kit (K-1510C). Linear regression equation utilised to calculate an unknown concentration of ammonia in ppm, X, is presented.

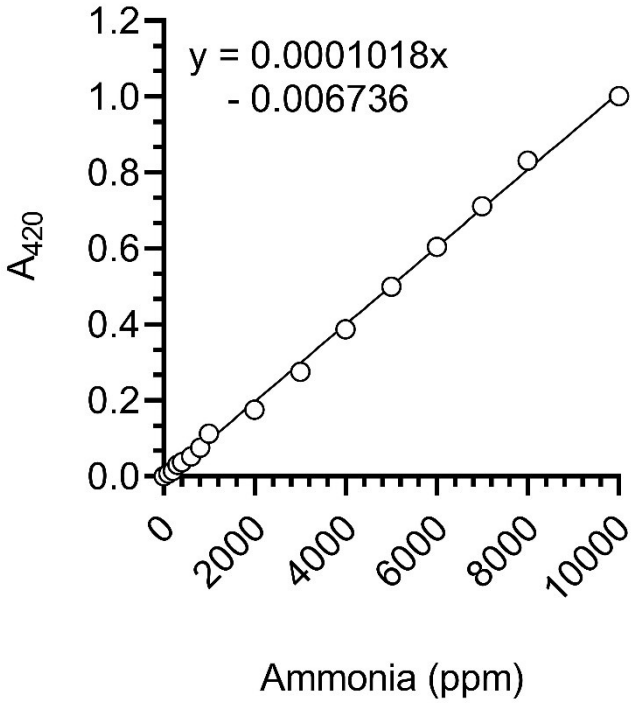

Supplementary Figure S3. Growth dynamics of H. meridiana directly and adjacently exposed to ammonia. Growth curves indicating optical density at 600 nm (OD_{600}) changes over time in *H. meridiana* directly exposed to and adjacently exposed to ammonia concentrations of (A) 0.1 M, (B) 0.25 M, (C) 0.5 M and (D) 1 M. All ammonia exposed cultures were compared to against growth of the control culture (0 M ammonia). Graph depicts mean ± S.D., with error indicated by area fill along error bands (*n* = 3).

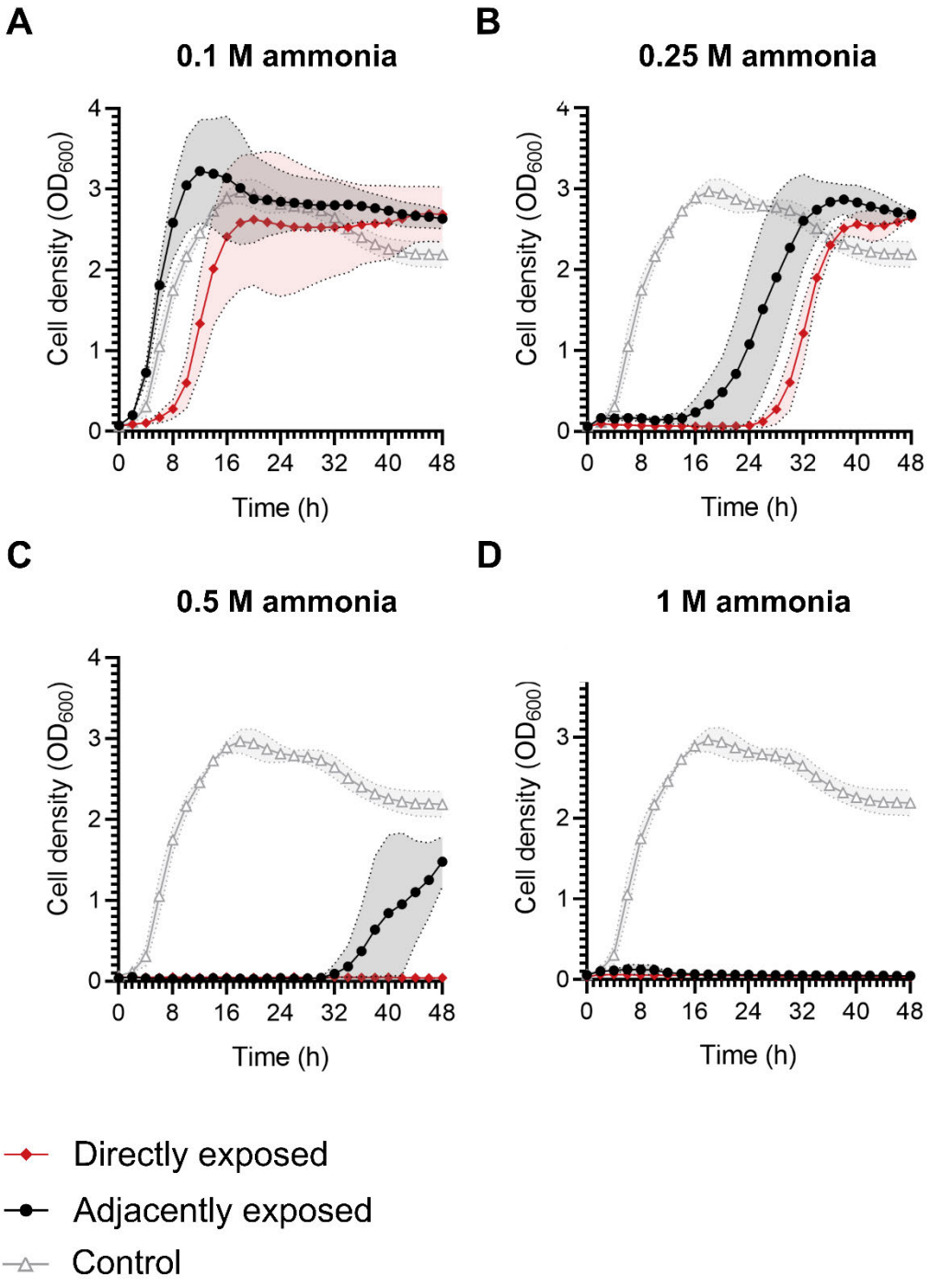

Supplementary Table S1. Statistical tests utilised in Figure 5 to compare mean lag phase, doubling time and Final OD_{600} of *H. meridiana* grown in control conditions (0 M ammonia), and directly and adjacently to ammonia solutions of 0.1 M, 0.25 M, 0.5 M and 1 M.

	Lag phase	**Doubling time**	**Final OD_{600}**
0.1 M	Kruskal-Wallis test, Dunn's multiple comparison test	One-way ANOVA, Tukey's multiple comparison test	Welch's ANOVA, Tamhane's T2 multiple comparison test
0.25 M	Kruskal-Wallis test, Dunn's multiple comparison test	Welch's ANOVA, Tamhane's T2 multiple comparison test	Kruskal-Wallis test, Dunn's multiple comparison test
0.5 M	Two-tailed unpaired t-test with Welch's correction	Two-tailed unpaired t-test with Welch's correction	One-way ANOVA, Tukey's multiple comparison test
1 M	n/a	n/a	Welch's ANOVA, Tamhane's T2 multiple comparison test

Microbial Ecology (2025) 88:111
https://doi.org/10.1007/s00248-025-02621-1

RESEARCH

Spatiotemporal Impacts of Enceladus- and Earth-relevant Ammonia Gas On Cultivation of Extremophile *Halomonas meridiana*

Cassie M. Hopton[1] · **Charles S. Cockell**[1]

Received: 26 June 2025 / Accepted: 28 September 2025

Abstract

One underexplored aspect of microbial growth is the impact of toxic gases transported through the atmosphere. Ammonia is a gas that can supply essential nitrogen but also exert cellular toxicity. Ammonia volatilized from a concentrated source into surrounding environments is therefore a crucial consideration when assessing the capacity of environments to support life, such as within terrestrial environments polluted with ammonia, or the ice crusts above ammonia–water oceans of icy moons. We cultivate *Halomonas meridiana* proximal to an ammonia source and examine the impact of ammonia volatilization on growth. Lower cell densities (OD_{600} = 0–1) occurred nearest the ammonia source. At 24 h, wells exhibiting an OD_{600} = 0–0.5 were evident when ammonia concentrations were ≥ 0.5 M. *H. meridiana* in proximity to 0 M, 0.1 M, 0.25 M, 0.5 M, and 1 M ammonia exhibited $OD_{600} > 2$ in 89.86%, 57.97%, 37.32%, 30.07%, and 18.48% of culture wells at 48 h, respectively. Alteration to growth kinetics and viability of *H. meridiana* cultivated adjacently to an ammonia source ("adjacently exposed") were not as severe compared to direct culture in ammonia ("directly exposed"). Compared to control, adjacent exposure to 0.1 M ammonia exerted no significant detrimental effect on growth kinetics and enhanced cell density, but adjacent exposure to ≥ 0.5 M ammonia greatly extended lag time, doubling time, reduced cell density, and reduced viability. Ammonia volatilized from 0.1 M sources may thus minimally affect, if not improve, habitability, whereas environments exposed to ammonia volatilized from sources at ≥ 0.5 M could constrain habitability.

Keywords Ammonia · Extremophiles · Habitability · Enceladus · Astrobiology · Pollution

Introduction

The habitability of an environment is influenced by its physicochemical conditions, the accessibility of chemical elements, nutrients and energy, and, distinctly, the availability of liquid water. Equally, the habitability of an environment can become constrained or limited by the presence of detrimental environmental components [1, 2]. One class of detrimental compounds is volatile toxic gases, which can be transported through the atmosphere. One such gas is ammonia (hereafter, the term "ammonia" is utilized to denote the total concentration of unionized ammonia, NH_3, and the ammonium ion, NH_4^+, in an environment). Ammonia is a bioavailable nitrogen source and metabolic input for many living organisms including bacteria [3–5]. However, the toxicity of ammonia has been demonstrated across a number of species, from bacteria to humans [6–9]. Notably, NH_3 possesses certain properties (e.g., small size and uncharged) which facilitates passive permeation through biological membranes. As a weak proton (H^+) acceptor, NH_3 readily reacts with H^+ to raise pH, disrupt proton motive force, and form NH_4^+ which impacts ionic balance [10–13]. The presence of NH_3 gas in the environment is therefore an important consideration when assessing habitability.

In aqueous environments, NH_3 exists in equilibrium with NH_4^+. The proportion of each species of ammonia is determined primarily by pH, but also temperature, pressure, and salinity [14–16]. Under standard Earth conditions (temperate and standard pressure) and pH exceeding 9.25, over half of ammonia is present as NH_3 gas. NH_3 is thus commonly released into the terrestrial atmosphere following application of ammonium fertilizer to alkaline soils. The process of release is known as volatilization—a

✉ Cassie M. Hopton
c.m.hopton@sms.ed.ac.uk

[1] UK Centre for Astrobiology, School of Physics and Astronomy, University of Edinburgh, James Clerk Maxwell Building, Peter Guthrie Tait Road, Edinburgh EH9 3FD, UK

Published online: 20 October 2025

phenomenon whereby ammonia transitions to the gas phase (NH_3) and escapes into the atmosphere. Due to volatilization, long-range dispersion and deposition of NH_3 has been well demonstrated [17–20]. Ammonia has been detected up to 3 km from a source pollution site and could be detected at a level of 5.1 μg/m^3 in natural reserves [20]. Despite the relatively short atmospheric lifetime of NH_3 which is in the order of hours to days [21–23], atmospheric transport can thus deposit ammonia into surrounding environments [24–26]. It is therefore possible for NH_3 to disperse from a concentrated, local source to distant environments. Such deposition may impact the habitability of afflicted environments.

As one of the simplest organisms on Earth, bacteria can provide a valuable foundation to examine growth limitations when considering habitability. Growth limitations in ammonia have been established for *Bacillus subtilis* [27, 28], *Escherichia coli* [28], *B. pasteurii*, *B. pumilus* [27], sulfate-reducing bacteria [29], and the extremophile *Halomonas meridiana* [30]. Increasing concentrations of atmospheric NH_3 has been found to reduce the number of viable bacteria [31]. NH_3 gas dissolved into environments from a distant source could thus be presumed to elicit one of two distinct effects. At low concentrations, the deposition of dispersed NH_3 could support the growth of organisms by providing essential nitrogen [32–36]. Alternatively, at high concentrations, NH_3 could exert adverse effects on the biodiversity of aquatic life, plants, invertebrates, and bacteria [37–41]. However, this binary effect of NH_3 has not been explicitly demonstrated in research. Additionally, NH_3 dispersed in the atmosphere can presumably alter growth over a wider spatial range than direct deposition but may be less toxic due to diminished concentration. The effects of NH_3 are also likely to be temporary as ammonia disperses into air over time. These facets of atmospheric NH_3 gas generate questions, such as what this spatial effect on bacterial growth could look like, and whether bacteria could recover from NH_3 gas exposure after complete dispersal. Such fundamentals are important when considering how terrestrial bacteria may be impacted by anthropogenic ammonia pollution.

Crucially, these fundamentals could also inform extraterrestrial habitability. Icy moons of our solar system feature liquid water subsurface oceans encased below thick ice shells [42–44]. The liquid state of the oceans has been thought to be preserved by anti-freeze components such as ammonia [45, 46]. Supporting this, mass spectrometry analysis by the Cassini–Huygens mission of the material ejected from the Southern plume of Saturn's icy moon Enceladus—presumed to originate from the subsurface ocean—measured ammonia at a volume mixing ratio of 0.4–1.3% [47, 48]. Enceladus features an availability of heat [49, 50], energy [51–53], nutrients [47, 48, 54, 55], and organics [47, 56], as well as liquid water, essential for prebiotic chemistry. Enceladus is thus a prominent target in astrobiology and the search for habitable environments beyond Earth.

On Enceladus, the spatial and temporal impact of NH_3 gas could be relevant to habitability prospects in the brine channels, veins, pockets, and fractures presumed to feature in the ice shell. These networks have been hypothesized as potentially habitable environments [57–60]. NH_3 gas may permeate into these environments through multiple pathways. In one pathway, NH_3 gas may be released and adsorbed onto the ice shell following exsolution from the ocean [61, 62] and migrate to the fluid networks by surface diffusion. Alternatively, ice fractures that are open to the surface may enable NH_3 volatilization on icy moons. This would depend on local temperature (−23 to 0 °C or higher) and pH (greater than pH 9) [63], as well as pressure. NH_3 can easily volatilize on Earth; the air contains trace amounts of ammonia, creating a strong gradient driving ammonia from environments to the air. On icy moons, NH_3 escape is governed by Henry's Law and vapor pressure equilibrium: colder temperatures reduce NH_3 volatility, and thus near-zero pressures are needed for NH_3 to escape, volatilize, from liquid. Such conditions could exist in ice shell fractures connected to the surface of Enceladus which is under near vacuum pressure. Volatilized NH_3 could then migrate along the fracture system and potentially solubilise into intersecting brine networks within the ice shell. As with exsolved NH_3, volatilized NH_3 may also absorb onto ice walls of the fracture and enter brine networks through ice diffusion [62]. It is not without mention that other prominent astrobiology targets, the icy moons Titan, Europa, Callisto and Ganymede, are also modelled with an internal ocean of NH_3 where spatial and temporal effects of NH_3 gas could be relevant [42, 46, 64]. However, the presence of NH_3 in these oceans has yet to be confirmed by direct measurements.

To characterize the habitability impacts exerted by volatilized and dispersed NH_3 gas, this work investigates the cultivation of *Halomonas meridiana* (nomenclature synonym: *H. aquamarina*) circumjacent to NH_3 gas. *H. meridiana* is a deep-sea bacterium with no specialized ammonia adaptations [65] but has extremophilic adaptations relevant to the physicochemical characteristics of the Enceladus ocean [66]. Indeed, we have previously shown *H. meridiana* can grow in concentrations of ammonia above the lower putative ammonia concentration threshold (0.01 M [61]) expected on Enceladus [30]. We utilize optical density readings to characterize the spatial impact of incrementally increasing concentrations of ammonia from 0.1 M to 1 M on growth. We analyze temporal recovery of cell density following exposure. Using growth kinetic and cell viability assays, we compare the growth kinetics of *H. meridiana* cultured adjacent to an ammonia source ("adjacently exposed") to those directly exposed to ammonia ("directly exposed"). Through this, we assess implications for the habitability of

environmental niches susceptible to NH_3 gas exposure such as those on the icy moon Enceladus as well as Earth.

Methods

Bacterial Strain Selection and Culture

The gram-negative bacterium *Halomonas meridiana* Slfth1 (DSM 15724) was obtained from the German Collection of Microorganisms and Cell Cultures (DSMZ). *H. meridiana* remains validly published as a heterotypic synonym according to the International Code of Nomenclature of Prokaryotes (ICNP). However, it should be noted this strain has been synonymized with *H. aquamarina* based on phylogenomic classifications [67]. *H. meridiana* was isolated from low temperature hydrothermal fluid at a depth of 2000 m. As such, *H. meridiana* presents physiological traits necessary for growth in this environment. This includes halophilic adaptations (growth in up to 22% NaCl), alkalitolerance (tolerance up to pH 12), psychrotolerant traits (growth at −1 °C and cold shock protein genes), and piezotolerance (growth at 550 bar) [65, 66, 68]. Evidence of hydrothermal systems is present on Enceladus [48, 52]. The isolation location and physiological adaptations exhibited by this organism therefore make it a suitable model for establishing the limits of life on Earth and potential for habitability on icy moons where cold, saline, alkaline, and high-pressure waters would be expected. Additionally, the strain genome hosts no known ammonia adaptations [65] (DDBJ, accession no. AP022821). This was an intentional choice. The estimated ammonia concentrations within icy moons oceans are low and may preclude the need for distinct ammonia adaptations. As such, the intention of this study was not to assess an already established ammonia adaptation, but to assess whether NH_3 gas acts as a chemical parameter that can affect habitability of organisms without ammonia adaptations. Pure cultures of *H. meridiana* were maintained in a simplistic yeast media consisting of 1 g/100 mL Bacto™ yeast extract (Becton, Dickinson and Company), 0.2 M NaCl (1.17% salinity) (Thermo Fisher Scientific, CAS Number: 7647-14-5), and distilled water (dH_2O) at pH 6. Cultures were cultivated aerobically in conical Erlenmeyer flasks with orbital agitation at 150 RPM and 28 °C.

Ammonia Preparation

All ammonia solutions were prepared from a stock solution of 35% liquid ammonia (Fisher Scientific, CAS Number: 1336-21-6). Stock ammonia was diluted in yeast media to molar concentrations of 0.1 M, 0.25 M, 0.5 M, and 1 M ammonia and maintained in air-tight falcon tubes to prevent gaseous escape. Control solutions of 0 M ammonia consisted of yeast media with no ammonia supplementation. The pH of all solutions was unaltered to preserve incrementally higher concentrations of NH_3 gas. The pH of each solution was recorded as follows: control (0 M), pH 6.06 ± 0.07; 0.1 M, pH 9.73 ± 0.01; 0.25 M, pH 10.18 ± 0.03; 0.5 M, pH 10.49 ± 0.01; and 1 M, pH 10.78 ± 0.02. The pH of solutions was determined with a Jenway 3510 benchtop pH meter.

Spatiotemporal Analysis of Ammonia Toxicity

Experiments were conducted in polystyrene 96-well plates. These plates were not air-tight and thus permitted ammonia to travel from wells to the exterior atmosphere. All wells, with exception of four central wells (D6, D7, E6, and E7), were plated with 190 µL yeast media inoculated with 10 µL overnight *H. meridiana* culture to an optical density at 600 nm (OD_{600}) of 0.05. A blank plate was created identically but without inoculation. The four central wells (D6, D7, E6, and E7) were plated with 200 µL ammonia at concentrations of either 0 M (control), 0.1 M, 0.25 M, 0.5 M, or 1 M, prepared as described above. Plates were incubated at 28 °C in a table-top orbital shaker at 150 RPM with OD_{600} readings taken at 24 and 48 h using a BMG SPECTROstar Nano Microplate Reader. Plates were shaken at 200 RPM before each reading. All plates were blank corrected against the blank plate before reading. Plate lids were utilized during incubation and analysis to ensure planar spread of NH_3 gas across the plate. The liquid culture depth was approximately 6 mm in a total well depth of 10.67 mm. An open space of 1 mm was between the well top and the plate lid.

Growth Experiments of Direct and Adjacent Ammonia Exposure

Growth experiments were conducted within polystyrene 96-well plates utilizing two distinct culture conditions: direct and adjacent ammonia exposure. In the direct ammonia condition, ammonia concentrations of 0 M (control), 0.1 M, 0.25 M, 0.5 M, and 1 M in yeast media were prepared as outlined above and dispensed into five wells. Ammonia solutions were inoculated with 10 µL overnight culture of *H. meridiana* to $OD_{600} = 0.05$ in a final volume of 200 µL (Fig. 1A). In the adjacent ammonia condition, five wells of yeast media were inoculated with 10 µL overnight culture of *H. meridiana* to $OD_{600} = 0.05$ in a final volume of 200 µL. Five wells directly adjacent to these culture wells were supplemented with ammonia in yeast media to concentrations of 0 M (control), 0.1 M, 0.25 M, 0.5 M, or 1 M ammonia (Fig. 1B). In both growth conditions, separate 96-well plates were used for each ammonia concentration. Negative controls had no inoculation.

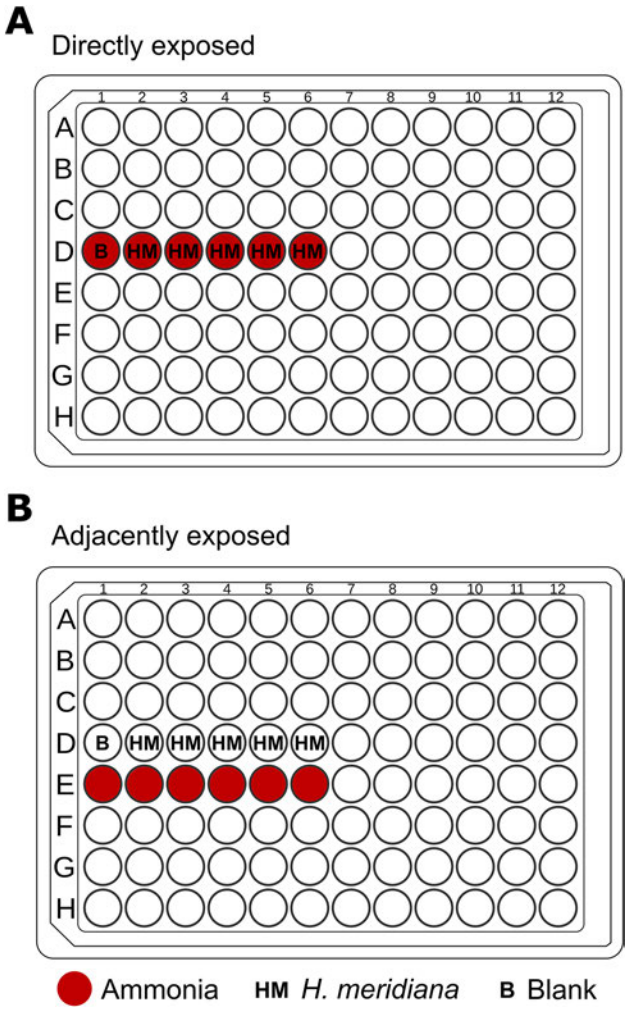

Fig. 1 Diagram of "directly" and "adjacently" exposed cultures to ammonia. (**A**) Depiction of *H. meridiana* cultures directly exposed to ammonia (red circles). *H. meridiana* (HM) is cultivated in yeast media with ammonia to concentrations of 0.1 M, 0.25 M, 0.5 M, or 1 M ammonia. (**B**) Depiction of *H. meridiana* cultures adjacently exposed to ammonia. *H. meridiana* is cultivated in yeast media without ammonia. Ammonia at concentrations of 0.1 M, 0.25 M, 0.5 M, or 1 M were placed in the wells directly below these cultures. Blank (B) solutions are identical but are without inoculation of *H. meridiana*

Kinetic Growth Assays and Parameters

Following preparation of the growth experiments as outlined above, growth over time was assessed using OD_{600} readings over 48 h in a BMG SPECTROstar Nano Microplate Reader. Plates were shaken at 200 RPM before each reading. Growth parameters of lag phase duration, doubling time, and final OD_{600} at 48 h were extrapolated from the OD_{600} growth curve. Lag phase duration was determined using the online microbial lag phase calculator developed by Smug et al. [69]. The following parameters were applied: algorithm = parameter fitting to a model; preprocessing applied: cut data at some time = yes, max time = 24 or 48 h; smooth data = no; initial biomass = first observation; model to fit = logistic; NLS fitting algorithm = auto; and max number of iterations = 100. Doubling time was derived from the growth rate, μ, by the equation $\ln 2/\mu$. Calculation of μ is presented in Eq. 1.0. N_0 is the OD_{600} at a beginning time interval (t_0) in the exponential growth phase. N is the OD_{600} at the end of a selected time interval (t) in the exponential growth phase. t and t_0 were recorded in minutes.

$$\mu = \left(\mathrm{Log}_{10}(N) - \mathrm{Log}_{10}(N_0)\right)2.303/(t - t_0) \quad (1)$$

Final cell density was determined at 48 h using the final OD_{600} value obtained. We defined no growth as any analysis where there was no defined lag or exponential phase after 48 h. Increases to OD_{600} were confirmed to correspond to increases in cell viability (Supplementary Fig. S1).

Cell Count

Cell viability of *H. meridiana* was assessed in cultures directly and adjacently exposed to ammonia. The experimental set-up of the two conditions occurred analogously to that described in the growth experiments. Then, 96-well plates were incubated for 4 h at 28 °C on a table-top orbital shaker at 150 RPM. This incubation period was found to be a suitable length of time to allow volatilization of NH_3 from the central ammonia wells and complete dispersal across adjacent wells utilized for testing. The duration is also within the doubling time range of *H. meridiana* (i.e., 1 to 2 h). Following incubation, cell numbers were determined using colony forming units (CFU) on yeast media agar plates incubated at 28 °C.

Evaluation of Ammonia Concentration

Volatilization and permeation of NH_3 from and into cultures that were directly and adjacently exposed to ammonia was assessed by using the CHEMetrics High Range VACUette Ammonia test kit (K-1510C). The K-1510C kit features a detection range of 0–10,000 ppm ammonia and a detection limit of 100 ppm. Precision data is not available for this kit. However, a related kit, K-1513, has shown precision of ± 11 ppm at 112 ppm. This kit measures ammonia by a direct nesslerization reaction. Direct nesslerization determines ammonia concentration by a reaction of ammonia with potassium mercuric iodide. This produces a yellow-colored complex, the Nessler reaction product, which can be measured at 420 nm [70]. The experimental set-up of the two conditions occurred as described in the growth experiments. A 4-h incubation period was identified as a suitable length of time that could allow NH_3 volatilization, dispersal, and dissolution into adjacent cultures. Plates were incubated

for 4 h at 28 °C on a table-top orbital shaker at 150 RPM. The parts per million (ppm) of ammonia in each culture was determined by colorimetric analysis of the Nessler reaction product at 420 nm. Ammonia content in ppm was determined by linear regression; the absorbance of the culture sample at 420 nm was compared against a calibration curve created by absorbance of known concentrations of ammonia at 420 nm (Supplementary Fig. S2). Molarity (M) was derived from ppm as shown in Eq. 2.0. Where 1 ppm ≅ 1 mg/L, and molar mass refers to the molar mass of ammonia at 17.031 g/mol.

$$M = \frac{(\text{ppm}/1000)}{Molar\ mass} \tag{2}$$

Statistics and Reproducibility

All data were compiled from a minimum of three biological replicates ($n = 3$ to 4). The Shapiro–Wilk test was utilized to assess normality of data. Where the assumption of normality was violated, two groups were analyzed by the Mann–Whitney test or, for three or more groups, by the Kruskal–Wallis test. Multiple comparison correction was applied using Dunn's test. Where normality was not violated, sample variance was assessed by an *F*-test for two groups. Samples of equal variance were analyzed by two-tailed unpaired *t*-test. If the assumption of variance was violated, a two-tailed unpaired *t*-test with Welch's correction was applied. For three or more groups, the Brown–Forsythe test was utilized to assess equal variance. Samples of equal variance were analyzed by analysis of variance (ANOVA) followed by Tukey's post hoc test. Samples of unequal variance were assessed by Welch's ANOVA test with Tamhane's T2 post hoc test. Data is presented as the mean ± standard deviation (SD). Significance was considered when $p < 0.05$. Statistical tests are specified in figure legends as well as the supplementary material when indicated. All figures and statistical analyses were produced using GraphPad Prism version 8.0.2 (GraphPad Software Inc.).

Results

Spatiotemporal Toxicity of Ammonia

NH_3 is a gas under temperate conditions and standard pressure. The spatiotemporal impact of NH_3 on bacterial cultures was assessed using 96-well plates. Plates were prepared with four central wells containing either yeast media (0 M ammonia, control) or ammonia at concentrations of 0.1 M, 0.25 M, 0.5 M, and 1 M. The peripheral wells were filled with yeast media inoculated with *H. meridiana*. Figure 2A-–2E is a heatmap illustrating the cell density of wells surrounding ammonia concentrations of 0 M (control, Fig. 2A), 0.1 M (Fig. 2B), 0.25 M (Fig. 2C), 0.5 M (Fig. 2D), and 1 M (Fig. 2E) at 24 h and 48 h post-inoculation. Cell density is given by optical density values at 600 nm (OD_{600}). Values of cell density are characterized as follows: 0—red, 0.5—orange, 1—yellow, 1.5—green, and ≥2—dark green. Figure 2F-G indicate the total number of wells, as a percentage of the total number of culture wells (92), that reached cell densities between 0–0.5, > 0.5–1, > 1–2, and > 2 OD_{600} at 24 h and 48 h, respectively, for each control and ammonia treatment condition.

Figure 2 demonstrates a pronounced suppression of cell density which was most severe in proximity to the ammonia source as ammonia concentration increases. Culture wells circumjacent to the control solution at 24 h and 48 h, with exception of a single well in each case, showed an average cell density at or exceeding 2 (Fig. 2A). At 24 h, 43.12% of culture wells in the control condition were at a cell density between $OD_{600} > 1$–2 and 55.8% of wells at a cell density $OD_{600} \geq 2$ (Fig. 2F). At 48 h, 89.86% wells exhibited a cell density of $OD_{600} \geq 2$ (Fig. 2G). The control represents typical growth densities that would be expected of *H. meridiana* when cultivated in optimal conditions. In culture wells circumjacent to 0.1 M ammonia, all wells with exception of one exceeded a cell density of $OD_{600} = 1$ (Fig. 2B). At 48 h, 57.97% of wells were $OD_{600} \geq 2$. This was lower than the number of wells at or exceeding a cell density of $OD_{600} \geq 2$ at 48 h in the control condition ($p < 0.01$), but higher than the number of wells at a cell density of $OD_{600} \geq 2$ when compared against the 0.25 M ($p < 0.05$) and 0.5 M ($p < 0.01$) ammonia conditions at 48 h (Fig. 2G).

The majority of cultures wells circumjacent to ammonia at a concentration of 0.25 M exhibited a cell density between $OD_{600} = 1$ and $OD_{600} = 2$ at both 24 h and 48 h (Fig. 2C). In this culture system, 19.93% of wells exhibited cell density values of $OD_{600} \geq 2$ at 24 h (Fig. 2F). This increased to 37.32% at 48 h (Fig. 2G). The number of wells at a cell density of $OD_{600} \geq 2$ was found to be nonsignificantly different from the 0.1 M ($p = 0.0664$), 0.5 M ($p = 0.808$) and 1 M ammonia ($p = 0.101$) conditions but lower than the control condition at 48 h ($p < 0.0001$) (Fig. 2G).

In the 0.5 M ammonia condition, 9.78% of wells exhibited a cell density of $OD_{600} \geq 2$ at 24 h (Fig. 2F). The number of wells at this level increased to 30.07% at 48 h but was still lower than that observed in control ($p < 0.0001$) and 0.1 M ammonia ($p < 0.05$) conditions (Fig. 2G). A cell density of $OD_{600} < 0.5$ at 24 was observed in 6.52% of wells (Fig. 2F), but none were observed at this level at 48 h (Fig. 2G). Comparatively, 7.97% of wells exhibited a cell density of $OD_{600} \geq 2$ when surrounding 1 M ammonia at 24 h, while 33.7% of wells exhibited an $OD_{600} < 0.5$ (Fig. 2F). At 48 h, the number of wells at a cell density of $OD_{600} \geq 2$

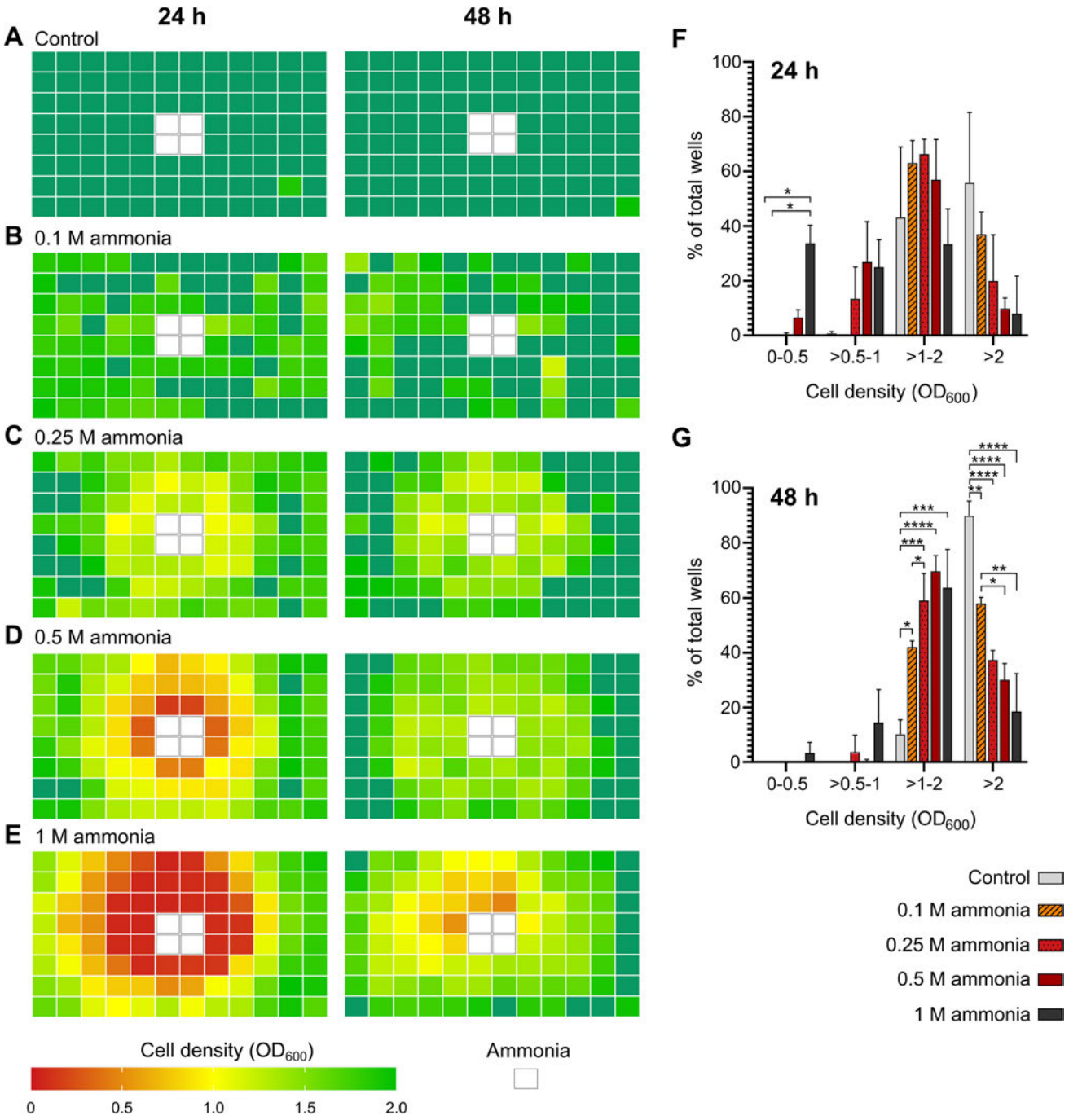

Fig. 2 Spatiotemporal effect of ammonia on growth of *H. meridiana*. (**A–E**) Heatmaps representing the mean OD_{600} of wells in a 96-well plate ($n = 3$). Central wells (D6, D7, E6, and E7) were filled with either 0 M (control), 0.1 M, 0.25 M, 0.5 M, or 1 M ammonia as indicated by white squares. Surrounding wells were yeast media inoculated with *H. meridiana*. OD_{600} values were recorded 24 h and 48 h post-inoculation to ammonia. OD_{600} values were coloured as follows: 0, red; 1, yellow; 2, green; and > 2, dark green. (**F, G**) Cell density changes with increasing ammonia concentrations. For each concentration of ammonia, the number of wells between OD_{600} 0–0.5, > 0.5–1, > 1–2, and > 2 at 24 h and 48 h post-inoculation was determined and calculated as a percentage of the total number of inoculated wells (92). The results are represented as a column graph with column heights and error bars indicating the mean ± S.D ($n = 3$). Statistical significance in (**F**) and (**G**) is given by the Kruskal–Wallis's test using Dunn's multiple comparison test for optical density groups 0–0.05 and > 0.5–1, and one-way ANOVA using Tukey's multiple comparison test for optical density groups > 1–2 and > 2. ns, no significance; *, $p < 0.05$; **, $p < 0.01$; ***, $p < 0.001$; ****, $p < 0.0001$

increased to 18.48%, but the majority of wells were between $OD_{600} = 1–2$ (63.77%) and 3.62% of wells were at a cell density of $OD_{600} < 0.5$ (Fig. 2G). Notably, there was no significant difference found between the mean percentage of wells between > 0.5–1, > 1–2, and > 2 OD_{600} compared across all treatment concentrations at 24 h, but treatment with 1 M ammonia significantly increased the number of wells between $OD_{600} = 0–0.5$ compared to control ($p < 0.05$) and 0.1 M conditions ($p < 0.05$) (Fig. 2F).

For *H. meridiana* cultivated proximal to 0.25 M, 0.5 M, and 1 M ammonia, lower cell density values ($OD_{600} < 1$) were nearer to the ammonia source at both 24 h and 48 h, while the horizontal and vertical perimeter wells showed higher cell densities ($OD_{600} > 1$) (Fig. 2C-–2E). In addition, the radial distribution of NH_3 was reflected in cell density alterations; the spatial zone of alterations became larger as ammonia concentration increased.

Kinetics of *H. meridiana* Cultivated Directly and Adjacently to Ammonia

Wells immediately adjacent to the ammonia source showed a lower cell density than those farther from the ammonia source. The lower cell density suggests an alteration to growth kinetics. Given the small (9 mm) distance from the ammonia source, the impact to growth kinetics could be similarly observed in *H. meridiana* directly exposed to ammonia. To explore this possibility, the growth dynamics of *H. meridiana* directly exposed to ammonia and adjacently exposed to an ammonia source were investigated and lag phase duration (Fig. 3A-–3C), doubling time (Fig. 3D-–3F), and final cell density (OD_{600}) at 48 h (Fig. 3G-–3J) extrapolated. The growth curves utilized to extrapolate these growth parameters is available in Supplementary Fig. S3. *H. meridiana* exhibited an extension to lag phase duration when directly cultivated in all concentrations of ammonia. Adjacent cultivation to ammonia increased the duration of the lag phase at concentrations of 0.25 M and 0.5 M ammonia, but not 0.1 M ammonia (Fig. 3A-–3D). *H. meridiana* cultivated adjacent to 0.1 M ammonia wells assumed a lag phase time of 0.2 h ± 0.141 (Fig. 3A). This was a shorter duration than those cultivated directly in 0.1 M ammonia (6.13 h ± 1.55). Differences between lag phase duration of *H. meridiana* cultivated adjacently to 0.1 M ammonia was found to be non-significant from cells cultivated directly in ammonia ($p = 2.00$) and in control conditions ($p = 0.665$). Similarly, *H. meridiana* cultivated adjacent to 0.25 M ammonia wells assumed a lag phase time of 18.15 h ± 4.62 (Fig. 3B). This was a shorter duration than those cultivated directly in 0.25 M ammonia (25.65 h ± 1.72). Differences between lag phase duration of *H. meridiana* cultivated adjacently to ammonia were found to be non-significant from cells directly exposed to ammonia ($p = 0.485$) and to control conditions ($p = 0.267$).

In Fig. 3D, the doubling time of cells cultivated adjacently to 0.1 M were comparable to growth in control conditions ($p = 0.989$) and faster than cells cultivated directly in 0.1 M ammonia ($p < 0.001$). Conversely, as ammonia concentration increased, cells adjacent to 0.25 M ammonia showed comparable doubling time to cells cultivated directly in 0.25 M ammonia ($p = 0.271$). This was longer when compared to control conditions ($p < 0.05$) (Fig. 3E). *H. meridiana* adjacently exposed to ammonia showed comparable final OD_{600} to cells cultivated directly in ammonia at concentrations of 0.1 M ($p = 0.991$) (Fig. 3G) and 0.25 M ($p = 0.999$) (Fig. 3H). Notably, the cell density at 48 h was significantly higher in cells cultivated adjacently to ammonia than those in control conditions at 0.1 M ammonia ($p < 0.05$) (Fig. 3G) and 0.25 M ammonia ($p < 0.05$) (Fig. 3H). *H. meridiana* did not show an observable lag, log or stationary phase when cultivated directly in 0.5 M ammonia but did show onset of growth at ~ 30 h post-inoculation when cultivated adjacently to a 0.5 M ammonia source (Supplementary Fig. S3). Consequently, cultures adjacent to 0.5 M ammonia exhibited a higher final cell density compared to cells cultivated directly in 0.5 M ammonia ($p < 0.0001$) (Fig. 3I). *H. meridiana* cultivated adjacently to 0.5 M were found to have a longer lag phase duration ($p < 0.01$) (Fig. 3C), slower doubling time ($p < 0.05$) (Fig. 3F) and lower final cell density ($p < 0.01$) (Fig. 3I) than *H. meridiana* in control conditions. No growth was recorded in *H. meridiana* cultivated directly in or adjacently to 1 M ammonia (Supplementary Fig. S3). OD_{600} at 48 h in both conditions thus remained at 0.05 (Fig. 3J).

Cell Viability and Ammonia Content in *H. meridiana* Cultures Directly and Adjacently Exposed to Ammonia

Lag phase duration of *H. meridiana* increased incrementally when cultivated adjacently to higher concentrations of ammonia. We have previously shown this extension to lag phase duration is a result of reduced viable cell populations correlating with ammonia concentration [30]. Figure 4 shows cell number of *H. meridiana* and ammonia content in cultures following 4 h of direct and adjacent exposure to ammonia. Control conditions without ammonia are also shown. Across all directly exposed ammonia cultures, the concentration of ammonia was diminished from original inoculation concentration at 4 h confirming ammonia volatilization from wells over time. Gaseous NH_3 solubilized into adjacent cultures from an ammonia source was indicated by detectable levels of ammonia in these wells.

Differences in cell number were nonsignificant between control cultures and cultures adjacent to 0.1 M ($p = 0.794$) (Fig. 4A). This aligned with a nonsignificant change in lag phase between this condition and control conditions in Fig. 3A. The ammonia content in 0.1 M ammonia adjacently

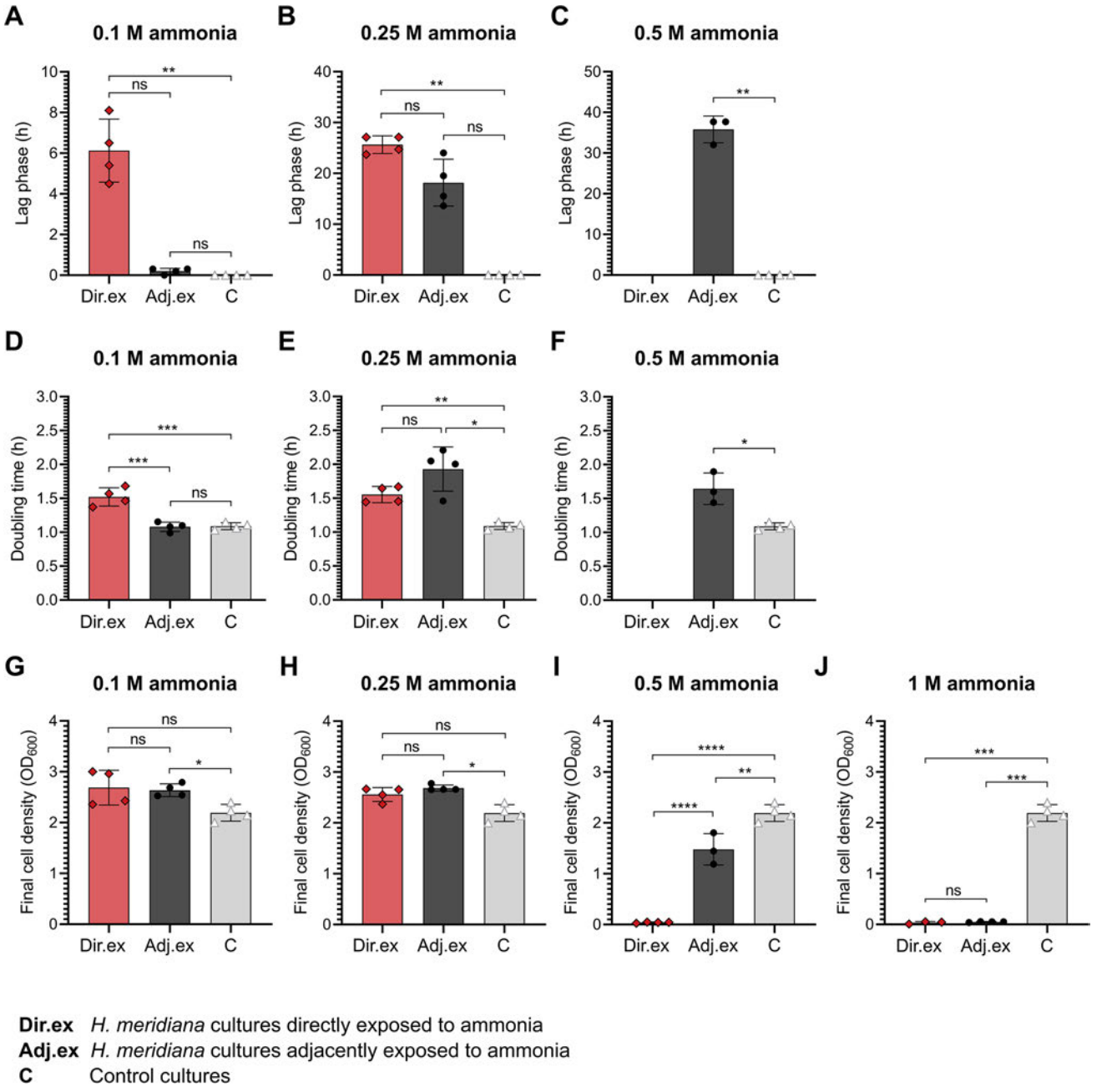

Fig. 3 Growth kinetics of *H. meridiana* cultivated directly and adjacently to ammonia. (**A–C**) Lag phase time, (**D–F**) doubling time, and (**G–J**) final OD_{600} of *H. meridiana* at 48 h extrapolated from growth curves of Supplementary Fig. S3. Column heights indicate the mean ± S.D. ($n = 3$ to 4). Statistical significance was calculated by one-way ANOVA, Welch's ANOVA, Kruskal–Wallis test and Welch's unpaired *t*-test. The individual tests utilised are outlined in Supplementary Table S1. ns, no significance; *, $p < 0.05$; **, $p < 0.01$; ***, $p < 0.001$; ****, $p < 0.0001$

exposed cultures at 0.0308 M ± 0.0002, however, was significantly higher than those in the control condition ($p < 0.0001$). This indicates 0.1 M was not a concentration that detrimentally impacts cell number, and in turn, lag phase duration. Cell number was lower in cultures directly exposed to 0.1 M ammonia compared to adjacently exposed to ammonia ($p < 0.01$) and control conditions ($p < 0.01$). In correlation with this, ammonia content in directly exposed cultures at 0.0538 M ± 0.004 was higher than those in adjacently exposed ammonia cultures ($p < 0.001$) or control cultures ($p < 0.0001$) (Fig. 4A). This correlates with the results of Fig. 3A that demonstrate direct exposure of *H. meridiana* to 0.1 M ammonia increases lag phase duration compared with control.

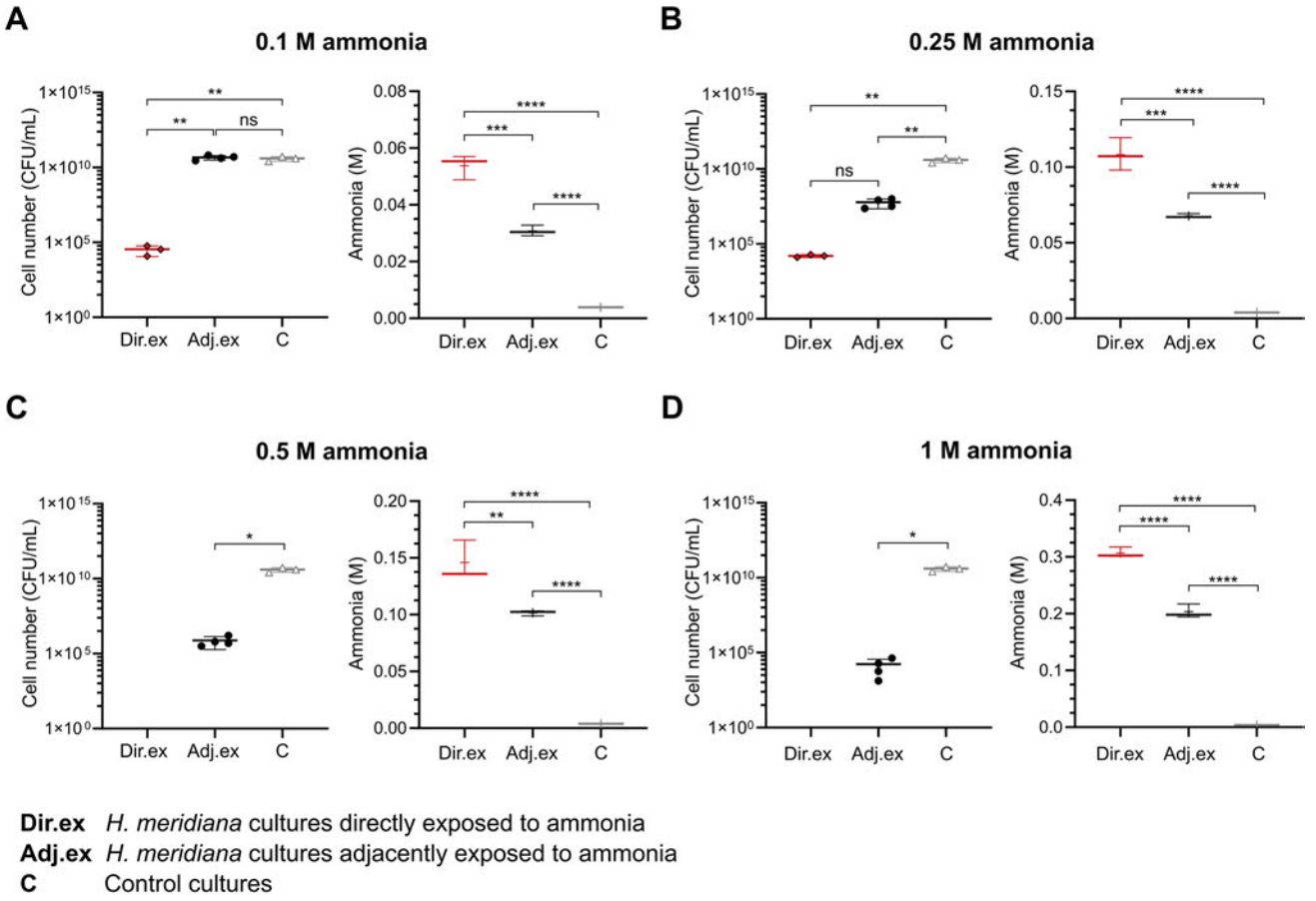

Fig. 4 Cell number and ammonia content of *H. meridiana* cultures exposed to ammonia. Cell number and ammonia content at 4 h in *H. meridiana* cultures following direct and adjacent exposure to ammonia concentrations of 0.1 M (**A**), 0.25 M (**B**), 0.5 M (**C**), and 1 M (**D**) are shown. Comparison to cell number and ammonia content in 0 M (control) cultures for each concentration is illustrated. Cell number is given by CFU/mL in individual value scatter plots. Mean is indicated by the central line between individual points ($n=3$). Error bars are ± S.D. Statistical significance was calculated by one-way ANOVA with Tukey's post hoc test (0.1 M and 0.25 M) or two-tailed unpaired *t*-test with Welch's correction (0.5 M and 1 M). Ammonia concentration is depicted in box plots that show molar concentrations of ammonia measured in culture solutions 4 h post direct and adjacent exposure to ammonia. Box plots represent the median as well as the 25% and 75% interquartile ranges. The whiskers represent 1.5 × the interquartile ranges. Plus sign (+) indicates the mean and the middle line indicate the median ($n=3$). All statistical tests here correspond to one-way ANOVA with Tukey's post hoc test. ns, no significance; *, $p < 0.05$; **, $p < 0.01$; ***, $p < 0.001$; ****, $p < 0.0001$

Differences in cell number were significant between control cultures and cultures adjacent to 0.25 M ammonia ($p < 0.01$) (Fig. 4B). Cultures adjacently exposed to 0.25 M showed a concentration of ammonia at 0.0677 M ± 0.000 which was significantly higher than control cultures ($p < 0.0001$). This level of ammonia may account for cell number reduction in ammonia-adjacent cultures. However, the level of viable cell loss was not found to impact lag phase duration significantly between ammonia-adjacent and control cultures, as indicated in Fig. 3B. As a result of viable cell loss, cell number changes in cultures adjacently exposed to 0.25 M were found to be non-significant from cultures directly exposed to 0.25 M ($p = 0.999$) (Fig. 4B). The non-significant change in cell number between directly and adjacently exposed cultures did not correlate with ammonia. Cultures adjacently exposed to 0.25 M showed a lower ammonia concentration than cultures directly exposed to 0.25 M, which were found to be 0.108 M ± 0.01 ($p < 0.001$). These results indicate, while not as cytotoxic as direct ammonia exposure, adjacent exposure to 0.25 M ammonia demonstrates detrimental effects on viability. This may account for the longer doubling time observed in cultures adjacently exposed to 0.25 M (Fig. 3E) which was not observable in cultures adjacently exposed to 0.1 M (Fig. 3D).

There were no viable *H. meridiana* cultivated directly in 0.5 M (Fig. 4C) and 1 M ammonia (Fig. 4D). These solutions also demonstrated the highest ammonia content compared to adjacent and control cultures, with ammonia concentrations of 0.146 M ± 0.02 and 0.307 M ± 0.009,

respectively. These concentrations were thus deleterious to *H. meridiana.* There were viable cells in cultures adjacent to 0.5 M and 1 M ammonia. This indicated adjacent cultures did not acquire ammonia to the concentrations observed in direct cultures at any point. Indeed, the ammonia content of ammonia-adjacent cultures was significantly lower than those in directly exposed cultures at 0.5 M (0.102 M ± 0.002, $p < 0.01$) and 1 M ammonia (0.203 M ± 0.01, $p < 0.0001$). Compared to control, the cell number in cultures adjacently exposed to 0.5 M ($p < 0.05$) (Fig. 4C) and 1 M ($p < 0.05$) (Fig. 4D) were lower. In accordance with this, the ammonia content was found to be significantly higher in cultures adjacent to 0.5 M ($p < 0.0001$) and 1 M ammonia ($p < 0.0001$) solutions compared to control.

Discussion

The aim of this work was to characterize the spatiotemporal effect of NH_3 gas on the cultivation of an extremophile, *H. meridiana.* Although the habitability of extraterrestrial environments is speculative, ammonia is known to be a component of extraterrestrial oceans [46, 47, 71]. Thus, our findings have relevance to the potential for habitability in these environments. Additionally, NH_3 volatilization, resulting from agricultural and industrial pollution [72, 73], can deposit ammonia at great distances and may alter habitability in environments on Earth beyond the local site of release [17–20]. These results therefore advance the current understanding on how the gaseous state of NH_3 may permeate into environments and impact the potential for a habitat to become or remain inhabited.

Although previous studies have investigated the effects of toxic gases on microbial growth, none of these studies have examined the spatial effects of gas on microbial growth. In literature, the growth of a diverse range of bacteria has shown to be disturbed most closely to a pollutant source. For example, as in the case of soils nearby tailing ponds of seepage pollution [74] or soils with crude oil contamination [75]. In accordance with this, we observed reduction of cell density nearest to an ammonia source. We also identified that increasing concentrations of NH_3 gas increased the spatial size of the zone affecting cell density. The effects we observed are analogous to diffusion-limited effects observed in agar plates. An increasing zone of inhibition with increasing concentration of a toxic substance has been demonstrated in agar diffusion assays using non-gas substances such as propolis extract [76], lauric acid-KOH [77], chromium [78], and a range of organics, inorganics and organometallics [79]. Likewise, an increasing spatial zone of antibacterial activity has been observed for application of increasing concentrations of reactive oxygen species on *Pseudomonas aeruginosa* [80] and *E. coli* [81]. Our findings show how microbial growth can also be influenced by compounds, such as NH_3, traversing through the atmosphere as well as through liquid media.

A notable alteration was that *H. meridiana* cultivated adjacently to ammonia at concentrations of 0.1 M and 0.25 M were able to establish a higher density at 48 h compared to control conditions. It is possible these concentrations were low enough, particularly following evaporation, that diffusion of NH_3 across the cytoplasmic membrane into the cell in equilibrium with NH_4^+ were sufficient to promote growth by providing additional nitrogen [82]. NH_4^+ is assimilated by either the glutamine synthetase-glutamate synthase (GS-GOGAT) or glutamate dehydrogenase (GDH) pathway. In enzymology, K_m is the substrate concentration at which an enzyme's reaction is half of its maximal velocity, V_{max}. K_m values for GS, GOGAT, and GDH have been reported at 0.033 M [83, 84], 0.0002 M [85], and 0.029 M [86] in bacteria. At 4 h, the ammonia concentration in wells adjacent to 0.1 M were 0.0308 M ammonia, and adjacent to 0.25 M ammonia were 0.0678 M ammonia. These concentrations are thus suitable for GS and GDH to achieve 50% velocity or higher according to Michaelis–Menten kinetics and may account for enhanced cell density compared to control.

In *Halomonas*, ammonia nitrogen removal, and thus assimilation, rates have been reported at 5 mg N L^{-1} h^{-1} in the species *H. salifodinae* [87], 9.10 mg N L^{-1} h^{-1} for strain HN2 [88] and 22 mg N L^{-1} h^{-1} in strain B01 [89]. This approximately corresponds to the respective removal, and possible assimilation, of NH_4^+ at ≈ 0.00036 M h^{-1}, ≈ 0.00064 M h^{-1}, and ≈ 0.0016 M h^{-1}. As aforementioned, cultures adjacent to 0.1 M and 0.25 M ammonia sources were found to accumulate ammonia at 4 h to concentrations of 0.0308 M and 0.0677 M, respectively. This indicates the ammonia provided into the wells were near 20-fold and 42-fold higher than the concentration utilised in assimilation per hour. Such abundance may have stimulated higher growth than the control which featured limited amounts of ammonia.

Such abundance of ammonia could also be deleterious to growth, however. While enhanced cell density was observed in cultures adjacent to 0.25 M ammonia, lag phase duration was higher, doubling time was slower and cell viability also lower compared to control. In contrast to 0.1 M ammonia, cultures adjacent to 0.25 M showed ammonia values that were substantially higher than the K_m values required for 50% V_{max} in nitrogen assimilation enzymes and typical rates of nitrogen assimilation. Ammonia at 0.25 M ammonia thus reflects a transition concentration whereby excess ammonia becomes deleterious to growth. It is notable adjacent exposure to NH_3 gas at a concentration of ≥ 0.5 M is the limit at which the following effects were observed: (i) reduced cell density surrounding the ammonia source ($OD_{600} < 0.5$); (ii) increased lag phase duration and doubling time; and (iii)

reduced cell number of *H. meridiana* from control conditions. Cultures adjacent to 0.5 and 1 M solutions may have experienced enhanced nitrogen assimilation but likely experienced an overriding toxicity effect including internal alkalization and disruption to the internal H^+ pool that ultimately led to the deleterious growth effects described. This is a function of ammonia concentration; we have previously demonstrated 0.05 M ammonia as a habitable limit for *H. meridiana* [30]. It is thus in accordance with this that cultures adjacent to 0.1 M ammonia showed an ammonia content below this limit. Concentrations above this limit were observed in 0.25 M, 0.5 M, and 1 M cultures where growth or viability was significantly impacted. Our findings indicating a correlation between increased concentrations of NH_3 gas and reduced cell growth has also been demonstrated using other forms of toxic gas [90–96].

In extraterrestrial icy worlds, ammonia is a primordial component incorporated into subsurface oceans. Fluid networks are expected within the overlying ice shells and could function as potential habitats [57–60]. It is possible fluids within the ice shell networks closely mimic, or are identical to, the composition of the ocean below and thus contain ammonia. However, it is feasible NH_3 gas may also be formed in these environments and thus influence habitability in addition to solubilised ammonia. For example, NH_3 gas may be produced by a process of exsolution at the plume vent region of Enceladus and expelled. NH_3 gas adsorbed onto the plume vent ice walls may then migrate through the ice shell to fluid networks. Alternatively, fractures through the ice shell that connect to the near vacuum surface could provide the pressure to facilitate NH_3 volatilization from connected fluid networks or the ocean if also permitted by pH and temperature. Volatilized NH_3 migrating up a fracture shaft may then disperse and dissolve into other fluid networks that intersect with the fracture region, impacting the potential for habitability in these environments.

The work presented here mimics an NH_3 exposure scenario. We have shown that the spatial migration of ammonia impacts the concentration of ammonia dissolved into a solution and thus the growth of *H. meridiana*. We provide proof-of-principle evidence that the concentration of ammonia solubilized determines whether growth is facilitated or hindered. At low concentrations, addition of bioavailable nitrogen in the form of ammonia can facilitate growth, while higher concentrations can exert toxic cellular effects. On Enceladus, a hypothetical scenario can be argued; NH_3 volatilized at the base of a fracture site may be more harmful at this site and less harmful as the gas migrates up, absorbs onto ice walls and fluid networks, and deceases in concentration.

We also demonstrated that environments neighbouring an ammonia concentration of 0.1 M improved growth of *H. meridiana*, while environments adjacent to concentrations exceeding 0.1 M became detrimental to growth and viability. This would indicate environments adjacent to such concentrations may be habitable but display an altered bacterial community structure. For example, alkaliphilic bacteria may survive and propagate with greater abundance than alkalitolerant bacteria, such as *H. meridiana*, that may grow slower. It is notable 0.1 M ammonia is the upper concentration boundary approximated for the ocean of Enceladus [61]. These thresholds are specific to *H. meridiana;* generalized habitability thresholds in NH_3 gas could be further constrained using a diversity of bacterial species. Indeed, comparisons with literature show that direct exposure to 0.1 M ammonia has been found toxic to neutrophilic *E. coli* and *B. subtilis* under icy moon conditions [28]. In accordance with our results, solutions where the NH_3 concentration exceeds 0.1 M can be survived by a diverse array of bacteria under standard terrestrial conditions including: *B. subtilis* T5 (0.15 M NH_3) [27], isolated sulfate-reducing bacteria (0.2 M NH_3) [29], *Staphylococcus aureus* (0.3 M NH_3), *Enterococcus faecium* (0.3 M NH_3), *Micrococcus luteus* (0.3 M NH_3), *Salmonella typhimurium* (0.3 M NH_3), *B. cereus* T41 (0.3 M NH_3), *Proteus pumilus* (0.5 M NH_3), *B. pumilus* (> 0.5 M NH_3), and *B. pasteurii* (> 0.5 M NH_3) [27]. Thus, there is reason to believe such concentrations of NH_3 gas volatilized from an ammonia source could be survived by a range of species, although growth may not be optimal.

The temporal effects of NH_3 gas were also demonstrated. Due to the use of an open-air system, cultures of *H. meridiana* exhibited cell density recovery with time when adjacently exposed to ammonia at all concentrations. This is comparable to our previous study which demonstrated *H. meridiana* cell numbers recovered over time with ammonia evaporation from culture media [30]. The spatial toxicity imposed by ammonia is therefore transient and suggests ecosystems exposed to NH_3 would only be temporarily affected if there is a pathway to ammonia dispersal into the bulk atmosphere. This may occur on Enceladus if NH_3 outgassing from the ocean is infrequent. Presumably, continuous exposure would exert a continuous deleterious effect on growth. It is crucial to note these results do not infer an increased or decreased likelihood of life existing on icy moons. Indeed, many other factors will influence habitability. It may be found these environments are habitable but not inhabited. Rather, these results show that NH_3 gas is a chemical parameter that could influence the potential for habitability in a spatiotemporal manner. The presence of NH_3 gas should thus be considered when constraining targets for astrobiological exploration.

On Earth, localised "point sources" of ammonia pollution have been identified in both agriculture and industry [72]. This would suggest long-term spatial effects on nearby bacterial communities according to the results of this study. *H. meridiana* was selected as an organism that could survive in

cold, saline and alkaline fluids under pressure. However, *H. meridiana* is also a mesophile, grows optimally at standard pressure and can grow at neutral pH. This organism, and the growth results presented, can thus represent bacteria without extremophilic adaptations and indeed our results are in accordance with other, diverse bacteria as outlined.

To more accurately assess the ecological impact of NH_3 gas, a natural extension of this work would be to consider evaporation rate of NH_3. The importance of evaporation rate in temporal toxicity may account for a discrepancy observed between the cell density achieved at 48 h in cultures surrounding 1 M ammonia (Fig. 2E) compared to the cell density reached at 48 h in cultures adjacent to 1 M ammonia in Fig. 3J. The evaporation rate of essential oils has been shown to effect the minimal inhibitory dose (MID) against *Staphylococcus aureus* and *E. coli*, with rapid evaporation producing a higher vapour concentration that reduces the MID required [97]. This research indicates discrepancies between experiments could be attributed to altered rate of ammonia evaporation, and thus delivery of NH_3, driven by differences in the culture instrumentation and shaking speed. A continuation of this work would be to alter atmospheric pressure or incorporate an air flow system. The incorporation of such measures could more accurately replicate in situ environments relevant to icy worlds and in anthropogenic NH_3 pollution.

Supplementary Information The online version contains supplementary material available at https://doi.org/10.1007/s00248-025-02621-1.

Acknowledgements The authors would like to acknowledge Peter Nienow, University of Edinburgh, for providing project guidance.

Author Contributions C.M.H. was involved in conceptualization of the project, methodology, validation, formal analysis, investigation, data curation, writing of the original draft, and visualization. C.S.C. provided conceptualization of the project, review and editing of the manuscript, supervision, project administration, and funding acquisition.

Funding Funding for this research was provided by the Natural Environmental Research Council (NERC) though an E4 Doctoral Training Partnership (DTP) studentship (NE/S007407/1) and the Science and Technology Facilities Council (STFC) through grants ST/V000586/1 and ST/Y001788/1.

Data Availability The raw data supporting the conclusions of this article are available in the supplementary dataset unless specified as part of the supplementary material.

Declarations

Competing Interests The authors declare no competing interests.

References

1. Cockell CS, Bush T, Bryce C et al (2016) Habitability: a review. Astrobiology 16:89–117. https://doi.org/10.1089/ast.2015.1295
2. Cockell CS, Simons M, Castillo-Rogez J et al (2024) Sustained and comparative habitability beyond Earth. Nat Astron 8:30–38. https://doi.org/10.1038/s41550-023-02158-8
3. Nagatani H, Shimizu M, Valentine RC (1971) The mechanism of ammonia assimilation in nitrogen fixing bacteria. Arch Mikrobiol 79:164–175. https://doi.org/10.1007/BF00424923
4. Burris RH, Roberts GP (1993) Biological nitrogen fixation. Annu Rev Nutr 13:317–335. https://doi.org/10.1146/annurev.nu.13.070193.001533
5. Stein LY, Klotz MG (2016) The nitrogen cycle. Curr Biol 26:R94–R98. https://doi.org/10.1016/j.cub.2015.12.021
6. Vines HM, Wedding RT (1960) Some effects of ammonia on plant metabolism and a possible mechanism for ammonia toxicity. Plant Physiol 35:820–825
7. Kelly LC, Cockell CS, Summers S (2012) Diverse microbial species survive high ammonia concentrations. Int J Astrobiol 11:125–131. https://doi.org/10.1017/S147355041200002X
8. Dasarathy S, Mookerjee RP, Rackayova V et al (2017) Ammonia toxicity: from head to toe? Metab Brain Dis 32:529–538. https://doi.org/10.1007/s11011-016-9938-3
9. Jurcă AD, Jurcă MC, Bembea M et al (2018) Clinical and genetic diversity of congenital hyperammonemia. Rom J Morphol Embryol 59:945–948
10. Rose C, Kresse W, Kettenmann H (2005) Acute insult of ammonia leads to calcium-dependent glutamate release from cultured astrocytes, an effect of pH. J Biol Chem 280:20937–20944. https://doi.org/10.1074/jbc.M412448200
11. Angelova PR, Kerbert AJC, Habtesion A et al (2022) Hyperammonaemia induces mitochondrial dysfunction and neuronal cell death. JHEP Rep 4:100510. https://doi.org/10.1016/j.jhepr.2022.100510
12. Bosoi CR, Rose CF (2009) Identifying the direct effects of ammonia on the brain. Metab Brain Dis 24:95–102. https://doi.org/10.1007/s11011-008-9112-7
13. Shi S, Xu F, Ge Y et al (2020) NH_4^+ toxicity, which is mainly determined by the high NH_4^+/K^+ ratio, is alleviated by CIPK23 in *Arabidopsis*. Plants 9:501. https://doi.org/10.3390/plants9040501
14. Hampson BL (1977) Relationship between total ammonia and free ammonia in terrestrial and ocean waters. ICES J Mar Sci 37:117–122. https://doi.org/10.1093/icesjms/37.2.117
15. Whitfield M (1974) The hydrolysis of ammonium ions in sea water - a theoretical study. J Marine Biol Assoc UK 54:565–580. https://doi.org/10.1017/S002531540002275X
16. Bower CE, Bidwell JP (1978) Ionization of ammonia in seawater: effects of temperature, pH, and salinity. J Fish Res Bd Can 35:1012–1016. https://doi.org/10.1139/f78-165
17. Sutton MA, Milford C, Dragosits U et al (1998) Dispersion, deposition and impacts of atmospheric ammonia: quantifying

local budgets and spatial variability. Environ Pollut 102:349–361. https://doi.org/10.1016/S0269-7491(98)80054-7
18. Bouet R, Duplantier S, Salvi O (2005) Ammonia large scale atmospheric dispersion experiments in industrial configurations. J Loss Prev Process Ind 18:512–519. https://doi.org/10.1016/j.jlp.2005.07.016
19. Leytem AB, Walker JT, Wu Z et al (2024) Spatial distribution of ammonia concentrations and modeled dry deposition in an intensive dairy production region. Atmosphere 15:15. https://doi.org/10.3390/atmos15010015
20. Lô S, Dohmen W, Heederik D et al (2025) Spatial and temporal variability of atmospheric ammonia using a dense network in an area with livestock, residential and natural environments intertwined. Atmos Environ. https://doi.org/10.1016/j.atmosenv.2025.121394
21. Pinder RW, Gilliland AB, Dennis RL (2008) Environmental impact of atmospheric NH_3 emissions under present and future conditions in the eastern United States. Geophys Res Lett. https://doi.org/10.1029/2008GL033732
22. Behera SN, Sharma M, Aneja VP, Balasubramanian R (2013) Ammonia in the atmosphere: a review on emission sources, atmospheric chemistry and deposition on terrestrial bodies. Environ Sci Pollut Res 20:8092–8131. https://doi.org/10.1007/s11356-013-2051-9
23. Xie Y, Wang W, Chen Y et al (2024) NH_3 emissions and lifetime estimated by satellite observations with differential evolution algorithm. Atmosphere 15:251. https://doi.org/10.3390/atmos15030251
24. Duce RA, Liss PS, Merrill JT et al (1991) The atmospheric input of trace species to the world ocean. Glob Biogeochem Cycles 5:193–259. https://doi.org/10.1029/91GB01778
25. Erisman JW, Draaijers GPJ (1995) Atmospheric deposition: in relation to acidification and eutrophication. Elsevier, Amsterdam
26. Krupa SV (2003) Effects of atmospheric ammonia (NH_3) on terrestrial vegetation: a review. Environ Pollut 124:179–221. https://doi.org/10.1016/S0269-7491(02)00434-7
27. Leejeerajumnean A, Ames JM, Owens JD (2000) Effect of ammonia on the growth of *Bacillus* species and some other bacteria. Lett Appl Microbiol 30:385–389. https://doi.org/10.1046/j.1472-765x.2000.00734.x
28. Deal PH, Souza KA, Mack HM (1975) High pH, ammonia toxicity, and the search for life on the Jovian planets. Orig Life Evol Biosph 6:561–573. https://doi.org/10.1007/BF00928904
29. Dai X, Hu C, Zhang D et al (2017) Impact of a high ammonia-ammonium-pH system on methane-producing archaea and sulfate-reducing bacteria in mesophilic anaerobic digestion. Bioresour Technol 245:598–605. https://doi.org/10.1016/j.biortech.2017.08.208
30. Hopton CM, Nienow P, Cockell CS (2025) Ammonia sets limit to life and alters physiology independently of pH in *Halomonas meridiana*. Sci Rep 15:1–16. https://doi.org/10.1038/s41598-025-03858-z
31. Eno CF, Blue WG, Good JM Jr (1955) The effect of anhydrous ammonia on nematodes, fungi, bacteria, and nitrification in some Florida soils. Soil Sci Soc Am J 19:55–58. https://doi.org/10.2136/sssaj1955.03615995001900010013x
32. Kleiner D (1981) The transport of NH_3 and NH_4^+ across biological membranes. Biochim Biophys Acta Bioenerg 639:41–52. https://doi.org/10.1016/0304-4173(81)90004-5
33. Raven JA, Wollenweber B, Handley LL (1992) A comparison of ammonium and nitrate as nitrogen sources for photolithotrophs. New Phytol 121:19–32. https://doi.org/10.1111/j.1469-8137.1992.tb01088.x
34. Britto DT, Siddiqi MY, Glass ADM, Kronzucker HJ (2001) Futile transmembrane NH_4^+ cycling: a cellular hypothesis to explain ammonium toxicity in plants. PNAS 98:4255–4258. https://doi.org/10.1073/pnas.061034698
35. Reitzer L (2003) Nitrogen assimilation and global regulation in *Escherichia coli*. Annu Rev Microbiol 57:155–176. https://doi.org/10.1146/annurev.micro.57.030502.090820
36. Li S-X, Wang Z-H, Stewart BA (2013) Chapter five - responses of crop plants to ammonium and nitrate N. In: Sparks DL (ed) Advances in agronomy. Academic Press, vol 118. pp 205–397. https://doi.org/10.1016/B978-0-12-405942-9.00005-0
37. Sutton MA, Reis S, Baker SMH (2009) Atmospheric ammonia. Springer, Dordrecht, London
38. Bobbink R, Hicks WK (2014) Factors affecting nitrogen deposition impacts on biodiversity: an overview. In: Sutton MA, Mason KE, Sheppard LJ, Sverdrup H, Haeuber R, Hicks W (eds) Nitrogen deposition, critical loads and biodiversity. Springer Netherlands, Dordrecht, pp 127–138. https://doi.org/10.1007/978-94-007-7939-6_14
39. García-Gómez H, Garrido JL, Vivanco MG et al (2014) Nitrogen deposition in Spain: modeled patterns and threatened habitats within the Natura 2000 network. Sci Total Environ 485:450–460. https://doi.org/10.1016/j.scitotenv.2014.03.112
40. Paoli L, Benesperi R, Proietti Pannunzi D et al (2014) Biological effects of ammonia released from a composting plant assessed with lichens. Environ Sci Pollut Res 21:5861–5872. https://doi.org/10.1007/s11356-014-2526-3
41. Hou L, Zhou Q, Wu Q et al (2018) Spatiotemporal changes in bacterial community and microbial activity in a full-scale drinking water treatment plant. Sci Total Environ 625:449–459. https://doi.org/10.1016/j.scitotenv.2017.12.301
42. Khurana KK, Kivelson MG, Stevenson DJ et al (1998) Induced magnetic fields as evidence for subsurface oceans in Europa and Callisto. Nature 395:777–780. https://doi.org/10.1038/27394
43. Tobie G, Čadek O, Sotin C (2008) Solid tidal friction above a liquid water reservoir as the origin of the south pole hotspot on Enceladus. Icarus 196:642–652. https://doi.org/10.1016/j.icarus.2008.03.008
44. Nimmo F, Pappalardo RT (2016) Ocean worlds in the outer solar system. J Geophys Res Planets 121:1378–1399. https://doi.org/10.1002/2016JE005081
45. Lewis JS (1971) Satellites of the outer planets: their physical and chemical nature. Icarus 15:174–185. https://doi.org/10.1016/0019-1035(71)90072-8
46. Spohn T, Schubert G (2003) Oceans in the icy Galilean satellites of Jupiter? Icarus 161:456–467. https://doi.org/10.1016/S0019-1035(02)00048-9
47. Waite JH, Lewis WS, Magee BA et al (2009) Liquid water on Enceladus from observations of ammonia and 40Ar in the plume. Nature 460:487–490. https://doi.org/10.1038/nature08153
48. Waite JH, Glein CR, Perryman RS et al (2017) Cassini finds molecular hydrogen in the Enceladus plume: evidence for hydrothermal processes. Science 356:155–159. https://doi.org/10.1126/science.aai8703
49. Roberts JH, Nimmo F (2008) Tidal heating and the long-term stability of a subsurface ocean on Enceladus. Icarus 194:675–689. https://doi.org/10.1016/j.icarus.2007.11.010
50. Nimmo F, Spencer JR, Pappalardo RT, Mullen ME (2007) Shear heating as the origin of the plumes and heat flux on Enceladus. Nature 447:289–291. https://doi.org/10.1038/nature05783
51. Matson DL, Castillo JC, Lunine J, Johnson TV (2007) Enceladus' plume: compositional evidence for a hot interior. Icarus 187:569–573. https://doi.org/10.1016/j.icarus.2006.10.016
52. Hsu H-W, Postberg F, Sekine Y et al (2015) Ongoing hydrothermal activities within Enceladus. Nature 519:207–210. https://doi.org/10.1038/nature14262

53. Zolotov MY (2007) An oceanic composition on early and today's Enceladus. Geophys Res Lett. https://doi.org/10.1029/2007GL031234
54. Postberg F, Sekine Y, Klenner F et al (2023) Detection of phosphates originating from Enceladus's ocean. Nature 618:489–493. https://doi.org/10.1038/s41586-023-05987-9
55. Xu W, Liu C, Zhang A et al (2025) Enough sulfur and iron for potential life make Enceladus's ocean fully habitable. ApJL 980:L10. https://doi.org/10.3847/2041-8213/adad65
56. Postberg F, Khawaja N, Abel B et al (2018) Macromolecular organic compounds from the depths of Enceladus. Nature 558:564–568. https://doi.org/10.1038/s41586-018-0246-4
57. Kargel JS, Kaye JZ, Head JW et al (2000) Europa's crust and ocean: origin, composition, and the prospects for life. Icarus 148:226–265. https://doi.org/10.1006/icar.2000.6471
58. Wettlaufer JS (2009) Sea ice and astrobiology. In: Thomas DN, Dieckmann GS (eds) Sea ice. John Wiley & Sons, Ltd, pp 579–594. https://doi.org/10.1002/9781444317145.ch15
59. Wolfenbarger NS, Fox-Powell MG, Buffo JJ et al (2022) Brine volume fraction as a habitability metric for Europa's ice shell. Geophys Res Lett 49:e2022GL100586. https://doi.org/10.1029/2022GL100586
60. Buffo JJ, Schmidt BE, Huber C, Meyer CR (2021) Characterizing the ice-ocean interface of icy worlds: a theoretical approach. Icarus 360:114318. https://doi.org/10.1016/j.icarus.2021.114318
61. Fifer LM, Catling DC, Toner JD (2022) Chemical fractionation modeling of plumes indicates a gas-rich, moderately alkaline Enceladus ocean. Planet Sci J 3:191. https://doi.org/10.3847/PSJ/ac7a9f
62. Richter C, Gholami S, Manoharan Y et al (2025) Uptake of ammonia by ice surfaces at atmospheric temperatures. Faraday Discuss 258:532–545. https://doi.org/10.1039/d4fd00169a
63. Bates RG, Pinching GD (1949) Acidic dissociation constant of ammonium ion at 0 to 50 °C, and the base strength of ammonia. J Res Natl Bur Stan 42:419. https://doi.org/10.6028/jres.042.037
64. Sohl F, Hussmann H, Schwentker B et al (2003) Interior structure models and tidal love numbers of Titan. Journal of Geophysical Research: Planets. https://doi.org/10.1029/2003JE002044
65. Takahashi Y, Takahashi H, Galipon J, Arakawa K (2020) Complete genome sequence of *Halomonas meridiana* strain Slthf1, isolated from a deep-sea thermal vent. Microbiol Resour Announc. https://doi.org/10.1128/MRA.00292-20
66. Kaye JZ, Márquez MC, Ventosa A, Baross JAY (2004) *Halomonas neptunia* sp. nov., *Halomonas sulfidaeris* sp. nov., *Halomonas axialensis* sp. nov. and *Halomonas hydrothermalis* sp. nov.: halophilic bacteria isolated from deep-sea hydrothermal-vent environments. Int J Syst Evol Microbiol 54:499–511. https://doi.org/10.1099/ijs.0.02799-0
67. Dobson SJ, Franzmann PD (1996) Unification of the genera *Deleya* (Baumann et al. 1983), *Halomonas* (Vreeland et al. 1980), and *Halovibrio* (Fendrich 1988) and the species *Paracoccus halodenitrificans* (Robinson and Gibbons 1952) into a single genus, *Halomonas*, and placement of the genus *Zymobacter* in the family *Halomonadaceae*. Int J Syst Evol Microbiol 46:550–558. https://doi.org/10.1099/00207713-46-2-550
68. Kaye JZ, Baross JA (2004) Synchronous effects of temperature, hydrostatic pressure, and salinity on growth, phospholipid profiles, and protein patterns of four *Halomonas* species isolated from deep-sea hydrothermal-vent and sea surface environments. Appl Environ Microbiol. https://doi.org/10.1128/AEM.70.10.6220-6229.2004
69. Smug BJ, Opalek M, Necki M, Wloch-Salamon D (2024) Microbial lag calculator: a shiny-based application and an R package for calculating the duration of microbial lag phase. Methods Ecol Evol 15:301–307. https://doi.org/10.1111/2041-210X.14269
70. Jeong H, Park J, Kim H (2013) Determination of NH_4^+ in environmental water with interfering substances using the modified nessler method. J Chem 2013:e359217. https://doi.org/10.1155/2013/359217
71. Fortes AD (2000) Exobiological implications of a possible ammonia-water ocean inside Titan. Icarus 146:444–452. https://doi.org/10.1006/icar.2000.6400
72. Van Damme M, Clarisse L, Whitburn S et al (2018) Industrial and agricultural ammonia point sources exposed. Nature 564:99–103. https://doi.org/10.1038/s41586-018-0747-1
73. Luo Z, Zhang Y, Chen W et al (2022) Estimating global ammonia (NH_3) emissions based on IASI observations from 2008 to 2018. Atmos Chem Phys 22:10375–10388. https://doi.org/10.5194/acp-22-10375-2022
74. Geng Y, Peng C, Wang Z et al (2022) Insights into the spatiotemporal differences in tailings seepage pollution by assessing the diversity and metabolic functions of the soil microbial community. Environ Pollut 306:119408. https://doi.org/10.1016/j.envpol.2022.119408
75. Jiao S, Liu Z, Lin Y et al (2016) Bacterial communities in oil contaminated soils: biogeography and co-occurrence patterns. Soil Biol Biochem 98:64–73. https://doi.org/10.1016/j.soilbio.2016.04.005
76. Boyanova L, Gergova G, Nikolov R et al (2005) Activity of Bulgarian propolis against 94 *Helicobacter pylori* strains *in vitro* by agar-well diffusion, agar dilution and disc diffusion methods. J Med Microbiol 54:481–483. https://doi.org/10.1099/jmm.0.45880-0
77. Hinton A Jr, Ingram KD (2011) Use of the agar diffusion assay to evaluate bactericidal activity of formulations of alkaline salts of fatty acids against bacteria associated with poultry processing. J Food Saf 31:357–364. https://doi.org/10.1111/j.1745-4565.2011.00307.x
78. Diaz-Baez MC, Roldan F (1996) Evaluation of the agar plate method for rapid toxicity assessment with some heavy metals and environmental samples. Environ Toxicol Water Qual 11:259–263. https://doi.org/10.1002/(SICI)1098-2256(1996)11:3%3c259::AID-TOX12%3e3.0.CO;2-6
79. Liu D, Chau YK, Dutka BJ (1989) Rapid toxicity assessment of water-soluble and water-insoluble chemicals using a modified agar plate method. Water Res 23:333–339. https://doi.org/10.1016/0043-1354(89)90099-7
80. Dwivedi S, Wahab R, Khan F et al (2014) Reactive oxygen species mediated bacterial biofilm inhibition via zinc oxide nanoparticles and their statistical determination. PLoS ONE 9:e111289. https://doi.org/10.1371/journal.pone.0111289
81. Goswami M, Mangoli SH, Jawali N (2006) Involvement of reactive oxygen species in the action of ciprofloxacin against *Escherichia coli*. Antimicron Agents Chemother 50:949–954. https://doi.org/10.1128/aac.50.3.949-954.2006
82. Müller T, Walter B, Wirtz A, Burkovski A (2006) Ammonium toxicity in bacteria. Curr Microbiol 52:400–406. https://doi.org/10.1007/s00284-005-0370-x
83. Tachiki T, Shirasu Y, Haruna M, Tochikura T (1978) Occurrence of glutamine synthetase/glutamate synthase pathway in *Gluconobacter suboxydans*. Agric Biol Chem 42:1689–1695. https://doi.org/10.1080/00021369.1978.10863232
84. Shatters RG, Liu Y, Kahn ML (1993) Isolation and characterization of a novel glutamine synthetase from *Rhizobium meliloti*. J Biol Chem 268:469–475
85. Hemmilä IA, Mäntsälä PI (1978) Purification and properties of glutamate synthase and glutamate dehydrogenase from *Bacillus megaterium*. Biochem J 173:45–52. https://doi.org/10.1042/bj1730045
86. Kanamori K, Weiss RL, Roberts JD (1987) Ammonia assimilation in *Bacillus polymyxa*. 15N NMR and enzymatic studies. J Biol

Chem 262:11038–11045. https://doi.org/10.1016/S0021-9258(18)60923-8
87. Hu J, Yan J, Wu L et al (2022) Insight into halotolerance of a robust heterotrophic nitrifying and aerobic denitrifying bacterium *Halomonas salifodinae*. Bioresour Technol 351:126925. https://doi.org/10.1016/j.biortech.2022.126925
88. Dong L, Ge Z, Qu W et al (2022) Characteristics and mechanism of heterotrophic nitrification/aerobic denitrification in a novel *Halomonas piezotolerans* strain. J Basic Microbiol 62:124–134. https://doi.org/10.1002/jobm.202100446
89. Wang T, Li J, Zhang LH et al (2017) Simultaneous heterotrophic nitrification and aerobic denitrification at high concentrations of NaCl and ammonia nitrogen by *Halomonas* bacteria. Water Sci Technol 76:386–395. https://doi.org/10.2166/wst.2017.214
90. Gee DL, Duane Brown W (1981) The effect of carbon monoxide on bacterial growth. Meat Sci 5:215–222. https://doi.org/10.1016/0309-1740(81)90004-8
91. Porter N, Drozd JW, Linton JD (1983) The effects of cyanide on the growth and respiration of *Enterobacter aerogenes* in continuous culture. Microbiology 129:7–16. https://doi.org/10.1099/00221287-129-1-7
92. Coyne FP, Hardy WB (1997) The effect of carbon dioxide on bacteria growth. Proceedings of the Royal Society of London Series B, Containing Papers of a Biological Character 113:196–217. https://doi.org/10.1098/rspb.1933.0041
93. Cheng J, Hu J (2021) Recent advances on carbon monoxide releasing molecules for antibacterial applications. ChemMedChem 16:3628–3634. https://doi.org/10.1002/cmdc.202100555
94. Mendes SS, Miranda V, Saraiva LM (2021) Hydrogen sulfide and carbon monoxide tolerance in bacteria. Antioxidants 10:729. https://doi.org/10.3390/antiox10050729
95. Seregina TA, Lobanov KV, Shakulov RS, Mironov AS (2022) Enhancement of the bactericidal effect of antibiotics by inhibition of enzymes involved in production of hydrogen sulfide in bacteria. Mol Biol 56:638–648. https://doi.org/10.1134/S0026893322050120
96. Couvert O, Koullen L, Lochardet A et al (2023) Effects of carbon dioxide and oxygen on the growth rate of various food spoilage bacteria. Food Microbiol 114:104289. https://doi.org/10.1016/j.fm.2023.104289
97. Inouye S, Takizawa T, Yamaguchi H (2001) Antibacterial activity of essential oils and their major constituents against respiratory tract pathogens by gaseous contact. J Antimicrob Chemother 47:565–573. https://doi.org/10.1093/jac/47.5.565

Chapter 6 appendix: Growth, physiology and metabolism of *Halomonas meridiana* in aqueous ammonium sulphate with implications for icy moon astrobiology

This following supplementary material originally appeared in *Frontiers in Microbiology*, 19th September 2025. DOI: 10.3389/fmicb.2025.1642998.

Supplementary Figure S1. Cell viability and optical density at 600 nm over 24 h. Column graph shows the PrestoBlue™ cell viability (black bars) against optical density at 600 nm (OD_{600}) (striped bars) of *Halomonas meridiana* sampled at 0, 2, 4, 6 and 24 hours. Column heights represent the mean ± s.d. (*n* = 3).

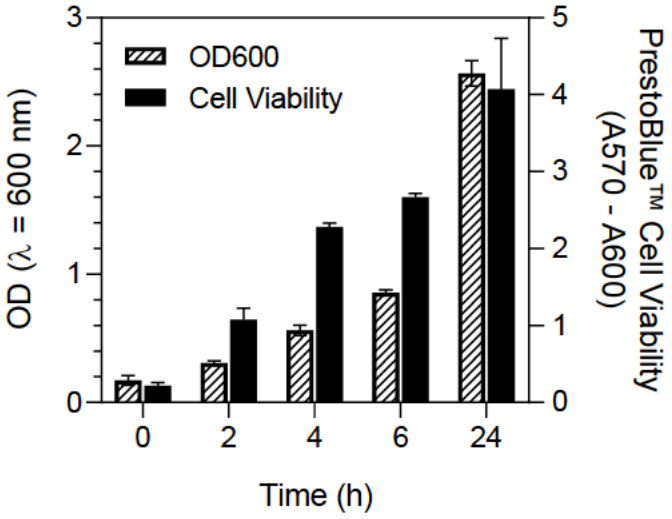

Supplementary Table S1. Statistical *p*-values for the mean OD_{600} of *H. meridiana* after 48 h growth in 0.5 M $(NH_4)_2SO_4$ vs. 0.5 M sulfate salts and 0.25 M $(NH_4)_2SO_4$ vs. 0.5 M ammonium salts, including HCl pH-matched solutions

	0.5 M					
	NH_4Cl	NH_4NO_3	HCl pH 5.9	Na_2SO_4	K_2SO_4	HCl pH 5.8
0.25 M $(NH_4)_2SO_4$	0.359	0.765	0.636			
0.5 M $(NH_4)_2SO_4$				>0.999	>0.999	>0.999

Supplementary Table S2. Statistical *p*-values for the mean a_w of $(NH_4)_2SO_4$ vs. sulfate salt and ammonium salt solutions at concentrations of 0.1 M, 0.5 M and 1 M.

	0.1 M			
	NH_4Cl	NH_4NO_3	Na_2SO_4	K_2SO_4
0.05 M $(NH_4)_2SO_4$	0.0558	0.233		
0.1 M $(NH_4)_2SO_4$			0.205	0.133
	0.5 M			
	NH_4Cl	NH_4NO_3	Na_2SO_4	K_2SO_4
0.25 M $(NH_4)_2SO_4$	>0.999	>0.999		
0.5 M $(NH_4)_2SO_4$			0.382	0.448
	1 M			
	NH_4Cl	NH_4NO_3	Na_2SO_4	
0.5 M $(NH_4)_2SO_4$	0.624	0.999		
1 M $(NH_4)_2SO_4$			0.126	

Supplementary Table S3. Metabolites significantly altered (*p*-value lower than 0.05, FDR corrected) between the treatment conditions assessed by unpaired *t*-test (*n* = 3). Unpaired t-test analysis was performed using the web-based software MetabAnalyst 6.0.

Metabolite	t.stat	p.value	-log10(p)	FDR
O-Succinyl-homoserine	284.81	9.12E-10	9.0401	0.000000482
Lumazine	-215.6	2.78E-09	8.5565	0.000000734
Fumarate	157.57	9.73E-09	8.0118	0.00000172
Poly-(glycine)5	118.74	3.02E-08	7.5204	0.00000281
N,N-Dimethylglycine	-115.03	3.42E-08	7.4654	0.00000281
N6-(delta2-Isopentenyl)-adenine	110.46	4.03E-08	7.3949	0.00000281
Glutamine	-109.44	4.18E-08	7.3787	0.00000281
4-Coumarate	-108.97	4.25E-08	7.3713	0.00000281
Dihydrobiopterin	87.054	0.000000104	6.9814	0.00000558
L-Serine	-86.816	0.000000106	6.9766	0.00000558
NVNDVIAPAFVK (Tryptic Peptide)	-80.982	0.000000139	6.8558	0.00000665
Hypoxanthine	-79.387	0.000000151	6.8213	0.00000665
Glutarylcarnitine	-75.613	0.000000183	6.7367	0.00000746
2-Deoxyadenosine-5-monophosphate	53.753	0.000000717	6.1444	0.0000271
PC 36:05	48.724	0.00000106	5.974	0.0000365
Indole-3-ethanol	-48.248	0.0000011	5.957	0.0000365
Inosine	-38.925	0.0000026	5.5847	0.000081
Imazapyr	-37.711	0.00000295	5.5297	0.0000828
Pyridoxine	-37.641	0.00000297	5.5265	0.0000828
PE 37:01	34.213	0.00000435	5.3611	0.00011517
D-allo-Isoleucine	31.901	0.00000576	5.2399	0.00014499
Indole-3-pyruvate	-31.113	0.00000636	5.1966	0.0001529
Guanosine	-28.125	0.00000951	5.0219	0.0002187
PS 40:01	-23.28	0.0000202	4.6951	0.00044474
Deoxyguanosine	-22.083	0.0000249	4.604	0.00052664
2-Amino-2-methylpropanoate	-20.833	0.0000314	4.5035	0.0006383
Stearic Acid (18:0)	16.285	0.0000832	4.0798	0.0016302
2-Methylnaphthalene	15.07	0.000113	3.9469	0.0021349
Oxoproline	-13.984	0.0001517	3.819	0.0027672
Protoporphyrin	-13.423	0.00017817	3.7492	0.0031417

Supplementary Table S4. Volcano analysis comparing molecular features in the 0.5 M $(NH_4)_2SO_4$ dataset against the control dataset (n = 3), where metabolites identified in the analysis exhibited a fold change (FC) greater than 2 and a p-value < 0.05 (adjusted using FDR correction). Volcano analysis was performed using the web-based software MetabAnalyst 6.0.

Metabolite	FC	log2(FC)	p.ajusted	-log10(p)
Glutarylcarnitine	1.23E-09	-29.595	7.46E-06	5.1272
Hypoxanthine	1.47E-09	-29.345	6.65E-06	5.177
Deoxyguanosine	1.50E-09	-29.31	0.00052664	3.2785
Indole-3-ethanol	1.72E-09	-29.115	3.65E-05	4.4377
Guanosine	3.16E-09	-28.239	0.0002187	3.6601
NVNDVIAPAFVK (Tryptic Peptide)	3.55E-09	-28.07	6.65E-06	5.177
Inosine	5.10E-09	-27.547	8.10E-05	4.0917
4-Coumarate	6.19E-09	-27.266	2.81E-06	5.5509
Lumazine	8.84E-09	-26.753	7.34E-07	6.1341
Glutamine	1.15E-08	-26.371	2.81E-06	5.5509
L-Serine	1.20E-08	-26.312	5.58E-06	5.2532
N,N-Dimethylglycine	2.81E-08	-25.083	2.81E-06	5.5509
Protoporphyrin	3.11E-08	-24.94	0.0031417	2.5028
Imazapyr	3.46E-08	-24.784	8.28E-05	4.0818
Indole-3-pyruvate	4.16E-08	-24.517	0.0001529	3.8156
Pyridoxine	5.48E-08	-24.12	8.28E-05	4.0818
PS 40:01	3.16E-07	-21.592	0.00044474	3.3519
N-Methylaspartate	0.10785	-3.2129	0.034078	1.4675
Oxoproline	0.11152	-3.1646	0.0027672	2.558
2-Amino-2-methylpropanoate	0.13412	-2.8984	0.0006383	3.195
2-Acetamindo-2-deoxy-beta-D-glycosylamine	0.1417	-2.8191	0.010995	1.9588
N-acetyl-L-aspartate	0.15917	-2.6514	0.026225	1.5813
Nicotinamide	0.30151	-1.7297	0.041236	1.3847
4-Guanidinobutanoate	0.43137	-1.213	0.03852	1.4143
Trigonelline	2.2167	1.1484	0.032461	1.4886
Stearic Acid (18:0)	2.4299	1.2809	0.0016302	2.7877
PC (18:1/18:1) (del9-trans)	4.8262	2.2709	0.0074116	2.1301
4-Quinolinecarboxylate	7.1661	2.8412	0.026225	1.5813
L-aspartate	7.2425	2.8565	0.03852	1.4143
D-allo-Isoleucine	8.4184	3.0735	0.00014499	3.8387
PC(16:1(9Z)/16:1(9Z))	11.35	3.5046	0.026225	1.5813
PE (O-34:03)	46.154	5.5284	0.022706	1.6439
2-Deoxyadenosine-5-monophosphate	5141100	22.294	2.71E-05	4.5671
2-Methylnaphthalene	41599000	25.31	0.0021349	2.6706
PE 37:01	70589000	26.073	0.00011517	3.9387

Poly-(glycine)5	95621000	26.511	2.81E-06	5.5509
N6-(delta2-Isopentenyl)-adenine	122200000	26.865	2.81E-06	5.5509
Dihydrobiopterin	200910000	27.582	5.58E-06	5.2532
Fumarate	743070000	29.469	1.72E-06	5.7655
O-Succinyl-homoserine	1.44E+09	30.421	4.82E-07	6.3166
PC 36:05	1559700000	30.539	3.65E-05	4.4377

Supplementary Table S5. Outcome of the pathway analysis depicting pathways identified in the metabolomics dataset as significantly changed (*p*-value = < 0.05; FDR = < 0.05). Pathway analysis was performed using the web-based software MetabAnalyst 6.0.

Pathway	Match	*p*-value	FDR
Sphingolipid metabolism	1/3	1.05×10^{-7}	6.54×10^{-6}
Nitrogen metabolism	2/6	5.71×10^{-7}	1.77×10^{-5}
Purine metabolism	22/70	5.36×10^{-5}	0.00111
Glyoxylate and dicarboxylic acid metabolism	7/32	3.03×10^{-4}	0.00382
Glycine, serine and threonine metabolism	5/33	3.08×10^{-4}	0.00382
Arginine biosynthesis	7/14	4.43×10^{-4}	0.00414
Alanine, aspartate and glutamate metabolism	11/28	4.67×10^{-4}	0.00414
D-amino acid metabolism	4/15	0.00352	0.0249
Folate biosynthesis	2/26	0.00361	0.0249
Pyruvate metabolism	3/23	0.00405	0.0251
Butanoate metabolism	3/15	0.00454	0.0256
TCA cycle	5/20	0.00862	0.0445